PROSPECTIVE SKY GUIDES:
DEVELOPING GUIDELINES FOR PILOT VISION AIDS

Thesis submitted in accordance with the requirements of
the University of Liverpool for the degree of Doctor in
Philosophy

by

Michael Jump

April 2007

Abstract

Airline transport operations are carried out in a wide range of visual and instrument meteorological conditions. For all but the most limiting of degraded visibility situations, the pilot can choose to fly the approach to the airfield and land the aircraft manually. S/he does this using the visual cues available through the cockpit windshield. The answer to the question - how is this achieved may seem rather obvious, but has actually challenged researchers for some time. The optical flow theory of visual perception offers solutions in terms of the way pilots pick up motion from the environment in which they move. In a relatively recent incarnation, flow theory transforms motion into the temporal, time-to-contact parameter, τ, defined as the time to close the motion gap to a surface or object at the instantaneous closure rate. This thesis reports on the development of novel display formats, using τ theory as a basis, for the fixed wing jet transport approach and landing manoeuvres.

A simulation model of a generic large jet transport aircraft is constructed and a number of repeatable flight test manoeuvres developed. Using these as a start point, a number of flight test trials are conducted. The first two of these is to establish whether or not coherent τ-based relationships exist for a series of motion gaps identified for each flight test manoeuvre. Here, it is discovered that for the localiser capture, glide slope capture and flare manoeuvre, pilots use constant rate of change of τ ($\dot{\tau}$) guidance strategies to close the motion gaps of interest. The use of such strategies is consistent with the pilots coupling onto the τ-guides that τ theory postulates. This result is consistent with previous work conducted using rotary wing aircraft.

Based upon the results obtained, a number of concept displays are developed. First, a two-dimensional lead aircraft concept is developed.

Here, the pilot must overlay a prediction of the aircraft position at some near-future time with that of the desired position. Speed cueing is provided by the lead aircraft 'looming' if there is a difference between desired and actual airspeed. Second, a flare command display is developed. It provides a commanded flight path angle to achieve a desired $\dot{\tau}$ of height. Again, the pilot must overlay the actual aircraft flight path with desired.

In order that these display designs could be finalised, the values of a number of parameters had to be established. A display development trial was conducted for this purpose. The specific values of interest and their final values were: optimum look-ahead time for a lead aircraft to guide the pilot along a given trajectory was found to be 2 seconds; for the localiser capture manoeuvre, the gap closure $\dot{\tau}$ was set at 0.6 and the gap closure duration fixed at 10seconds; for the glide slope capture manoeuvre the gap closure $\dot{\tau}$ was also set at 0.6 and the duration at 5 seconds; for the flare command display, the $\dot{\tau}$ commanded was 0.75 and the initiation τ at 3.5 seconds.

The novel display formats were tested by comparing them with a conventional head-down primary flight display, a 'state-of-the-art' head up display and a highway-in-the-sky concept. The comparison was performed using objective measurement of actual and desired trajectories and subjective measurement using the NASA display flyability rating scale and the Bedford workload scale. During this testing, the looming cue was found to be insufficient for the purposes of accurate speed control. However, the lead aircraft concept is shown to provide superior trajectory tracking over the alternative display formats in both good and degraded visual environments. The improved performance comes at the expense of slightly higher pilot-perceived workload. The τ-based flare command display is shown to provide landing touchdown performance as least as

good as a current state-of-the-art head-up display in both good and degraded visual environments.

Based upon the design process followed and the results obtained, a number of conclusions are drawn. The most important is that τ-based motion gap closure strategies are a fundamental means by which pilots guide aircraft through the environment. As such, the future display designers should incorporate the methods and approach discussed in this thesis.

A c k n o w l e d g m e n t s

'*Time is an illusion. Lunchtime doubly so*'

Douglas Adams

The above quotation seemed particularly apt to a thesis that is concerned with a theory the primary dimension of which is measured using time and to the author who has had to find the time to write it.

No PhD thesis is truly a solo effort and the author wishes to express sincere appreciation to Professor Gareth D. Padfield who provided an escape from his (the author's) 'wilderness years' and the opportunity to fulfill a long-held but dormant ambition in one go.   The entire Flight Science & Technology Research Group has, at some time, provided much needed assistance but a few special mentions are deserved. The first is Dr. Mark White who has continuously imparted the technical and political knowledge required to make the research project happen in an academic environment. The second mention must go to Dr. Ben Lawrence who has provided tireless guidance through the mysteries that FLIGHTLAB can present to a newcomer. Mr. Heath Lockett must be congratulated on his mastery of the eye-tracking equipment, leaving the author one less thing to sort out. On the same note, Dr. Keith Nuttall must be both thanked and congratulated on his perseverance with the manual analysis of the eye-tracker video footage. Mr. Steve Bode deserves an honourable mention as the provider of outside world databases and assorted 3-D models.

The final mention must go to the three women in my life: my wife, Kath, my daughter, Emily and my mum, Ann. They have provided the support, space and a much needed series of reality checks that have ultimately made this research possible. Normal service will now be resumed.

A c r o n y m s

2,3,4-D	Two, Three or Four Dimensional
ADI	Attitude Direction Indicator
ADF	Automatic Direction Finder
ADS-B	Automatic Dependent Surveillance-Broadcast
AEO	All Engines Operative
AI	Artificial Intelligence
AMSL	Above Mean Sea-Level
ASL	Applied Science Laboratories
ASN	Aviation Safety Network
ATC	Air Traffic Control
ATM	Air Traffic Management
CAA	Civil Aviation Authority
CAP	Civil Aviation Publication
CAVOK	Cloud and Visibility OK
CDA	Continuous Descent Approach
CFIT	Controlled Flight Into Terrain
CHIN(L,R)	Chin window visual channel (Left, Right)
CNS	Central Nervous System
CRM	Crew Resource Management
CRT	Cathode Ray Tube
DH	Decision Height
DTI	Department of Trade and Industry
EFB	Electronic Flight Bag
EM	Electro-magnetic
EPSRC	Engineering and Physical Sciences Research Council
EVS	Enhanced Vision System
FAA	Federal Aviation Administration
FD	Flight Director

FL	Flight Level
FLIR	Forward Looking Infra Red
FMS	Flight Management System
FOV	Field of View
FPV	Flight Path Vector
FST	Flight Science & Technology
GA	General Aviation
GLTA	Generic Large Transport Aircraft
GPS	Global Positioning System
GPWS	Ground Proximity Warning System
GS	Glide Slope
HDD	Head Down Display
HITS	Highway In The Sky
HMO	Head-Mounted Optics
HSI	Horizontal Situation Indicator
HUD	Head Up Display
ICAO	International Civil Aviation Organisation
ILS	Instrument Landing System
IMC	Instrument Meteorological Conditions
INSTR	Instrument (visual channel)
ISA	International Standard Atmosphere
MDA	Minimum Decision Altitude
MTE	Mission Task Element
MTOW	Maximum Take-Off Weight
ND	Navigation Display
NDB	Non-Directional (radio) Beacon
NTSB	National Transportation Safety Board
OEI	One Engine Inoperative
OS	Operating System
OTW(L, C, R)	Out of The Window (Left, Centre, Right)
PFD	Primary Flight Display
RNP	Required Navigation Performance

RoC	Rate of Change
RPM	Revolutions Per Minute
RTO	Rejected Take-Off
SA	Situational Awareness
SAR	Search and Rescue
SVS	Synthetic Vision System
TTC	Time-To-Contact
TTP	Time-To-Passage
UoL	University of Liverpool
UNK	Unknown
USAAC	United States Army Air Corps.
UK	United Kingdom
VAPS	Virtual Avionics Prototyping Software
VGS	Visual Guidance System
VHF	Very High Frequency
VMC	Visual Meteorological Conditions
VOR	VHF Omni Range (radio beacon)
VSD	Vertical Situation Display
w.r.t	with respect to

Nomenclature

Capitals

A, C   integration constant (nd)

C   aerodynamic coefficient e.g. CL (nd)

C1   constant value of $\dot{\tau}_{\Delta y}$ (nd)

C3   constant value of $\dot{\tau}_{\Delta xz}$ (nd)

P   distance between pilot eye position and lead aircraft cg (ft)

K   constant of proportionality for τ coupling (nd)

P   test pilot number prefix (nd)

R   square root of linear regression correlation coefficient (nd)

T   total duration of motion gap closure (s)

T   value of time to contact to initiate flare command signal (s)

V   IAS (kts)

V   visual condition prefix (nd)

X   horizontal distance to generic point in observers field of view (ft)

Z   vertical distance to generic point in observers field of view (ft)

Lower Case

a   constant value of τ (s)

b   wing span (ft)

c   constant value of $\dot{\tau}$ (nd)

d   distance from observer to retinal plane (ft)

d   fog density value (ft-1)

f   fog obscuration factor (nd)

h   inertial height above ground level (ft)

v   screen height (pixels)

v   body-axis component of perturbation velocity in 'y' direction (ft/s)

w   velocity in body 'z' direction (ft/s)

w   body-axis component of perturbation velocity in 'z' direction (ft/s)

x   generic motion gap variable (ft)

x   earth-referenced 'x' coordinate (ft)

xz   right-angle distance between aircraft cg and extended runway glide slope (ft)

h	screen width (pixels)	y	right-angle distance between aircraft cg and runway (extended) centre-line (ft)
k	constant of proportionality for intrinsic τ guidance	y	generic motion gap variable (ft)
m	pitching moment (ft-lb)	y	earth-referenced 'y' coordinate (ft)
m	slope of linear regression curve	z	force in body 'z' direction (lb)
n	total number of data points (nd)	z	distance from eye-point to object (ft)
t	instantaneous time during a motion gap closure (s)	z	earth-referenced 'z' coordinate (ft)
u	body-axis component of perturbation velocity in 'x' direction (ft/s)		

Symbols

α	angle of incidence (rad)	γ	flight path angle (rad)
Δ	indicates an incremental value (nd)	η	elevator angle (rad)
Δ	indicates a motion gap (nd)	$\overline{\eta}$	normalised elevator angle (nd)
δ	control surface deflection angle (rad)	θ	Euler pitch angle (rad)
δ	throttle input (%)	σ	standard deviation
δ	visual angle (deg)	τ	time-to-contact surface or obstacle (s)
ϕ	Euler roll angle (rad)	ψ	Euler yaw or heading angle (rad)

Subscripts

0	initial condition value	gs	glide slope
1	take-off decision speed	h	w.r.t elevator deflection angle
2	take-off safety speed	horizon	horizon line
3	steady initial climb speed	i	initial
a/c	aircraft	IAS	indicated airspeed
actual	current instantaneous	inertial	earth-referenced axes

Symbol	Definition
	value
appr	steady-state approach value
body	aircraft body axes
cg	centre of gravity
chase	of the chase aircraft
climb	pertaining to climb out phase of take-off
command	commanded value
δ	with respect to elevator deflection
des	desired instantaneous value
Δgsdev	of the glide slope capture angular deviation motion gap
Δh	of the inertial vertical distance gap
Δlocdev	of the localiser angular deviation motion gap
$\Delta\theta$	of the pitch angle motion gap
Δxz	of the inertial right-angle vertical distance gap between aircraft cg and extended glide slope
Δy	of the heading angle motion gap
Δy	of the inertial lateral distance gap between aircraft cg and (extended) runway centre-line
e	earth i.e. inertial
engfail	engine failure speed
eye	of the eye point
f	final
flareT1	Type 1 flare

Symbol	Definition
k	coupling constant for intrinsic τ guides
L	lift
lead	of the lead aircraft
loc	localiser
m	maximum value
m	pitching moment
max horizon	maximum horizontal
max vert	maximum vertical
n	normalised
P	generic point in observers field of view
pred	pertaining to the prediction or 'look-ahead'
q	w.r.t body pitch rate
r	take-off rotation speed
r/w	runway
r/w c/l	runway centre-line
screen	pertaining to display screen
t	tail plane
take-off	pertaining to take-off MTE
target	desired instantaneous value
td	value at main gear touch down

flareT2	Type 2 flare	td	touch down value
G	pertaining to general intrinsic τ guide	trim	trimmed value
g	pertaining to constant acceleration τ guide	v	vertical
ground roll	pertaining to ground-roll during take-off	w	w.r.t velocity of body in 'z' direction

Miscellaneous

$$\dot{a} = \frac{da}{dt}$$ First derivative w.r.t time $\qquad$ $$\ddot{a} = \frac{d^2 a}{dt^2}$$ Second derivative w.r.t time etc.

$\bar{x}$ $\qquad$ mean value of x $\qquad$ x' $\qquad$ Value of x in alternative reference frame

a_b $\qquad$ $\frac{da}{db}$ (when considering aerodynamic coefficients)

CONTENTS

C h a p t e r 1

INTRODUCTION

1.1 The Future Development of Air Traffic Management

The demand for air transport is forecast to increase between twice and three times present day levels by the year 2030[1]. This will put increasing strain on an already crowded airspace system in terms of both the economics and safety of air transport operations. The major cause of this problem is seen as the inflexibility of the present day air traffic management (ATM) system [2]. The ATM system in use today dates from the 1950's. It is defined by a series of ground-based radio-navigation beacons that link a set of fixed routes called airways. Aircraft are vectored along these routes and around airports by air traffic control (ATC) whose remit is to ensure that legal vertical and lateral separation of the aircraft is maintained. Aircraft operators are therefore forced to fly fixed routes, often at fixed speeds at a number of pre-determined flight levels[1].

Flight-deck technology has, to some degree, raced ahead of the ground based system used to support it. Modern jet transport aircraft are equipped with on-board computers that provide a Flight Management System (FMS). Such a FMS can provide functions that will allow the aircraft to automatically fly more efficient trajectories point to point within defined accuracy tolerances. These so-called RNAV operations (Required Area Navigation) are slowly being introduced to current ATM systems but their

---

[1] A Flight Level (FL) is a nominal aircraft altitude of constant atmospheric pressure that is related to a specific pressure datum (1013.25 hPa) and is not necessarily the actual measured altitude of the aircraft above sea-level. It is conventionally given a numerical value to the nearest 1000 ft in units of 100 ft in accordance with the structure of the ICAO Standard Atmosphere. For example, the 500-hPa level is written as FL 180, the ICAO standard height being 18 289 ft.

utilisation is not yet widespread or optimal. To fully adopt the flexible ATM system, the airways system would have to be abandoned.

In a parallel development, satellite and data link technologies (e.g. Global Positioning System (GPS) and Automatic Dependent Surveillance-Broadcast (ADS-B)) can now provide the capability for aircraft to broadcast their intended route and negotiate efficient trajectories with ATM computers taking into account other relevant traffic. The use of modern technology to make global air transport operations more efficient (including, for example, investigation into the utilisation of other aircraft platforms to reduce capacity problems at busy airports) is the subject of a number of studies including Ref. [3].

The danger in rushing to use technology in any realm of human endeavour is that the *human* element is either forgotten or over-relied upon. Pilots are highly trained individuals and one of their primary drivers is the safe conduct of any flight. Reducing aircraft separations and allowing flight in non-defined airways has the potential to reduce flight safety. In such an environment, it is therefore incumbent upon flight-deck equipment providers to present information about both the aircraft status and the surrounding environment to an aircraft's flight crew that will allow a rapid and intuitive assessment of the safety and appropriateness of the current situation (flight path selected, execution of that flight path etc.). Such a system must allow easy manual intervention or the simple monitoring of the automatic processes.

1.2   The Pilot as a Systems Monitor

It is perhaps more often the case that the human element of a system is not forgotten, but rather, his /her needs are not attended to appropriately. This may seem strange since for as long as there has been powered aircraft there have been attempts to provide pilots with additional information to allow

the flight to be conducted in a more controlled and safe manner. Pilots of large jet transport aircraft, at least, no longer fly by the 'seat-of-the-pants' but are 'system-information-monitors' [4]. Flight control system technology is mature enough to allow automatic take-off, en-route flight and landings to be carried out without the need of pilot intervention. The pilot monitors the actions of the automation, ready to intervene and take control if a system failure occurs. Failure of the automatic systems must not lead to a catastrophic loss of the aircraft or those on board and aircrew are legally required to maintain their manual flying skills. Manual flight is still performed but usually with reference to a Flight Director (FD). The FD is a display that provides the pilot with automated steering information. All of this has led to concerns that:

1. whilst manual workload has decreased, mental workload has increased [5, 6];

2. human beings do not perform at all well in monitoring task situations [7];

3. removal of the crew from the control loop of the aircraft reduces their ability to maintain an awareness of the aircraft's situation [8];

4. flight-deck technology has become so complex that it is difficult for flight crew to understand the principles on which the automation is operating [9] and

5. the extensive use of automation has reduced the proficiency of pilots to perform flight tasks manually [7].

It is clear that there is a conflict between the desire to use increasingly sophisticated automation to facilitate more efficient air transport and the current level of understanding of how aircrew will be able to safely be part of and utilise such systems. The most common question in modern cockpits is reported to be 'what's it doing now ?' [10]. It is perhaps time, therefore, to take a fresh look at how human crew use their senses to guide

3

an aircraft through its environment and apply this learning to the design and development of the flight deck systems of the future.

1.3 The Perception of Motion

The primary sense utilised by humans to guide themselves through their environment is sight. Sight has evolved into a precision system that enables light rays impinging on the 2-dimensional retinal surface to be interpreted instantly ('at-a-glance'), intuitively and in three dimensions. When moving through that environment, the visual field must not only provide information concerning where the observer is *now*, but where the observer *will be* in the near future. If an obstacle stands in the path of this *prospective* trajectory, avoiding action can be made in a timely fashion.

A review of airline transport safety statistics reveals that fatal accidents do still happen and a majority of them occur either during or shortly after take-off or during the approach and landing phases of flight. Understandably, manoeuvres in close proximity to the ground are less tolerant to crew error. There is an argument that a proportion of these accidents are a result of modern electronic 'glass-cockpit' displays being evolutions of their mechanical counterparts. These displays have been in use for the last half-century and the evolutionary process has added a few sets of symbols. By definition, this development process has not always been coherent or part of a long term plan. The displays provide an almost entirely two dimensional representation of the information required for flight. The instruments provide information on the *now* but the pilot must assimilate the data presented to him and construct the *will be* mental picture of the flight path of the aircraft in three dimensions from rather limited information. This may not be intuitive and will certainly not be instant, particularly in unfamiliar situations.

As previously mentioned, the reliability of the pilot's mental model is particularly critical when flying close to the ground or near to obstacles. In a good visual environment, the pilot can obtain sufficient cues from the visual scene to correlate with that of the cockpit instruments. As the visual environment degrades, for example, due to adverse weather conditions, the visual cues available become less reliable. The pilot must rely on the cockpit instruments alone. To counteract this degradation in visual information, the pilot will require some form of guidance vision aid.

To provide such a guidance aid, a complete reconstruction of the natural world from active/passive sensors coupled with terrain databases can, in principle, be achieved. Even where this has already been achieved, the cost of adopting and retro-fitting suitable equipment to aircraft is proving prohibitive in the short to medium term, resulting in the US government funding the equipment for national carriers and a voluntary equipage policy for the remainder [11]. This begs the question: what is the minimum necessary and sufficient visual information required by a pilot to develop a reliable mental model, rather than a dangerous illusion, that will allow safe flight through the surrounding environment ? The implication here is that a minimum information display will be cheaper and less complex to implement than one with extraneous data displayed.

The starting point to try to answer this question is the results of previous work performed at The University of Liverpool that used the ecological approach to visual perception as a basis. Proponents of this approach emphasise that the pilot perceives the aircraft and hence his/her own motion (known as ego-motion) *directly* from the *optic flow* of surfaces in the field of vision [12]. Optic flow specifies how the observer is moving in relation to their environment. It has been shown that optic flow rate can provide the pilot with, for example, information on ground speed in body-scaled units - eye-heights per second [13], or surface slant [14]. Lee has

developed the theory of optic flow and direct motion perception by introducing an optical variable, 'tau' (τ) – the time to contact or close to an obstacle or surface at the current closure rate [15]. Tau theory provides a framework for perceiving motion in terms of time and serves as a universal variable for controlling motion-gaps. Evidence for pilots using τ-guidance strategies has been demonstrated in simulated helicopter manoeuvring at The University of Liverpool [16]. It was shown that when helicopter pilots fly stopping manoeuvres close to the ground, there is a close correlation between the motion-τ (instantaneous time to reach the stop point) and a pilot-generated τ-guide that can follow constant deceleration or acceleration laws. It is postulated that the correlation is so good, that the τ model of pilot visual perception and motion is suitable for extension to other flight manoeuvres.

1.4   Research Aims and Objectives

Whilst evidence for the use of τ guidance strategies has been demonstrated in rotary wing flight, the equivalent literature for fixed-wing flight remains sparse. The research presented within this thesis aims to start to fill this gap. It tries to answer the question posed earlier regarding minimum sufficient information by:

1. Establishing a coherent engineering basis for the design of pilot aids that will support flight in degraded visual conditions, particularly when close to the ground.

2. Evaluating synthetic displays that recover the visual cues necessary to allow flight in degraded visual conditions for a range of manoeuvres.

The project objectives established to support these aims are as follows:

1. Quantify the informative optical flow field variables that a pilot requires for prospective flight control in a range of mission tasks.

6

2. Demonstrate equivalent performance and workload for:

   a. Mission tasks flown in good visual conditions and

   b. Mission tasks flown in degraded visibility whilst utilising vision aids that synthesise the available optical flow field information.

3. Quantify the impact of the synthetic vision aids on the level of task performance and pilot workload during critical phases of flight.

4. Produce guidelines for the design, evaluation and certification of prospective flight systems.

1.5 Thesis Scope, Structure and Content

With the motivation and objectives of the project outlined, the scope of this thesis can now be described.

1.5.1 Thesis Scope

It is easier to define the scope of this thesis by first eliminating elements of work that are definitely *not* in scope. The first of these relates to τ theory itself. Section 2.4.2 provides a discussion on the research that debates whether τ theory is a useful concept in the natural world. The work contained within this thesis does not set out to prove (or otherwise) that τ theory is valid in terms of an observer's perception of motion. Rather, the assumption is made that τ information is used by observers and should therefore be considered in gap closure scenarios. Should τ be shown to be invalid as a visual perception mechanism, the research contained within this thesis is not invalidated. The work shows that the mathematical relationships that τ defines for aircraft motion gap closures can neatly describe the manoeuvres. It provides an alternate, time-based framework, to allow a motion gap to be controlled.

If τ is assumed to exist in theory, at the practical end of things, further assumptions have been made. The goal of the project is to develop guidelines for display development. It was considered that the best way to do this was to go through the display design process itself. However, this thesis does not deliver a production standard display ready for marketing. A small number of concepts were developed and tested during the course of the research. It is also assumed that all problems associated with the measurement of the required aircraft states (whose gaps are being closed) have been solved satisfactorily. For instance, a major part of the work concentrates on the fixed-wing aircraft flare manoeuvre during a landing. The gap to be closed is aircraft height. In a simulation environment, it is easy to measure aircraft height to the precision allowed by the simulation computer. In the real world, of course, radar altimeters provide one solution for height estimation, but account would have to be taken of their respective accuracy and position aboard the aircraft in any calculation of the τ of height. The simulated flight trials conducted during the course of this research were 'ideal' and did not model any errors that may be produced by such a device (or any other). Hence, there is no measure of the effect of position estimation errors on display performance.

The effects of automation on display design were not considered in this work. Only manual fixed wing flight is investigated. Similarly, the only sense considered as providing the pilot with perceptual information as to motion of the aircraft is the *visual system*. Vestibular, haptic and aural stimuli were not investigated in this research.

The analysis of fixed-wing aircraft flight in terms of τ is a novel concept in itself. The use of such a theory for display design is also novel. The scope of the thesis is therefore defined by the subject matter being at an early stage of development. As such, the thesis includes the definition of basic jet transport aircraft manoeuvres using the concept of the mission task

element (MTE). The motion gaps of interest for each MTE are then described and basic τ analyses performed upon them. Using results from these analyses, a small number of new display concepts are developed and tested against existing operational and research display concepts.

1.5.2 Thesis Structure and Content

The thesis is divided into a number of chapters, each with a specific purpose in mind. Chapter 2 reviews the current state-of-the-art in the technical areas across which this thesis cuts. Safety statistics are evaluated in more detail than covered in this Section to establish the phases of flight that would most benefit from pilot guidance vision aids. Existing production and research technology that provides guidance to the pilot of a jet transport aircraft is reviewed. It is noted that current technology in particular is still functionally based and using natural perceptual processes might well yield benefits in terms of new display design. This leads into a description and brief assessment of competing motion perception theories. Ultimately, the research has been guided by the ecologically based Tau Theory and so Chapter 2 also contains a detailed examination of that theory. Finally, Chapter 2 concludes with an identification of the research questions which support the project aims and objectives that have driven the experimentation. The novelty of the resulting work is summarised in Section 1.6. The remainder of the thesis then starts to address the identified gaps in knowledge.

Chapter 3 provides a description of the work that had to be carried out to bring the facilities at The University of Liverpool to a point were the research could be started. This comprised the definition of a jet transport experimental manoeuvre set, the upgrading of the research facilities to incorporate the capability to generate realistic degraded visual conditions and construct aircraft displays and the building of a jet transport aircraft simulation model using FLIGHTLAB multi-body modelling software.

Chapters 4-6 provide the experimental investigation method and results which includes the design and testing of a small number of display concepts. They are arranged around specific jet transport MTEs. Chapter 4 reports on the investigation into the Flare MTE and includes results starting from the basic τ analysis, through eye-tracking results, the development of a flare command display and the testing of that display against other relevant concepts.

Chapter 5 reports on the investigation into the localiser and glide slope capture MTE. The basic τ analyses are performed and a different approach to eye-tracking presented. Again, a display concept is developed and tested against other formats.

Chapter 6 provides a more limited set of results on MTEs that require a full approach to the airfield to be made. These are essentially 'super-MTEs' that link together localiser capture, glide slope capture and the flare MTE. However, given the potential move towards alternative uses of airspace, results from a Curved Approach are also reported for each of the display formats tested.

Chapter 7 provides the conclusions of the work performed and recommendations as to how future related research can be continued or directed.

1.6   Original Contribution to Learning

The work contained within a PhD thesis must provide an 'original contribution to learning'. This can be made in a number of ways:

- discovering new knowledge;
- connecting previously unconnected facts;
- developing a new theory

- or revising established views [17].

The original contribution to learning of the work presented in this thesis meets these criteria as follows:

1. The development of fixed-wing aircraft pilot displays in the context of motion perception and specifically the ecological approach to motion perception connects, in itself, previously unrelated disciplines.

2. The analysis of such a wide range of fixed-wing jet transport manoeuvres in the τ-domain has not been previously performed. The discovery of a number of strategies that close in-flight motion gaps using constant $\dot{\tau}$ relationships is new knowledge. Furthermore, this discovery has shown that pilots perform flight manoeuvres using one of the mostly widely found relationships in nature – the power law.

3. The lessons learned from implementing the observed $\dot{\tau}$ relationships into algorithms that control aircraft displays constitutes the discovery of new knowledge.

4. A linear relationship has been discovered between aircraft touchdown velocity and the rate of change of the aircraft τ of height for one specific type of flare manoeuvre. This has been linked to existing theory for τ-based flight guidance for rotary-wing aircraft.

5. The development and analysis of pilot elevator input as a function of τ, using the reduced aircraft equations of motion as a start point is the start of the development of a new theory of pilot control strategy and can also be considered to be the connection of previously unrelated topics.

Chapter 2

TECHNICAL REVIEW

The research reported in this thesis encompasses a number of technical areas that include the perception of self (or ego)-motion and pilot guidance display technology. This Chapter will examine each of the relevant technical areas in turn and identify the gaps in knowledge that have driven the research described within the subsequent Chapters.

2.1 Aviation Safety Statistics Review

The primary aim of the research is to develop guidelines to assist with the development of future pilot guidance displays for jet transport aircraft. Ideally, the guidelines would cover all phases of flight for a typical jet transport operation. However, it was considered both necessary and important to target the research to phases of flight where the most impact could be made in terms of benefits to the aerospace industry. One of the hoped-for benefits of any new guidance system would be an increase in flight safety. Aviation safety statistics were reviewed to provide information on those phases of flight that would most benefit from enhanced safety systems, whatever their form. This Section therefore provides a summary review of available aviation fatal accident data. It summarises aircraft fatal accidents where, by definition, manned flight is being conducted, but a chain of events have occurred that have led to loss of life. Only fatal accidents have been considered for two reasons:

1. Safety statistics are more prevalent for aircraft fatal accidents in the public arena.

2. Whilst non-fatal accidents that cause injury or destruction of aircraft/property are regrettable, it is fatal accidents that cause the most upset and what might be termed 'bad press'.

The purpose of the review was to enable an informed decision to be made on the phases of flight that would most benefit from a pilot vision aid in terms of increased aviation safety and, as an additional consequence, reduced costs to the aircraft operators (due, for example, to a reduction in hull losses).

2.1.1   Organisations that provide Aviation Accident Data Statistics

Accident data have been reviewed from the United Kingdom (UK) Civil Aviation Authority (CAA), the United States (US) National Transportation Safety Board (NTSB) and the Aviation Safety Network (ASN). The CAA has responsibility for [18]:

- Ensuring that UK civil aviation standards are set and achieved. Regulating airlines, airports and National Air Traffic Services economic activities and encouraging a diverse and competitive industry.

- Managing the UK's principal travel protection scheme.

- Bringing civil and military interests together to ensure that the airspace needs of all users are met as equitably as possible.

The NTSB is a United States Federal Agency mandated to [19]:

- Investigate transportation accidents and determine the probable causes of the accidents.

- Issue safety recommendations.

- Study transportation safety issues.

- Evaluate the safety effectiveness of government agencies involved in transportation.

The ASN is a private independent initiative founded in 1996 and charges itself with 'Providing everyone with a (professional) interest in aviation with up-to-date, complete and reliable authoritative information on airliner accidents and safety issues' [20].

A number of individual data sources have been consulted from the organisations described above. Each of these publications is discussed in the following Sections.

2.1.2 Global Fatal Accident Data Statistics: CAP 681

The CAA produces Civil Aviation Publications or CAPs on a variety of topics including global fatal accidents. CAP 681 is the most up-to-date version of the publication containing this information [21]. It provides a summary analysis of 621 global fatal accidents to jet and turboprop aircraft with a Maximum Take Off Weight (MTOW) above 5,700kg between 1980 and 1996 inclusive.

The assessment of each accident consists of three main parts:

- Causal Factors: an event or item judged to be directly instrumental in the causal chain of events leading to the accident.

- Circumstantial Factors: an event or item judged not to be directly in the causal chain of events but could have contributed to the accident.

- Consequences: a record of the outcomes of the fatal accident.

The two most frequently identified primary causal factors of the 589 fatal accidents that were judged to have sufficient information available were:

1. Lack of positional awareness in air (20.9%). This generally involved a lack of appreciation of proximity to the ground, frequently when the aircraft was not equipped with a Ground Proximity Warning System (GPWS) or when precision approach aids were not available. This primary causal factor has shown an increasing trend over the period considered.

2. Omission of action / inappropriate action (19.7%). This causal factor commonly referred to the crew continuing their descent below the Decision Height or Minimum Descent Altitude[2] without a visual reference or when visual cues were lost. This primary causal factor has shown a decreasing trend over the period considered.

The analysis method used in Ref. [21] meant that an accident could be allocated more than one causal factor. When all causal factors are analysed (i.e. not just the primary causal factor), the 2 most frequently attributed causal factors to the same 589 accidents were still:

1. Lack of positional awareness in air (41.4%).

2. Omission of action / inappropriate action (36.7%).

The 2 most frequently identified circumstantial factors were:

1. Non-fitment of presently available safety equipment (39.8%). This referred in most cases to the lack of GPWS or enhanced GPWS being fitted to the aircraft (even if it was not available at the time).

---

[2] For an approach to a runway, a height is reached where the pilot must transition from instrument to visual flight. If insufficient visual cues cannot be acquired at this height, the landing must be aborted. For a precision approach (vertical guidance provided to pilot via e.g. ILS), this height is termed the Decision Height. For a non-precision approach (no vertical guidance is provided), this height is termed the Minimum Descent Altitude.

2. Failure in CRM (37.7 %). This relates to whether, if the crew had worked more effectively together, the accident could have been avoided.

The 2 most frequently identified consequences were:

1. Collision with terrain / water / obstacle (46.5%).

2. Controlled Flight Into Terrain (CFIT, 35.3%).

Fig. 7.3 from Ref. [21] is recreated as Fig. 2-1. It shows an analysis of fatal accidents by phase of flight. Of the 621 aircraft accidents, 310 (50%) occurred during approach and landing phases (including go-around). A further 23% of all fatal accidents occurred during the take-off and climb.
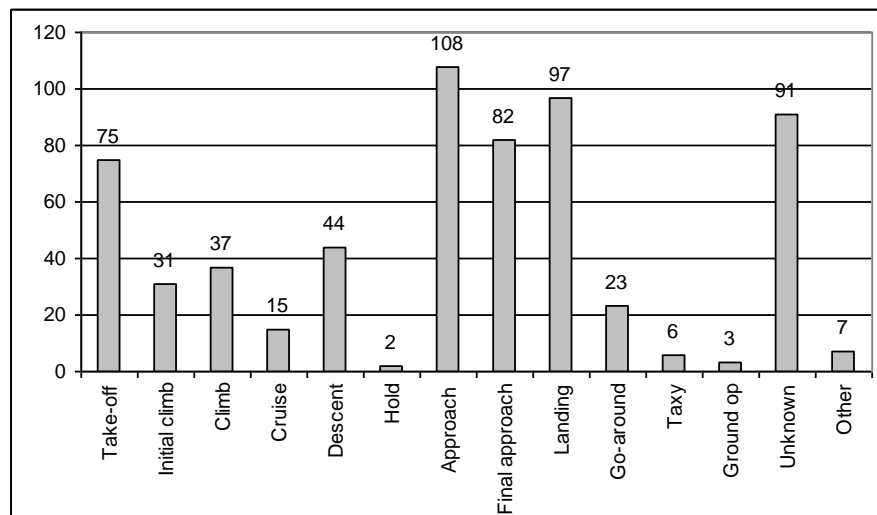

Fig. 2-1. Global fatal accidents broken down by phase of flight

2.1.3 Global Fatal Accident Data Update: CAP 701

Ref. [22] provides a review of UK civil aviation safety between 1990 and 1999. It differs from Ref. [21] in that as well as providing a worldwide accident analysis, it provides analysis of non-fatal accidents and also divides this analysis between aircraft types. It does not, however, provide analysis on causal factors, circumstantial factors and consequences by UK aircraft mission type. The pertinent points from the fatal accident statistics are summarised in the Section below.

Ref. [22] provides an additional three 3 years worth of aircraft accident data to that of Ref. [21]. The two most frequently identified fatal accident primary causal factors for Large Jet and Turboprop fatal accidents are:

1. Lack of positional awareness in air.

2. Omission of action / inappropriate action.

The 3 other major primary causal factors are given as: 'Flight Handling', 'Pressonitis' (i.e. the decision to continue in order to reach the destination when conditions are deteriorating and a decision to turn back/divert should have been made) and 'Poor professional judgement / airmanship'.

The two most commonly identified fatal accident circumstantial factors are given as:

1. Failure in CRM.

2. Non-fitment of presently available safety equipment.

The two most commonly identified fatal accident consequences are given as:

1. Collision with terrain / water / obstacle.

2. CFIT.

Ref. [22] also provides the five most prevalent primary causal factor–consequence combinations. These are:

1. Lack of positional awareness in air – CFIT.

2. Flight handling – collision with terrain / water / obstacle.

3. Omission of action / inappropriate action – collision with terrain.

4. Omission of action / inappropriate action – CFIT.

5. Flight handling – loss of control in flight.

2.1.4 NTSB Accident Statistics 1983 – 1999

The NTSB issues annual reviews of US air carrier (operators that fly aircraft in revenue service) aircraft accident data such as that provided at Ref. [23]. The NTSB also provides the raw accident data in a convenient spreadsheet form from 1983 to 1999 [24]. It is these data that have been used to provide the analysis detailed in this Section. It is recognised that, in some cases, these data form a subset of those provided in Ref. [21]. However, the provision of raw data has allowed a wider variety of analyses to be performed to provide more insight than that available from the CAA data alone.

All of the analysis presented is for operations under Title 14, Parts 121 and 135 of the Code of Federal Regulations (CFR). Broadly speaking, Part 121 refers to major airlines and cargo carriers whilst Part 135 applies to commercial operators referred to as commuter airlines and air taxi services (note - a change in the definitions of these regulations in 1997, however, now means that most commuter airlines operate under Part 121 of the CFR).

2.1.4.1 Fatal Accident Review by Phase of Flight

Fig. 2-2 presents a breakdown of fatal accidents of Turbofan, Turbojet, Turboprop and Turboshaft US Air Carrier Aircraft by phase of flight (where it is reported). As such, it provides some means of comparison
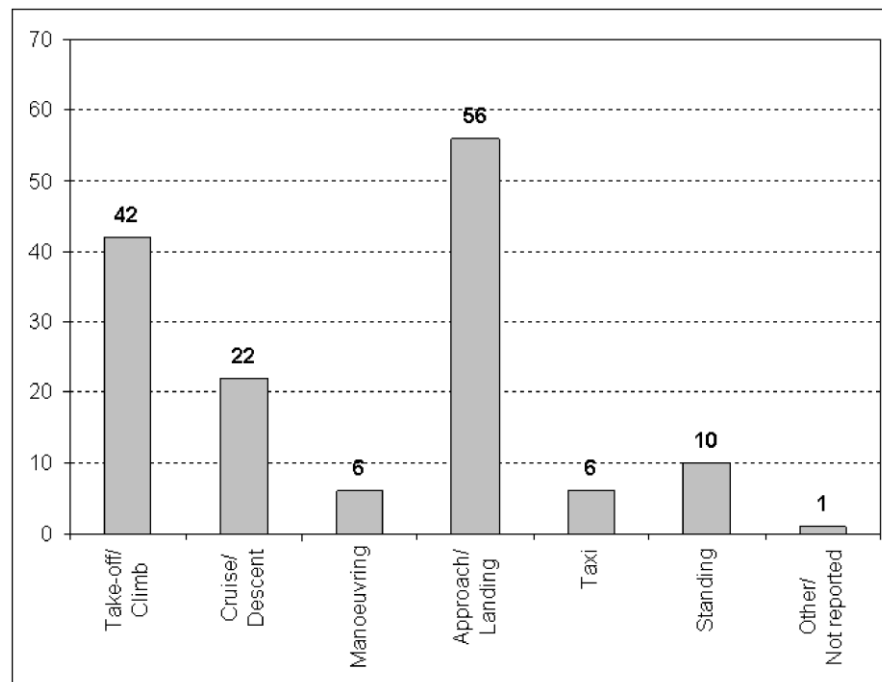

Fig. 2-2 - **Air Carrier Fatal Accidents by Phase of Flight 1983 – 1999**

with Fig. 2-1. Fig. 2-2 shows that of all 143 aircraft accidents, 56 (39.2%) occurred during approach and landing phases. A further 29.4% of all fatal accidents occurred during the take-off and climb.

2.1.4.2 Fatal Accident Review By Phase of Flight and Weather Condition

Fig. 2-3 presents a further breakdown of the data presented in Section 2.1.4.1 as a function of general weather condition (Visual Meteorological Conditions (VMC) and Instrument Meteorological Conditions (IMC) have strict definitions but generally speaking, IMC weather represents a degraded visual situation when compared to VMC). Where the visual conditions were unknown, they are recorded as such (UNK).
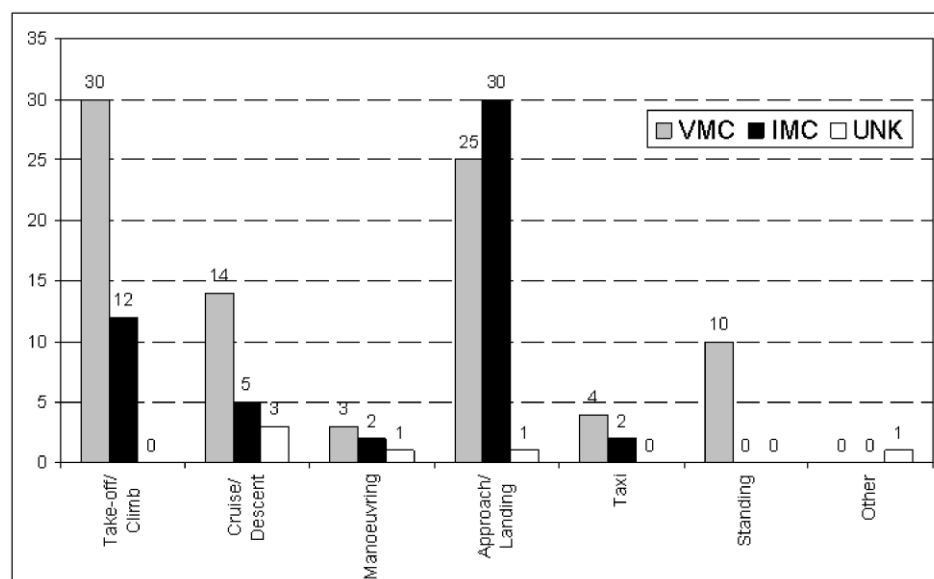

Fig. 2-3. US Air Carrier Fatal Accidents by Phase of Flight and Weather Condition 1983 - 1999

It can be seen from Fig. 2-3 that for the two phases of flight where accidents are most prevalent (Approach/Landing and Take-Off Climb):

- More fatal accidents occur on Approach and Landing in IMC than in VMC

- A significant number of additional accidents occur on Take-Off/Climb in VMC when compared to IMC.

2.1.4.3 Fatal Accident Review By Phase of Flight and Weather Condition

Table 2-1 presents a breakdown of accident first occurrence for fatal accidents of Turbofan, Turbojet, Turboprop and Turboshaft US Air Carrier Aircraft in varying weather conditions.

First Occurrence	Basic Weather Conditions			
	IMC	VMC	UNK	Grand Total
Loss Of Control - In Flight	18	24	1	43
In Flight Collision With Terrain/Water	10	7	2	19
Airframe/Component/System Failure/Malfunction	2	13		15
In Flight Encounter With Weather	10	4		14
On Ground/Water Collision With Object	4	7		11
In Flight Collision With Object	3	3	1	7
Miscellaneous/Other	1	5		6
Propeller/Rotor Contact To Person		4		4
Midair Collision		3		3
Altitude Deviation, Uncontrolled		1	1	2
Collision Between Aircraft (Other Than Midair)		2		2
Loss Of Control - On Ground/Water	2			2
Loss Of Engine Power(Partial) - Mech Failure/Malf		2		2
Loss Of Engine Power(Total) - Mech Failure/Malf		2		2
Loss Of Engine Power(Total) - Nonmechanical		2		2
Abrupt Manoeuvre		1		1
Cargo Shift	1			1
Explosion		1		1
Fire		1		1
Loss Of Engine Power		1		1
Missing Aircraft			1	1
On Ground/Water Encounter With Weather		1		1
Propeller Failure/Malfunction		1		1
Undetermined		1		1
Vortex Turbulence Encountered		1		1
Grand Total	51	87	6	144

Table 2-1. US Air Carrier Fatal Accidents by First Occurrences per Phase of Flight and Weather Condition 1983 – 1999

Table 2-1 shows that of all 144 aircraft accidents with a first occurrence listed, 43 (29.9%) were 'Loss of Control – In Flight'. A further 13.2% of first occurrences were 'In Flight Collision with Water/Terrain'.

Other major first occurrence data of interest to the research are 'In Flight Encounter with Weather' (9.7%) and 'On Ground/Water Collision with Object' (7.6%).

Further observations can be made from the IMC data:

- 'Loss of Control in Flight' happened most frequently during the 'Approach/Landing' and the 'Take-off/Climb' phases of flight.

- 'In-flight Collision with Terrain/Water' exclusively occurred during the 'Approach/Landing' phase of flight.

- 'In-flight Encounter with Weather' most often happened during the 'Approach/Landing' and 'Cruise/Descent' phases of flight.

Additional observations can be made from the VMC data:

- 'Loss of Control in Flight' happened most frequently during the 'Approach/Landing' and the 'Take-off/Climb' phases of flight.

- 'In-flight Collision with Terrain/Water' occurred most frequently during the 'Approach/Landing' phase of flight but also during the 'Take-off/Climb', 'Cruise/Descent' and 'Manoeuvring/Hovering' phases of flight.

- 'In-flight Encounter with Weather' most often happened during the 'Approach/Landing' and 'Cruise/Descent' phases of flight.

- 'On Ground Collision with Object' occurred during all phases of flight except 'Cruise/Climb' and 'Manoeuvring/Hovering' (by definition).

- 'Airframe/Component/System Failure/Malfunction' occurs as a high proportion of VMC first occurrence fatal accidents.

2.1.5　Aviation Safety Network Statistics

The ASN issues an annual summary of fatal accident statistics for multi-engine airliners taken from official sources, including NTSB. The latest of
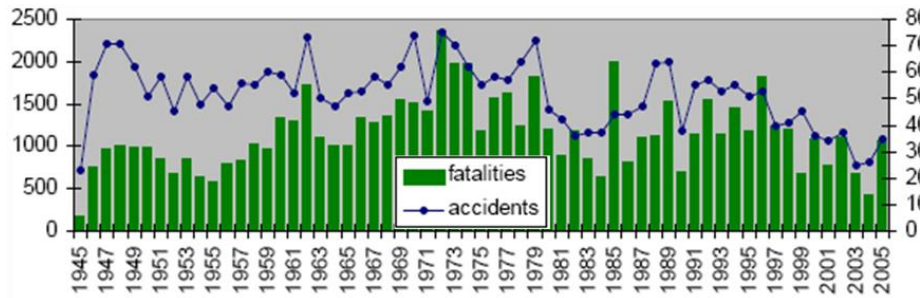

Fig. 2-4. Historical aviation accident statistics

these is Ref. [25]. Fig. 2-4, taken and adapted from this reference, shows the number of individual accidents and consequent fatalities that resulted over the last 60 years from 1945. In general, since the mid 1990's, there has been an overall decreasing trend in both accidents and fatalities, with 2005 being an unfortunate exception. This trend is reflected by aircraft driven by all forms of propulsion in Fig. 2-5 (also taken from Ref. [25]).
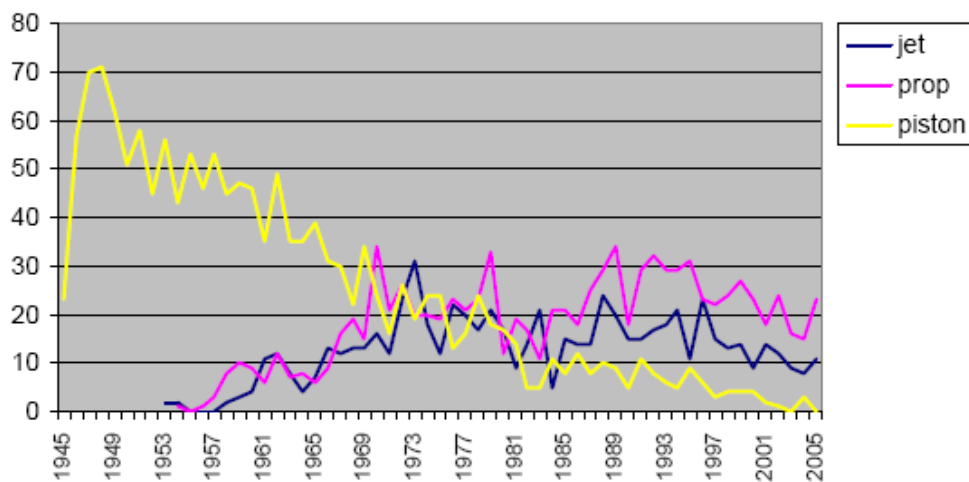

Fig. 2-5. Fatal airliner accidents by propulsion type

2.1.6　Accident Statistics Discussion

The purpose of the technical review is to identify the current state-of-the-art and any gaps in the knowledge in the area of interest. It is difficult to reconcile aviation statistics with this intention but it is clear from the

review conducted that the 'state-of-the-art' technology used to conduct aircraft transport operations has reduced the overall number of accidents from that observed in the 1940's, '50's and '60's. However, the number of accidents and consequent fatalities cannot be considered insignificant and more work must be done to continue to reduce both sets of figures. The following Sections identify the 'gaps' that the review has identified in terms of where to focus these efforts.

2.1.6.1 Causal Factors

Refs. [21, 22] show that if a visual aid could be developed to recreate pilot visual cues to indicate the aircraft's proximity to the ground or to a Decision Height or Minimum Descent Altitude, then a large proportion of fatal accidents could potentially be avoided. In addition, if the same display could recreate cues to generally increase pilot positional awareness, increase 'visibility' of the outside world in degraded visual conditions and provide a substitute for current ground aids, then the fatal accident rate could be further reduced.

The data from Ref. [24] suggests that if a display were developed that could:

- prevent loss of control in flight (by increasing situational awareness);

- prevent in-flight collision with terrain/water (by increasing the pilot's awareness of the aircraft's proximity to it);

- increase the safety of flight when adverse weather conditions are encountered and

- prevent on-ground collisions with objects (by providing the pilot with information about conflicting locations of those objects)

then a high proportion of fatal accidents could be avoided.

2.1.6.2 Phase of Flight

Fig. 2-1 and Fig. 2-2 show broad agreement in that the majority of fatal accidents occur during or shortly after take-off (including initial climb and climb) or during approach and landing. Approach and landing is cited as a key safety priority area in Ref. [26].

Fig. 2-3 provides an interesting statistic. It shows that a high number of fatal accidents occur in VMC during the take-off and landing phases of flight. Table 2-1 shows that some of these are attributable to mechanical failure (which it is unlikely that a visual aid could prevent). However, it shows that loss of control and in-flight collisions also have a high incidence. The original project concept was to develop guidelines for displays for use in degraded visual conditions to try to help prevent such accidents. Fig. 2-3 shows that, for the approach and landing phase of flight at least, such displays will also be important in good visual conditions.

2.2   Review of Civil Pilot Guidance Display Technology

The pilot of a modern civil transport aircraft has a significant number of systems at his/her disposal that provide guidance information. Despite this technology, the statistics show that accidents continue to occur. There is still, therefore, a need to reduce or eliminate such occurrences. One way to do this is to improve upon existing pilot display formats. To avoid 're-inventing the wheel', it is useful to consider both the state-of-the-art guidance display technology available in the airline transport industry today, how this state has come to be and the displays that are already being explored for the future. Relatively up-to-date treatments of modern aircraft display technology can be found in Refs. [27] and [28] and these have been the primary sources of information for the discussion that follows.

2.2.1   Context of and Terminology Associated With Display Systems

2.2.1.1 Navigation, Guidance and Stabilisation

Before starting the discussion on guidance technology, the term 'guidance' needs to be defined. Classically, there are three tasks that a pilot must carry out during a flight: navigation, guidance and stabilisation [29]. The navigation task deals with the pilot knowing the current and next desired position of the aircraft with respect to the Earth's surface, with timescales measured in minutes and distances measured in miles. Stabilisation of the aircraft, at the other extreme, involves the continuous correction of small localised errors in the desired flight path or aircraft attitude induced by, for example, atmospheric disturbances. Much of this task is automated for large transport operations but will still be required for example, during a manual approach and landing in gusty conditions. The stabilisation task involves timescales of the order of a second and rotations of a few degrees. The guidance task falls between the stabilisation task and navigation task in terms of both the timescales and spatial measures with which the pilot is concerned. It deals with, for example, the avoidance of obstacles when close to or on the ground and involves timescales of several seconds and distances of several hundreds of feet [30]. It is the aircraft guidance function for which this research project has sought to develop guidelines for novel vision aid formats.

2.2.1.2 The Future Use of the Airspace System

The pilot of a jet transport aircraft will have to navigate, guide and stabilise the aircraft in a managed airspace system that dates from the 1950's. It is defined by a series of ground-based radio-navigation beacons that link up a set of fixed routes called airways. Aircraft are vectored along these routes and around airports by air traffic control (ATC) who are mandated to ensure that legal vertical and lateral separation of the aircraft is maintained.

Aircraft operators are therefore forced to fly fixed routes, often at fixed speeds at a number of pre-determined altitudes or flight levels [2].

The use of airspace is beginning to change and further changes are planned. So-called RNAV operations (Required Area Navigation) are slowly being introduced to current air traffic systems but their utilisation is not yet widespread or optimal. These allow aircraft to fly more efficient trajectories point to point. This is only the beginning. Programs such as those defined at Ref. [3] have been initiated to try to modernise air transport operations, making them more efficient whilst reducing the environmental impact of existing aircraft e.g. by reducing/removing inefficient level flight segments with flaps and gear deployed. GPS will be a key enabler to allow the required increased accuracy trajectories that these programs will demand to be flown using a wider variety of aircraft platforms (e.g. tilt-rotor aircraft).

Satellite-based navigation systems will make the transformation of airspace usage possible. The people that will have to interpret and act upon the information that the technology provides are the aircrew. Their ability to use the new systems and procedures put in place will be determined largely by the way that information is presented to them and their ability to assimilate it. Problems already exist. For current jet transport operations, pilots no longer fly by the 'seat-of-the-pants' but are 'system information monitors' [4]. The pilot's task is to monitor the actions of the automation, ready to intervene and take control if a system failure occurs. The extensive use of automation has led to concerns that:

- whilst manual workload has decreased, mental workload has increased [5, 6];

- human beings do not perform at all well in monitoring task situations [7];

- removal of the crew from the control loop of the aircraft reduces their ability to maintain an awareness of the aircraft's situation [8];

- flight-deck technology has become so complex that it is difficult for flight crew to understand the principles on which the automation is operating [9] and ;

- the proficiency of pilots to perform flight tasks manually has been steadily reduced [7].

This situation is unlikely to improve. The technology already exists to allow on-board aircraft computers to negotiate with air-traffic management computers to move through the new airspace system [2]. This will further distance the pilot from the operational environment.

2.2.1.3 Enhanced/Synthetic Vision Systems

Two terms in common use with reference to display systems are Enhanced and Synthetic Vision System (EVS and SVS respectively). An EVS and SVS are two different approaches to providing the pilot with a view of the outside world when the environmental conditions surrounding the aircraft prevent an adequate view from being obtained through the cockpit windscreen.

An EVS provides the pilot with a 'real' view of the world obtained from on-board sensors that use parts of the electro-magnetic spectrum other than the visual range. Forward-looking infra-red (FLIR) or millimetre range sensors are utilised to 'see through' degraded visual conditions (fog, dark etc.).

Fig. 2-6 – Example Enhanced Vision System Image

The output of these sensors is processed into an 'image' that

would be what the pilot could see if human eyes were sensitive to that band of EM radiation. Fig. 2-6, taken from Ref. [31] shows a typical EVS image. It can be seen that symbology can be overlaid onto such systems to provide additional flight information to the pilot. EVS can be presented on conventional PFD and on HUD installations.

Although undoubtedly improving the pilot's vision, EVS do suffer from some issues, including: 1) relatively narrow field of view (FOV). The full view that would be available from the cockpit window cannot be re-created by the sensor; 2) reduced contrast sensitivity which can lead to earth-sky blending and the appearance of 'false-horizons'; 3) reduced visual acuity leading to impairment of the visibility of manmade structures and altered monocular depth perception and 4) lack of registration with the pilots line of sight due to the sensor location on the aircraft [32].

A SVS, rather than providing a sensed image, provides the pilot with a software-generated view of the outside world as it would appear in good
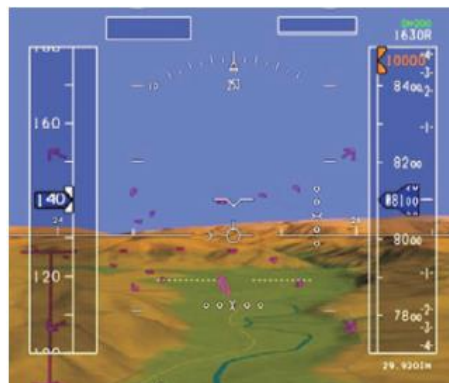
visual conditions. An example of such an image is shown in Fig. 2-7 (also from Ref. [31]). The image is computed from on-board global terrain and obstacle databases based upon an estimation of the aircraft's

Fig. 2-7 - Example Synthetic Vision System Image current position and attitude from Global Positioning System (GPS) and Inertial Navigation System (INS) data feeds. The success of such a system relies upon the accuracy of data sources which it uses. The resolution of the terrain database, the level of detail provided by the obstacle database and the accuracy of the estimation of current position will all determine how well the software

generated view of the outside world correlates with what the pilot would see if the view from the cockpit window was not obscured.

It is one thing to provide the pilot with an enhanced or reconstructed view of the outside world, but these do not necessarily provide any extra direct guidance to the pilot over and above those that he would receive from a view of the outside world. In order to receive extra guidance, additional symbology would need to be overlaid onto the displays (as shown in Fig. 2-7). The research reported in this thesis deals specifically with the symbology sets and logic used to drive them that may well end up being overlaid on an SVS or EVS.

2.2.1.4 Situational Awareness

In many situations in flight, but primarily in degraded visual conditions, there are occasions when the view from the cockpit window does not provide the pilot with the necessary information to conduct a flight. In this case, the pilot must rely on the aircraft instrumentation to provide information to construct a mental model of the outside world and the aircraft's relationship to it. The pilot's appreciation of the aircraft's orientation, the state of its systems, the en-route weather, its navigational position etc. can all be termed as his/her situational awareness (SA). More formally, it is defined as a pilot's 'perception of the elements in the [aviation] environment within a volume of time and space, the comprehension of their meaning, and the projection of their status in the near future' [28]. It can be seen from this definition that an effective guidance system, particularly one with a predictive capability, must contribute to the pilot's SA.

2.2.1.5 Prospective Guidance

The term 'prospective' features in the title of this thesis. This term relates to the supposition for that any observer under motion, guiding themselves

successfully through the environment to some target destination (e.g. a bird landing on a branch of a tree) , will not generally be reacting to the situation that instantaneously presents itself, but will be modifying their motion with reference to some future point in time. This modification will be based upon the identification of obstacles that lie in the path of the future trajectory and the urgency will be based upon the time to any collision that would occur if no changes were made.

2.2.2   Historical Development of Pilot Guidance Technology

2.2.2.1 Head-Down Displays

For as long as there has been powered flight there have been instruments to give the pilot extra information to assist with the flight task: contemporary film footage shows that the Wright Brothers used a piece of cloth tied between the landing skids of their aircraft. If it streamed approximately parallel to the skids, then any turn that they were in was safe; the Bleriot monoplane had a rev-counter added to it to give an indication of engine speed. Much of the development in early aviation, however, was necessarily devoted to aerodynamic and structural considerations. Even in 1927 when Lindbergh crossed the Atlantic in a Ryan monoplane, the majority of the instruments provided the pilot with the state of the aircraft e.g. airspeed and altitude and its all important engine parameters e.g. fuel pressure and engine RPM. The only 'guidance' information available to the pilot was a compass and turn and slip indicator. It is arguably not until 1929 that the first true guidance system was successfully tested by Lt. James Doolittle. Lt. Doolittle's aircraft (a Consolidated NY-2 single-engine biplane) was modified with a Hood such that the pilot could not see the horizon or the ground. A radio guidance system was used, in conjunction with aircraft instruments that even today's pilot would recognise (including a gyroscopic artificial horizon and a vertical speed

indicator), to successfully fly a circuit around the airfield and land safely with recourse only to the instrumentation [27].

As air travel became more routine, the need to rationalise and standardise flight deck instrumentation was recognised. This led to the 'basic 6'
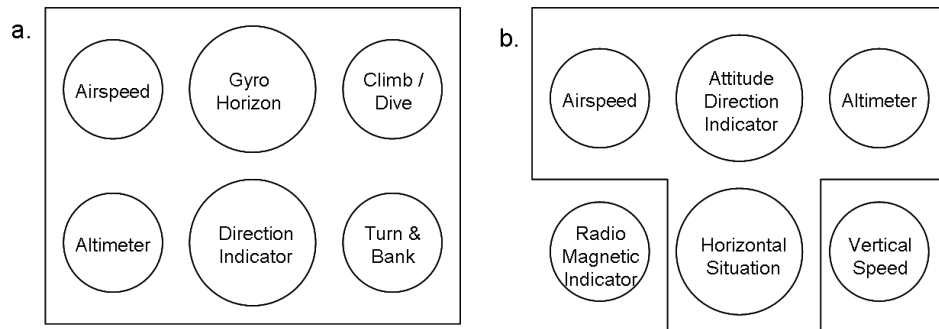

Fig. 2-8. Development of the Instrument Panel: a. 'Basic 6' and b. 'Basic T' Configurations

configuration of electromechanical instruments and then the 'basic T' configuration that can still be found in some aircraft today. These configurations are shown in Fig. 2-8 (adapted from Ref. [27]). Formats and procedures were developed that made displays easier to follow and check (e.g. how pointers should move and flags be displayed). For instance, the Horizontal Situation Indicator (HSI) was developed to combine the function of three of the 'basic 6' instruments into one (gyroscopic and magnetic compass, radio magnetic indicator and distance measuring indicator). This process of rationalisation, however, led to increasingly complex mechanisms with their associated maintenance costs. Under ever increasing financial pressure, the aviation transport industry has, over the last two decades, been upgrading flight decks to solid-state or the so-called 'glass' cockpit format.

Modern transport aircraft are now fitted with 'glass-cockpits' to provide the pilot with flight information. That is, flight data are displayed using software-generated displays using cathode ray tube (CRT) technology. Although cockpit designers are free to choose any symbols for a given

display, at present, the software-generated instruments, in many cases, are similar to the analogue devices that they replace [10]. This is particularly true when 'glass' instruments are retro-fitted into aircraft and must fit into the same space in the panel where their mechanical counterparts were housed. Replication is considered to be advantageous in reducing the need for flight crew re-training.

Typically, there are two CRT displays per flight crew member mounted side-by-side: a Primary Flight Display (PFD) and a Navigation Display (ND). A typical layout is shown in Fig. 2-9.
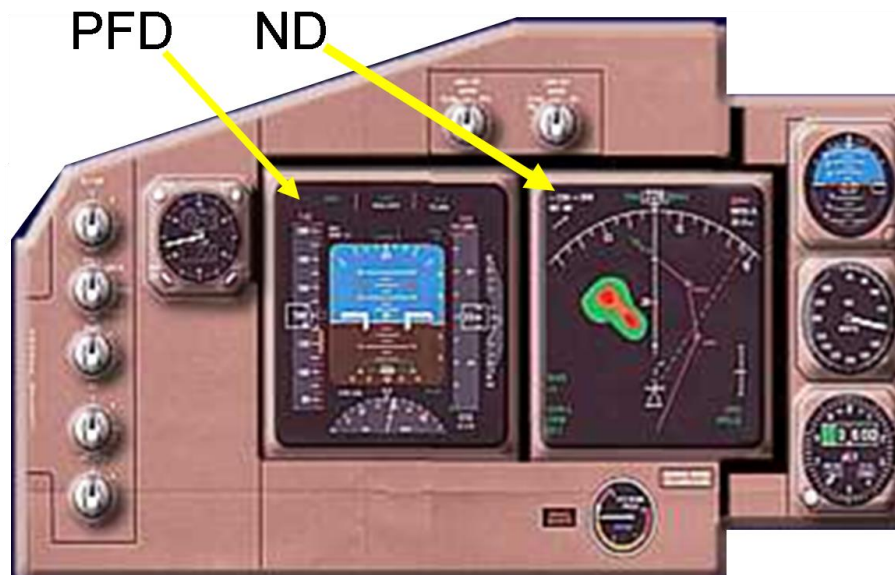
Fig. 2-9. Illustration of dual CRT layout in jet transport cockpit

The PFD typically provides the following information to assist guidance and stabilisation:

- aircraft attitude information;

- speed and altitude information (including trends for projected speed at current power setting in 10 seconds);

- flight path deviations obtained from, for example, an Instrument Landing System (ILS);

- flight director command bars;

- lateral acceleration;

- a flight path vector (FPV, shows the aircraft horizontal and vertical flight path angles) and

- a flight path target (the desired aircraft horizontal and vertical flight path angles).

The ND provides the pilot with either a plan view of the aircraft position with respect to the planned track or an electronic version of the Horizontal Situation Indicator (HSI). Due to their positions in the cockpit, the PFD and ND are sometimes referred to as Head-Down Displays (HDD).

2.2.2.2 Head-Up Displays

Although in use with the UK military since 1961, it is only in the last decade that Head-Up Displays (HUDs) have appeared on the flight decks of civil transport aircraft [33]. The HUD derives its name from the fact that flight information is displayed using a

Fig. 2-10. Head-Up Display Combiner

glass 'combiner' (see Fig. 2-10) that sits between the pilot and the outside world. Key features of such a display image are (1) some symbology can be conformal and (2) it is displayed at infinity or is collimated. A conformal display element is one where angles are preserved between the display and the outside world. For example, the FPV on a HUD shows the pilot where the aircraft is heading in real world space. So, by placing and maintaining the FPV on the touchdown markers of a runway, the pilot can

ensure that a steady approach will be achieved. Providing images at infinity means that the pilot can maintain his view out of the cockpit window and does not have to continually refocus on the instruments on either the HDD or HUD. This is advantageous in poor visibility on the approach when the flight crew needs to maintain station on defined vertical and lateral descent profiles and, with only tens of feet to touchdown, look for visual cues to allow them to land within legal requirements.

A number of manufacturers produce HUDs for civil aircraft. One example is the BAE Systems 2020 Visual Guidance System (VGS) [34]. The VGS provides all of the usual flight information in a standard conformal format. Its 'look and feel' is based upon HDD symbology. In addition, the VGS is capable of providing the pilot with:

- a clear touchdown point, even at airfields where precision approach equipment does not exist;

- acceleration cues to assist with total energy management;

- a guidance cue to assist with making precise corrections to flight path, the flare and ground roll-out;

- precision take-off guidance in the form of runway centre-line cueing and

- a mode to provide cues to support recovery from unusual attitudes.

The VGS was designated the current 'state-of-the-art' for this research project. It was used as a baseline against which novel displays developed during the course of the project were tested and compared.

2.2.3   Key Guidance Display Symbology in Use Today

There are a number of key symbols/displays that are used to provide flight guidance to the pilot on a modern PFD and/or ND. These are described in the following Section. The first three guidance solutions are essentially

electronic versions of the electro-mechanical devices that they replaced. The remaining guidance solutions are software-based systems and would have been difficult, if not impossible to develop mechanically. These solutions incorporate an element of prediction of where the aircraft will be in the future. These displays are termed 4-D (i.e. four dimensional: three spatial dimensions plus time).   They allow the pilot to monitor the aircraft's predicted position against some desired position and modify the aircraft trajectory accordingly.

2.2.3.1 Flight Director

Flight directors (FDs) come in a variety of forms which mimic their electro-mechanical predecessors. A common form is shown in Fig. 2-11
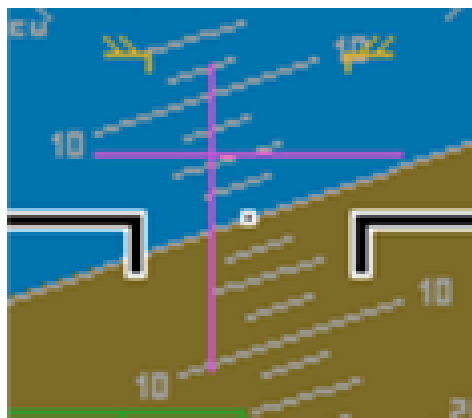

Fig. 2-11. Typical Flight Director Symbology

(the magenta lines). The FD symbol is superimposed upon the Attitude Direction Indicator (ADI). The horizontal line moves up and down to command pitch angle. The vertical line moves left and right to command roll. The pilot must match the motion of the FD symbols with that of

the aircraft symbol (the white dot). The command signals are generated by information coming from, e.g. the aircraft navigation systems. In the example given in Fig. 2-11, the FD is commanding a pitch up and roll to the left. Although the FD makes use of navigation aid technology, it is considered a guidance aid as the manoeuvres commanded will take place over periods of time and distances consistent with the definition of Section 2.2.1.1. Furthermore, the FD does not blindly command a bank angle, but (via the control law driving it) will react and modify its command signals in response to the control inputs that the pilot makes.

The FD is not considered to be a final solution to the pilot guidance problem. Because the FD provides a *command* signal, the pilot is obliged to follow it. It reduces the pilot's role to that of a series of control surface actuators [35]. The pilot must focus his/her attention on the FD to reduce the lag between command and response. This, in turn, reduces the time available for scanning the other instruments. The pilot's ability to form a mental image of the aircraft's state and its environment must only be reduced.

2.2.3.2 Instrument Landing System Deviation Indicators

Glass cockpit ILS deviation indicators also tend to be facsimiles of their electro-mechanical counterparts. Lateral and vertical deviations from target localiser (alignment with runway centre-line) and glide slope (alignment with desired vertical flight path to runway) are shown respectively. The 'target' is indicated by the central bar of the display and
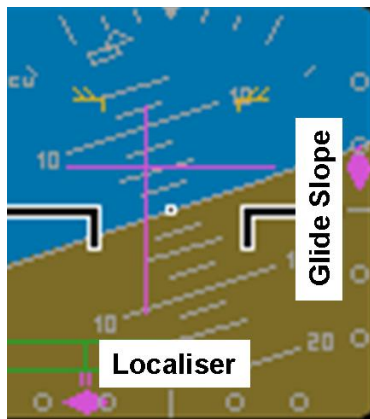

Fig. 2-12. Localiser and glide slope deviation indicator formats

a magenta arrow, diamond or, sometimes line, indicates the relative position of the localiser or glide slope to the aircraft. Typical display formats are shown in Fig. 2-12. In this example, the aircraft is shown low on the glide slope and to the right of the localiser (the target positions are the lines at the centre of the respective lines of dots). Unlike the FD, the ILS indicators only provide the aircrew with guidance information rather than direct commands. It is the responsibility of the pilot to manoeuvre the aircraft onto the localiser or glide slope as appropriate.

2.2.3.3 Non-Directional Radio Beacon/Automatic Direction Finder

Non-directional radio beacons (NDB) are one of the earliest forms of radio aid technology but can still be found in use today. NDBs are simple beacons that broadcast in all directions simultaneously. When the pilot

Fig. 2-13. ADF Indication to NDB

tunes into a particular NDB frequency on the aircraft's radio navigation systems, the Automatic Direction Finder (ADF) will indicate the direction from which the signal emanates. To fly directly to a beacon, the pilot has to simply turn the aircraft such that the NDB needle points 'straight ahead' (the 12 'o' clock position, as illustrated by the cyan needle in Fig. 2-13). The distinction between guidance and navigation here is perhaps a little blurred, but an NDB can be argued to be a guidance aid when used for non-precision approaches to an airfield. NDB indications are used to navigate to an airfield but will then be used as a guidance aid to align the aircraft with the runway in use.

Care must be taken when using NDB displays as they are subject to a number of potential reductions in accuracy, including:

- NDB needles will point towards thunderstorms and away from the selected radio beacon;

- interference from beacons transmitting on similar frequencies and from radio waves reflecting from the ionosphere, particularly at dusk and dawn and

- 'needle dip' where the direction needle moves towards the lower wing in a turn (caused by the NDB aerials on the aircraft taking finite time to resolve the incoming radio waves during the turn) [36].

The technology that drives the preceding displays, i.e. a world-wide network of radio and microwave beacons, originated in the 1950's. It is becoming increasingly expensive to maintain and, in an increasingly uncertain world, make secure from potential malicious tampering. There is therefore an impetus to use satellite-based information to drive guidance technologies. The remaining guidance displays make use of such information to provide aircraft position to the pilot in relation to its external environment.

2.2.3.4 Turn Prediction Display

The Turn Predictor display is the first of the 4-D displays to be described in this Section. It provides the pilot with a bird's-eye view of the aircraft and a line showing the aircraft's predicted trajectory in a turn. This is overlaid onto the ND with the planned aircraft track displayed. In this way, the pilot can adjust the trajectory by steering in to or out of the turn to line the predicted trajectory up with the desired ground track. An example of such a display is shown in Fig. 2-14.

Fig. 2-14. Example Turn-prediction Display

2.2.3.5 Vertical Situation Display

In order to relieve some of the mental burden of recreating the vertical aircraft situation in relation to surrounding terrain, Boeing have developed the
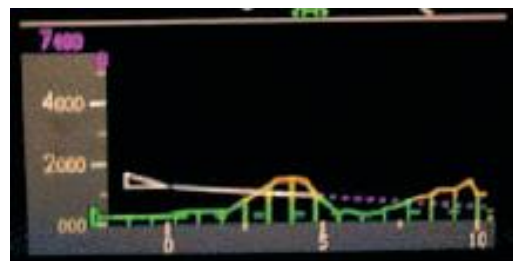

Fig. 2-15. Vertical Situation Display Showing Terrain Profile

Vertical Situation Display (VSD) [37]. The VSD depicts a side view of the local terrain and current aircraft flight path to the pilot as shown in Fig. 2-15 (from Ref. [37]). In this way, there is an early indication to the pilot of any conflict between aircraft flight path and local terrain. The VSD is a corollary in the vertical plane to the existing plan view representations of the aircraft position that is presented on a typical ND.

2.2.3.6 Electronic Flight Bag

The average pilot's flight bag contains, amongst other items, the airport diagrams, departure and approach plates and assorted charts that are required for the forthcoming flight(s). These create a burden on crew, airline and supplier in terms of storage, maintenance i.e. keeping charts up to date and additional weight that has to be carried on the aircraft.

The move to a digital form of these navigation aids is slowly starting to take place with the introduction of the Electronic Flight Bag (EFB) [38]. There are various types of EFB hardware and software that are currently available and these vary in permanence of installation on the aircraft and technical capability. The combination of Class 3 hardware (either a permanent stand-alone installation or part of a standard multi-function display avionics suite) with Type C software (software applications that allow the position of the aircraft to be overlaid onto the electronic document) provides the pilot with direct guidance information. Having the aircraft's position overlaid on, for instance, a precision approach plate will allow the pilot to guide the aircraft onto and then maintain the correct spatial position in order to intercept the appropriate radio aid for that approach (strictly speaking, this type of equipment has to be certificated and must not be used for navigation purposes).

2.2.3.7 Highways in the Sky

The use of perspective flight-path displays has been of interest to the research community since the 1950's [2]. It is only with the advent of modern computing, however, that these concepts have become a real possibility. The favoured concept is of a pre-planned route overlaid onto a representation of the out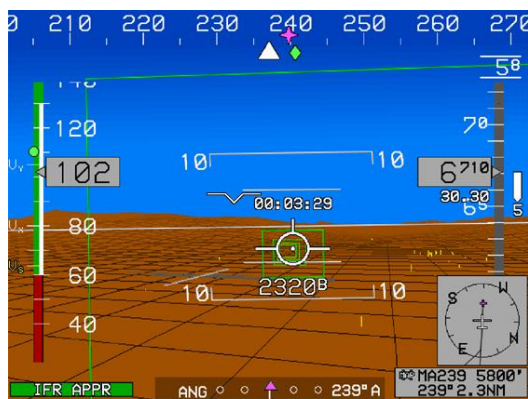side world. The pre-planned route generally takes the form of a perspective tunnel or highway in the sky (HITS) and a FPV or predictive FPV is overlaid onto this. The pilot's task is to maintain the FPV (and hence the aircraft) within the route prescribed by the tunnel. Fig. 2-16 shows an operational example of a HITS display

Fig. 2-16. Highway In The Sky Display

(courtesy Chelton Flight Systems).

Such a system is advantageous when compared to, for example, a FD because it provides a level of flight path performance as good as a FD (for the approach task) but provides all elements of a given flight situation (e.g. position, attitude and flight path angle) and allows the pilot to act on them accordingly [39]. In addition to this, the pilot can select their own strategy to intercept the defined track rather than slavishly following the rule-based FD command [2]. However, other research has shown that whilst flight path performance is improved with this form of display, global situation awareness is reduced [40].

In an attempt to reduce the high accident rates that occurred during the 1990's [41], the General Aviation (GA) community and FAA in Alaska have been the driving force behind the certification of HITS systems into operational aircraft via the 'Capstone' program. In order for these systems

to be used, special permission has had to be granted to deviate from existing FAA regulations in order for them to certificated [42]. Whilst the safety benefits are not in question, the reliability of the systems being implemented and the cost of re-equipping aircraft with the required technology have considerably slowed progress of the Capstone initiative [43, 44].

2.2.4 Emerging Advanced Guidance Technology

Section 2.2.3 provides a brief tour of the guidance display formats in use in today's glass cockpits. The development of such guidance technology/symbology continues today. This Section describes some of those technologies that are being actively researched but that have not yet made it on to a commercial aircraft flight-deck.

2.2.4.1 More Highways in the Sky

HITS have been a major contender for the next generation of pilot display for some time and, as discussed in Section 2.2.3.7, are now being used commercially. However, these solutions are displayed on HDDs. This means that the pilot still has to make a visual and mental adjustment to correlate display with the outside world when a look out of the cockpit window is required (this, of course, is less of a problem in IMC then VMC). The merits of HUD symbology have already been described and it therefore seems a logical next step to display the tunnel concept to pilots using a HUD. This has been done by Rockwell-Collins and is undergoing evaluation [45]. This display also incorporates a wire-frame mesh of the surrounding terrain. One of the criticisms of the display as tested was that the wire frame tunnel was difficult to see, particularly when overlaid with other information or when flying in bright sunshine.

The Capstone HITS already reported provides a FPV to assist the pilot in guiding the vehicle through the tunnel. There is an issue here in that the

FPV provides the pilot with information about where the aircraft is heading now, whilst tunnel elements ahead provide information about where the aircraft needs to be at some point in the future. To rectify this, there is research into providing some form of predictive FPV with longitudinal/lateral control system coordination algorithms such as that described in Refs.[46-48]. The benefits of such an arrangement are reported as being enhanced flight-path control performance and reduced pilot workload.

The HITS concepts described thus far, whether head-up or head-down, are restricted to line drawings to limit the amount of the outside view that is obscured. This limits any image to a two-dimensional representation of a three-dimensional world. In an attempt to address this issue, a stereoscopic HUD has been developed and integrated into a fixed-base flight simulator for research purposes [49]. This offers a number of claimed advantages such as: (1) improved perception of information in the outside view; (2) a de-cluttered display as information is spatially separated so is less likely to merge; (3) flight-path, terrain and obstacles can be seen in their spatial position and (4) new 3D symbology can be introduced to enhance spatial awareness and motion perception.

The question arises as to what would happen if a pilot were to find his/her aircraft outside of the tunnel, intentionally or otherwise ? If the tunnel were still visible from the display, then of course, the aircraft could be flown back into it. If it were not, a mechanism to enable the pilot to fly the aircraft back onto the desired track would be required. A number of methods have been proposed including arrows to indicate to the pilot the correct turn direction to recover the tunnel trajectory, deviation indicators (similar to current ILS indications) and a return tunnel that is automatically generated to guide the pilot back to the original highway tunnel. There is some evidence to suggest that the return tunnel concept is preferable [50]

but it is not clear what would happen in the case that the pilot flies out of the newly generated return tunnel (one could imagine a whole series of tunnels being required in this instance).

Whilst HITS is favoured for the next generation of guidance displays, research has been conducted along similar lines, but which is sufficiently different to be of worthy note. Ref. [51] reports on a comparison between perspective pavers (the desired track is displayed as a series of perspective rectangular paving blocks), a perspective tunnel i.e. HITS and conventional format symbology. All of these were displayed Head-Up. The pilot performance using pavers and tunnel displays was comparable and both were superior to that using the conventional format display.

2.2.4.2 Enhanced Vertical Guidance

Vertical guidance is provided on a limited number of (Boeing 737-700) aircraft using the VSD shown in Section 2.2.3.5. Whilst this display has been shown to be useful at increasing pilot situational awareness, it was less helpful at providin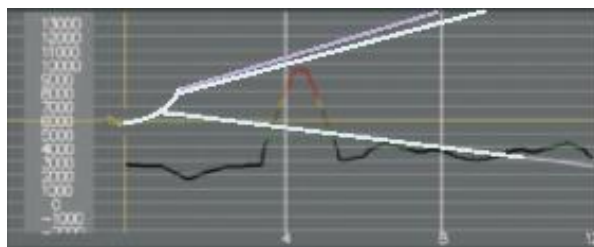g information relating to how the terrain was rising in relation to the current aircraft altitude [52]. Although it is clear from the VSD that terrain is rising ahead of the aircraft, it provides no

Fig. 2-17. Enhanced Vertical Guidance Display (courtesy TU Delft)

information on when a manoeuvre to initiate terrain avoidance should be commenced or indeed how aggressive that manoeuvre should be. These issues are starting to be addressed with investigations into enhanced vertical situation displays that provide the pilot with climbing and descending flight path indications based upon the performance limitations of the aircraft [31]. These limitations are shown as the white lines in front of the aircraft symbol in Fig. 2-17, taken from Ref. [31]. In this way, the

pilot is provided with an indication of whether or not the aircraft will be able to climb above or glide clear of terrain that lies ahead at any given moment.

2.2.4.3 Pursuit Guidance

An alternative guidance concept exists in the form of pursuit guidance and this can take various forms. Two display formats use a 2D line drawing of an aircraft to provide a 3D representation of an aircraft flying some distance ahead of the piloted aircraft. Military research has used this 'follow-me' aircraft symbol in conjunction with either a paver or HITS representation of the intended flight path [53, 54]. This display format has been shown to improve pilot performance with respect to maintenance of commanded airspeed, altitude and heading during instrument landing [55]. This increase has been shown to be independent of the external visibility conditions [53]. A similar pursuit aircraft/HITS concept has been used to conduct rotorcraft precision approaches and very precise approach profiles resulted with excellent situational awareness maintained throughout the manoeuvres.

Finally, the BAE Systems VGS uses a simpler pursuit concept for airfield approaches in that the flight director guidance simply represents an aircraft at a fixed distance ahead of the piloted vehicle. This format resulted in both increased flight path tracking performance and reduced pilot workload [56].

2.2.4.4 Abstract Concepts

The preceding discussion has concentrated on display concepts that portray a version of the world that bears some semblance to 'reality'. Another class of display technology exists at the other extreme. These attempt to provide the pilot with the same information using more abstract representations of the world and aircraft state. One of the most recent of
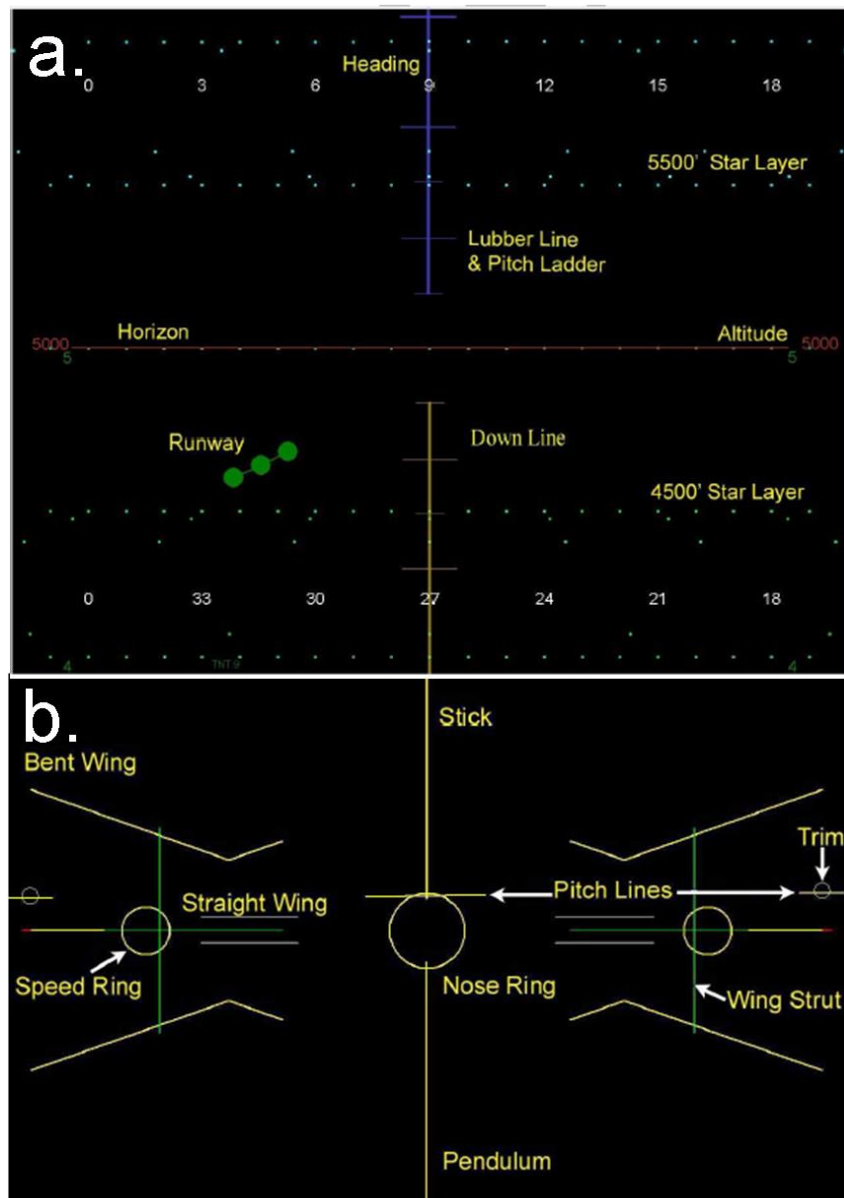

Fig. 2-18. Illustration of the Two 'Oz' Metaphors: (a) star-field and (b) aircraft

these is a display named 'OZ' [57] that uses two 'metaphors' to provide flight information to the pilot. A 'star field metaphor' provides aircraft attitude information and a sense of forward motion. An overlaid 'aircraft metaphor' provides aircraft configuration and flight envelope information. Both of the metaphors are illustrated in Fig. 2-18, taken from Ref. [58]. Use of this display with non-pilots has demonstrated improved flight performance (e.g. speed and trajectory control) compared with the same test subjects using conventional flight displays.

2.2.5 Discussion of Display Technology

The history of display development shows that instruments were added as pilots or engineers discovered a need for them. Even today, new flight deck technologies tend to follow a design process that is focused on component functionality and technical performance rather than pilot usage and operability [59]. Section 2.1 provides a safety-related perspective on why current display technology and design processes is needed Section 2.2.1.2 provides an operational imperative. The vision of airline operations highlighted here is one where more aircraft and more aircraft types are operating:

- more frequently;

- with fewer or no delays;

- in all weather conditions;

- using non-standard procedures (compared with those used today) and

- with an increased requirement for trajectory precision.

Clearly, the technology employed to assist pilots in the guidance of their aircraft using these procedures must be capable of coping with such a scenario.

The HITS concept offers one possible solution to this problem but a criticism of this format is that the display can quickly become cluttered. In addition, there is a danger that the tunnel will mask an important feature on either the real or synthetic terrain that it overlays.

It is argued that all of the technology discussed that is currently in use in this Section requires the pilot to interpret the spatial information being presented into a mental model of the aircraft state and its environment. The HITS and the pursuit guidance concepts have started to address this problem but these too retain shades of legacy symbology.

The question has to be asked, 'if pilot vision aid was to be designed making the most of visual perception mechanisms that have already evolved in nature, would any of the formats in use today be the result ?' The challenge for the display designer is to provide the pilot with information that can be interpreted as effortlessly as in the 'natural world'. The provision of an EVS or SVS might seem to be the answer but these display systems have their own issues. These include how to provide correct views of the outside world to more than one eye position (there are usually two crew members on a jet transport aircraft) and how to provide the correct binocular cues that a real outside world view would provide [60].

EVS and SVS systems and the associated equipment required to produce the images are also expensive. This is perhaps less of a problem for new aircraft where this expense can be built into the cost price but for maximum benefit, any display system would have to be retro-fitted to existing jet transports. The display formats developed within this research have therefore been kept simple partially as only simple concepts were being tested but also on the basis that this will provide a low(er) cost display system should any of the ideas be adopted.

To start to tackle the problems highlighted, the display designer must understand the processes that humans use to perceive and guide themselves through their environment. The perception of motion therefore forms the next review topic to define the current state-of-the-art for the 'knowledge space' in which the presented research resides.

2.3   Perception of Motion

The study and development of aircraft flight deck technologies displays must not ignore the end user i.e. the aircrew. The study of human behaviour and mental processes falls under the remit of the science of psychology. The meeting of psychology and aerospace engineering is generally referred to as the study of Human Factors. The following Section reviews those elements of psychology and human factors that are pertinent to the reported research.

2.3.4   Visual Perception in Psychology

2.3.4.1 Sensing our Environment

The world around us is made up of atoms, molecules and energy. Atoms and molecules can also be considered to be forms of energy. In order to be able to perceive and interact with its environment, an organism must be able to sense the various forms of energy that surround it that are important to its survival. The process by which an organism mentally acquires information about the world through the reception of it various forms of energy can be regarded as a working definition of *sensation* [61]. For humans, the sense/energy relationship is defined in Table 2-2. The research in this thesis is primarily concerned with vision so the

Sense	Type of Energy
Sight	Light
Hearing	Sound
Touch	Mechanical
Smell	Airborne Chemical
Taste	Chemical

Table 2-2. Human senses and their corresponding energy source

remainder of this Section will concentrate on the sensation and then perception of light energy.

49

The light energy received by a human observer, must first be converted by the appropriate structure in the body to allow interpretation by the brain. Specific receptor cells exist within the structures to convert or 'transduce' the received energy into electrochemical or 'neural' energy for processing by the brain. Transduction of light is carried out on the retina of the eye. The retina lies at the back of the eye-ball and contains special receptor cells that convert light into neural energy:

- Rods are able to react to very low levels of light and assist with peripheral vision.

- Cones respond to different wavelengths of light and are involved in the 'seeing' of colour. There are two opposing colour vision theories in existence but discussion of these is beyond the scope of this work.

These receptor cells contain chemicals that are broken apart when light makes contact with them. This reaction triggers further reactions that cause a neural signal to be sent to the visual cortex of the brain, the region of the brain responsible for analysing visual stimuli[3] [61].

2.3.4.2 Perceiving our Environment

The world that a human experiences through the sense of sight is more complex than the summation of the sensed energy. The pilot of an aircraft sees runways, signposts and other aircraft rather than photons of light. This process of organising, analysing and providing meaning to sensation is defined as perception [61].

2.3.5   Theories of Visual Perception

There are two main competing views of how the complex process of perception is accomplished [62]. These are:

---

[3]Stimulus: an event, situation or object that triggers a psychological response; a sensory experience.

- The Constructionist view states that perception relies upon previous knowledge and information to construct reality from fragments of sensation. Organisms do not passively receive stimuli but are actively processing and constructing the world around us.

- The Ecological viewpoint states that the environment provides all of the information required to perceive the world. Interpretation or construction of the world around us is rarely required when controlling motion.

The research contained within this thesis has been guided by the ecological approach to visual perception based upon results obtained at The University of Liverpool in Ref. [16]. The following Sections provide a review of both perception viewpoints and then a brief justification of the approach adopted.

2.3.6   Constructionist View of Visual Perception

The start point for the Constructionist theories of perception is the impoverished two-dimensional image that is formed on the retina. The eye, in this case, is sometimes likened to a camera, and the image on the retina is the resultant photograph. However, humans do not 'see' photographically i.e. in two dimensions where all objects are flat, they see in three dimensions. The Constructionist argument is therefore that some form of recovery of information must take place between the retina and the brain. The three-dimensional world has to be constructed from a two-dimensional image. Attempts to explain how this occurs have taken place over many centuries and by many researchers. Many of these have led to 'schools of thought' which sub-divide the Constructionist viewpoint.

2.3.6.1 Marr's Computational Theory

Computational vision theory stems from Information Theory (the quantification of information flowing through any system), Cybernetics

(the application of mathematics to systems that show self-regulation) and Digital Computing (which became a metaphor for the human brain) [63]. Developments in these fields led to the creation of the Artificial Intelligence (AI) research community. AI provides an engineering approach to the representation of organisms. Organisms are treated as machines that are controlled by processes. Some processes are perceptual and vision is one of these. Psychologists aim to understand visual processes by building computer models of them. Vision is seen as the process of forming a description of what is in the scene from the retinal images. The task of the visual system is to recover the causes of the scene from the images on the retina. Computational vision aims to specify mathematically how this is done and to assign a functional role to neural components involved in this computation.

2.3.6.2 Empiricism

Ref. [63] asserts that the dominant paradigm for perception research in the 20th century was empiricism. That is, perception is more than a direct registration of sensations; somehow, other events intervene between the stimulus and the observer's experience. To make sense of an image, sensory data has to be interpreted. This interpretation is carried out on the basis of stored knowledge acquired through learning.

In the earliest version of empiricism (Helmholtz), the visual system drew "unconscious inferences" about the visual image. General conclusions were drawn from these inferences. For example, if all the crows ever seen are black, then the conclusion can be drawn that "all crows are black". This is the same process as is used in the formation of scientific hypotheses.

In a later version of empiricism, Gregory takes the scientific argument further and argues that perception is a collection of hypotheses about the world. In the case of vision, light falls on the retina to trigger neural

energy signals. Appropriate knowledge interacts with these signals to create psychological information. This information is then used to advance hypotheses to both predict and make sense of the environment causing the light to impinge upon the retina in the first place.

2.3.6.3 Gestalt Theory

The Gestalt theory describes perception as a dynamic but organised process. It differs from the empiricist viewpoint in that no learning or hypothesising is required. The processing that is performed between retinal image and perception is considered innate to the organism. Gestalt Theory can be conveniently summarised into its laws of organisation:

(1) Proximity: One of the most important factors in perceiving a visual scene is the proximity of the elements within it. Items that are close to one another will be grouped together and associated with each other;

(2) Similarity: Objects in the visual scene that look similar will be grouped together;

(3) Common Fate: Elements of a visual scene that move together are grouped together e.g. a flock of birds are seen as belonging to the same 'object' in motion;

(4) Good Continuation: Perceptual organisation will tend to preserve smooth continuity rather than yielding abrupt changes;

(5) Closure: The perceptual process will favour an organisation that provides a 'closed' rather than an 'open' figure;

(6) Relative Size, Surroundedness, Orientation and Symmetry: For all other things being equal, the smaller of two areas will be seen as a figure against a larger background.

2.3.7 Ecological Theory of Visual Perception

The Ecological Theory of visual perception sits in stark contrast to the Constructionist view. Instead of an impoverished retinal image, Ecological Theory maintains that the information in the observer's field of vision, particularly when the observer moves, is rich. The observer and its environment are inextricably linked (hence ecological).

The roots of ecological psychology are based in aviation. Its pioneer, J.J. Gibson investigated the use of pictures, both static and motion, for the selection of aircrew for the USAAC [64]. He was particularly attracted to the motion picture as a training aid due to the additional information that was available to the observer due to the movement of objects in the film. Gibson later hypothesised that this extra information came from the optic flow field – the way in which individual points in the scene move from moment to moment – that the motion caused [12, 65]. Optic flow is the first of a number of key concepts that underpin this approach to visual perception. The others are optical invariance and affordance. These three concepts will be described in more detail in the following Sections.

2.3.7.1 Optic Flow

Gibson's ecological approach to visual perception comprises a number of key concepts. The first of these is the nature of light. Classical drawings of light rays show one or two rays entering the eye. In reality, if light is assumed to be made up of rays, the eye will be subjected to millions of them. Some will have travelled directly from the sun but others will be reflected from objects in between. To Gibson then, the world is comprised of surfaces under illumination.

Second, because light travels in straight lines (unless under the influence of strong gravitational forces), it can carry information. An example of evidence for this claim comes in the form of holograms. The holographic

plate used to generate a hologram does not contain an image of the object in question, merely the interference pattern created whilst under laser illumination. Shining light onto this pattern recreates a three-dimensional image of the original object.

The result of the above observations is that contrary to the impoverished retinal image of single visual stimuli used in experimental laboratories, in the real world, an observer has a huge amount of information available to perceive the environment. When the observer moves, his/her movement is then perceptible by the way that the optic field changes from moment to moment. This change is termed 'optic flow'. If that observer happens to be the pilot of an aircraft, it has been shown that optic flow rate can provide the pilot with information about ground speed in eye-heights per second [13] , surface slant [14] and heading [66, 67]. Furthermore, this phenomenon is used for practical applications such as autonomous robotic vehicle guidance [68-70]. Fig. 2-19 shows an everyday example of optic flow – approaching a garage door. Fig. 2-19(a) shows the view from a 'distant point' with a number of points in the viewing field highlighted.
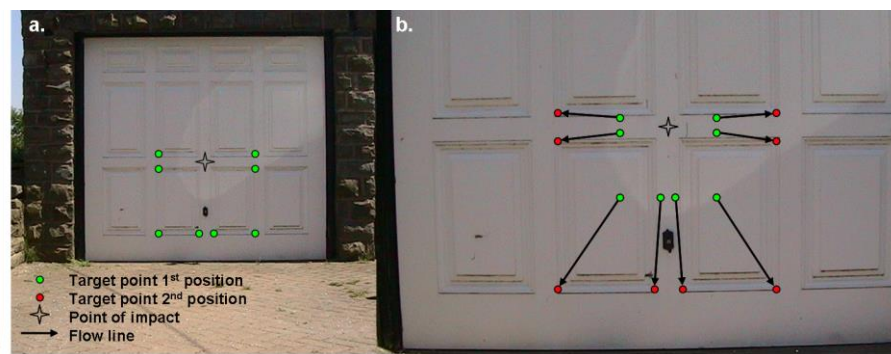

Fig. 2-19. Illustration of optic flow when approaching a textured surface

Fig. 2-19(b) then shows how these points move as the observer approaches the surface. Also marked are the 'vectors' that mark the target point's trajectory during the motion. At any instant during the motion, these define the 'optic flow'. The star marks the point that does not move which represents the point of impact if the motion is continued to the surface.

55

The situation illustrated in Fig. 2-19 is the Gibsonian ideal. However, the situation is slightly more complicated than this. It is suggested that, for practical purposes, the human eye cannot detect motion below about 50min arc/sec [14]. This is shown for a pilot approaching an airfield to modify the 'shape' of the flow field detected in Ref. [71]. The principle, nevertheless, still applies.

2.3.7.2 Optical Invariants

Motion is a key component of the ecological approach to visual perception. However, the flow of the visual scene due to the motion will not be random, but will follow a lawful progression. Adjacent components of the scene will move in a correlated manner. This correlation is a source of information about the environment through which the observer moves and is primarily received from optical invariants. They are the properties of patterns of stimulation which remain constant during changes associated with the observer, the environment or both [63]. Examples if such optical patterns or structures are[72]:

- texture gradients (e.g. the texture of a field of grass is more apparent for regions close to the observer than regions further away);

- occlusions (accretion or decretion of texture) i.e. an object that passes in front of another object is closer to the observer and vice-versa;

- motion perspective e.g. in a moving train, if the observer looks out of the carriage window, close objects will be moving through the visual field very quickly whilst motion of objects in the distance will be barely perceptible;

- focus of expansion i.e. the point denoted by the star symbol in Fig. 2-19 and

- the rate of expansion about the focus.

2.3.7.3 Affordances

A key concept in Gibson's later writing is that of affordances [73]. This is where the concept of the link between observer and environment is particularly important. The affordance of an object, Gibson maintains, contains invariant information that has (survival) value for the perceiver. So, a hut might afford 'shelter', water might afford 'pouring' or 'drinking'. Where this claim is controversial is that the affordances are perceived directly. The patterns of light reflected from an object allow the observer to perceive what the object can do for him/her without any intervening processing.

2.3.7.4 Engineering Analogy – Resonance and Pickup

A useful analogy to consider that helps to explain Gibson's ecological approach to perception to an engineering mind is that of resonance and pickup [65]. In the ecological view of the world, the perceptual system is likened to a traditional analogue radio [63]. Radio signals surround us all of the time. When an analogue radio is not tuned correctly, all that the listener can hear is static. However, when the radio is tuned to a particular radio station's frequency, its components resonate and the broadcast can be heard clearly. There is not one particular part of the radio that can be isolated as the component that is performing the function of that radio. Remove one component and the radio will cease to work. In the same way, the visual system picks up information from the optic flow field that is around us all of the time by resonating with it. Remove any part of the system, the flow field or the perceptual system and perception is lost. At the same time however, there is not one isolated component of that system that is 'perceiving'.

2.3.8   Discussion of Visual Perception Theories

The research contained within this thesis is of an engineering nature and the author is certainly not a trained psychologist. It is therefore difficult to provide a definitive, confident critique of the various theories of visual perception and the gaps in the knowledge of each of those fields. However, within the literature, there are arguments and evidence presented for and against each theory (see, for example, Refs. [63, 74]). Images can be successfully generated on a computer monitor using Marr's mathematics but this does not necessarily imply that the methods used by the programmers and within the computational hardware are those used by a human vision system. Gestalt theory draws heavily on optical illusions to illustrate its position, but optical illusions are often highly contrived (though interesting) and rarely affect an observer in real life. If, as the empiricists might claim, the visual system has to continuously test hypotheses, then what data are used by the perceptual systems in this process? Finally, from an ecological standpoint, if there is so much information available directly to an observer from any particular viewpoint, why is it that ambiguities can still exist in the visual field that need to be resolved by closer inspection or a view from a different angle i.e. requiring movement ?

From the literature available, there is clearly a marked variation in views across the psychology community as to how motion is perceived. Evidence exists for and against those theories described briefly in the preceding Sections (and for those that weren't). So, which to choose as a guide for the research ? The first question that an organism must be able to answer when it is moving is 'where am I heading?'. Once this can be established, the next question must be 'will I collide with anything?'. If the answer to this question is 'yes', then the questions 'when will a collision occur?' and 'is the corrective action having the desired effect?'

must be answered if a destructive collision is to be avoided. Any theory regarding a living organism's perception of self-motion must be able to explain how those questions are answered. The ecological approach, using optic flow as a basis, provides explanations for how each of these questions can be answered directly from the motion itself.

As a secondary issue, in the context of engineering display design, it would be useful if the theory were amenable to mathematical manipulation and analysis. The theory must also provide relevance to the research subject matter. Ecological psychology places the environment at the heart of perception [63] and does not rely on experiments involving isolated stimuli in laboratory conditions (organisms did not evolve under such conditions). This 'real-world' approach is compelling to an engineering mind that must deal with 'real-world solutions'. From a mathematical perspective, ecological psychology and the use of optic flow has been developed into a simple but elegant theory known as 'Tau Theory'. The University of Liverpool has had some success in analyzing aircraft flight in terms of τ theory [16]. As such, this branch of psychology has been used to guide the research described in this thesis. The review of 'state-of-the-art' and an analysis of where the gaps in knowledge exist must therefore now concentrate on the theory of τ.

2.4   'Time-to-Contact' (Tau) Theory

It has already been noted that one of the key facets of the ecological approach to visual perception is that the motion of the observer and the perception of the environment are inextricably linked. Motion leads to an optic flow-field that contains optical invariants that the observer can utilise to perceive that motion. The observer must use the invariant information about the perceived environment and the affordances that perceived objects provide to navigate around and survive within it. This must include, for

59

example, avoiding obstacles and predators and finding shelter and food. To perform these tasks, the observer must be able to estimate when an obstacle will be reached or when a predator will reach their prey in order to be able to take the appropriate manoeuvring action. The organism must also be able to reach for an object by anticipating when its hand/paw/claw will contact it. By their very nature, these actions are not based just in the present, but must contain some form of prediction capability as to where an object/hand/predator/prey etc. will be in the future. There must be, therefore, a time-based variable (in Gibson's view, an optical invariant) available to an observer that can be used to perform these actions. This variable must explain how such prospective guidance of movement can be perceived and it must be biologically plausible. Such an invariant comes in the form of *the time to close a motion-gap at its current closure rate*, designated tau or τ [75].

2.4.1   Time to Close a Motion Gap, Tau

2.4.1.1 Motion Gaps and the Definition of Tau

In τ theory, a motion gap is defined as being the changing gap between the state that an organism is currently in and the state is desires itself to be in [75]. In the examples given above, the gap is one of distance. However, the concept is more general than that and can be any gap that an animal will encounter. This will include, for example, the angular gap of the head when turning to look at something, the force gap required to take a pace or a pitch gap when singing a tune. What's more, at any given moment, there are likely to be several motion gaps that need to be closed at any one time. All of the gaps noted so far are in different units of measurement and it is argued that a perceptual system that had to cater for differing units of motion would be unnecessarily complex and that nature and the evolutionary process would have provided a more compact and highly efficient solution. Tau theory postulates that the most likely candidate for

a dimension of an optical variable is one that underlies all motion-gap changes, time [75].

The single temporal variable that is proposed for use in controlling motion is the τ of a motion gap and is defined as follows and shown in
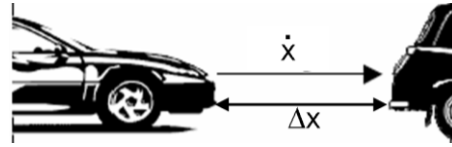

Fig. 2-20. Tau definition variables

Fig. 2-20 (adapted from Ref. [76]. If an observer is under motion and approaching a surface with velocity $\dot{x}$ and the current distance to the target is x then the τ of the motion gap, Δx, is given by:

$$\tau_x = \frac{\Delta x}{\dot{x}} \tag{2-1}$$

In the case of an approach to an object or surface, τ_x is termed the time-to-contact (TTC) and is the inverse of the closure rate. In the event that an organism is not heading straight for an object, τ_x is termed the time-to-passage (TTP).

2.4.1.2 Perceiving Tau

It would seem at first sight, from Eq. (2-1) that to perceive τ, the observer must first detect the size of the motion gap and then the rate of change of the size of the gap. This is not the case. τ is directly available to the observer from the view of the surrounding environment. It is useful at this point to consider how this might be so.

Ref. [15] shows that if two τs are coupled i.e. maintained in constant ratio, then the motions to which they relate are governed by a power law. If $\tau_u = K\tau_v$ then by the definition of τ in Eq. (2-1):

$$\frac{u}{\dot{u}} = K\frac{v}{\dot{v}} \tag{2-2}$$

Inverting Eq. (2-2), integrating with respect to time and rearranging gives:

$$u = Cv^{\frac{1}{\kappa}} \qquad (2\text{-}3)$$

where 'C' is an arbitrary constant. This relationship is only useful if it can be shown that a particular motion of an observer allows τ information to be picked up from an external scene. Ref. [15] provides a number of cases of motion that result in the observer being able to directly perceive τ information due to motion of the visual scene. For the sake of brevity, only one example will be included here. Much of the work contained within this thesis relates to a fixed-wing aircraft landing flare manoeuvre, which is primarily a change in motion in the vertical sense. The following example therefore considers only vertical motion and to further simplify matters, assumes monocular vision and that the observer's retina (the projection plane) to be flat.

Fig. 2-21 shows an observer, O, travelling in the inertial Z (vertical) direction at a velocity dZ/dt parallel to a vertical plane. A point, P,
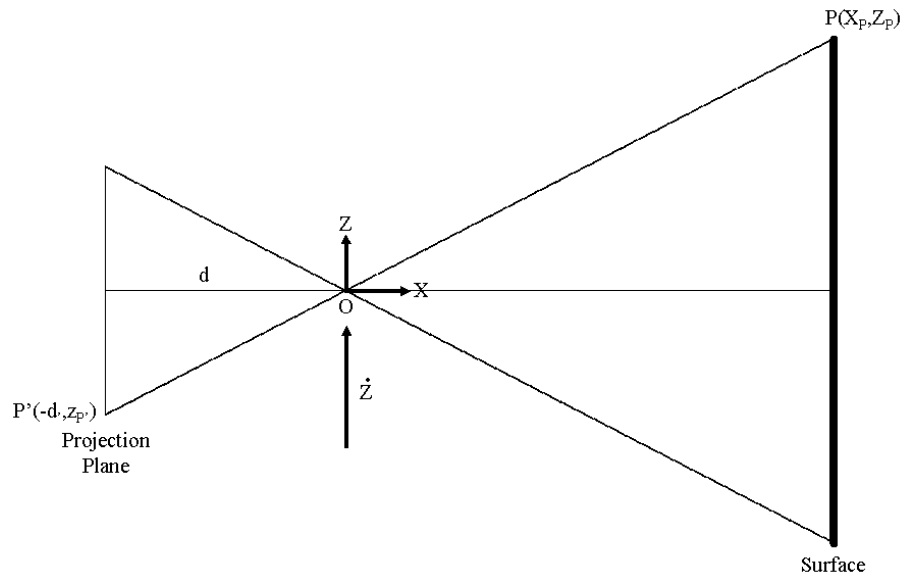
Fig. 2-21. – Schematic Representation of an Observer, O, Moving in the Vertical Plane

makes up part of the image of that plane on the projection plane at point P'. From similar triangles we have:

$$\frac{z_{P'}}{d} = \frac{Z_P}{X_P}$$
(2-4)

When O is moving at dZ/dt, d and X_P are constant, so:

$$z_{P'} = \frac{d}{X_P} Z_P$$
(2-5)

Eq. (2-5) is equivalent to Eq. (2-3) with C=(d/X_P) and K=1. We can therefore formally say that:

$$\tau_{ZP'} = \tau_{ZP}$$
(2-6)

i.e. a sensory flow-field τ is coupled to an externally perceived τ. In this way, information picked up by the observer's eyes from a vertical motion can be converted into information about the vertical gap being closed.

2.4.1.3 Coupling Tau

Tau theory, as described at this stage, will enable a single motion gap closure to be perceived. There may be many motion gaps to be closed in a single manoeuvre. Tau theory offers a hypothesis that may go some way to explain how this occurs. It is postulated that for the control of motion where multiple motion gaps are to be closed, the τs of those motion gaps are coupled i.e. kept in constant ratio [15]. Such a coupling can be intrinsic or extrinsic. An extrinsic coupling means that two externally perceived motion gaps are kept in constant ratio. So, if a motion gap 'x' is being closed at a rate '$\dot{x}$' and a motion gap y is being closed at a rate '$\dot{y}$' and both gaps need to be closed together, then a possible means of achieving this through the observer's perception of that motion is:

$$\tau_x = K\tau_y$$
(2-7)

As noted in Section 2.4.1.2, such a relationship implies that the two gap variables, x and y are linked by a power-law relationship.

Such a hypothesis accounts for guided motion using two externally perceived gaps but no explanation is provided for motion where a greater number of gaps are involved.

Intrinsic τ-coupling is hypothesised as a means for guiding motion where only one external gap is perceived by the observer. In this case, an internally generated τ-guide is postulated as a means by which τs can be coupled.

2.4.1.4 Intrinsic Tau Guidance

Intrinsic τ coupling is based upon the premise that an internally generated, so-called, 'τ-guide' provides a basis onto which an externally perceived variable can be coupled. Such a guide, it is believed, is generated in the brain's neural network by an as yet undiscovered bodily process [15]. This idea maps onto the concept of the visual field resonating with the observer. A number of τ-guides, denoted τ_g, have been proposed. These are:

1. Constant velocity τ-guide:

$$\tau_g = (t - T)$$ (2-8)

2. The constant deceleration τ-guide:

$$\tau_g = \frac{1}{2}(t - T)$$ (2-9)

3. The constant acceleration τ-guide:

$$\tau_g = \frac{1}{2}\left(t - \frac{T^2}{t}\right)$$ (2-10)

where t is the current time during the motion and T is the total duration of the motion (0<t<=T) [15].

The names are self explanatory with perhaps the exception of the guide of Eq. (2-10). This is valid for guiding motion of an object accelerating from rest and stopping at a goal. As such, both acceleration and deceleration are experienced by the observer. The intrinsic τ-guide model has since been developed further into the *General Intrinsic* τ-guide model. This applies to guiding the motion of an object that is approaching or receding from a destination and that starts at rest or starts with some initial velocity [75]. It assumes that observer's perceptual systems that have evolved within the Earth's gravitational field will be sensitive or 'tuned' to motion that this field causes. This general τ-guide, designated τ_G, is given as:

$$\tau_G = \frac{t(T+t)}{T+2t} \qquad (2\text{-}11)$$

where T is the total motion duration and t is current time during the motion (in this case, $-T <= t <= 0$). For an external spatial variable 'x' to τ-couple onto the general intrinsic τ guide:

$$\tau_x = k\tau_G \qquad (2\text{-}12)$$

where τ_x is the τ of the spatial variable x, τ_G is the general intrinsic τ guide and k is the coupling constant. Both τ_x and τ_G vary with time. The constant acceleration τ_g, it turns out, is a special case of τ_G, corresponding to the second phase i.e. the deceleration of the motion generated by τ_G [15, 75]. This can be shown as follows, using the original (constant acceleration) τ-guide, τ_g, from Ref. [15]:

$$\tau_g = \frac{1}{2}\left(t - \frac{T^2}{t}\right) \qquad 0 < t \le T \qquad (2\text{-}13)$$

Ref. [75] provides the defining equation for the General Intrinsic τ-guide, τ_G, viz:

$$\tau_G = \frac{t(T + t)}{T + 2t} \quad -T \le t \le 0 \tag{2-14}$$

where T is the total duration of the motion and t is the current time during the motion. Now, τ_g is equivalent to τ_G for the last half of a τ_G motion. For this period of the motion:

$$T_g = \frac{T_G}{2} \tag{2-15}$$

and:

$$t_g = t_G + \frac{T_G}{2} \tag{2-16}$$

where T_g is the duration of the motion guided by τ_g, t_g is the current time during this motion, T_G is the duration of the equivalent motion guided by τ_G and t_G is the current time during this motion. Substituting (2-15) and (2-16) into (2-13) (with t=t_g and $T = T_g$):

$$\tau_g = \frac{1}{2} \left(\frac{\left(\frac{2t_G + T_G}{2} \right)^2 - \left(\frac{T_G}{2} \right)^2}{\left(\frac{2t_G + T_G}{2} \right)} \right) \tag{2-17}$$

and hence:

$$\tau_g = \frac{t_G(t_G + T_G)}{T_G + 2t_G} \tag{2-18}$$

Eq. (2-18) is now in the same form as Eq. (2-14).

When coupled onto such a guide as per Eq. (2-12), an object in motion will follow one of the theoretical normalised motion profiles shown in Fig. 2-22. These curves were plotted using Ref. [75]. This reference derives the

defining equation for the General Intrinsic τ-guide, τ_G, and the resulting

motion that is implied by coupling onto such a guide as follows:

$$\tau_G = \frac{t(T+t)}{T+2t} \qquad -T \le t \le 0 \qquad (2\text{-}19)$$

where T is the total duration of the motion and t is the current time during

the motion. To normalise equation (2-19), define $t_n = t/T_G$, giving:

$$\tau_G = \frac{T_G(1+t_n)t_n}{1+2t_n} \qquad (2\text{-}20)$$

If a body under motion, closing a gap 'x', is coupled onto a General

Intrinsic Tau Guide then:

$$\tau_x = \frac{x}{\dot{x}} = k\frac{T_G(1+t_n)t_n}{1+2t_n} \qquad (2\text{-}21)$$

Integrating Eq. (2-21) with respect to time successively yields:

$$x = x_m 2^{\frac{2}{k}}(t_n - t_n^2)^{\frac{1}{k}} \qquad (2\text{-}22)$$

and:

$$\dot{x} = \frac{x_m}{T_G}\frac{2^{\frac{2}{k}}}{k}(-1-2t_n)(t_n - t_n^2)^{\frac{1}{k}-1} \qquad (2\text{-}23)$$
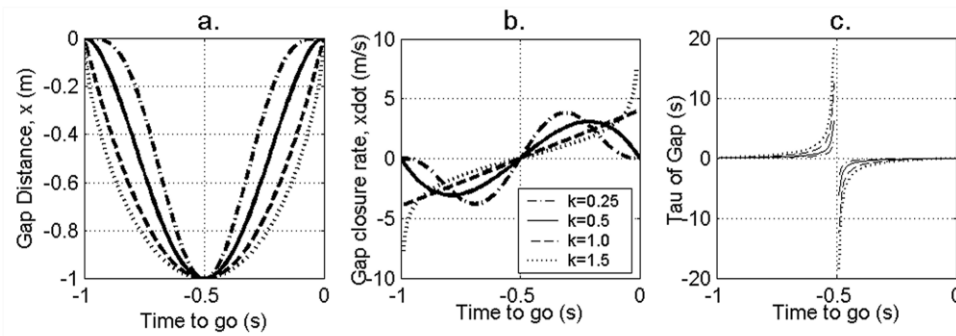
Fig. 2-22. Theoretical normalised motion profile of a 1kg mass coupled to the General Intrinsic τ guide for varying values of coupling constant, k: (a) distance of mass from target; (b) instantaneous velocity of mass and (c) τ of distance for the mass

Inspection of the τ_G-coupled motion profiles reveals that the value of 'k'

selected will provide differing responses when approaching a target surface

or object (from time to go -0.5 to 0.0). A value of k<1.0 results in a series of acceleration - deceleration motions. As k approaches 1.0, the deceleration phase of the motion starts at an increasingly later time. If k=1.0, the resulting motion is performed under constant acceleration. The body under motion reaches the target with some residual velocity. If a value of k>1.0 is selected, then the object continues to accelerate towards the target.

2.4.1.5 Constant Rate of Change of Tau Strategy

One of the earliest hypotheses for the use of τ came in the form of drivers braking to avoid either a moving or a stationary obstacle ahead [77]. Rather than using τ directly, it was proposed that effective braking strategies could be achieved by maintaining a constant value of its first derivative with respect to time, $\dot{\tau}$. That is:

$$\frac{d\tau}{dt} = \dot{\tau} = c \tag{2-24}$$
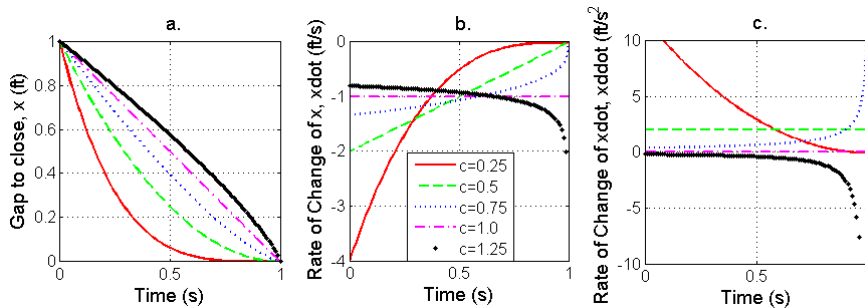
Fig. 2-23. Normalised theoretical trajectory data assuming motion gap is closed using a constant $\dot{\tau}$, 'c': (a) motion gap being closed; (b) rate of gap closure and (c) acceleration during gap closure

Holding $\dot{\tau}$ constant, it turns out, is a particular example of τ coupling [15]. Fig. 2-23 shows the normalised trajectory for an observer in motion using such a strategy to decelerate to a stop before striking an obstacle or surface. The derivation of the calculations used to create these curves is as follows:

For a constant rate of change of τ of a motion gap, 'c':

68

$$\frac{d}{dt}\left(\frac{\Delta x}{\dot{x}}\right) = c \tag{2-25}$$

where 'Δx' is current gap to be closed and $\dot{x}$ is the instantaneous rate of closure of that gap. For an instantaneous position, 'x', and target 'x_t', Δx is given by $(x-x_t)$. Integrating both sides with respect to time, bearing in mind that, by convention, at time t=0, τ_x=0:

$$\frac{\Delta x}{\dot{x}} = ct \tag{2-26}$$

Rearranging Eq. (2-26) yields:

$$\frac{c}{\Delta x}d\Delta x = \frac{1}{t}dt \tag{2-27}$$

Evaluating the integrals and rearranging gives:

$$\ln(\Delta x^c) = \ln(Ct) \tag{2-28}$$

To find the constant of integration, C: at t =-T, manoeuvre duration, $\Delta x=x_0$, initial gap value yielding:

$$\Delta x = -\left[\frac{x_0^c}{T}t\right]^{\frac{1}{c}} \tag{2-29}$$

Differentiating Eq. (2-29) once to provide velocity and a second time to find acceleration gives:

$$\dot{x} = \frac{x_0}{cT^{\frac{1}{c}}}t^{\frac{1-c}{c}} \tag{2-30}$$

and:

$$\ddot{x} = \left(\frac{x_0}{T^{\frac{1}{c}}}\right)\left(\frac{1-c}{c^2}\right)t^{\frac{1-2c}{c}} \tag{2-31}$$

69

It is evident that two special cases exist. The first, if 'c' is maintained at 0.5, results in a motion under constant deceleration. In this case, the surface or obstacle is just reached. The second special case, maintaining 'c' at a value of 1.0, results in motion with constant velocity. Ref. [75] states that if 'c' is maintained at less that or equal to 0.5
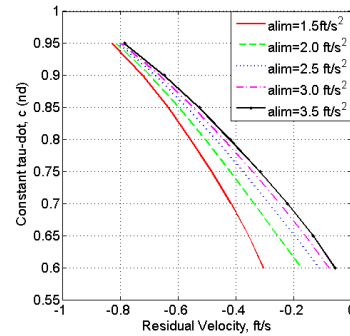

Fig. 2-25. Residual velocity at target surface using a constant $\dot{\tau}$ closure strategy with a limiting deceleration value, 'alim'

then stopping before reaching the surface or obstacle in question is assured. However, it can be seen from Eq. (2-30) that all motion for values of 'c' < 1.0 will result in zero velocity at the end of the motion (when t=0.0). However, to achieve this, for values of 'c' above 0.5 and particularly for values that approach 1.0, an increasing magnitude of deceleration is required. This might be because it is beyond the physical limits of the observer or the vehicle in motion or it may simply be the observer's choice. If this is the case, then the gap will be closed/surface reached with a residual velocity. If the surface or obstacle is a solid one, then a controlled 'crash' will result. Fig. 2-24 shows how the normalised trajectory of Fig. 2-23 with c=0.75 is modified if a nominal limit is applied to the deceleration (1.5 ft/s^2).
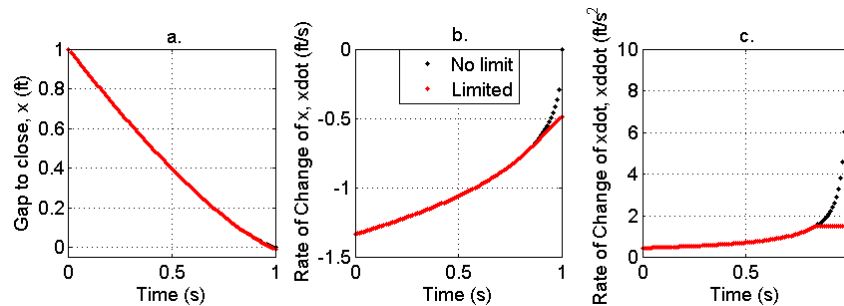

Fig. 2-24. Comparison of normalised theoretical trajectory data with trajectory limited in acceleration (at 1.5 ft/s^2) for 'c'=0.75: (a) motion gap being closed; (b) rate of gap closure and (c) acceleration during gap closure

The modified behaviour is summarised in terms of the residual velocity observed for a number of values of constant $\dot{\tau}$ and limiting deceleration ('alim') values in Fig. 2-25. It can be seen that pseudo-linear relationships are defined by this form of closure strategy.

2.4.2   The Arguments For and Against Tau Theory

There is vigorous debate as to the truth or otherwise of τ theory and for every piece of evidence that supports the theory, it seems that there is a contradictory argument against. The following Section presents examples of both sides of the argument.

Ecological psychology emphasises the importance of the interaction between the environment and the observer. Naturally enough, therefore, much of the evidence that supports τ theory comes from experiments that observe an organism's behaviour in their own environment. Specific examples of these are:

- Plummeting Gannets [78]. In this analysis, evidence is presented for the existence of a time-to-contact strategy employed by gannets in controlling the moment to fold their wings when diving into the sea from a height of up to 30m i.e. wings were folded at a constant τ value. However, an alternative approach (dynamical systems), has shown that modelling the gannets dive can be regulated successfully by $1/\tau$ [79].

- Grasping movements e.g. catching a ball. One of the constraints given for τ theory is that the outline of an object must not change since this would change the shape of the image and hence its flow over the retina, leading to false time-to-contact information. However, Ref. [80] provides evidence that a time-to-contact strategy is employed in timing a grasping action by observers catching a ball that is deflating during the approach. However, the

71

same author revises this to include the requirement that such interceptive action requires online regulation during the catching activity i.e. contrary to the theory, τ is not the sole piece of information that is required [81].

- Pigeons landing on a perch [82]. This experiment examined the deceleration strategy of pigeons approaching a perch under both binocular and monocular conditions (one eye covered). The results claim that the birds regulated braking by maintaining the rate of change of τ of the distance of their feet from the perch constant. Objections are raised to this claim, however, in Ref. [83]. Here, simulated results are presented for similar pigeon flights that take account of a pigeon's natural head-bobbing and the fact that the image of the perch is projected onto a spherical, rather than flat surface. In this case, the τ of the foot-perch distance (and hence its first derivative with respect to time) is shown to be non-linear and discontinuous.

- Coordination of Movement [84]. A number of τ-coupling hypotheses are tested, including intrinsic τ guidance, for the movement of hand to mouth e.g. when feeding. It was found that an extrinsic coupling relationship existed between the τ of the angle of approach of the hand to the mouth and the τ of the distance between the hand and mouth. An intrinsic coupling relationship was found between the τ of the distance between the hand and mouth and the original version of the intrinsic τ guide, τ_g (see Section 2.4.1.4). These results were unaffected whether the test subjects had their eyes open or closed. It was therefore concluded that the τ information was obtained from muscular information as well as optic flow information. Some researchers object to and

warn against this extension of τ from a purely optical retinal expansion variable to the more generic motion gap case [85].

2.4.3   The Investigation of Tau in Aerospace Applications

The application of τ theory to aerospace applications is relatively sparse. Refs. [86] and [87] investigate the effects of texture and pictorial detail of a simulated visual field for the initiation of the landing flare manoeuvre. These conclude that the inclusion of texture improves the test subject's ability to perceive time to contact the runway surface (based upon an indication of flare commencement) and that when insufficient information is available to make TTC judgements, flare initiation height is judged using the runway visual angle, Ψ (the angle subtended between the runway surface and a line drawn from the pilots eyes to the aiming point).

Ref. [88] examines observers judgement of TTP of an object rather than TTC and concludes that the test subjects were able to demonstrate a robust ability to utilise such information. It is therefore proposed that τ might well be a useful metric for pilots to employ in planning and orchestrating vehicular control.

Further evidence for the use of τ strategies in flight comes from work conducted at The University of Liverpool Research [16]. This work showed that when helicopter pilots fly stopping manoeuvres close to the ground, there is a close correlation between the motion-τ (instantaneous time to reach the stop point) and a pilot-generated τ-guide that can follow constant deceleration or acceleration laws.

Related research effort within the aerospace field has been conducted around optic flow and possible spatial optical invariants rather than τ itself. J.J. Gibson, the 'founder' of the ecological approach to motion perception worked in association with the USAAC on an analysis of the landing flare

[89]. In this work, Gibson argues that the contemporary thinking of the time regarding the information available to the pilot for a flare was insufficient. He then derived an alternative, optic flow based account, called motion perspective and proposes that this is the mechanism used by pilots to perceive their motion during a flare. This work was extended in [71] to show that the area of imperceptible motion, as optic flow would have it, is not just a point, but a larger area whose shape varies with angle of approach. Interestingly, in this work, it is suggested that helicopter pilots making steep approaches may be able to make better use of this information than pilots in fixed-wing aircraft using more shallow approaches due to the relative velocity rates induced by the perceived optic flow.

At around the same time as the Gibson analysis, perspective analysis has been carried out in the UK to establish the visual information available to a pilot during the final phases of the approach. Based upon this analysis, it was argued that conventional instrumentation, that provided only angular error indications were insufficient to allow the pilot to make predictive corrections to the aircraft flight path. Flight directors were seen as one answer but it was also suggested that information be presented to the pilot *in a manner analogous to that in which it appears in the visual field* [90].

From an optical invariant perspective, a body of research has been conducted into how a pilot maintains station on the correct glide slope when flying with reference only to visual cues. There are a number of cues available to the pilot that will allow him to do this that relate to the relative size and shape of the runway, the layout of its surroundings and its position in the windscreen in front of the pilot (the optical invariants). For example Refs. [91-94] document various attempts to quantify, by analysis, how a glide-slope angle is detected and maintained using variables visually available to the pilot. The conclusions from this work are that the size and

shape of the runway are key parameters in the judgement of approach angle. However, the situation is more complex that that. At greater distances from the runway, the angle in the vertical plane between the line from the eye-point to the horizon and the line from the eye-point to the runway aim-point provide less uncertainty for estimating glide slope angle and information from the runway shape provides less uncertainty in estimating glide slope angle when closer in to the runway.

2.4.4 Discussion of Tau Theory

There is a body of evidence that might well account for the universal use of τ-based strategies to guide animal (including human) motion which includes humming birds docking at a feeder [95], bats navigating through their environment using echo-location [96] and athletes performing various motions during the course of competition [97, 98]. Further evidence exists that the steering of vehicles is a time-based perceptual task, rather than a spatial one [99]. This evidence, perhaps coupled with the simplicity of the theory itself, seems to have led to a widespread acceptance. There are those researchers however, that maintain that such acceptance is not warranted given the evidence [83, 100, 101]. They propose alternative strategies that, they maintain, also fits the data. For example, relative distance is proposed as an alternative strategy for an observer falling under gravity [83]. In this perceptual theory, an event might be triggered when the observer has travelled a fixed proportion of the distance towards the destination. Ref. [83] asserts that the observer simply has to learn the critical proportion that will allow for motor delays and movement time (e.g. wing folding in the gannets experiment of Ref. [78]). For this specific example, one wonders whether the requirement to learn holds evolutionary benefit for the organism involved. Over-cautious gannets i.e. gannets that folded their wings late, might risk injury to their wings and under-cautious gannets might risk being knocked unconscious or worse if their arrival velocity at the water surface was too high.

The proving or otherwise of τ theory is beyond the scope of this thesis. The success of a theory lies in its general explanatory power and the degree to which it is supported by empirical evidence. Tau theory does possess explanatory power for motion perception and has an attractive simplicity that lends itself to analysis. There is significant empirical evidence in support of τ theory as well as evidence for other mechanisms to control motion. It would seem likely, from a survival perspective, that there is room for multiple control strategies in an observer's armoury to provide guidance information that will allow movement through their environment. The strategy selected will be based upon the information (or lack of it) available at the time [86]. One of these, it seems, might well be τ.

Tau theory, or the application thereof, also provides the means to define types of trajectory that may well find a use in aerospace applications. Using either constant $\dot{\tau}$, τ_g or τ_G as guidance strategies will provide the closure of a particular aircraft state gap with no overshoot e.g. turning onto a heading or with a small residual collision velocity e.g. a landing flare. This coupled with the results of Ref. [16], where it was shown that helicopter acceleration-deceleration manoeuvres where closely correlated with τ guidance strategies warrants further investigation of the use of Tau Theory for aerospace applications.

The question would be, therefore, which strategy to use. Given that this is the first application of τ to display design, the simplest would be desirable. τ_g is the latter half of τ_G and $\dot{\tau}$ strategies are a particular case of τ coupling (with either extrinsic or intrinsic guidance) [75]. On that basis, whilst none of the strategies are particularly complex, constant $\dot{\tau}$ strategies were selected for the starting point for the display work conducted during the research. The other strategies have not been completely ignored during

the research, however, and some limited findings on τ_G control strategies can be found in Refs. [30, 102].

2.5 Contribution of the Research

The vision of airline operations described in Section 2.2.1.2 is one of more aircraft and more aircraft types operating more frequently, without delays, in all weather conditions using non-standard procedures (compared with today) with an increased requirement for trajectory precision. Section 2.1.5 shows that whilst aviation safety has improved considerably over the last half-century, there is still room for improvement. Sections 2.1.2, 2.1.3 and 2.1.4 illustrate that the most improvement can be made in phases of jet transport flight that are closest to the ground, in both good and degraded visual environments. The review suggests that the following phases of flight should be targeted as a priority:

        a.   Take-off and Initial Climb.

        b.   Approach and Landing (to include go-around).

These are exactly the phases of flight where new airspace procedures will require the most stringent adherence to inertial position.

The increase in flight safety can be attributed in part to an increased level of automation in jet transport operations. However, an increasing reliance on automated technological solutions to effect these changes has resulted in a disconnect between the flight deck displays and the crew. There are many reasons for this but it is asserted that the problem is exacerbated by the displays in current use have evolved over a long period of time to provide spatial information in a rather symbolic manner. A more natural (i.e. intuitive) display might well utilise the natural mechanisms that organisms use to move through their environment. There are many theories that provide an explanation for how this might be achieved (Sections 2.3.5, 2.3.6 and 2.3.7). One of the more compelling from a

motion-guidance perspective is the Ecological Approach using optic flow as its basis (Section 2.3.7.1). More specifically, a spatial representation of the world might well be ignoring the natural, time-based, guidance mechanism, τ (described in Section 2.4).

Previous results obtained at The University of Liverpool (UoL) have indicated that τ-based guidance mechanisms are involved in at least some aspects of rotary wing flight [16]. One of the logical extensions to this work is to investigate fixed-wing flight in terms of the parameter, τ, and, in an attempt to make cockpit displays more intuitive, to use the results to start to design nature-inspired flight-deck display concepts.

The research reported in this document begins to tackle this issue and provides rudimentary solutions to it. Natural motion perception mechanisms are used to provide information to cockpit pilot guidance displays. These are compared with existing display formats. Specifically, the following research questions are addressed:

1. What are the visible motion gaps available to the pilot for the target flight phases and aircraft manoeuvres ?

2. For the identified motion gaps, are coherent τ-based relationships evident in the same way that they have been for rotary wing flight ?

3. If τ-based relationships are evident for key phases of flight, can these be used as a basis for pilot displays to conduct flight in both good and degraded visibility

Chapter 3

RESEARCH EXPERIMENTAL SET-UP

Some of the key aspects of the research described in this thesis pertain to the design of display formats to assist with large jet transport flight manoeuvres in degraded visual conditions. At the start of the research project, there were a number of constraints on the Flight Science and Technology (FST) Research Group's ability to do this:

- simulation facilities were unable to provide realistic degraded visibility outside world views;

- there was no capability to generate new displays over and above those already in existence;

- the Group's knowledge base did not extend specifically to large jet transport operations and

- a large jet transport simulation model did not exist.

A considerable amount of preparation was therefore required before the research effort could begin. The areas of focus for this task were to upgrade FST's flight simulation facility to:

1. Allow the simulation of more realistic degraded visibility outside world visual scenes (i.e. fog).

2. Allow the development of cockpit HDD and HUD systems.

3. Incorporate a generic large jet transport aircraft (GLTA) simulation model into the aircraft library.

Section 3.1 reports upon the upgrades carried out and Section 3.2 reports on the development of the GLTA simulation model. Once the new

capabilities of the upgraded facility were established, then suitable experiments could be designed to use them effectively. Experimental design comprised three main stages:

1. The division of jet transport operations into mission task elements (MTEs) that could then be developed into (simulated) repeatable flight test manoeuvres.

2. The design of a number of experiments to first investigate each MTE in terms of the closure of τ-based motion gaps and then the application of these research results to the design, implementation and testing of novel display concepts and control laws.

3. The development of cockpit displays and the simulation environment to support the designed experiments.

Section 3.3 reports upon the development of jet transport MTEs and Section 3.4 explains the background of the experiments that were designed around them. The results of the experiments are then reported in Chapters 4 - 6.

3.1   HELIFLIGHT Upgrades

The key FST research group facility is the research flight simulator 'HELIFLIGHT'. This comprises a cockpit with six visual channels mounted upon a six-axis motion base. The name originates from the original intended use of the device, namely for rotary wing flight simulation. However, the aircraft modelling simulation software in use at UoL, 'FLIGHTLAB', can also be used to model fixed-wing aircraft. The interface between the hardware and the software is controlled by 'PILOTSTATION'. At the start of the research project, the simulation facility was at a state defined by Ref. [103]. This configuration did not offer the functions required to conduct the research to answer the questions posed by the technical review of Chapter 2. An element of upgrade work

was therefore required. The following upgrades to the simulation facility were carried out:

1. The six simulator visual channels (five outside world and one instrument panel) were converted to use BAE Systems' 'Landscape' software [104]. This provided not only the capability to simulate degraded visibility but also increased the flexibility of the simulation environment by allowing the addition or subtraction of 3D models e.g. runway lighting from the outside world scene without having to create entirely new databases.

2. Engenuity Technologies' VAPS (Virtual Avionics Prototyping Suite) software was integrated with both Landscape and FLIGHTLAB. This provided the capability to create software-based user interfaces (in the context of this research, HDDs and HUDs) in a user-friendly graphical environment [105].

3. An ASL-501 eye-tracking system was purchased [106]. The intention was to use this equipment to help establish how the pilot's information requirements were changed as the visual scene was degraded. Fig. 3-1 shows the key elements of the head-mounted system.
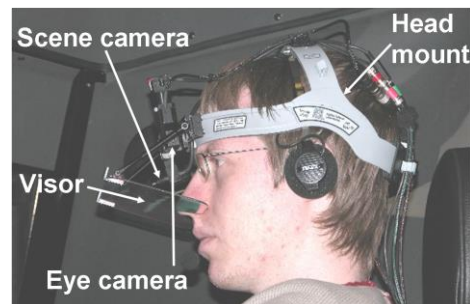
Fig. 3-1. Eye tracker head-mounted installation

Each of these upgrades is described in more detail in the following Sections. The new facility is shown in schematic form in Section 3.1.4.

3.1.1 Outside World Visualisation / Cockpit Display Software

3.1.1.1 Limitations of the Existing Visual Channel Software

The original HELIFLIGHT configuration is described in Ref. [103]. With this system in place, the outside world view for a given simulation trial was

originally driven by PILOTSTATION. Aircraft could be 'flown' around databases created and/or modified using FST Mulitgen-Paradigm's Creator software tool. Flight was limited to daytime CAVOK[4]. The only mechanism to degrade the visual scene was to either change the quality of the textures associated with database surfaces or remove elements of the database altogether. Whilst a valid approach to scene degradation, a more realistic means to perform this function was required. BAE Systems' 'Landscape' software (based upon SGI's OpenGL Performer graphics software tool) was procured for this purpose. The key features that Landscape provided was a relatively easy to use interface and more importantly, the ability to degrade the visual conditions in the outside world database using fog modelling software.

3.1.1.2 New HELIFLIGHT Outside World Display Capabilities
Landscape provides a number of enhancements to the HELIFLIGHT facility including the ability to: add animated models to the simulation environment; visualise the simulation real-time from almost any angle and customise existing databases more flexibly than was previously possible, allowing many more outside world databases to be used per simulation trial than was previously possible. The key desirable feature of Landscape used for this research was the ability to obscure the visual scene to a greater or lesser extent using 'fog'.

Landscape provides two levels of fog: 'Ground Fog' and 'Sky Fog'. The dividing altitude for these is approximately 100ft but if the two values selected are different, then a linear blending is performed. In either case however, the fog is modelled in the same way using the OpenGL Performer squared exponential fog model. The fog colour is blended with the colour of the object being obscured by a factor 'f' where:

---

[4] CAVOK – aviation term for 'Cloud and Visibility OK' i.e. good visual conditions.

$$f = e^{(d \times z)^2}$$

'd' is the fog density (default = 1.0) and 'z' is the distance from the eye-point to the object. In this way, the fog does not just appear to be a wall of colour at a fixed distance from the eye-point, but, as in reality, objects are gradually obscured until there comes a point were the fog obscures all objects behind it. This position is set as the 'fog distance' in Landscape. In practice, the user merely needs to set this distance to a suitable value to provide total degradation of the visual scene beyond that range. Examples of outside world visual scenes containing fog are shown in 3.4.2.4.

3.1.2 Cockpit Display Software

3.1.2.1 Limitations of the Existing Cockpit Display Software

For the original HELIFLIGHT configuration, only one head-down cockpit instrument panel was available and a basic HUD could be switched on or off. There was no easy means to modify the existing displays or create new ones.   Engenuity Technologies' VAPS rapid prototyping display software was purchased to fill this capability gap.   VAPS provided a straight-forward mechanism for drawing display symbols and then animating them using aircraft simulation model data without having to resort to low-level code generation. Furthermore, integration between the two software tools had already been performed by Engenuity/ BAE Systems so there was minimal risk that the software suite selected would not work in an integrated manner.

3.1.2.2 New HELIFLIGHT Cockpit Display Generation Capability

Engenuity Technologies produces a display rapid prototyping tool called VAPS (Virtual Avionics Prototyping Software). This allows the user to draw symbols, shapes and primitives (in the same way as one would in Microsoft PowerPoint, for example) and connect data channels to various properties of the graphical object in question e.g. size, colour, shape etc. to animate them as required. There are also pre-configured object types e.g.

knobs and dials that allow for the rapid creation of cockpit (or any other type of) displays. Conceptually, the user simply has to connect up the graphical object data channel to the appropriate simulation model variable. In practice, this means that a FLIGHTLAB aircraft simulation model must have the variables in question being broadcast out on the simulation network in one or more variable lists by PILTOSTATION. Each visual channel that contains a VAPS display must then be 'listening' out for those variable lists in order for the animation to work. In this way, HELIFLIGHT gained the capability to be able to create displays, the only limitation being the imagination of the user.

Communications software was coded and added into the Landscape compilation process to 'listen' for the FLIGHTLAB model broadcast and the corresponding variable lists added to the GLTA model to stream the data to the VAPS display at run-time. Various permutations of this solution were tried during the course of the research project and the latest version is shown in Fig. 3-2.
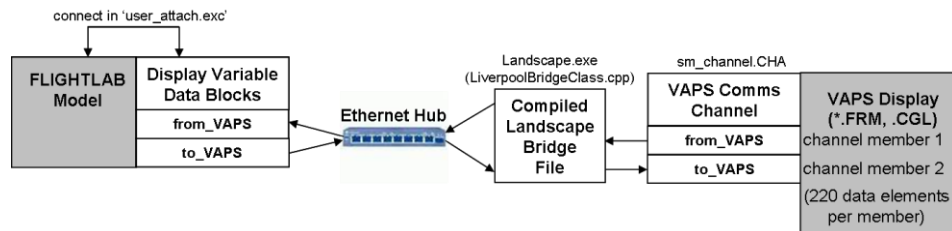
Fig. 3-2. Schematic illustration of FLIGHTLAB – VAPS integration

3.1.3   Eye Tracking System

At the start of the research project, no eye-tracking capability existed within FST. It was envisaged that such a system would provide useful information concerning pilot's information sources for flight in a good visual environment. After trialling a small number of systems, an ASL 501 eye tracking system with head-mounted optics (Ref. [107]) was selected

and purchased in conjunction with Mangold (Ref. [108]) video analysis software.

The eye-tracking apparatus, when properly calibrated, provides a video image of the scene that is presented to the pilot with a super-imposed cross-hair that indicates the pilot's 'point of gaze' i.e. where the pilot's eye is 'looking'. An example of a still image taken from such a video is shown in
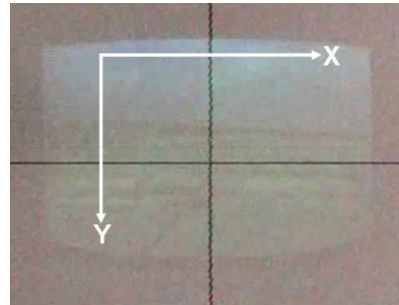
Fig. 3-3. Eye tracker coordinate system

Fig. 3-3. This figure also shows the orientation of the coordinate system used for the cursor position. A corresponding data file containing the cross-hair x-y coordinate positions can be recorded for subsequent off-line analysis. Two types of x-y data can be generated.

1. An 'x-y' time-history of the pilot's point of regard. The software provide with the system could then produce a number of analyses from these data. The key analysis for the research described in this thesis was the 'fixation analysis'. This analysis is based upon the principle that just because the eye is 'looking' in a particular direction, it does not necessarily mean that the viewer is processing the visual information. The assumption is made that to be cognisant of the image being looked at, the point of gaze must remain in approximately the same area of the visual scene for a minimum amount of time. The default setting was used for the results presented in this thesis. This corresponds to a fixation being recorded if the point of gaze remained with 1 degree visual angle for a minimum of 100ms.

2. Assuming that the eye-tracking system scene camera video output was recorded, then a visual record of the pilot's point of regard is obtained by a cross-hair being superimposed upon the scene camera

85

image. These video scenes can then be post-processed (e.g. to count how many times a particular flight instrument or piece of information was sought by the pilot) using the Mangold video-analysis software.

The procedure used for eye-tracking trials is as follows:

1. Connect up eye-tracker head-mounted optics to control box.

2. Upload the control box software from the eye-tracking system laptop.

3. Ensure that both scene and eye camera images are 'sensible'.

4. Fit head-mounted optics to pilot and obtain a suitable image of the pilot's pupil from the eye –camera (in situ in simulator pod using the remote colour monitor purchased for that purpose). It is helpful to have two people to do this such that the second person in the control room can modify the eye illumination intensity and the intensities of the automated pupil and corneal reflections. In this way, loss of pupil and corneal reflections over the viewing area of interest can be minimised at an early stage.

5. Ask the pilot to adopt his/her normal flying position and adjust the scene camera such that all of the items of interest (instruments, external views etc.) are contained within the image.

6. Simulator pod door was now closed and the eye-tracker calibration procedure commenced. Nine computer desktop icons were used as target points for the calibration process. The pilot was again asked to adopt the normal flying position and maintain his/her head as still as possible. The target icons were then identified to the eye-tracker system. The pilot was then instructed to look at each icon in turn. This provides the system with a means to identify where the pilot is looking. The icons need to be placed over the viewing

area of interest as the accuracy of the system degrades outside the calibrated area.

7. The pilot is then asked to relax and to look at each of the icons in turn. If the scene camera cross-hairs indicate that the pilot's point of regard is correct, the simulation trial outside world view and instruments are started. The pilot is then asked to look at specific features/instruments. If the point of regard is indicated correctly, the trial is commenced. If not, the calibration process is repeated.

8. Steps 6 and 7 are repeated at the end of each trial test point. If the point of regard is indicated satisfactorily, the next test point is commenced. If not, the results are ignored and the test point repeated, time permitting.

3.1.4 Schematic of the Current HELIFLIGHT Facility

Fig. 3-4 shows a schematic diagram of the upgraded facility and Table 3-1 provides more detail on the key upgraded elements.
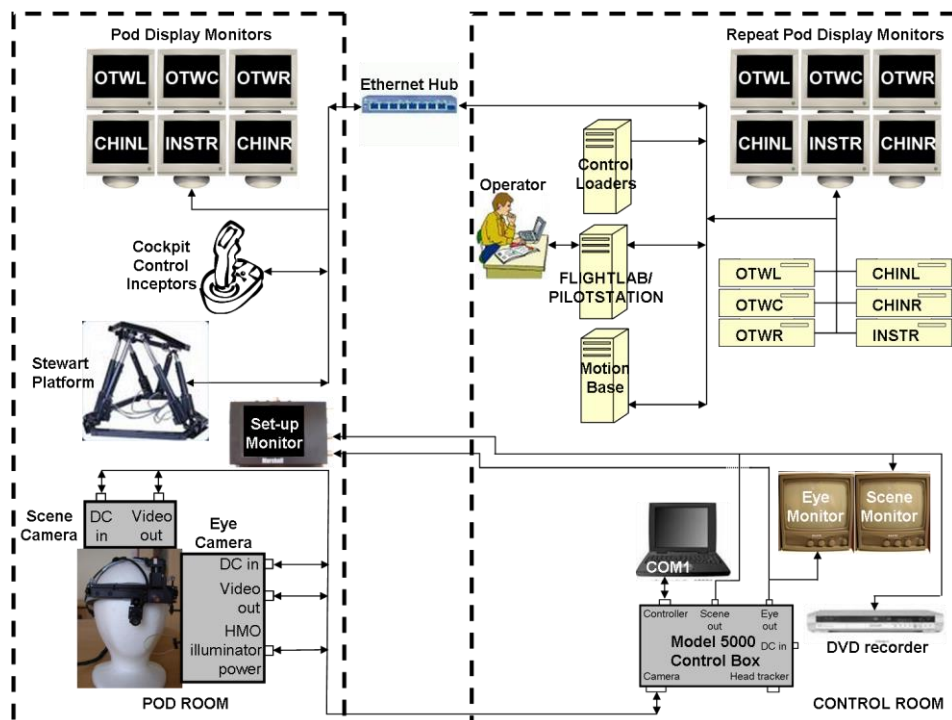
Fig. 3-4. Upgraded simulation facility schematic

Upgraded Element	Description
Visual channel computers (OTWL, OTWC, OTWR, CHINL, CHINR, INSTR)	• Processor: AMD XP 3000 or higher • Graphics: NVIDIA GeForce 5950 256Mb DDR or higher • RAM: 512Mb • OS: Linux (Red Hat 8.0)
Eye Tracking System	• ASL 501 with head-mounted optics (HMO, 50Hz) • Model 5000 eye-tracker control unit • Eye-head integration hardware (laptop pc: (Pentium III, OS: Windows)) and software • Mangold INTERACT video analysis software • SANYO VM-6609A black and white remote scene and eye camera video monitors • Marshall V-LCD4-PRO-L LCD video monitor – this repeated the eye and scene camera video images on two separate channels to allow the optics to be set up with the pilot in the cockpit seat.

Table 3-1. Description of key simulation facility upgraded items

3.2 Generic Large Transport Aircraft Simulation Model

At the start of the research project, the HELIFLIGHT facility had a reasonably extensive library of rotary wing aircraft, including a number of tilt-rotor aircraft e.g. XV-15. A smaller number of powered fixed-wing aircraft were available but the largest (in terms of aircraft Maximum Take-Off Weight, MTOW) simulation model in existence was the Handley-Page Jetstream (for a description see e.g. Ref. [109]). The anticipated main beneficiaries of the research output are the large jet transport operators. It was therefore necessary to construct a FLIGHTLAB simulation model of this type of aircraft. The decision was taken, due to the relatively easy access to a limited amount of publicly available aircraft data for the type, to construct a simulation model *based upon* the Boeing 707-120B (B707) marque. Unfortunately, insufficient data were available to build a high fidelity B707 simulation model. Where data required by FLIGHTLAB was missing for the B707, it was obtained from alternative sources. For this reason, for the purposes of this thesis, the FLIGHTLAB aircraft simulation model used for the research will be termed the Generic Large Transport Aircraft (GLTA). Fig. 3-5, taken from Ref. [110], shows the basic key dimensions of the modelled aircraft. The philosophy behind the development of this simulation model was to provide a flight vehicle that

behaved in a manner representative of a large jet transport aircraft. No claims are made as to it ability to specifically simulate a Boeing 707-120B (or any other aircraft) faithfully. Appendix A shows a number of results from the model validation exercise that was carried out.
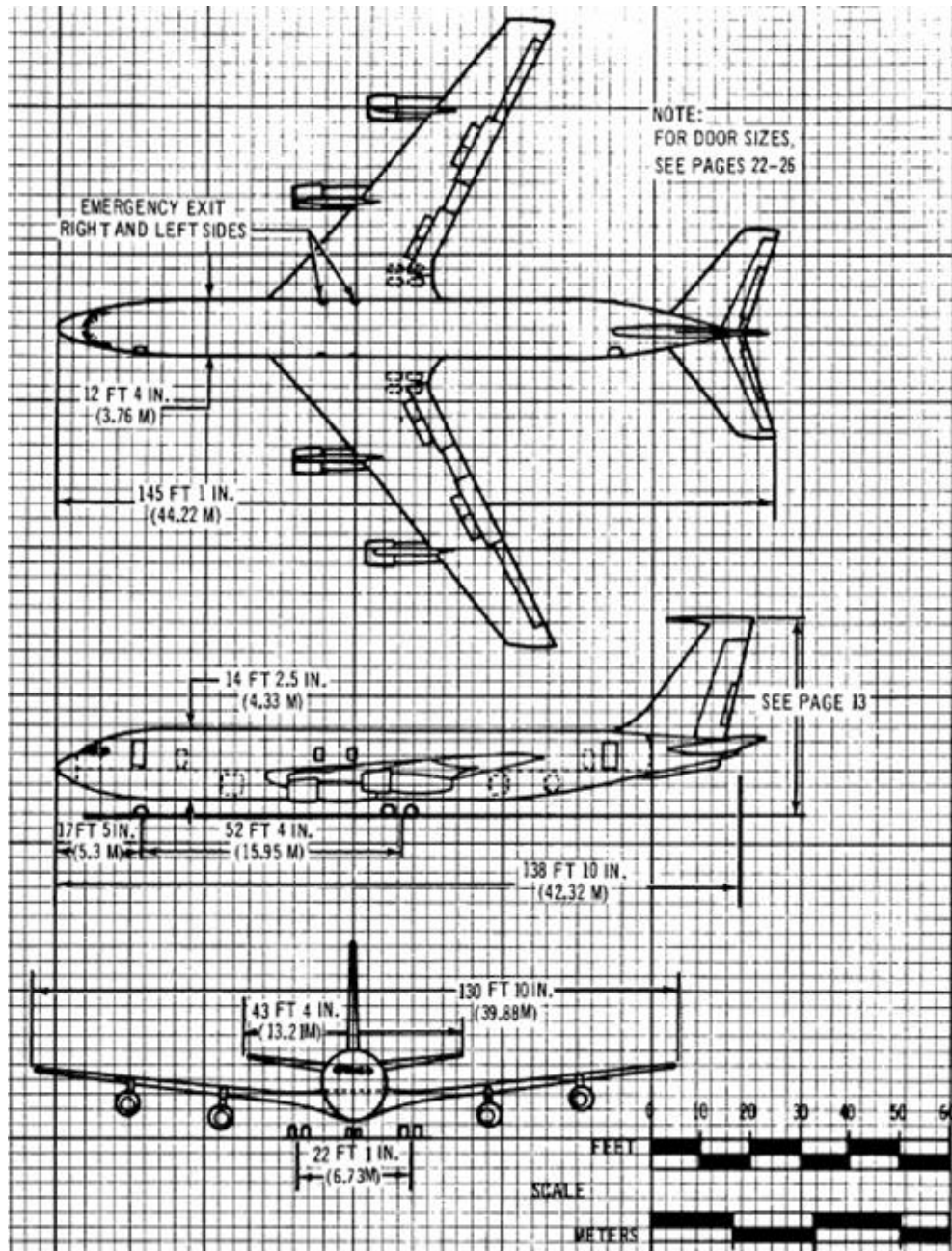

Fig. 3-5. Key Dimensions for Boeing 707-120B

3.3 Mission Task Element Definition for a Jet Transport Aircraft

To be able to evaluate jet transport operations analytically, it is first necessary to break down a typical aircraft sortie into smaller, repeatable flight manoeuvres that can be tested in the laboratory. An accepted way of doing this is to create individual mission task elements (MTE) for the vehicle in question [10, 111]. The process to define individual MTEs is as follows.

First, all aircraft operations can be broken down into types of 'Mission'. A mission can be defined as the purpose for which the aircraft is being utilised [29] e.g. Transport, Training etc.

Second, each mission can be broken down further into a number of 'Phases'. A mission phase can be defined as a portion of the aircraft mission where a specific objective has to be achieved e.g. Take-off, Climb, Cruise, Descend, and Land etc.

Finally, the mission phases can then be further sub-divided into a number of MTEs. An MTE is an individual component of a mission phase that:

1. Has a distinct start and end condition (usually trimmed).

2. Exercises the aircraft's flight or ground-handling characteristics.

The definition of an MTE includes:

1. The operational objectives of the task (including 'desirable' and 'adequate' performance requirements).

2. Piloting requirements, including those needing special attention.

An analysis as outlined above was carried out for fixed-wing aircraft operations and the results pertinent to the research reported in this thesis are detailed in Appendix B. The key jet transport MTEs of interest are also contained in Appendix B.

90

3.4   Experimental Approach

The preceding two Chapters have identified the need for a re-examination of the design of pilot displays, a means by which this might be achieved and the research questions that this approach raises. The preceding Sections have also briefly discussed the experimental apparatus and facilities available to answer these questions. What follows is a description of the experimental regime adopted to conduct the research.

3.4.1   Planned Experimental Regime

It was considered that the most instructive way to formulate relevant guidelines for display design was to go through the design process and discover the learning points/pitfalls through practical experience. A number of individual simulated flight experiments were performed to start to answer the research questions and develop guidelines as follows:

1. Experiment SKYG-FW-0001: The Search for Coherent Tau Motion Gap Closure Relationships. The purpose of this initial investigation was to isolate aircraft state variables for motion gaps being closed during the MTEs described in Appendix B that exhibited coherent τ relationships. In this way, those state variables could be used as design parameters for future display concepts. The objectives of the testing and analysis were:

    a. Identify the key motion gaps that a pilot closes during each MTE of interest.

    b. Establish whether the motion gap is closed using a coherent τ relationship e.g. constant τ, constant rate of change of τ, coupled to τ guide etc.

2. Experiment SKYG-FW-0002a: Detailed Evaluation of the Motion Gap Closures with Coherent Tau Relationships. The purpose of experiment FST-SKYG-FW-0002a was two-fold:

a. To increase the number of sample test points for any MTEs where evidence for coherent τ-based relationships exists in the results of experiment SKYG-FW-0001. If and when such relationships were established:

b. Investigate the degradation of the established τ relationships as the visual scene is degraded.

3. <u>Experiment SKYG-FW-0002b</u>: Eye Tracker Evaluation of the Flare Manoeuvre. Analysis of the flare manoeuvre in the τ-domain has yielded many interesting results during the course of the investigation. An eye-tracking experiment was planned with the following purpose:

    a. To qualitatively assess the pilot's point of gaze during the flare to gain an understanding of the details in the field of view that contribute to any observed coherent τ relationships.

    b. To qualitatively assess how the point of gaze changes during the flare as the visual scene is degraded. In this way, the intention was to try to understand how these changes contributed to any degradation of the observed coherent τ relationships.

4. <u>Experiment SKYG-FW-0003a</u>: Display Design Parameter Shakedown. Having conducted research into the nature of any coherent τ relationships that exist in fixed-wing flight motion gaps, it was then necessary to use the findings of that research to inform the design of cockpit displays. A small number of concepts were developed (see Section 3.5 for details) and the control laws associated with them constructed. However, this left a number of

design parameter values undecided.   The purpose of this experiment was therefore:

    a.   To establish the values of the unknown parameters to allow a 'finalised' display design to be tested and compared with existing design concepts.

    b.   To select which of the flare display concepts should be selected for the final display design.

5.   Experiment SKYG-FW-0003b: Display Design Evaluation. Having finalised the design of the novel display concepts, the final task of the research project was to assess their effectiveness. The assessment would be in terms of both objective measurable aircraft (simulated) flight data parameters and subjective pilot opinion ratings. Identical assessments would also be made for a small number of existing and alternative concept displays. In this way, the ability of the novel concepts to actually assist the pilot with aircraft guidance and the acceptability of its format could be assessed in comparison to alternatives rather than as a stand-alone solution. The purpose of SKYG-FW-0003b was to:

    a.   Assess the capability of the novel approach concept to assist the pilot of a large jet transport aircraft in the guidance task for a range of flight manoeuvres, including non-standard arrivals at an airfield.

    b.   Compare the trajectory control performance of an aircraft flown using the novel approach display concept with that flown using alternative display formats (including the project benchmark display – the BAE Systems 20/20 VGS).

    c.   Assess the capability of τ-based control laws to drive a flare command display concept.

d. Compare the performance of the novel flare command
      display (in terms of vertical touchdown velocity) with flare
      MTEs flown using alternative display formats.

   e. Measure the pilot's ability to control pre-defined trajectory
      parameters and the workload required.

3.4.2   Experimental Design

In line with standard experimental practice, experiments SKYG-FW-0001
and SKYG-FW-0002a started with a hypothesis and the resulting
experiment was designed to test it (them). The starting hypothesis for
these experiments was:

   '*For the motion gap(s) of interest, the pilot closes the gap using a*
   constant rate of change of τ ($\dot{\tau}$).'

The remaining experiments were either more investigative or were
designed to test specific display designs and so did not lend themselves
easily to a 'hypothesis'. In either case, the first stage of the design process
was to identify the specific motion gaps of interest for the MTE in
question. A generic approach profile then had to be constructed for both
standard and non-standard approaches. This naturally led on to a set
defined start conditions for each of the flight test manoeuvres. The results
of this design process are outlined below.

3.4.2.1   MTE Motion Gaps Per Phase of Flight

3.4.2.1.1 Approach

Fig. 3-6 shows the motion gaps of interest for the approach flight phase.
Table 3-2 indicates the motion gap applicability to the approach MTEs.

Approach MTE	Δy	Δlocdev	Δxz	Δgsdev	Δψ
Localiser capture	o	o			o
Glide slope capture			o	o	
Full standard	o	o	o	o	o
Curved		o		o	o

Table 3-2. Spatial Gaps Closed by Pilot During Take-Off MTEs

The localiser can be defined as a line that extends the centre-line of either end of the runway to (±) infinity. The glide slope is a notional flight path angle, γ_{gs}, which takes the aircraft over the threshold of the runway at a nominal 50 ft screen height. The glide slope angle is typically 3.0° [36].
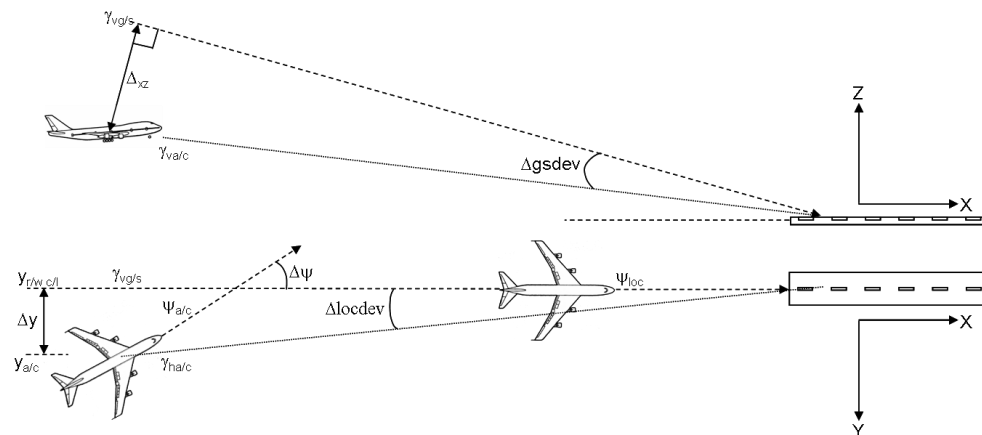
Fig. 3-6. Primary Motion Gaps Closed by Pilot During Full Standard Approach MTE

More extreme examples do exist. For example, due to its location, London City Airport has a glide slope angle of 5.5° [108]. For the purposes of this and all other experiments, the glide slope angle was 3.5°. This angle is steeper than average. It was used to ensure correct vertical ground clearance for the airfield being used in the simulation database.

For normal transport operations, under ideal conditions, an aircraft will be vectored towards the runway localiser with no more than a 30° difference between the aircraft heading, $\psi_{a/c}$ and the runway heading $\psi_{r/w}$[5]. The pilot must then turn the aircraft onto a heading that results in the aircraft track across the ground following that defined by the localiser. For still-air conditions, this will be the same as the runway heading. Where a cross-wind component exists to the prevailing breeze, the aircraft heading and runway heading will be different. For manual flight instrument approaches (MTEs Non-Precision and Precision Approach), this turn will usually be accomplished with reference to the localiser deviation indicator or a flight

---

[5] Based upon discussions with pilots P1 and P2

director. For the Visual Approach MTE, the turn must be made with reference to the view of the outside word available through the aircraft windscreen.

The localiser capture manoeuvre is usually performed first so that the glide slope is intercepted from below, as illustrated in Fig. 3-6[6]. The pilot must transition the aircraft from its current flight path angle (this will usually but not always be zero degrees, i.e. straight and level flight) to the glide slope angle of the runway in question. Again, for instrument-based manual flight, this will be accomplished with reference to either a glide slope deviation indicator or a flight director. Once captured, the glide slope can be maintained both with reference to this instrument and by setting an appropriate rate of descent for the airspeed flown. For visual flight, the moment to transition to descending flight and then maintenance of an appropriate flight-path angle must be judged visually.

3.4.2.1.3 Land
Fig. 3-7 shows the motion gaps of interest for the land MTE.
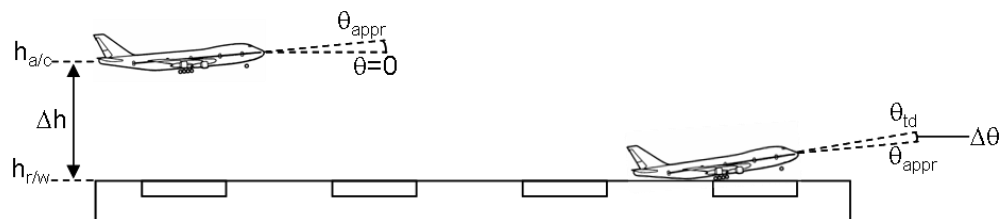
Fig. 3-7. Primary Motion Gaps Closed during the flare MTE

The flare is described in more detail in Appendix B. In brief, during this manoeuvre, the pilot must arrest the aircraft rate of descent from that of the approach to one that will provide a comfortable and safe touchdown. This is achieved by pitching the aircraft nose up to increase the pitch attitude from that of the approach, θ_{appr} to a value at touchdown, θ_{td}. In doing so, the gap between the aircraft height, $h_{a/c}$, and the ground, $h_{r/w}$ is reduced to

---

[6] Based upon discussions with pilot P1

96

zero (and, by implication the vertical descent rate ($\dot{h}$) is reduced from $\dot{h}_{appr}$ to $\dot{h}_{td}$. $\dot{h}_{td}$ is rarely zero for large transport aircraft as pilots are advised to fly the aircraft 'positively' onto the runway surface rather than risk floating just above it [112].

3.4.2.2   Approach Profiles

An approach profile was constructed by pilot P1 that satisfied regulatory authority requirements for terrain clearance etc. for the outside world database to be used during the research. The approach profile is represented schematically in Fig. 3-8.
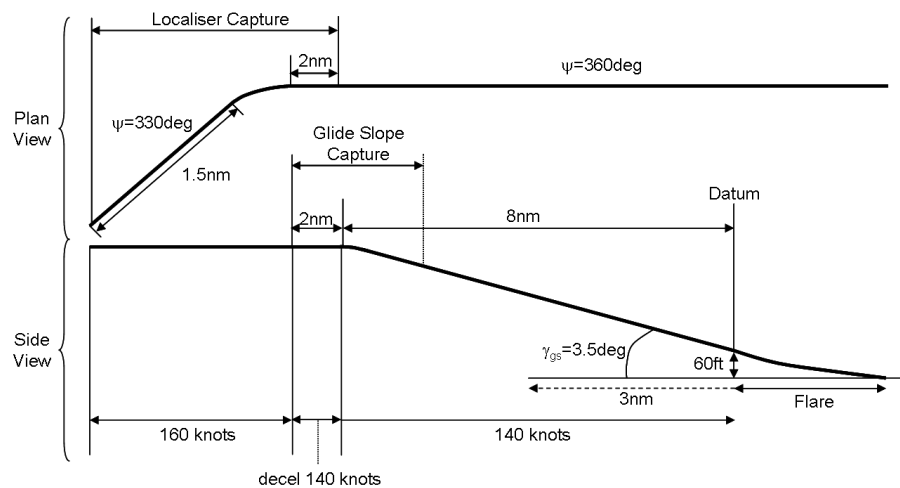
Fig. 3-8. Schematic representation of intend approach profile to airfield

In order that this information could be communicated in a way that professional pilots could assimilate quickly, a set of approach and airfield plates were also constructed by pilot P1 and are shown in Appendix C. These provide all of the information required to navigate around an aerodrome and have been constructed in the same style as would be presented in professional pilot publications such as Ref. [113].

To incorporate a non-standard arrival, a curved approach profile was developed as shown in Fig. 3-9. No approach plates were developed for this
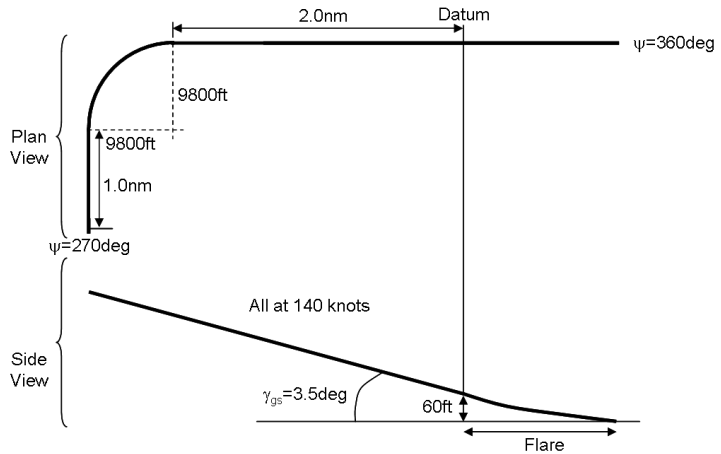
Fig. 3-9. Schematic representation of curved approach profile

approach, rather, the pilots were given a verbal brief prior to any trial sortie.

3.4.2.3   Experimental Start Conditions

Each experiment design incorporated a number of aircraft model start positions. Fig. 3-10 shows the start positions used during this research for
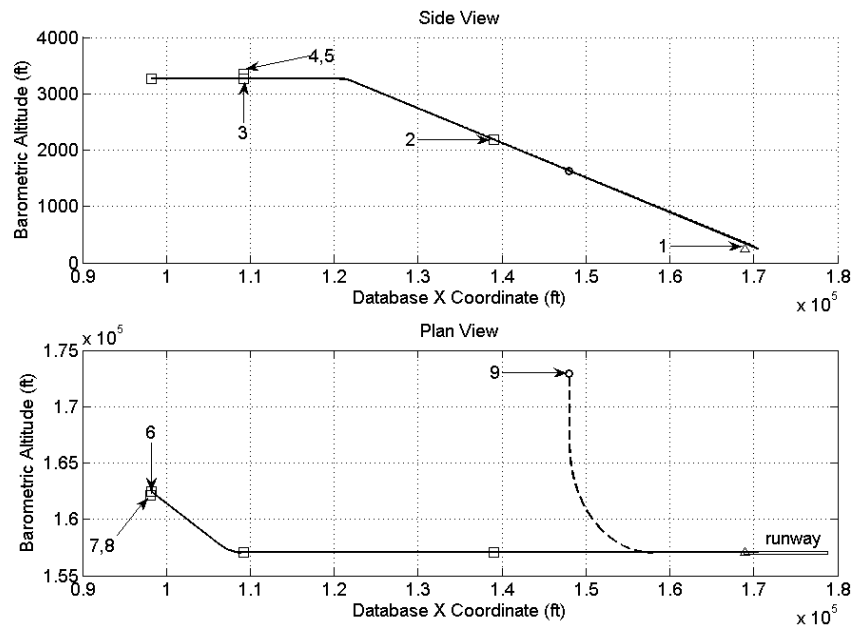
Fig. 3-10. Experimental Inertial Start Positions, standard approach

98

the MTEs incorporated on the standard approach profile (note: positive 'x-coordinate' = North and positive 'y-coordinate' = East).

Table 3-3 provides more detail on the initial conditions. Start conditions 4, 5, 7 and 8 were included to establish the capability of each display to guide the pilot back to nominal 'on condition' track.

No.	Description	Alt AMSL (ft)	IAS (kts)	Heading (deg)	Lateral Offset (ft)	Vertical Flight Path Angle (deg, +ve up)
1	Take-off (not used for work described in thesis)	242	0	360	0	0
2	Flare	1407	140	360	0	-3.5
3	Glide slope capture, on condition	3265	140	360	0	0
4	Glide slope capture, vertical offset	3345	140	360	0	0
5	Glide slope capture, vertical & flight path angle offset	3345	140	360	0	3.5
6	Localiser capture, on condition	3265	160	330	0	0
7	Localiser capture, lateral offset	3265	160	330	360	0
8	Localiser capture, lateral & heading offset	3265	160	320	360	0
9	Curved approach, on condition	1635	140	270	0	0

Table 3-3. Start condition definition for experiment SKYG-FW-0002

For each start condition, the aircraft model was released to pilot control in a trimmed condition. All simulated flight testing was conducted in nil-wind and nil-turbulence conditions.

3.4.2.4   *Experimental Visual Conditions*

The acquisition of BAE Systems' Landscape software allowed the introduction of more realistic degraded visibility outside world scenes into the simulation environment (the previous method used in FST flight vision research projects was to reduce the texture content of the database that makes up that scene). This is achieved by a fog model whereby the user can specify the 'fog distance' which is effectively a visual range. Landscape also allows the introduction of cloud layers and the visual range within that cloud layer can also be specified. Table 3-4 shows the visual ranges and cloud bases used during the research.

Visibility Condition Code	Visibility (ft)	Day /Night	Cloud Base (ft)	Comment	Scene Content
V1	60000	Day	-	Baseline condition	Rich
V2	60000	Night	-	Runway lights only	Impoverished
V3	8000	Day	-	Visual range = one runway length	Rich
V4	4000	Day	-	Visual range = half runway length	Rich
V5	1800	Day	-	Equivalent Category I RVR	Rich
V5b	1800	Day	200	Equivalent Category I RVR	Rich
V6	700	Day	-	Equivalent Category IIIa RVR	Rich
V6b	700	Day	50	Equivalent Category IIIa RVR	Rich
V7	150	Day	-	Equivalent Category IIIb RVR	Rich

Table 3-4. Visibility conditions used during the research project

The visual range achieved was calibrated against that entered in the Landscape set-up scenario files by qualitatively assessing when a test model was just not discernible to the naked eye. Fig. 3-11 outlines the calibration process. A 3D model of a multi-coloured box was created and placed at the required RVR (Fig. 3-11(a)). The fog range was then adjusted within Landscape such that all of the coloured segments on the box were obscured from view (Fig. 3-11(b)). This iterative process only had to be carried out once per visual condition and then could be saved in a configuration file for use during the research flight trials.
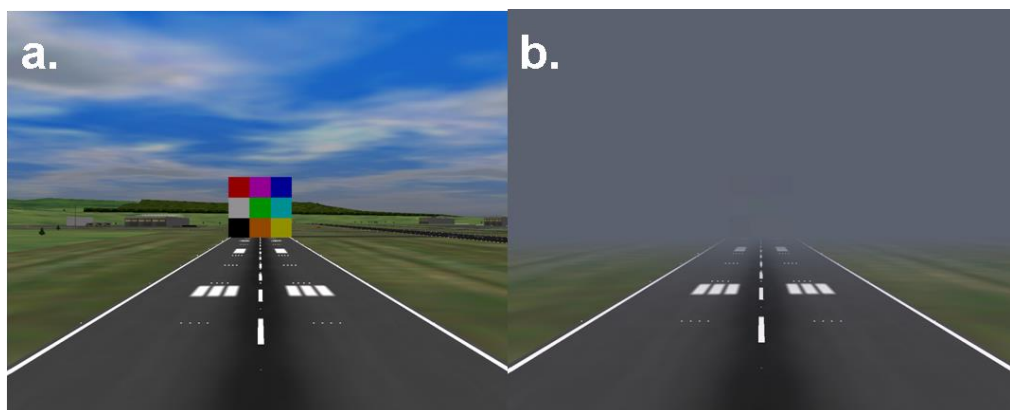
Fig. 3-11. Degraded visual environment calibration process

The visual scene presented to the pilot if the aircraft were crossing the runway threshold at a radar altitude of 50ft for the different visibility conditions of Table 3-4 are shown in Fig. 3-12-Fig. 3-18. Fig. 3-12 shows

the cockpit view at the runway threshold for visibility condition V1. The runway edges 'warp' slightly as the figures that follow are a flat 2D representation of what is, in essence, a scene that should 'wrap-around' the viewer.

Fig. 3-12. Visual condition V1

Fig. 3-13 shows the cockpit view at the runway threshold for visibility condition V2.
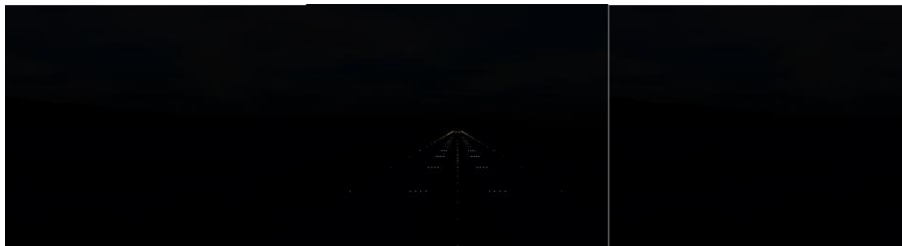
Fig. 3-13. Visual condition V2

Fig. 3-14 shows the cockpit view at the runway threshold for visibility condition V3.

Fig. 3-14. Visual condition V3

Fig. 3-15 shows the cockpit view at the runway threshold for visibility condition V4.

Fig. 3-15. Visual condition V4

Fig. 3-17 shows the cockpit view at the runway threshold for visibility condition V5 and V5b.

Fig. 3-17. Visual condition V5 and V5b

Fig. 3-17 shows the cockpit view at the runway threshold for visibility condition V6 and V6b.

Fig. 3-16. Visual condition V6 and V6b

Fig. 3-18 shows the cockpit view at the runway threshold for visibility condition V7.

Fig. 3-18. Visual condition V7

The point should be made that even in the simulated good visual environment (V1, Fig. 3-12), the pilots visual environment is already degraded by the simulator framework (which is analogous to the windscreen frame in a real aircraft). Fig. 3-12-Fig. 3-18

Fig. 3-19. Visual scene as viewed from within the Bibby flight simulation facility

are not truly representative of the pilots view as they are amalgamated screen shots of the three out-the-window visual channels of the simulator. Fig. 3-19 shows the inside of the simulator and gives some indication of the degradation in the visual scene caused by its framework.

The 'Categories' given in Table 3-4 refer to the aircraft operating minima for making an approach and landing to a runway. The Runway Visual Range (RVR) values used for the trial test points were taken from Ref. [27]. Where a cloud base setting has been specified, this equates to the decision height (DH) for that category, assuming a precision approach is being flown. Category IIIb landings have no decision height. 'Rich' scene content refers to the use of a highly detailed outside world database in terms of both texture and objects in the scene. This effectively meant that the approach was carried out during the day in a good visual environment. The 'impoverished' scene used the same database but was not 'lit', so all objects appeared black. The only objects visible to the pilots were a set of runway lights that provided an outline of the runway and that also marked its centre-line. For the night case, the visibility was 'unlimited' at 60km but there simply was not much to see. Of course, for the degraded visual condition test cases, the texture and object detail of the outside world database is obscured to a greater or lesser degree by the fog model.

3.4.3   Experimental Procedure

The implementation of each experiment might be considered to only be the running of a flight simulation trial itself. However, a number of individual tasks were undertaken per trial as follows.

1. Pilot Briefing. Prior to the simulation trial, the pilots due to fly were sent a written brief outlining the objectives of the session, the MTEs to be flown with their respective 'desirable' and 'adequate' performance criteria. Immediately prior to flying a sortie, this briefing was repeated orally. This provided all involved with an opportunity to discuss and resolve any outstanding queries.

2. Experiment - learning and measurement phases. Each MTE was conducted a number of times prior to collecting any results. The initial runs allowed the pilot to familiarise himself with the general handling of the aircraft simulation model during the MTE and the layout of the outside world database (airfield, terrain etc,) being used. Once the pilot was satisfied that the MTE could be conducted in a manner representative of a real aircraft manoeuvre, then data was collected for the MTE.

3. Questionnaire/Pilot Rating. At the end of each MTE test flight, the pilot was asked to provide ratings and comments regarding the performance of the aircraft simulation model in response to a questionnaire. Section 3.4.4.4 deals with this topic in more detail.

4. De-brief. At the end of each test day, a de-brief session was conducted to allow the pilot to elaborate on and summarise any comments made during the trial and to allow the experimenter to clarify any issues raised.

3.4.4   Experimental Analysis

Raw data obtained from the experimental flight simulation trials have been subjected to a variety of analyses. This Section briefly describes each of these analyses.

3.4.4.1   Basic Tau Analysis

Having identified the motion gaps of interest per MTE, the τ of that gap has to be calculated to ascertain whether or not any coherent relationships existed. The process for doing this was:

1. Identify motion gap closures from the simulated flight time-histories.

2. Identify the 'target' motion gap variable value i.e. the value of the data variable that, when reached, the motion gap can be considered to have been closed.

3. Calculate the value of the motion gap, its rate of change and hence the τ of that gap.

4. Plot the τ time-history for the gap closure.

The process is best illustrated by an example. Fig. 3-20(a) shows the
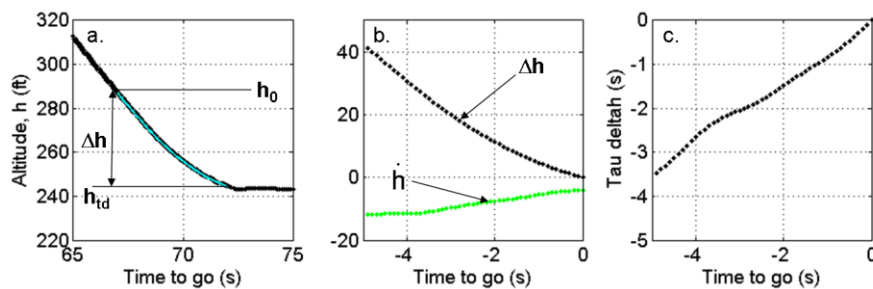
Fig. 3-20. Example τ analysis process

aircraft cg height time history for a flare and land manoeuvre. At the flare initiation height, h_0, the pilot pitches the aircraft nose up to reduce the rate of descent until touchdown on the runway surface at h_{td}. The motion gap can now be defined as:

105

$$\Delta h = h_{td} - h \qquad\qquad (3\text{-}2)$$

(Fig. 3-20(b)) and $\tau_{\Delta h}$ calculated as:

$$\frac{\Delta h}{\dot{h}} \qquad\qquad (3\text{-}3)$$

(Fig. 3-20(b) and (c)).

3.4.4.2   Residual Velocity Analysis

The research has been primarily concerned with decelerative or constant velocity motion gap closures. Section 2.4.1.5 has already discussed the consequences of the observer not possessing the decelerative capability required to maintain a constant $\dot{\tau}$ closure strategy. It has been shown that when such limiting deceleration values are applied, the gap target is reached with a residual rather than zero velocity and that for a given limit, a pseudo-linear relationship exists between the residual velocity and the value of $\dot{\tau}$ used. Flare manoeuvres rarely end with zero vertical velocity. As such, the relationship between touchdown velocity and $\dot{\tau}_{\Delta h}$ was investigated, primarily to establish whether τ theory could be used as a basis to first predict and then define a touch down velocity for a landing manoeuvre.

3.4.4.3   Trajectory Performance Analysis

In order to be able to objectively compare the performance of each of the display formats tested, the trajectory of each MTE test point is compared to the target value and the desired and adequate performance boundaries of the MTEs defined in Appendix B. 'Trajectory' information is defined here to mean inertial 'x', 'y' and 'z' position, IAS, localiser and glide slope angle deviations and touchdown velocity at touchdown.

In order to gather sufficient comparative results, a relatively large number of test points have been conducted over the course of the research. To plot

each trajectory analysis individually would make this document unwieldy. The data is therefore summarised by two processes:

1. Averaging. Where a target value for a parameter, 'x', is defined, the average value of that parameter ($\overline{x}$) is calculated for the duration of each of the test points conducted for a particular MTE. This averaged value provides an indication of how close the pilot was able to maintain the aircraft to target throughout each MTE.

2. Standard Deviation (s.d., σ). The standard deviation from the average value is calculated against the target value for a given MTE. This provides some measure of the scatter of the parameter from the calculated mean [114]. All of the data recorded has been used in this calculation and so the s.d. has been calculated using the general formula:

$$\sigma = \sum_{1}^{n} \frac{(x - \overline{x})^2}{n} \tag{3-4}$$

where 'n' is the number of readings taken.

3.4.4.4   Pilot Ratings

To complement the objective assessment of the display format performance, subjective pilot ratings were provided by each test pilot used. Two rating scales are used, both based upon the Cooper-Harper flight handling qualities rating scale [115]. These are:

1. Display flyability/controllability [116]. This scale provides a subjective measure of the adequacy of the display dynamics during the selected task or manoeuvre and is shown in Appendix D.

2. Bedford Workload Scale [117]. This scale provides a subjective measure of the workload experienced by the pilot during the MTE and is shown in Appendix D. It does this by asking the pilot to

consider how much spare capacity for other tasks was available during the MTE.

These scales were selected as the pilots used during the research were familiar with the Cooper-Harper rating format/style which provides a less complex method of obtaining rating information than, for example the NASA TLX workload assessment method of Ref. [118].

In order to be able to present the results of this type of assessment, individual ratings per pilot and per MTE have been averaged. In some cases, this results in non-integer values which strictly, do not make sense as the scales are ordinal in nature. However, the values being averaged are never more than 2 rating scale points different and so the averaging process provides an indication of the relative values assigned to each display without masking extreme differences in assigned ratings

3.4.4.5   *Eye Tracking Analysis*

To complement primarily the objective trajectory performance analyses and the subjective pilot assessments, eye tracking analyses were conducted for the approach and flare MTEs. The eye-tracking system provided raw point of regard data i.e. where it calculated that the eye was pointing at a given moment. The eye of an observer may be pointing in a particular direction but this does not necessarily mean that anything is being looked at or seen. The eye may not be 'fixated' on that part of the image. The eye-tracking software therefore also performs a 'fixation analysis'. That is, a position is only considered to be being 'looked at' if the point of regard remains in a small region for a pre-defined amount of time. For the results presented in this thesis, the default fixation settings were used. This means that a fixation was recorded of the point of regard remained within one degree of visual angle for a minimum of 100ms.

3.5   Display Development

3.5.1   Display Design Principles

Before commencing a description of the cockpit displays developed for the research, it is first necessary to describe the general principles on which such a display is based. The displays used were both 'head-down' and 'head-up'. In the latter case, where appropriate, the symbols were conformal with the outside world. Conformal symbology means that viewing angles are preserved so the symbol appears on a display where it would appear in the visual field if the pilot were simply looking through the aircraft windscreen.
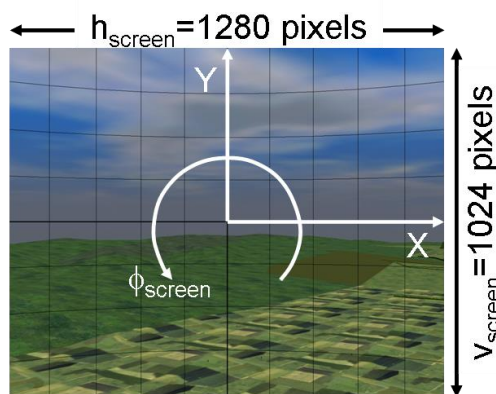
Fig. 3-21. Display Coordinate System

The first issue to understand, therefore, is that the view of the outside world corresponds to a set of horizontal and vertical viewing angles. Fig. 3-21 shows the forward view, as seen by the pilot, divided into a grid of 5-degree vertical and horizontal lines.

The second issue to comprehend is that these viewing angles must be mapped onto the coordinate system being used to generate the display symbology. For the purposes of the research reported in this document, the symbol coordinate system and screen dimensions used are shown overlaid on the viewing angles in Fig. 3-21.

109

In order to position display symbols conformally, a basic understanding of how aircraft angles in flight correspond to features in the outside world visual scene. These are shown in Fig. 3-22. From top to bottom, the 'gull-wing' symbol is the aircraft bore-sight and can be thought of as the direction in
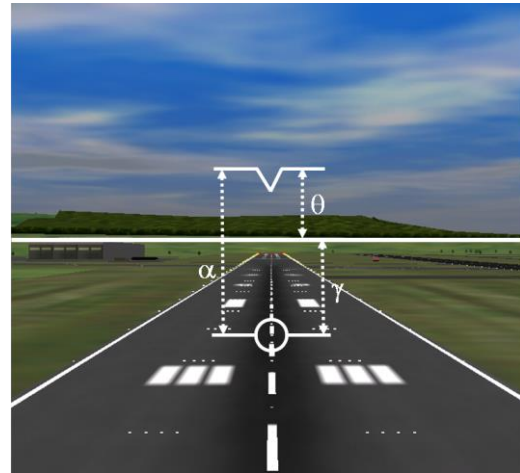
Fig. 3-22. Key aircraft display angles

which the aircraft nose is pointing. The horizontal line represents the zero pitch angle position and the aircraft symbol provides flight path vector information i.e. the direction in which the aircraft is actually moving. The aircraft pitch angle (θ), incidence angle (α) and flight path angle (γ) are marked in relation to these symbols.

Finally, it must be recognised that a correction has to be made to the display coordinates to account for aircraft roll. Any calculated display x-y coordinates must be converted to the coordinate system x'-y' that accounts for aircraft roll using the following transformation:

$$x' = x\cos(-\phi) + y\sin(-\phi) \qquad (3\text{-}5)$$

$$y' = -x\sin(-\phi) + y\cos(-\phi) \qquad (3\text{-}6)$$

3.5.2   Specific Displays Developed

The displays developed during the course of the research can be divided into two groups:

1. Novel displays developed as a consequence of the research effort. These are denoted LEAD and LEAD* throughout this document. In brief, these formats consisted of:

a. A 'lead aircraft' symbol to provide an indication of the desired trajectory t_{pred} seconds in the future. This symbol also provided a speed cue by looming as would a real lead aircraft if the chase aircraft's speed did not match its own.

b. A 'predictor aircraft' symbol that provided the pilot with an indication of the aircraft position t_{pred} seconds hence.

c. A flare command algorithm to bring the aircraft into contact with the runway surface at an acceptable rate.

d. The LEAD* differs from the LEAD format in that a digital IAS value is also displayed to the pilot.

2. Displays developed to provide comparative data for the novel formats. These are:

a. a generic basic glass cockpit primary flight display (denoted PFD);

b. the BAE Systems' 2020 Visual Guidance System (denoted VGS)

c. and a rudimentary highway-in-the-sky display (denoted HITS).

The detailed development of these displays is described in Sections 3.5.3 and 3.5.7.

3.5.3 Lead-predictor Concept

3.5.3.1 Background

It is clear from the discussion in Section 1.1 that aircraft will be increasingly required to follow constrained, predictable trajectories. One way to follow a predictable path is to follow something that is taking the same path. Furthermore, if the lead object's aspect remains constant, the speed of the observer must also be constant i.e. if the chase object gets no nearer or farther away, the shape and form of the lead object will remain

constant in size (assuming the object to be solid and fixed in shape). For example, when driving (at a safe distance) behind another vehicle on a motorway, by maintaining the lead car at a fixed aspect in the window, the chase car will follow the lead car's path at the same speed. If the lead car pulls away, its visual angle (the angle subtended at the eye by, for instance, its left and right tail lights) will decrease and vice-versa. This is an example of optical looming. It follows, therefore, that if the pilot is presented with the position of a lead aircraft at some time ahead of his own, t_{pred}, plus information about his own aircraft's (the 'chase' aircraft) position at that same time ahead, then by overlaying the two, the chase aircraft will follow the prescribed trajectory of the first. Additionally, if the lead aircraft symbol is allowed to expand and contract, then information should be available to the pilot regarding the chase aircraft's actual speed in relation to the desired lead aircraft's speed. These principles form the basis for the lead-predictor concept tested during the research. The looming concept is illustrated in Fig. 3-23 (note, arrows included for illustrative purposes only).

A question immediately arises regarding whether this concept is a useful one. Informal discussions with pilots P1 and P2 revealed that
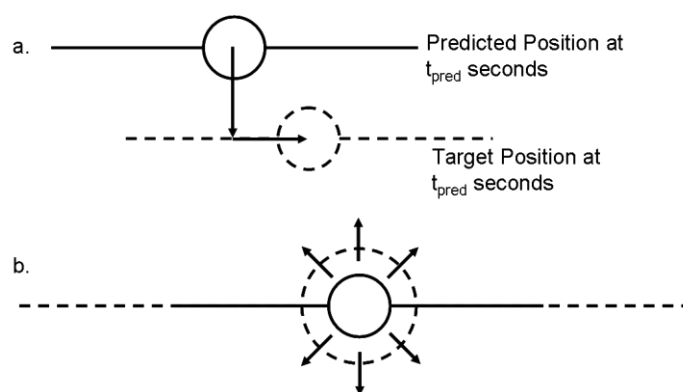
Fig. 3-23. Predictor-lead symbol concept showing (a) current predicted position high and left of target and (b) chase aircraft speed high compared to target

formation flying is one of the hardest tasks that they can be asked to perform. However, the pilots were from a military background and were referring to tight formation tactical low-level flying, in-flight re-fuelling or display flying. In both cases, the lead and chase aircraft are much less than

a second and only a matter of a few feet away from each other. At the other extreme, self-fly aircraft safaris are available to private (and hence often inexperienced) pilots (e.g. Ref. [119]) where the primary means of navigation for all but the lead participant is to follow the aircraft in front. Of course, this is at much lower airspeeds and the difference in time measured in fractions of minutes. Prior to t_{pred} being fixed, it was anticipated that the required prediction time would be some value between these two extremes.

3.5.3.2 Symbol Set
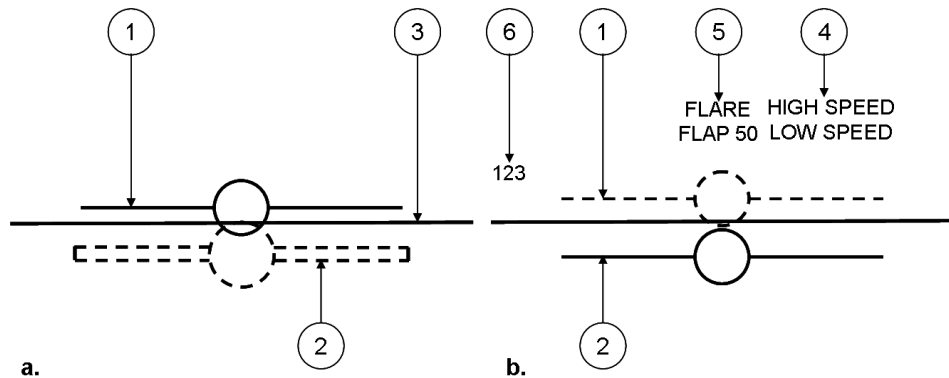
Fig. 3-24. Lead-predictor display concept evolution: (a) original (LEADI) and (b) final (LEAD AND LEAD*) design concepts

Fig. 3-24 illustrates the evolution of the lead-predictor concept display set and Table 3-5 defines, for the final display format, each symbol's purpose.

Symbol	Description	Purpose	Used on Display
1	Lead aircraft [note1]	Provide target trajectory and airspeed cueing	LEADI, LEAD, LEAD*
2	Aircraft predicted position	Provide actual trajectory and airspeed cueing	LEADI, LEAD, LEAD*
3	Horizon line	Provide aircraft pitch and roll attitude cueing	LEADI, LEAD, LEAD*
4	Speed annunciations	Indicate to pilot when 5 & 10 knots above/below target[note2]	LEAD, LEAD*
5	Pilot information annunciations	Indicate to pilot to set land flap and flare initiation [note3]	LEAD, LEAD*
6	Indicated airspeed	Provide IAS	LEAD*

Table 3-5. Novel concept display symbol definition

Note:

1. All symbols coloured green as per current HUD practice.

2. When $5 \leq \left| \text{IAS}_{\text{actual}} - \text{IAS}_{\text{t arget}} \right| < 10 \, \text{knots}$, symbol 2 starts to flash and symbol 4 (with 'HIGH' or 'LOW' as appropriate) appears and flashes simultaneously. When $\left| \text{IAS}_{\text{actual}} - \text{IAS}_{\text{t arget}} \right| \geq 10 \, \text{knots}$, both symbols turn green → red. These symbols were primarily added to assist the pilots with the provision of ratings.

3. FLAP 50 indicated to remind pilot to perform this action following turn onto localiser for 5 seconds (flashing). FLARE indicated (flashing) 3 seconds prior to pitch up for flare to warn pilot that this was about to happen.

3.5.3.3 Display Control Algorithms

The specific idea for this symbol set is to provide translational guidance information to the pilot of the chase aircraft via the relative positions of the lead and predictor aircraft symbols on the screen. Changes in chase aircraft translational location are driven by constant $\dot{\tau}$ trajectory gap closures. Timing guidance is provided via the chase aircraft symbol looming when compared to the lead aircraft as it would if there were a real aircraft ahead. Finally, a general indication of roll and pitch attitude is provided by an artificial straight-line horizon. By implication, these symbols need to be conformal with the outside world. The following Sections describe the algorithms used to drive each symbol.

3.5.3.3.1   Horizon Line

To position the horizon line correctly on the display screen, it is necessary to consider the forward view as being made up of a series of viewing angles. For the horizon line, only the vertical depression or elevation angle (and hence the horizontal grid lines) are of concern. The positioning of the horizon line symbol was calculated based upon the negative value of the aircraft Euler pitch angle, θ. If the screen has a vertical resolution of v_{screen} pixels and a vertical viewing angle of δ_{maxvert} degrees, then the vertical

114

position of the horizon line $v_{horizon}$, where the symbol origin is at the middle-centre of the screen is computed as:

$$v_{horizon} = -\theta \times \frac{v_{screen}}{\delta_{max\,vert}}$$

(3-7)

3.5.3.3.2 Lead Aircraft Symbol

The lead aircraft symbol requires four values:

1. x-coordinate position on display screen;

2. y-coordinate position on display screen;

3. roll angle of lead aircraft and

4. scale at which to display.

The start point for the calculation of the x- and y-coordinates was to define the trajectory to be followed in terms of database x, y, z coordinates and aircraft roll angle, ϕ. Fig. 3-25 shows the nominal 3-D full standard
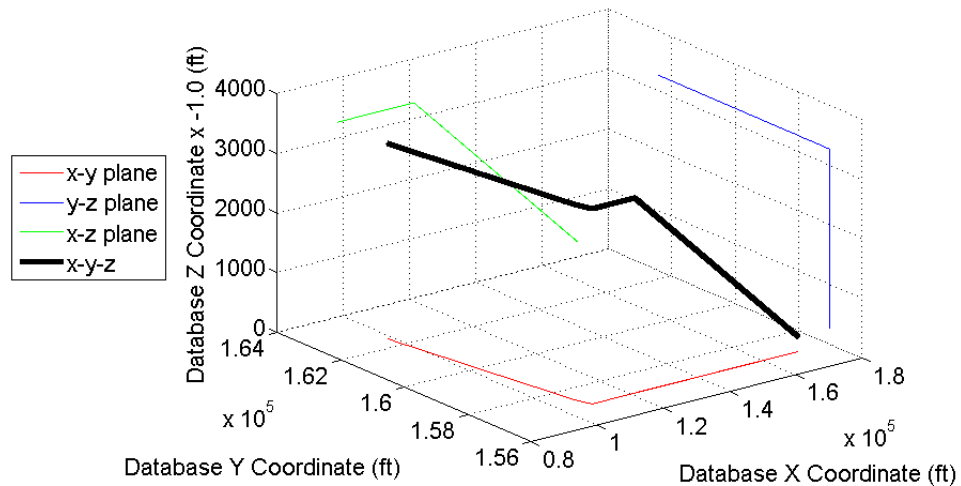
Fig. 3-25. Example full approach profile in inertial coordinates

approach trajectory in the database x,y,z coordinate system. The equivalent 2-D plots of the data are also shown in the figure to more fully illustrate the trajectory (N.B. the axis scales are not equal so the trajectory

115
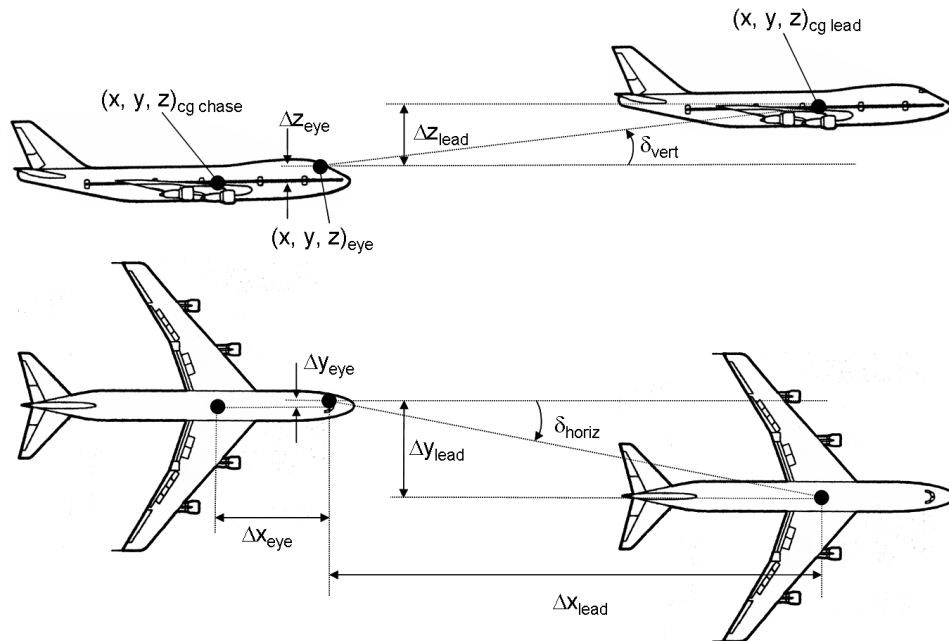
Fig. 3-26. Definition of variables used to compute screen position of lead aircraft symbol
proportions are distorted with respect to reality). The trajectory for the
Curved Approach MTE is shown in Appendix B. Each portion of the
approach was calculated at a specified true airspeed. The localiser glide
slope capture phase trajectories were calculated as motion gaps closed
using constant $\dot{\tau}$ strategies. These trajectory data are loaded into the
aircraft model as a table. For any simulation time step, the positions of the
centre-of-gravity of both the lead and the chase aircraft are known. The
calculation to ascertain the screen position of the lead aircraft can then
proceed as follows, with reference to Fig. 3-26:

1. Calculate pilot eye position in database (inertial) coordinates. The
   offset values for the pilot eye position from the modelled aircraft
   centre of gravity ((Δx, Δy, Δz)$_{eye}$) are known in body coordinates:

$$\begin{bmatrix} x_{eye} \\ y_{eye} \\ z_{eye} \end{bmatrix}_{body} = \begin{bmatrix} x_{cgchase} \\ y_{cgchase} \\ z_{cgchase} \end{bmatrix}_{body} + \begin{bmatrix} \Delta x \\ \Delta y \\ \Delta z \end{bmatrix}_{eye} \tag{3-8}$$

116

The pilot eye position coordinates of the chase aircraft can now be converted into inertial coordinates through the usual transformation:

$$\begin{bmatrix} x_{eye} \\ y_{eye} \\ z_{eye} \end{bmatrix}_{int\,ertial} = [D]^{-1} \begin{bmatrix} x_{eye} \\ y_{eye} \\ z_{eye} \end{bmatrix}_{body} \tag{3-9}$$

Where $[D]^{-1}$ is defined for an aircraft at an Euler pitch angle θ, Euler roll angle, ϕ and Euler yaw angle, ψ as [120]:

$$[D]^{-1} = \begin{bmatrix} \cos\psi\cos\theta & \cos\psi\sin\theta\sin\phi & \cos\psi\sin\theta\cos\phi \\ & -\sin\psi\cos\phi & +\sin\psi\sin\phi \\ \\ \sin\psi\cos\theta & \sin\psi\sin\theta\sin\phi & \sin\psi\sin\theta\cos\phi \\ & +\cos\psi\cos\phi & -\cos\psi\sin\phi \\ \\ -\sin\theta & \cos\theta\sin\phi & \cos\theta\cos\phi \end{bmatrix} \tag{3-10}$$

2. Calculate the x, y and z offsets of the lead aircraft c.g. from the chase aircraft pilot eye position.

$$\begin{bmatrix} \Delta x_{lead} \\ \Delta y_{lead} \\ \Delta z_{lead} \end{bmatrix}_{inertial} = \begin{bmatrix} x_{cglead} \\ y_{cglead} \\ z_{cglead} \end{bmatrix}_{inertial} - \begin{bmatrix} x_{eye} \\ y_{eye} \\ z_{eye} \end{bmatrix}_{inertial} \tag{3-11}$$

3. Calculate the horizontal and vertical visual angles of the lead aircraft c.g. from the chase aircraft pilot eye position.

$$\delta_{horiz} = a\tan\left(\frac{\Delta y_{lead}}{\Delta x_{lead}}\right) \tag{3-12}$$

$$\delta_{vert} = a\tan\left(\frac{\Delta z_{lead}}{\Delta x_{lead}}\right) \tag{3-13}$$

4. Calculate the screen x and y coordinates for the symbol. If the screen has a horizontal resolution of h_{screen} pixels and a horizontal

viewing angle of $\delta_{maxhoriz}$ degrees, then the horizontal position of the chase aircraft symbol, h_{chase}, where the symbol origin is at the middle-centre of the screen is computed as:

$$h_{lead} = \delta_{horiz} \times \frac{h_{screen}}{\delta_{max\,horiz}}$$ (3-14)

Similarly, if the screen has a vertical resolution of v_{screen} pixels and a vertical viewing angle of $\delta_{maxvert}$ degrees, then the vertical position of the chase aircraft symbol, v_{chase} is given by:

$$v_{lead} = \delta_{vert} \times \frac{v_{screen}}{\delta_{max\,vert}}$$ (3-15)

5. Compensate the screen x and y coordinates for any chase aircraft roll angle using Eqs. (3-5)and (3-6) with x=h_{lead} and y=v_{lead}.

$$\phi_{lead} = \phi_{leaddmd} - \phi_{chase}$$ (3-16)

The display concept also calls for the lead aircraft symbol to provide some indication of roll angle during any turn manoeuvres. The symbol cannot simply be rolled through the required angle because account must also be taken of the chase aircraft roll angle from which the lead aircraft is being 'viewed'.

The scale of the symbol was driven by the idea that the symbol should be as simple and yet as realistic as possible. To provide as realistic an impression as possible of the lead aircraft with only a 2-D aircraft symbol, it was considered necessary to provide an image that appeared to be, in at
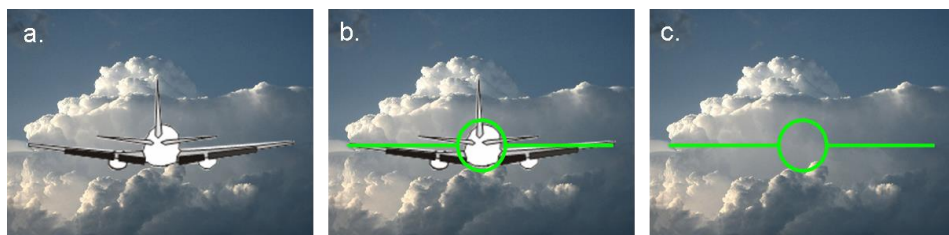
Fig. 3-27. Illustration of the concept for sizing the lead aircraft guidance symbol: (a) lead aircraft as it would appear; (b) lead aircraft symbol matched to real lead aircraft wing span visual angle and (c) lead aircraft as it appears to the pilot
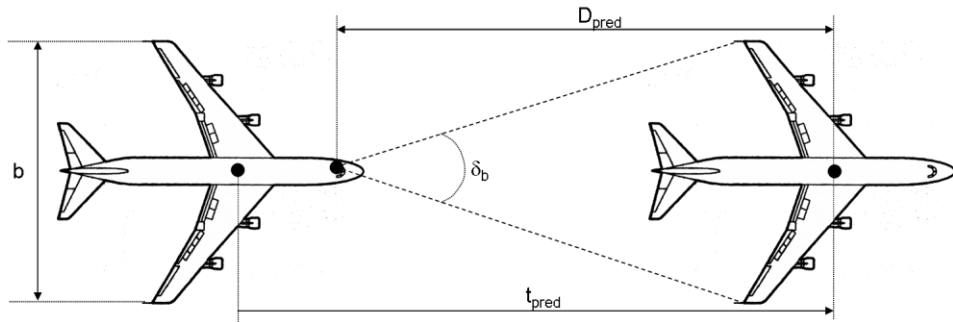
Fig. 3-28. Definition of parameters used to compute scaling factor for lead aircraft symbol

least one dimension, the actual size that the lead aircraft would be at a time t_{pred} ahead of the chase aircraft. The dimension chosen to be matched was wing span since this is the major dimension illustrated in a 2D symbol. The animated symbol has a wing span that provides a visual angle subtended at the observer as would be by a real lead aircraft. This concept is illustrated in Fig. 3-27. The calculation to perform the scaling of the lead aircraft is performed as follows, with reference to Fig. 3-28:

1. Compute the visual angle of the lead aircraft wingspan.

$$\delta_b \cong a \tan\left(\frac{b}{2D}\right) \tag{3-17}$$

where b, the lead aircraft wing span is known and taken as 130.8ft which is the GLTA model wing span taken from Ref. [121].

2. Compute the screen scaling factor, σ_b, to apply to the lead aircraft graphical symbol. This is achieved by knowing that when the scale factor is 1.0, the symbol wing tips touch the screen edges, which provides a horizontal viewing angle of 48 degrees.

$$\sigma_b = \delta_b \times \frac{v_{screen}}{\delta_{max\ horiz}} \tag{3-18}$$

119

3.5.3.3.3 Predictor Aircraft Symbol

The predictor aircraft symbol requires the same 4 pieces of information as the lead aircraft symbol. However, the method by which these values are obtained differs from that defined in Section 3.5.3.4.2 for the lead aircraft symbol. A prediction time, t_{pred}, has to be defined to establish how far ahead the predictor aircraft should be placed. Of course, this 'look ahead' time then has to be matched to the lead aircraft start position for any given
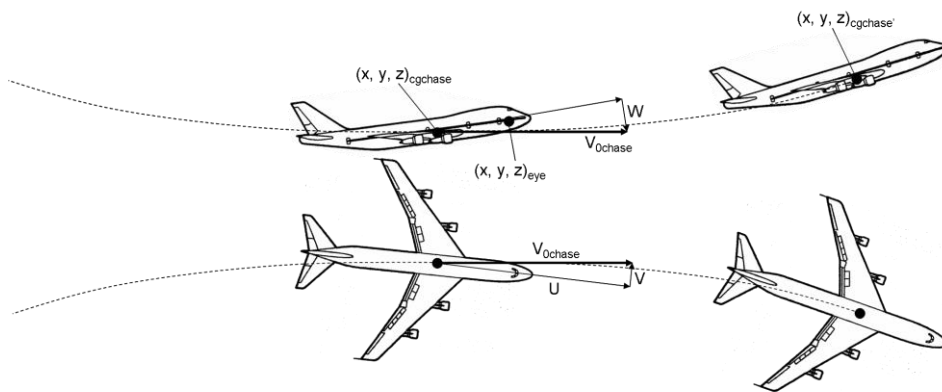
Fig. 3-29. General illustration of aircraft motion parameters used to define predictor symbol algorithm

trial test point. Once t_{pred} is defined, the calculation for the translational of the aircraft can proceed for the general case shown in as follows:

1. Compute the horizontal and vertical translational offsets through which the aircraft will travel assuming constant acceleration over the next t_{pred} seconds.

$$\begin{bmatrix} \Delta x_{cgpred} \\ \Delta y_{cgpred} \\ \Delta z_{cgpred} \end{bmatrix}_{body} = \begin{bmatrix} u \\ v \\ w \end{bmatrix} t_{pred} + \frac{1}{2} \begin{bmatrix} \dot{u} \\ \dot{v} \\ \dot{w} \end{bmatrix} t^2_{pred} \tag{3-19}$$

2. Convert these offsets into inertial coordinates.

$$\begin{bmatrix} \Delta x_{cgpred} \\ \Delta y_{cgpred} \\ \Delta z_{cgpred} \end{bmatrix}_{int\,ertial} = [D]^{-1} \begin{bmatrix} \Delta x_{cgpred} \\ \Delta y_{cgpred} \\ \Delta z_{cgpred} \end{bmatrix}_{body} \tag{3-20}$$

120

$$\Delta\phi_{pred} = \dot{\phi}t_{pred} + \frac{1}{2}\ddot{\phi}t_{pred}^2 \tag{3-21}$$

Where $[D]^{-1}$ is defined in Eq. (3-10).

3. Compute the predicted aircraft centre of gravity inertial position based upon current inertial position plus prediction of translational offsets.

$$\begin{bmatrix} x_{cgchase'} \\ y_{cgchase'} \\ z_{cgchase'} \end{bmatrix}_{inertial} = \begin{bmatrix} x_{cgchase} \\ y_{cgchase} \\ z_{cgchase} \end{bmatrix}_{inertial} + \begin{bmatrix} \Delta x_{cgpred} \\ \Delta y_{cgpred} \\ \Delta z_{cgpred} \end{bmatrix} \tag{3-22}$$

4. The computation can now proceed as for the lead aircraft from Eq. (3-12), the pilot eye position having already been calculated in Eq. (3-9), substituting $[X]_{cgchase}$ for $[X]_{cglead}$.

The chase aircraft would be indicating roll angle to the pilot and so the predictor aircraft would also be required to indicate roll angle. A similar scheme to the translational prediction routines was implemented. This simply estimated the increment in roll angle that would be achieved at current roll rate and acceleration:

The scale of the predictor aircraft symbol is calculated in the same manner as for the lead aircraft symbol. However, in Eq. (3-17), the distance ahead used to calculate the scale parameter is not calculated from a pre-computed track but is obtained using:

$$D_{pred} = V_0 t_{pred} \tag{3-23}$$

3.5.3.4 Display Validation

Prior to any formal assessments, it was necessary to ensure that the algorithms were functioning correctly and that the display symbology was being positioned on the display screen appropriately. In addition, although not always explicitly mentioned in the algorithm development, a number of approximations have been included as follows:

1. The horizon line algorithm of Eq. (3-7) is valid at the aircraft cg but the actual flight simulation viewing point is ahead and above the aircraft cg (in aircraft body axes).

2. The scaling algorithm is only truly valid if the simulation viewing position were on the notional fuselage longitudinal centre-line. The eye point is actually offset to the left (to model the pilot sitting the captain's seat).

The effect of these approximations needed to be assessed and this exercise was conducted during the initial testing phase of the algorithms and display symbology. The results are presented in the following Sections.

3.5.3.4.1 Horizon Line

Fig. 3-30 shows a small number of screen shots taken during the development of the positioning of the horizon line (the line has been
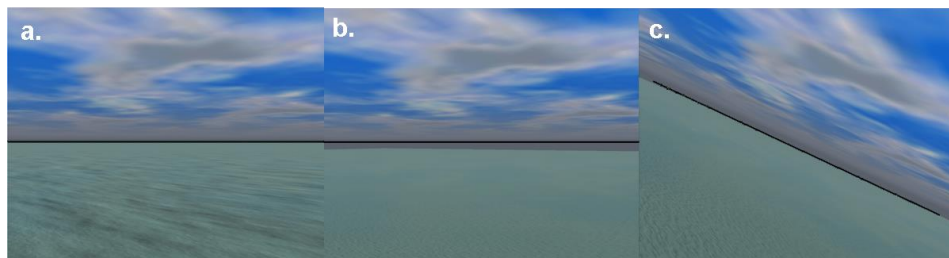
Fig. 3-30. Development of horizon line algorithm

artificially enhanced for the sake of clarity). A seascape was chosen for this exercise as, by default, this represented zero altitude for the scenery database and there were no hills to confuse the issue of horizon placement. Fig. 3-30 (a) and (b) show the horizon line with the aircraft cg positioned at 100ft and 4000ft respectively. It can be seen that at low level, the raw algorithm of Eq. (3-7) works well but an offset is introduced as aircraft altitude is increased. To counter this, a correction value, calibrated against aircraft altitude, was added to the simulation algorithm. Fig. 3-30(c) shows the results of this correction plus evidence that the roll algorithm also functioned correctly (aircraft at 3000ft and 25 degree roll).

3.5.3.4.2   Lead Aircraft Symbol

Fig. 3-31 shows screen shots taken during the development of the lead aircraft symbol algorithm. The figures show the lead aircraft symbol itself and also a 3D model of a Boeing 707 aircraft that is placed at the lead aircraft cg position within the outside world database itself.

Fig. 3-31(a) shows the 'ideal' scenario with the chase aircraft flying straight and level behind the lead aircraft. The scaling of the wing span appears correct. The symbol itself is low compared to the 3D model of the lead aircraft. This was considered acceptable as the symbol was not intended to be a completely faithful representation of the 3D aircraft. Some of the offset was also accounted for by the incorrect positioning of the 3D aircraft model origin (the point being driven by the algorithm) compared to the notional aircraft cg position of the simulation model itself. Fig. 3-31(b) shows the scenario where the pilot is having to re-acquire the correct trajectory position. Again the scaled wing span appears correct and the roll algorithm is shown working in the correct sense. For each of these
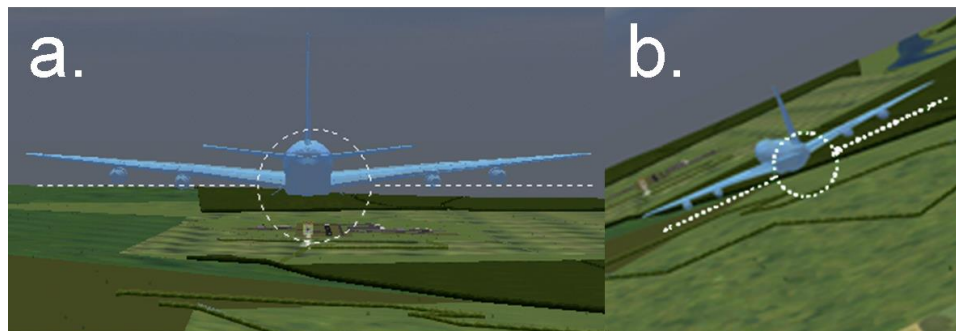
Fig. 3-31. Development of lead aircraft symbol

cases, a zoomed image is shown to improve image clarity. The display symbology in the zoomed images has been artificially enhanced to improve image clarity.

3.5.3.4.3   Predictor Aircraft Symbol

Two methods were used to verify that the predictor symbol algorithm was working correctly. The first test was simply that at the start of a given run, the predictor and the lead aircraft symbol should be the same size and overlay each other exactly. This was indeed the case (Fig. 3-32).
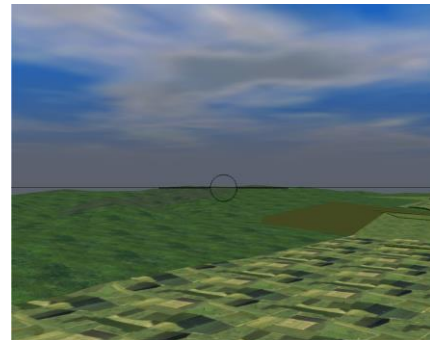

Fig. 3-32. **Illustration of predictor symbol overlaying chase aircraft symbol at start of test run**

Indirect validation evidence is shown in Fig. 3-33. Fig. 3-33(a) and (b) compare the trajectory of the chase aircraft flown for a glide slope capture MTE and against the target trajectory. Fig. 3-33(c) and (d) show the same information for a localiser capture MTE. Both of these were flown by EP1 during the display development phase of the project. The trajectory following is particularly good during the straight-and-level portions of the MTE and degrades slightly during the transition phases, particularly the height during the turn onto localiser. At this stage, the observed deviations were attributed to the piloting proficiency of EP1.
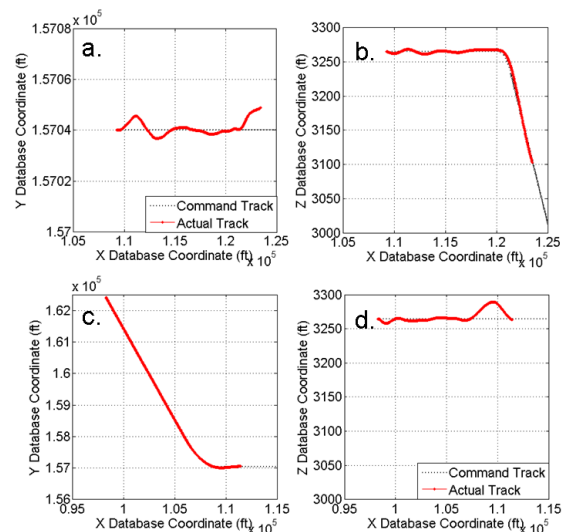
Fig. 3-33. EP1 trajectory comparison between actual flown and target (a) and (b) glide slope capture (c) and (d) localiser capture

The looming functionality of the display was tested by EP1 simply monitoring the aircraft indicated airspeed (IAS) and relative size of the predictor and lead aircraft symbols. If the symbols remained the same size

as one another, the IAS remained constant at its desired value. If the lead aircraft symbol loomed and became larger than the predictor symbol, the IAS was noted to have increased and vice-versa. As such, this function was deemed to work as planned

3.5.4 Flare Command Concept

3.5.4.1 Background

A predictor-lead concept was considered acceptable for aircraft manoeuvring were there are no local solid surfaces to constrain the motion. However, such a solution would not be as useful for the flare because, particularly if t_{pred} is large, the resulting chase aircraft motion would not follow the lead aircraft due to the dynamic non-linearity introduced to its motion by the 'impact' with the runway surface. Alternative methods were therefore required.

It was considered that a command-type display would be more suitable for a flare (e.g. VGS). The simplest method for providing a τ-based trajectory command is to provide the pilot with raw τ information. In order to be able to do this, the decision as to whether to use a Type 1 or Type 2 flare profile had to be made. For the Type 2 flare (i.e. constant $\dot{\tau}_{\Delta h} < 1.0$ to touchdown), only one parameter has to be displayed to the pilot. For the Type 1 flare, the display has to transition from showing $\dot{\tau}_{\Delta h}$ information, to $\tau_{\Delta h}$ and then back to $\dot{\tau}_{\Delta h}$ again. Consequently, the decision was made to concentrate on the Type 2 flare τ profile.

A common method for identifying the aircraft flight path to the pilot is via a 'flight path vector' symbol. This symbol identifies the vertical and horizontal angles of aircraft motion. Displayed on a HUD, it provides the pilot with an instantaneous indication of where the aircraft is heading. If the symbol overlays the ground, then that is the point where the aircraft will strike the Earth if no correction is applied. An indirect method of

obtaining a specific τ-based trajectory would therefore be to derive and display the target flight path angle required to achieve it. The pilot would then have to overlay the aircraft flight path vector onto this symbol to achieve the desired trajectory.

Two concepts were therefore developed using the Type 2 flare command:

1. Direct τ command using raw $\dot{\tau}_{\Delta h}$ target and actual information.

2. Indirect τ command using vertical flight path angle, γ_v target and actual information to prescribe a given constant $\dot{\tau}_{\Delta h}$ trajectory.

3.5.4.2 Display Symbology

The format of the lead-predictor concept symbols essentially fixed the design of the flare symbology since if both were to be used in one final display format, they would have to blend seamlessly into each other. As such, symbols 1 and 2 from Fig. 3-24 also form the 'target' and 'actual' values for the flare τ command display concepts. As for the lead-predictor concept, the pilot's task is to overlay the former with the latter.

3.5.4.2.1   Direct Tau Flare Command Symbology

For the flare portion of any given manoeuvre, both the command and actual symbols were constructed as VAPS scale objects displaying $\dot{\tau}_h$ ranging between 0 (corresponding to
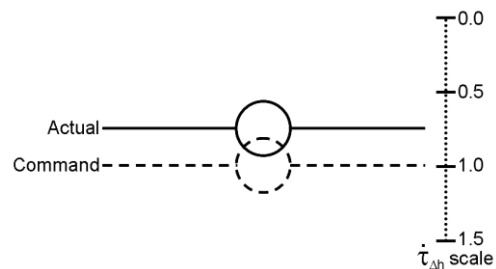

Fig. 3-34. Definition of direct τ flare guidance display

level flight if the surface height does not change) and 1.5 (corresponding to accelerative flight towards the surface). As such, only vertical guidance is provided. Values of $0.0 < \dot{\tau}_{\Delta h} \leq 1.0$ were anticipated to be required in the design but an upper limit of 1.5 was selected to try to avoid the symbols hitting 'hard stops'. The positioning of the symbols did not have any specific meaning i.e. they were not conformal with the outside world but

were simply placed directly in the pilot's line of sight. The concept is shown in Fig. 3-34. The scale shown in this figure is for illustrative purposes only and did not form part of the display symbol set. It should be noted that the scale has been constructed so that the command symbol transition from approach to flare is in the correct sense i.e. a pitch up is required so the symbol moves upward.

3.5.4.2.2   Indirect Tau Flare Command Symbology

The same symbols were used for the indirect τ flare command symbols as for the direct concept. In this case however, because the symbols were indicating flight path vector, a simple scale was insufficient and additional logic had to be incorporated to ensure that they were conformal with the outside world. In this way, in good visual conditions, they would also provide information regarding the direction of travel in relation to the outside world.

3.5.4.3 Display Control Algorithms

3.5.4.3.1   Direct Tau Flare Command Symbol

For the direct flare τ command symbol, at the appropriate value of $\tau_{\Delta h}$, the target $\dot{\tau}_{\Delta h}$ value was indicated to the pilot.

3.5.4.3.2   Direct Tau Flare Actual Symbol

For the direct flare τ actual display symbol, the $\dot{\tau}_{\Delta h}$ value to be displayed was calculated as (see Fig. 3-7):

$$\dot{\tau}_{\Delta h actual} = \frac{d}{dt}\left(\frac{\Delta h}{\dot{h}}\right) = \frac{\dot{h}^2 - \Delta h \ddot{h}}{\dot{h}^2} = 1 - \frac{\Delta h \ddot{h}}{\dot{h}^2} \qquad (3\text{-}24)$$

3.5.4.3.3   Indirect Tau Flare Command Symbol

The computation of the equivalent flight path angle to give a prescribed $\dot{\tau}_{\Delta h}$ trajectory is as follows (for the vertical plane only):

1. Compute current instantaneous time-to-contact runway surface.

127

$$\dot{\tau}_{\Delta h} = \frac{\Delta h}{\dot{h}} \qquad (3\text{-}25)$$

2. At $\tau_h=t_{transition}$ (= 4.0s), blend to the flight path angle $\dot{\tau}_h$ flare control law over t_{blend} (= 0.5s). This is given by:

$$\gamma_{vcommand} = \theta - \frac{1}{\cos\theta\cos\phi}\left[\frac{1}{u}\sqrt{\frac{\Delta h\ddot{h}}{1-c}} + \sin\theta\right] \qquad (3\text{-}26)$$

The expression of Eq. (3-25) is derived in Eqs. (3-28)-(3-34).

3. Compute symbol vertical (y) screen coordinate as:

$$v_{\gamma command} = -\gamma_{vcommand}\frac{v_{screen}}{\delta_{vert}} \qquad (3\text{-}27)$$

3.5.4.3.4   *Indirect Tau Flare Actual Symbol*

The actual flight path angle symbol position was calculated as follows:

1. Compute chase aircraft vertical flight path angle:

$$\gamma_{vchase} = \theta - \alpha \qquad (3\text{-}28)$$

2. Compute symbol vertical (y) screen coordinate as:

$$v_{\gamma chase} = -\gamma_{vchase}\frac{v_{screen}}{\delta_{vert}} \qquad (3\text{-}29)$$

3.5.4.4 *Derivation of Flight Path Angle for Constant Tau-dot*

This Section contains the derivation of the expression used to drive the indirect τ flare command display, $\gamma_{vcommand}$. The result is a flight-path angle command that guides the aircraft along a constant $\dot{\tau}_h$ trajectory. To start the derivation, Eq. (3-24) must be rearranged to the form:

$$\dot{h} = \sqrt{\left(\frac{\Delta h\ddot{h}}{1-c}\right)} \qquad (3\text{-}30)$$

128

Perturbations in vertical flight path angle, γ_v, may be expressed in terms of perturbations in pitch attitude, θ, and incidence angle, α [120].

$$\gamma_v = \theta - \alpha \cong \theta - \frac{w}{u} \qquad (3\text{-}31)$$

Rearranging Eq. (3-31) for w yields:

$$w = u(\theta - \gamma_v) \qquad (3\text{-}32)$$

Now, $\dot{h}$ is the vertical velocity of the aircraft c.g. referenced to Earth or inertial axes. If lateral motion is ignored (an aircraft on final approach should be sufficiently stabilised in its ground track such that this assumption holds), it can be shown that the perturbation in aircraft height is [120]:

$$\dot{h} = u \sin\theta - w \cos\theta \cos\phi \qquad (3\text{-}33)$$

Substituting Eq. (3-32) into Eq. (3-33) for w and equating Eq. (3-33) with Eq. (3-30), then rearranging for γ_v gives:

$$\gamma_{v\text{command}} = \theta - \frac{1}{\cos\theta \cos\phi}\left[\frac{1}{u}\sqrt{\frac{\Delta h \ddot{h}}{1-c}} + \sin\theta\right] \qquad (3\text{-}34)$$

3.5.4.5 Display Validation

3.5.4.5.1   Direct Tau Symbols

Fig. 3-35 shows a selection of example $\tau_{\Delta h}$ ($\dot{\tau}_{\Delta h}$ =c_{flareT2}=C6) trajectories flown by pilot EP1 during development testing of the direct flare command
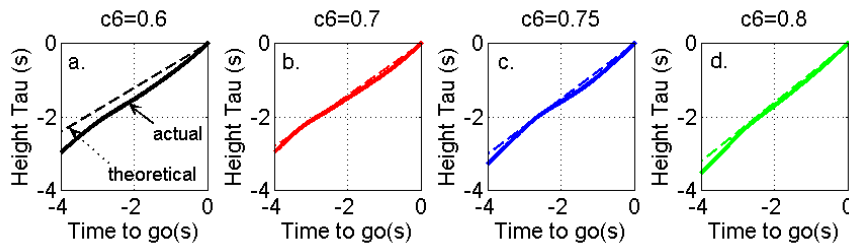
Fig. 3-35. Example trajectories flown by EP1 during development of the direct flare display concept

129

concept display. The theoretical $\tau_{\Delta h}$ curve expected by using the commanded value of $c_{flareT2}$ is also shown. In each case, the transition from approach to flare command was initiated at $\tau_{\Delta h}=3.0s$. For the cases of $c_{flareT2}=0.7$, 0.75 and 0.8, that the actual τ trajectory closely follows the theoretical curve. The $c_{flareT2}=0.6$ case is less impressive. However, the initial aircraft $\tau_{\Delta h}$ response does parallel the theoretical line i.e. the correct $\dot{\tau}_{\Delta h}$ is being flown. However, analysis revealed that the pilot did not follow the symbol all the way to the surface and this is evident in the increase in $\dot{\tau}_{\Delta h}$ in the final second or so before touch down.

Fig. 3-36 shows the vertical velocity at touchdown against the commanded $\dot{\tau}_{\Delta h}$ value. Also shown is the averaged best-fit line of Eq. (4-2) and (4-3) i.e. $\dot{\tau}_{\Delta h} = -0.032\dot{h}_{td} + 0.529$.

With the exception of the $c_{flareT2}=0.6$ case, the display concept results in a lower vertical touchdown velocity than would be predicted by the linear regression of observed flight test and simulated flight test data. This is considered acceptable as it is safer than the alternative.
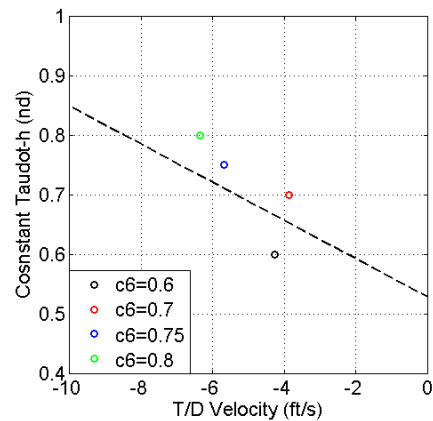

Fig. 3-36. Direct τ flare display concept touchdown vertical velocities compared with observations

130

3.5.4.5.2   Indirect Tau Symbols

Fig. 3-37 shows a selection of example $\tau_{\Delta h}$ ($\dot{\tau}_{\Delta h} = c_{flareT2}$) trajectories flown
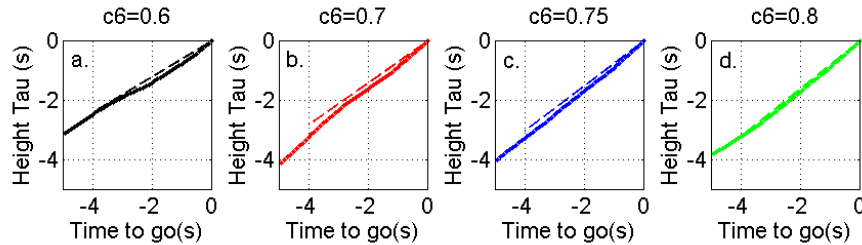

Fig. 3-37. Example trajectories flown by EP1 during development of the indirect flare display concept

by pilot EP1 during development testing of the indirect flare concept

display. The theoretical $\tau_{\Delta h}$ curve expected by using the commanded value

of $c_{flareT2}$ is also shown. As for the previous examples, the transition form

approach to flare command was initiated at $\tau_{\Delta h}$=3.0s.

In each case, the aircraft τ-domain trajectory follows that of the theoretical

value, the most accurate being when $c_{flareT2}$=0.8. In the other cases, the

aircraft trajectory lies parallel with the theoretical value for the majority of

the flare with an increase in the value of $\dot{\tau}_{\Delta h}$ during the final moments of

the flare.

As for the analysis in the previous Section, the vertical velocity at

touchdown was plotted against the commanded $\dot{\tau}_{\Delta h}$ value and compared with the averaged best-fit line of Eq. (4-2) and (4-3). The results are shown in Fig. 3-38. With the exception of the $c_{flareT2}$=0.8 case, the display concept results in a somewhat higher vertical touchdown velocity than would be predicted by
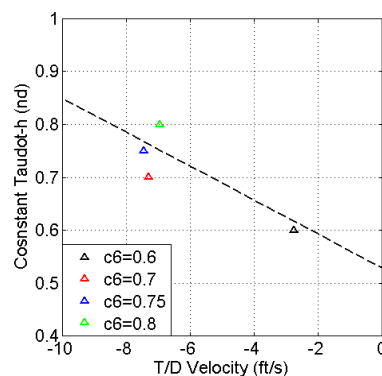

Fig. 3-38. Indirect display concept touchdown vertical velocities compared with observations

the linear regression of observed flight test and simulated flight test data. This is considered less acceptable than the direct case as this is less safe than the alternative. This is attributed to the piloting experience level of EP1.

The development testing highlighted an issue that, whilst predictable with the benefit of hindsight, wasn't anticipated. It was found that with the indirect display in particular (although the problem was encountered with the direct concept on a few occasions), the flare was commanded, but either shortly before or just after touchdown, a pitch up was commanded that resulted in the aircraft taking flight again. The reason, of course, is that $\dot{\tau}_{\Delta h}$ can be equal to $c_{flareT2}$ whether the aircraft is in a descent or a climb. If the aircraft bounced on its main gear, for instance, then the upward stroke would result in a negative Δh and a positive $\dot{h}$. The symbology would then continue to indicate a pitch up to obtain a flight path angle to give $\dot{\tau}_{\Delta h} = c_{flareT2}$. The following logic was therefore implemented and resolved the problem:

1. Identify an acceptable touchdown velocity, $\dot{h}_{des}$. 2.0 ft/s was (arbitrarily) decided upon in this case.

2. Calculate the aircraft flight path angle that would give rise to this touchdown velocity.

$$\gamma_{tdh\dot{d}es} = a\sin\left(\frac{\dot{h}_{des}}{V_0}\right) \qquad (3\text{-}35)$$

3. Once this flight path angle is achieved, symbology to maintain command at this value.

3.5.5 Display Control Algorithm Blending

The final display concept comprises two differing information display philosophies:

1. For the approach to the runway threshold, the aircraft's target 'position' is displayed to the pilot as a function of future desired position.

2. For the flare, the aircraft's target 'position' is commanded on an instantaneous basis.

Both philosophies are implemented by displaying the target 'position' (be it future or instantaneous) to the pilot. The pilot's task is to overlay a symbol representing the aircraft's current 'position' with that of the target. At some time between the approach and the flare proper, therefore, the two differing signals have to be blended together so that the transition is as seamless as possible for the pilot. How this is achieved for the lead-predictor display concept is described below, in conjunction with Fig. 3-39.
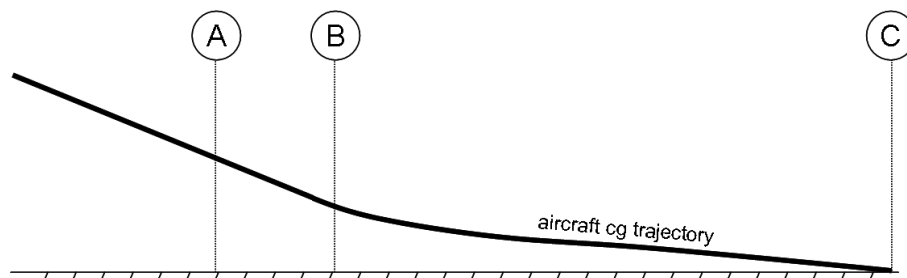
Fig. 3-39. Schematic illustration of lead-predictor and flare algorithm blending

Before point (A) is reached, the lead-predictor algorithms of Sections 3.5.3.3.2 and 3.5.3.3.3 are used to drive the display symbology. (A) is the algorithm transition start point and is defined as being $\tau_{\Delta h}=-4.0s$. (B) is the nominal position when all of the lead-predictor signals have been blended out and the flare command algorithms commence. Point (B) is when $\tau_{\Delta h}=-3.5s$. Point (C) is main gear touchdown ($\tau_{\Delta h}=0.0s$). Beyond this, the pilot was instructed to ignore display commands.

3.5.4.6 Lead Aircraft Symbol

During the blending, the lead aircraft symbol becomes the flare flight path command symbol. At (A):

1. If radar altitude < 70ft, fix lead aircraft symbol scaling (Eq. ((3-18)) otherwise wait until radar altitude <70ft.

2. Begin to linearly blend aircraft command flight path angle information (3-33) converted to screen units) with the lead aircraft symbol signal (Eq. (3-15)) over 0.5s.

3. Calculate initial flare initiation height for point (B) based upon current height and vertical velocity.

$$h_B \cong h_A + 0.5\dot{h}_A \qquad (3\text{-}36)$$

4. Calculate the initial acceleration for the flare command.

$$\ddot{h}_B = \left(\frac{1-c}{c^2}\right)\frac{h_A}{T^2} \qquad (3\text{-}37)$$

5. Calculate the initial $\dot{\tau}_{\Delta h}$ using Eq. (3-24).

At (B):

1. If $\ddot{h}_{a/ccg} < \ddot{h}_B$ then hold $\dot{\tau}_{\Delta h}$ at value using $\ddot{h}_B$ in Eq. (3-37) otherwise use $\ddot{h}_{a/ccg}$ in Eq. (3-37).

3.5.4.7 Predictor Aircraft Symbol

During the blending, the predictor aircraft symbol becomes the actual aircraft flight path symbol. At (A):

1. Begin to linearly blend actual aircraft flight path angle information (Eq. (3-28)) with the predictor aircraft symbol signal over 0.5s.

3.5.6 Display Control Algorithm Implementation

A number of options were available to implement the algorithms detailed above:

1. Utilise VAPS 'collector objects' (assorted variations on C++ coding) to manipulate the raw FLIGHTLAB aircraft simulation data.

2. Use the so-called Landscape 'Bridge' file. The 'Bridge' allows user-define code to be executed during Landscape run time.

3. Perform algorithm calculations using FLIGHTLAB. Here, there are two possible methods.

    i. Develop user-defined components (blocks of FORTRAN code).

    ii. Use the Control System Graphical Editor (CSGE) to develop control system-type diagrams to represent the mathematical operations required.

Option (3)(ii) was the method opted for as it offered a number of advantages:

a. All calculations remain within the FLIGHTLAB modelling environment making data and calculation house-keeping more robust.

b. CSGE is a graphical editor and as such, a visual representation of the calculations was considered to be easier to manipulate and manage than lines of code.

c. CSGE offers a reasonably extensive range of pre-defined mathematical 'blocks' e.g. matrix manipulation (in a manner that MATLAB Simulink users would be familiar with) that speed up the process of calculation 'coding'.

d. CSGE offers a range of de-bugging facilities that make the tracing of mistakes through calculations simpler.

e. Using CSGE lends itself to being an 'open-source' implementation of the calculations. The calculations can easily be imported to other FLIGHTLAB models by opting for this method.

Presentation of all of the CSGE networks used to implement the symbol algorithms would be unwieldy as some are quite large and hence difficult to see clearly on A4 paper. However, an example is presented in Fig. 3-40. This illustrates the pilot's eye position calculation of Eqs. (3-8) and (3-9).
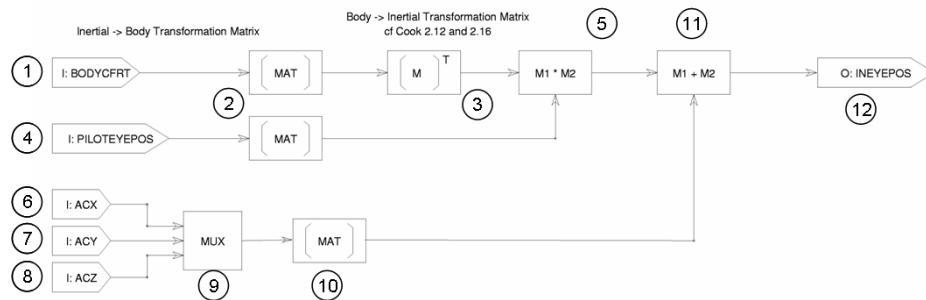

Fig. 3-40. Example display algorithm implementation in CSGE

The transformation matrix [D] is automatically computed by the FLIGHTLAB simulation environment and is input to the calculation as 'BODYCFRT' (block 1). This vector is converted to the more usual 3x3 matrix format (block 2). The required inverse, $[D]^{-1}$ is obtained, in this case, by transposing [D] (block 3). The aircraft body-referenced pilot eye position offsets from the cg are input using block 4 and is converted to matrix format via block 2. The two resultant matrices are multiplied together by giving the result of Eq. (3-9) (block 5). The aircraft inertial cg position is input as three individual (x, y, z) values (blocks 6, 7 and 8). These are multiplexed together into vector format and converted to a 3x1 matrix (blocks 9 and 10). The inertial pilot eye offset coordinates and aircraft cg coordinates are then summed in block 11 to give pilot eye coordinates in inertial coordinates and the result output as a 3x1 matrix to the simulation space (block 12).

136

3.5.5 Comparative Displays: Basic Primary Flight Display (PFD)

Fig. 3-41 shows the basic PFD used during the course of the research. Table 3-6 provides the key to the important display elements. This is display is not intended to be a facsimile of any particular display currently in service but features common symbol formats for existing display elements with the exception of a dedicated flight director.
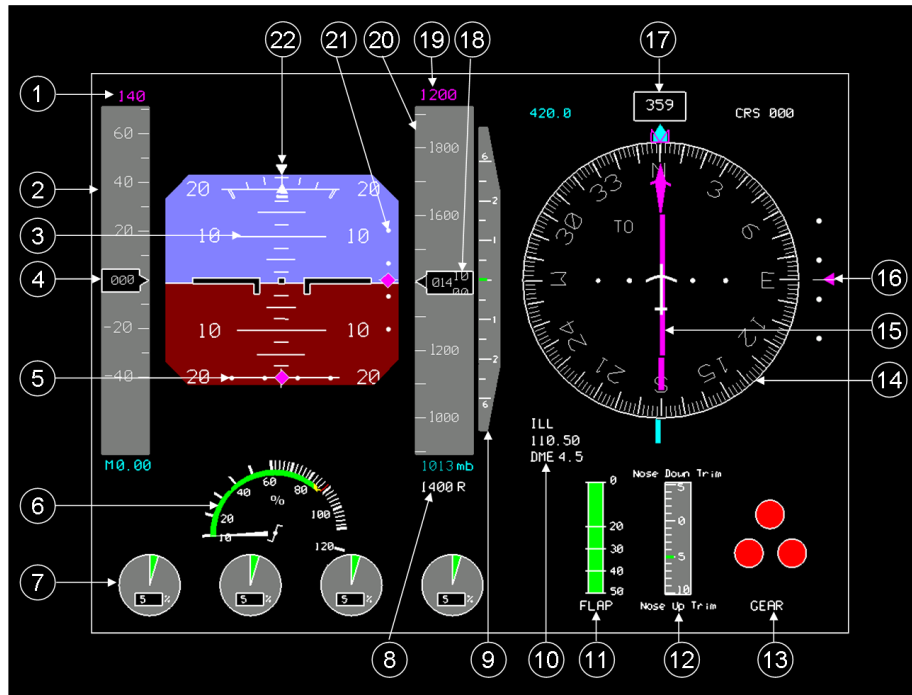

Fig. 3-41. Basic primary flight display

No.	Description	Comment
1	Target airspeed	Adjusted by simulator operator as required by test point
2	Airspeed tape	
3	Pitch ladder	
4	Digital indicated airspeed	
5	Localiser deviation indicator	Full scale deflection = +/- 1 degree
6	Cockpit throttle lever position	0% = closed; 100% = fully open
7	Engine thrust	Indicated as a percentage of maximum available
8	Radar altitude	Only displayed when below 2500ft radar
9	Vertical speed indicator	
10	Distance to navigation beacon	
11	Flap position indicator	Shown in full flap i.e. FLAP 50 position
12	Pitch trim indicator	Shows stabiliser position in degrees
13	Landing gear position indicator	Red = up; grey = travelling; green = down
14	Compass rose	
15	Localiser deviation indicator	Full scale deflection = +/- 3 degrees
16	Glide slope deviation indicator	Full scale deflection = +/- 1 degree
17	Digital heading	
18	Digital altitude	
19	Target altitude	Adjusted by simulator operator as required by test point
20	Altitude tape	
21	Glide slope deviation indicator	Repeat of item 16
22	Bank angle indicator	

Table 3-6. Primary flight display symbol descriptions

3.5.6 Comparative Displays: Visual Guidance System (VGS) Head-Up Display

The HUD used for the research was a version of the BAE Systems' 20/20 Visual Guidance System (VGS). The form of the symbology was replicated as faithfully as possible and the control laws for those symbols recreated as closely as the information provided by BAE Systems allowed. For reasons of commercial sensitivity, those control laws will not be published within this thesis.

Fig. 3-42 shows the UoL implementation of the VGS and Table 3-7 provides the key to the important display elements (note: where comment indicates that an element of the display is 'pilot selectable', this value was actually set by the simulator operator to a suitable value for the test point in question). The image in Fig. 3-42 has been artificially enhanced to try to improve the contrast between display and background.
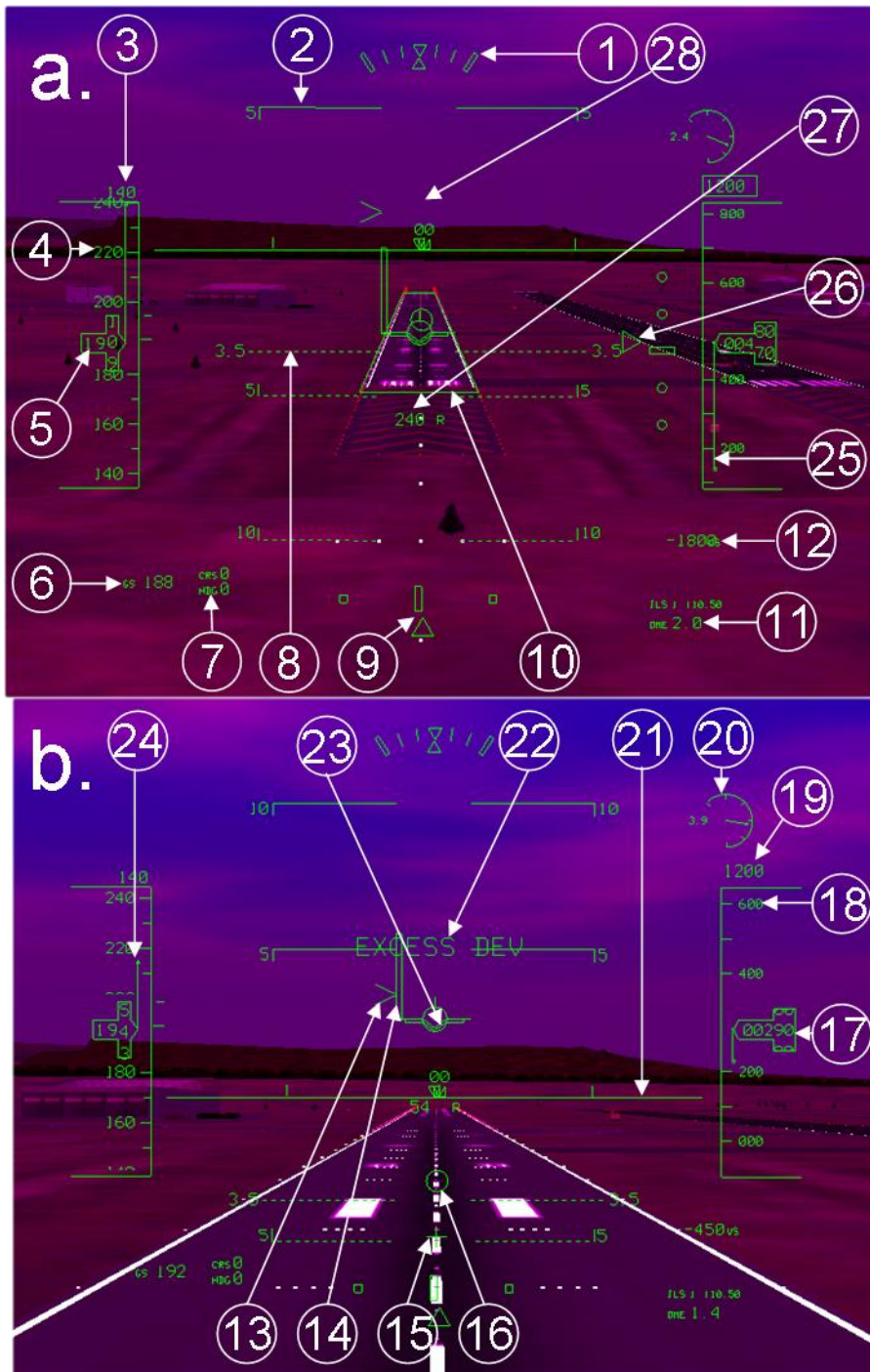
Fig. 3-42. BAE Systems VGS HUD layout

No.	Description	Comment
1	Bank angle indicator	
2	Pitch ladder	
3	Target airspeed	Pilot selectable target indicated airspeed.
4	Indicated airspeed tape	
5	Digital indicated airspeed	
6	Digital ground speed	
7	Target course/heading	Pilot selectable navigation course/magnetic heading. The values selected define the position of the course and heading markers on the horizon line. Only the heading marker was used for the research.
8	Glide slope reference line	Pilot selectable glide slope reference line. Switched off for all research test points.
9	Localiser deviation indicator	Full scale deflection = +/- 1 degree.
10	Runway outline	Provides a line-drawing representation of the runway edges between specified altitudes AGL.
11	Distance to navigation beacon	
12	Vertical speed	
13	Flight path acceleration cue/caret	Defines the 'potential flight path angle' or the flight path angle where speed will not change at a given power setting. So, when the caret is aligned with flight path vector left wing, the aircraft will remain at a constant speed at the current power setting. If the caret is above the left wing, the aircraft will accelerate and vice-versa.
14	Flight path marker / Speed error worm	Provides quickened flight path direction information such that the symbol dynamic characteristics in response to elevator inputs is that of pitch attitude at high frequency and flight path angle at low frequency. The error bar/worm indicates the actual airspeed in relation to the pilot selected airspeed (above the left wing = actual speed above target and vice versa).
15	Flare alert cue	Symbol that provides an indication to the pilot of the pitch rate at which the flare will be performed.
16	Guidance cue	For the purposes of the research, provides flight direction guidance (pitch and roll) onto the active localiser and glide slope and pitch-only guidance for the flare.
17	Digital barometric altitude	
18	Altitude tape	
19	Target altitude	Pilot selectable target altitude.
20	Angle of incidence indicator	
21	Horizon line / heading tape	
22	Warning annunciations	Not used during the research.
23	Boresight	Shows where aircraft nose is pointing in space
24	Airspeed trend arrow	Predicted speed at a defined time in the future.
25	Altitude trend arrow	Predicted altitude at a defined time in the future .
26	Glide slope deviation indicator	Full scale deflection = +/- 1 degree
27	Radar Altitude	
28	Selected heading indicator	

Table 3-7. VGS display symbol descriptions

3.5.7   Comparative Displays: Highway in the Sky (HITS)

Sections 2.2.3.7 and 2.2.4.1 reports that much attention has been focused by the display research community on the so-called 'highway-in-the-sky' concept and indeed, a version of this display format is already available for operational use in Alaskan airspace. A version of this concept was implemented for the purposes of the research and this is shown in Fig. 3-43. Table 3-8 describes each of the display symbols. Based upon pilot feedback, only 5-6 tunnel segments were displayed ahead to avoid

obscuring distant but useable reference points e.g. runway threshold which is visible in Fig. 3-43(a). The concept also featured a flight path vector to assist the pilot in maintaining station within the tunnel. This displayed unmodified, instantaneous flight path information to the pilot.
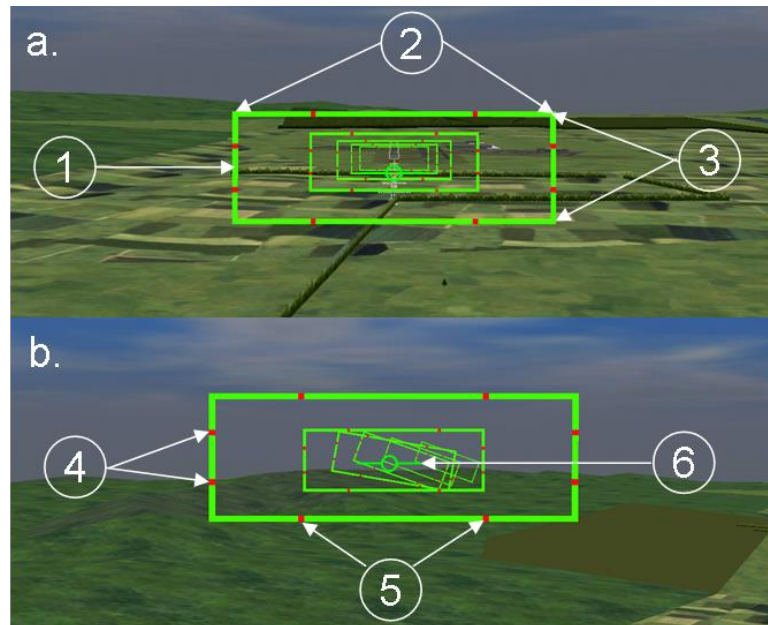

Fig. 3-43. Highway-in-the-sky display layout: (a) glide slope descent and (b) localiser capture turn

No.	Description	Comment
1	Tunnel element	Static 3D models placed in simulation database.
2	'Adequate' lateral trajectory performance limits	Set at ±0.02nm. This is the proposed Cat. I precision approach required navigation performance (RNP) taken from Ref. [3].
3	'Adequate' vertical trajectory performance limits	Set at ±40ft. This is the proposed Cat. I precision approach required navigation performance (RNP) taken from Ref. [3].
4	'Desired' vertical trajectory performance limits	Set at ±15ft. This is the proposed Cat. I precision approach required navigation performance (RNP) taken from Ref. [3].
5	'Desired' lateral trajectory performance limits	Set at ±0.01nm. This is the proposed Cat. II precision approach required navigation performance (RNP) taken from Ref. [3].
6	Instantaneous flight path indicator	

Table 3-8. Highway-in-the-sky display element description

141

3.6   Test Pilot Recruitment

Each of the experiments was performed using at least one current professional jet transport aircraft pilot. These are designated (in no particular order) P1 – P3 throughout the thesis. Each has a background in test-pilot flying and is familiar with fixed- and rotary-wing operations. Their aviation curriculum vitae are included in Appendix E for reference purposes as is that of engineering pilot, EP1. EP1 is an engineer based in FST with some, albeit limited, flying experience who was used to test fly the displays prior to any assessment by pilots P1 – P3.

C h a p t e r   4

FLARE MTE

4.1 Introduction

This Chapter reports on the results obtained for the Flare MTE. Section
4.2 reports on the preliminary testing performed to establish whether
coherent τ relationships were observed and whether such relationships are
affected by degradation in the visual environment. Section 4.3 describes
the investigation of residual aircraft vertical velocity at touchdown.
Section 4.4 details an evaluation undertaken using the eye-tracking
capability developed during the research project. These results are used to
try to provide some explanation for the results in the previous two
Sections. Section 4.5 reports on the development of novel τ-based flare
displays. Section 4.6 provides a comparison of the performance results
obtained for each of the display formats tested. Section 4.7 reports upon
the associated pilot display controllability and workload ratings. Section
4.8 provides an introduction to how the τ analyses can be used i.e. for
modelling the pilot elevator command during the flare. Finally, Sections
4.9, 4.10 and 4.11 bring together and summarise all of the learning points
for the flare MTE.

4.2 Basic Tau Analysis

As discussed in Section 3.4.4.1, the 'basic τ analysis' consisted of the
selection of a number of potential motion gaps over which the pilot might
have visual control. The τ of these gaps was then calculated during the
flare (using the value at main gear touch down as the 'target' value) and
observations made about the coherence (or otherwise) of the τ value with

time. For the flare, as per Fig. 3-7, aircraft height and pitch angle were selected as the motion gaps of interest.

4.2.1 Aircraft Height Motion Gap

4.2.1.1 Flight Test Data

Ref. [122] investigates the behaviour of experienced pilots transitioning to the McDonnell-Douglas DC-10 aircraft during the landing manoeuvre. A proportion of the pilots received their transition training using DC-10 simulators. The remainder had performed the transition on the actual aircraft type. It was found that the simulator-trained pilots had a slightly inferior landing technique that was carried through to their check-rides in the real aircraft that resulted in heavy or inconsistent landings. Ref. [122] analysed this behaviour using a pilot-in-the-loop model of the landing manoeuvre. It was found that the simulator-trained pilots exhibited a larger effective lag in commanding the flare.

From an ego-motion perspective, it might be said that the simulator-trained pilots were either unable to pick up suitable motion-gap closure cues or picked up erroneous motion-gap closure cues from the simulator displays that were then carried across to the real aircraft. It was felt that this would make a relevant τ study. From the data available in the reference, it was only possible to analyse the τ of the height motion gap. It was considered instructive to consider the variation of $\tau_{\Delta h}$ for the various groups of pilots defined in the reference. It should be noted that the $\tau_{\Delta h}$ information presented was calculated by the author and did not form part of the results of Ref. [122]. The procedure adopted is as follows. The data available from Ref. [122] was almost exclusively height and vertical descent rate information presented in phase plane format i.e. h vs. $\dot{h}$. These data were scanned into electronic format to be used in the analyses described in Chapter 3. However, to be suitable for analysis in the τ domain, time-histories of the data had to be derived. Fig. 4-1 shows the schematic

144

representation of how this was achieved. The time taken to travel from

heights h_1 to h_2 can be approximated as:

$$t_{12} \approx \left(\frac{h_2 - h_1}{1/2\,(\dot{h}_2 + \dot{h}_1)} \right)$$

(4-1)

To validate the routine written to perform this task, a comparison was

made with the limited set of time-history data that had been provided in the

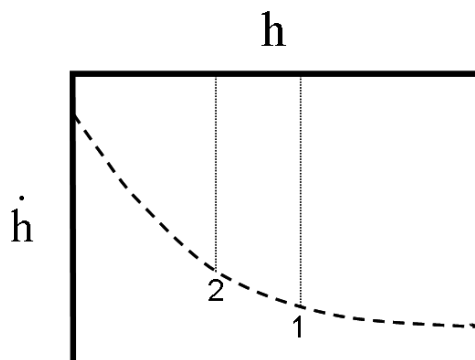reference. Fig. 4-2 presents the results of this comparison. Fig. 4-2 (a)

Fig. 4-1. Schematic representation of phase-plane portrayal of flare data

shows a comparison of scanned and derived altitude data over the final seconds of a landing manoeuvre. Fig. 4-2 (b) shows the scanned and derived vertical velocity data and Fig. 4-2 (c) presents the resulting $\tau_{\Delta h}$, calculated using Eq. (4-1), for both sets of data (where x=Δh).
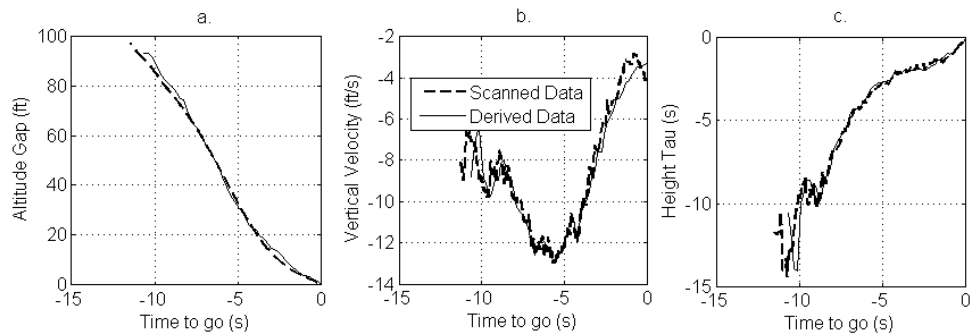
Fig. 4-2. Validation of data extraction routine

It can be seen that small differences do exist between the two sets of

altitude and vertical velocity data, but the resulting $\tau_{\Delta h}$ curves, particularly

close to touchdown, are insensitive to these differences. The routine as
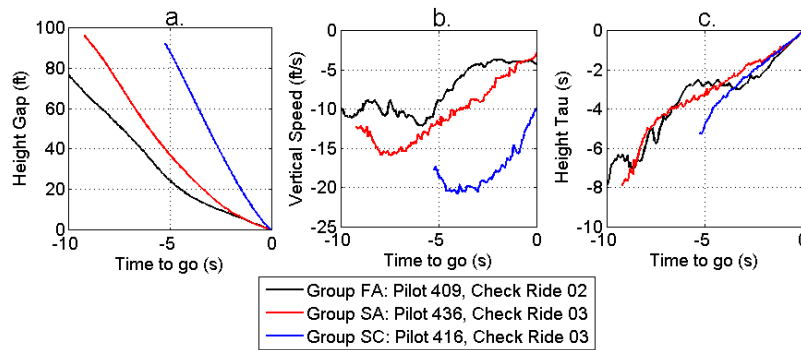
developed was therefore considered to be valid.

145

Fig. 4-3. Sample flight-test data: (a) height gap, (b) vertical speed and (c) height-τ ($\tau_{\Delta h}$).

Fig. 4-3 shows a representative sample of the results obtained from the analysis performed on the flight test data. Fig. 4-4 shows an example of the $\dot{\tau}_{\Delta h}$ analysis that was conducted. The 'Group' label on Fig. 4-3 relates to how the pilots were divided in Ref. [122], namely:
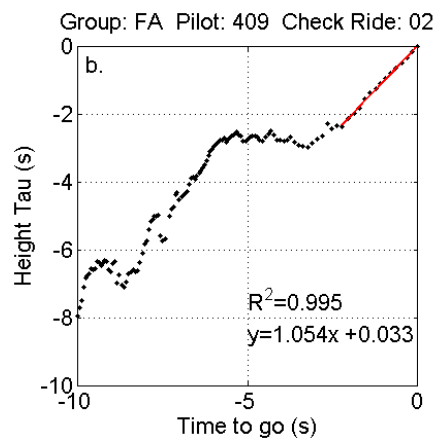

Fig. 4-4. Example analysis results for basic tau analysis

- FA (flight trained pilots with check ride landings consistently less than 5 ft/s vertical touchdown velocity);

- SA (simulator trained pilots with check ride landings consistently less than 5 ft/s);

- FC (flight trained pilots with check ride landings harder than 5 ft/s or height misjudgement tendencies). No data is shown for this group in Fig. 4-3 for the sake of clarity;

- SC (simulator trained pilots with inconsistent check rides i.e. no discernible improvement) and

- SB: simulator trained pilots where the first check ride landing was harder than 5ft/s but followed by continual improvement).

146

The pilot's number relates to the individual pilot in question and the check ride number indicates which of the 3 check rides used for data acquisition is displayed. The latter data i.e. Group SB were not investigated. They were given the lowest priority in the limited time available to conduct the analyses.

From this investigation, the constant $\dot{\tau}_{\Delta h}$ hypothesis appears to be correct during the last few seconds before touchdown. Furthermore, two different techniques for the flare are apparent:

- Pilot 433: The pilot commences the flare and decelerates the aircraft to a vertical speed that is maintained to touchdown. One additional feature of this technique is that τ_h is held approximately constant for a period prior to touchdown. This strategy is designated 'Type 1' for the remainder of this document.

- Pilots 416 and 436: The pilot commences the flare and continues to decelerate the aircraft in the vertical axis (not necessarily at a constant rate) until touchdown. This results in an approach and flare that features a constant rate of change of $\tau_{\Delta h}$. In the case of pilot 416, the same technique was adopted but at a much higher descent rate (and value of $\dot{\tau}_{\Delta h}$) resulting in a touchdown with a high vertical speed. This gives the pilot less time to assimilate the (arguably stronger) cues provided by the view of the outside world from the flare height. This strategy is designated 'Type 2'.

4.2.1.2 Simulated Flight Test Data

The first analysis conducted was to ascertain whether both forms of flare technique observed in the flight test data were used by pilots in the research simulation environment. In this way, additional confidence could be gained from both the aircraft simulation model and the outside world scenes being used for the experiments. Fig. 4-5 shows sample flare time-
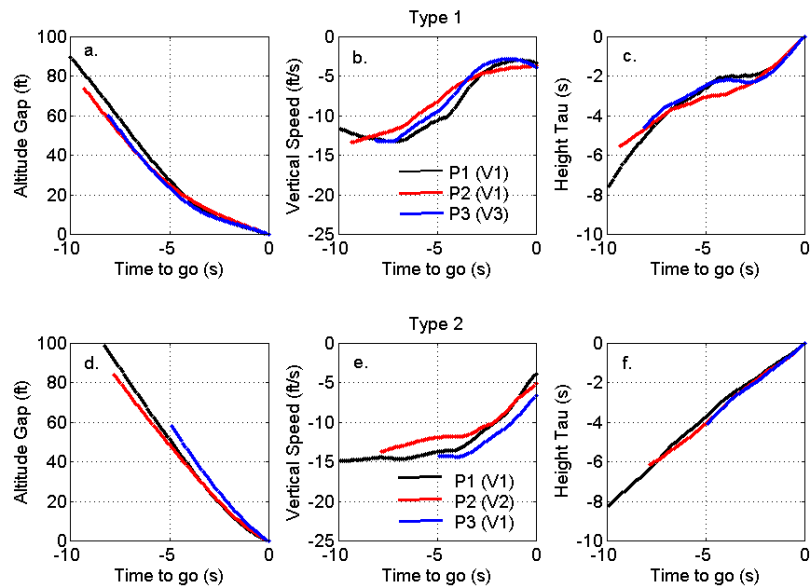
147

Fig. 4-5. Example flare time-histories for pilots P1, P2 and P3: (a) and (d) Altitude gap, Δh; (b) and (e) vertical velocity and (c) and (f) τ_h

histories for pilots P1, P2 and P3. It shows that all pilots used both Type 1 and Type 2 strategies to land the simulated aircraft. The techniques to flare and land a fixed-wing aircraft observed in the flight-test data had been, therefore, recreated. This provided a good level of confidence that any further observations made in simulated flight tests would be valid ones.
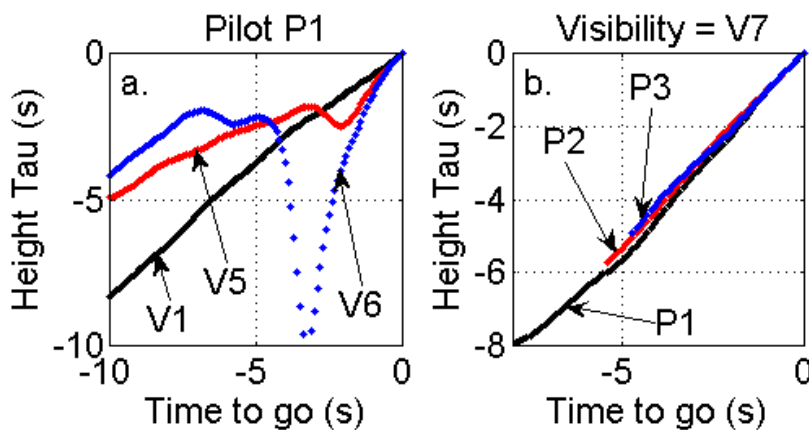
Fig. 4-6. Extreme effects of degrading visibility on $\tau_{\Delta h}$ relationship: (a) non-linearity and (b) runway not seen

An assessment was made as to any effect that degrading the visual conditions had upon the nature of the $\tau_{\Delta h}$ relationships observed in the flight test data. The key points are summarised in Fig. 4-6. There is a

148

marked break down in the $\tau_{\Delta h}$ relationship as the visual conditions are degraded for a small number of the landings carried out. Otherwise, both Type 1 and Type 2 landings are carried out by all pilots for all visibility conditions. In extreme cases, where the visibility is V6b or V7, the pilot never becomes visual with the runway and flies into it with a τ_h approximately equal to or greater than one (indicating a constant velocity or accelerative approach to the surface).

4.2.2 Aircraft Pitch Angle Motion Gap

Fig. 4-7 shows the second τ analysis for the flare manoeuvre, that of the τ of pitch angle, $\tau_{\Delta\theta}$. All runs are for a good visual environment (V1). Elements of coherence are evident in the $\tau_{\Delta\theta}$ time-histories, but the 'hunting' for the correct touchdown attitude evident in Fig. 4-7(a) masks any overall linear relationship that may exist to the moment of touchdown. As such, no linear regression or degraded visual condition results are presented for these cases.
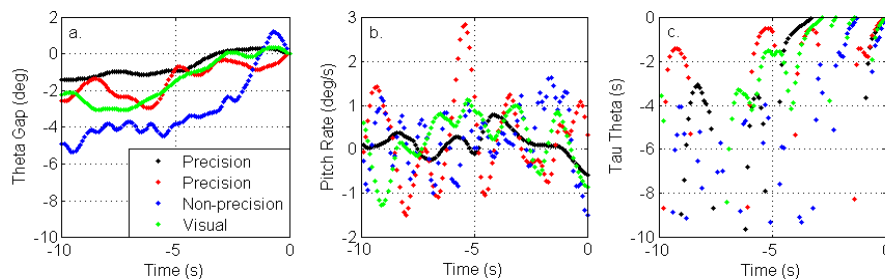

Fig. 4-7. Pitch Angle Tau Analysis of the Flare Manoeuvre: a. Pitch Angle Gap Closure; b. Pitch Rate and c. Tau of Pitch Angle

149

4.3 Residual Velocity Analysis

For the Type 2 flares in particular, there is an apparent relationship, in the examples given in Fig. 4-3, between the value of $\dot{\tau}_h$ used and the touchdown velocity achieved. A full analysis of the flight test data was therefore undertaken to establish the touchdown velocity achieved for a given $\dot{\tau}_h$ observed to touchdown. The results of this analysis are summarised in Fig. 4-8. This shows the constant value of $\dot{\tau}_{\Delta h}$ maintained by
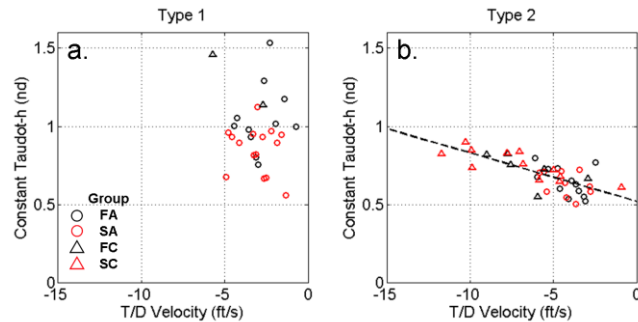

Fig. 4-8. Summary analysis of variation of touchdown velocity with $\dot{\tau}_{\Delta h}$ for the observed flight test flare techniques: (a) Type 1 and (b) Type 2

the check ride pilots to touchdown. It is clear from this figure that both Type 1 and 2 techniques are used successfully by pilot groups FA and SA (success being measured by achieving a touchdown velocity < 5ft/s). The Type 2 flare is predominantly used by pilot groups FC and SC for landing flares that would be judged unsuccessful. The Type 1 landing technique appears to be the almost exclusive technique used by 'successful' pilots. Perhaps most striking is the approximately linear relationship that is apparent between $\dot{\tau}_{\Delta h}$ and touchdown velocity for Type 2 landing flares. A linear regression was performed upon the data of Fig. 4-8 (based upon the results presented in Section 2.4.1.5 and Fig. 2-25) with the following result:

$$\dot{\tau}_{\Delta h} = -0.031\dot{h}_{td} + 0.5203 \qquad (4-2)$$

The regression line is shown in Fig. 4-8(b).

To be consistent with the flight test data, the results for the simulation results have also been designated Type 1 or 2. Fig. 4-9 shows the respective values of $\dot{\tau}_{\Delta h}$ plotted against the vertical velocity at touchdown. The results show similarity with the flight test data for both Type 1 and Type 2 flare control strategies. For Type 1 flares, there is a wide range of $\dot{\tau}_{\Delta h}$ values used to achieve low
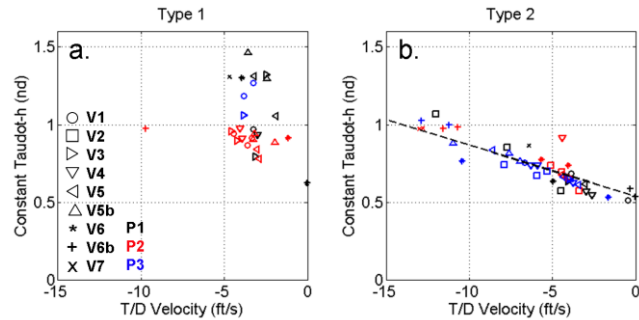

Fig. 4-9. Summary analysis of variation of touchdown velocity with $\dot{\tau}_{\Delta h}$ for the observed simulated flight test flare techniques: (a) Type 1 and (b) Type 2
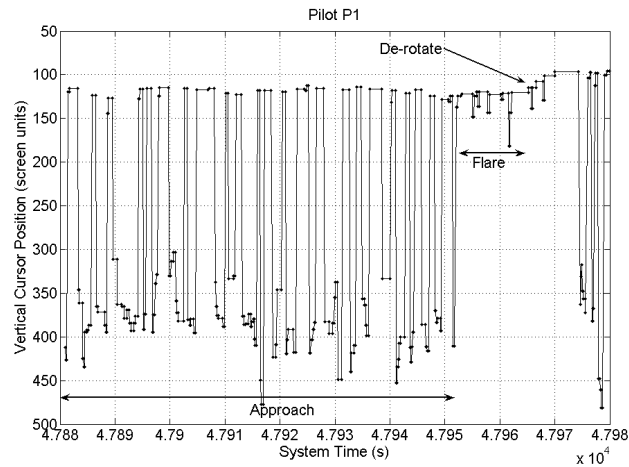
touchdown speeds (< 5 ft/s) for all but one case. For Type 2 flares, the linear relationship between touch down velocity and $\dot{\tau}_{\Delta h}$ is again evident. What is perhaps most remarkable is that the two linear regression 'curves' that can be calculated for these data are consistent between the two sets of results. For the simulated flight test results, the linear regression line is given by:

$$\dot{\tau}_{\Delta h} = -0.033\dot{h}_{td} + 0.538 \tag{4-3}$$

The linear regression line is shown in Fig. 4-9(b).

4.4 Eye Tracking Analysis

To try to help explain the occasional degraded height-τ responses observed during the flare as the visibility is reduced (Fig. 4-6), a number of landing manoeuvres were performed with the pilot wearing the eye-tracking apparatus described in Section 3.1.3. A typical fixation analysis for an approach and landing flare is shown in Fig. 4-10.

Fig. 4-10. Example fixation analysis for pilot P1 in visual conditions V1

An element of interpretation is required in conjunction with the scene camera video to assess the data provided by the eye-tracking analysis tool. Fig. 4-10 shows how different portions of the fixation analysis data correspond to different portions of the approach. The initial data shows a gaze oscillation between the instruments and the outside world view. There is then a transition to a different point-of-gaze strategy to initiate the flare. As contact with the runway surface becomes imminent ($\tau_{\Delta h}<10s$), in the good visual conditions of the example, at least, the instruments become less important and the point-of-gaze transfers exclusively to the outside world view. There is then a final apparent shift upwards of gaze due to the pilot rotating the aircraft to bring the nose-wheel into contact with the runway. The pilot's gaze position actually remains constant but the aircraft rotation downward shifts the outside world scene upwards, resulting in the apparent upward shift in gaze position observed in the data.

152

Fig. 4-11 illustrates a sample of the fixation results obtained for both pilots that cover the main observations in the eye-tracking analysis data. Only two visual conditions are shown to avoid the figure becoming cluttered. The figure shows the vertical element of the pilot's fixation analysis during the final 25 seconds of the approach to touchdown and then de-rotation.
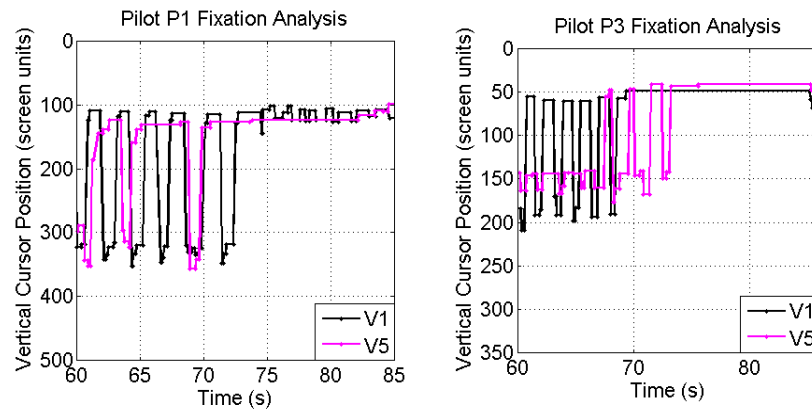

Fig. 4-11. Fixation analysis for pilots P1 and P3 in visual conditions V1 and V5

Fig. 4-12(a)-(d) show a sequence of still frames from the captured video sequences to complement the description of the events highlighted in Fig. 4-11. There are a number of interesting points to note from Fig. 4-11. The first is that even in good visual conditions (V1), it is evident that pilots P1 and P3 have differing techniques in terms of where they look during the flare. During the final approach in V1, both pilots continually shift their gaze between the touchdown markers on the runway and the instrument panel (Fig. 4-12(a) and (c) stills 1 and 2 (for pilot P1, the cursor is not visible on the scene camera image due to the nature of the calibration performed)). This action accounts for the oscillations in gaze during the first 10-15s of the data. During the transition to and execution of the flare, which accounts for the final ten seconds or so of the data, pilot P1 continues to switch gaze position between the horizon and a position closer to the aircraft (Fig. 4-12(a) stills 3, 4 and 5). Pilot P3 however, maintains the gaze position on the horizon (Fig. 4-12(c) stills 3, 4 and 5). When the visibility is reduced to V5, pilot P1 continues to scan both inside and
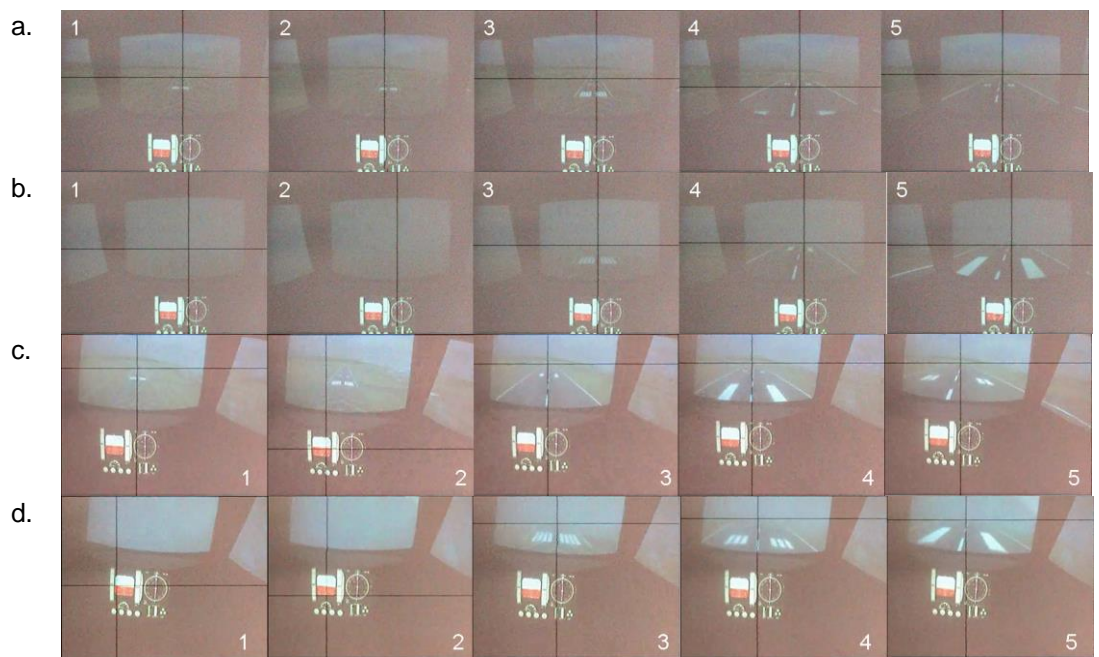
153

Fig. 4-12. Eye tracker stills to illustrate variation of pilot point-of-gaze position with visual conditions: (a) P1 V1, (b) P1 V5, (c) P3 V1 and (d) P3 V5

outside the cockpit (albeit, less frequent scans outside, Fig. 4-12(b) stills 1 and 2). However, during the transition to and execution of the flare, he no longer shifts gaze position during the flare but maintains a more or less constant gaze position at the boundary between the runway surface at the limit of the fog visibility (Fig. 4-12 b) stills 3, 4 and 5). During the approach, pilot P3 concentrates his scan primarily on the instrument (Fig. 4-12(d) stills 1 and 2). This is evident in Fig. 4-11 as a much smaller peak-peak fixation oscillation. During the transition to the flare and the flare itself, pilot P3 maintains a more or less constant gaze position at the boundary between the runway surface at the limit of the fog visibility (Fig. 4-12(d) stills 3, 4 and 5). Again, the lower point of regard position is due to the degraded visual environment bringing the furthest visible point of regard position closer and hence lower in the visual field available from the cockpit wind screen. This is not apparent from the data in Fig. 4-11 and may be due to the inherent accuracy tolerance that is associated with the eye-tracker apparatus (quoted as ±0.5 degrees of the visual field).

4.5 Initial Display Design for the Flare MTE

4.5.1 Display Options

For each MTE, and specifically in this instance for the flare, there are a number of options that have to be considered for the design of a guidance display. These can be summarised in the following questions:

1. What information does the pilot require to allow him/her to successfully guide the aircraft along the required path ?

2. In what form should that information be presented ?

The answer to question (1), from the results presented thus far, appears to be that the pilot needs sufficient information to allow the τ of the motion gap (between aircraft and the runway surface) to be perceived. The rate of change of the τ can then be controlled by the pilot. With this in mind, two potential answers to question (2) are:

1. Present the τ-based guidance information directly to the pilot or

2. Present the τ-based guidance information indirectly to the pilot.

The remainder of this Section briefly explores both of these possibilities. It details the selection process used to reduce the options to a manageable number to be tested and evaluated. Section 4.5.4 then reports on a flight simulation trial that investigated pilot preferences for various design parameters required by the selected options.

4.5.2 Direct vs Indirect Tau Display Information

One of the principle tenets of Tau Theory is that organisms control their motion through the closure of gaps. One of the design drivers for the displays from the research was that it must enable the pilot to close the required motion gap. To achieve this, the pilot must be aware of both a target gap value and the current actual gap value in order that the closure can be completed. The first option for a display format, therefore, is to provide the pilot with the τ information required to close the motion gap

155

directly. To explain what is meant by the term, 'directly', an example is required. The Type 2 flare will be used for this purpose. For the Type 2 flare, results have been reported that show that a τ-domain relationship exist for the closure of the aircraft height to the runway surface, namely:

$$\dot{\tau}_{\Delta h} = c_{flareT2} \qquad (4\text{-}4)$$

The term 'direct' simply means that a display would provide two pieces of information to the pilot:

1. The desired value of the constant value '$c_{flareT2}$' and

2. The current actual value of the constant values of '$c_{flareT2}$'.

Each of these values would be represented by a symbol and the pilot's task would be to overlay the 'actual' and the 'desired' symbol to allow the aircraft trajectory to move along the desired flight-path.

The corollary to this argument is that indirect τ information is information that is displayed to the pilot that results in the same desired trajectory being accomplished but using a means other than displaying the desired and actual values of '$c_{flareT2}$' to the pilot. It still means, however, that whatever the source of the information provided to the pilot, a target value and an actual value must be presented. This is not a new idea in itself. Displays already in existence use this method to present information to the pilot. The Flight Director provides target roll and pitch attitude to the pilot. When flying manually, the pilot must match the aircraft roll and pitch information to the commanded motion to achieve the desired motion. The new idea in this instance is that the commanded motion be based upon the information that the pilot naturally uses from the visual field to perceive their self-motion and hence the motion of the aircraft.

The τ analysis results for the flare analysis present a number of initial possibilities for the design of an 'actual-target' type display to bring the aircraft onto the runway surface. The key parameters are shown in Fig. 3-

156

7. The final approach phase of flight to the runway threshold can be accomplished by setting a target display value as:

$$\dot{\tau}_{\Delta h} = 1.0 \qquad (4\text{-}5)$$

However, once the closure phase i.e. the flare is initiated, a number of possibilities present themselves. For a Type 1 flare, the target display would indicate:

$$\tau_{\Delta h} = c_{flareT1} \qquad (4\text{-}6)$$

for a period, $t_{constant\,\tau}$ until a suitably low vertical velocity was achieved and then return back to:

$$\dot{\tau}_{\Delta h} = 1.0 \qquad (4\text{-}7)$$

to maintain that velocity to touchdown. Inspection of the flight test and simulation trial results presented indicated that the transition can be initiated at a $\tau_{\Delta h}$ value of anywhere between 3.0 and 8.0 seconds, that the value of $c_{flareT1}$ is in the region of 2.0 to 4.0 seconds and that this value is maintained for the period $t_{constant\,\tau}$ between 1.0 to 3.0 seconds. These values are, of course, inter-dependent and are likely to be specific to aircraft type – the heave constant of the aircraft will have a significant role to play on the selection of a suitable initiation point and a comfortable value of $c_{flareT1}$.

For a Type 2 flare, the target display is transitioned to:

$$\dot{\tau}_{\Delta h} = c_{flareT2} \qquad (4\text{-}8)$$

Inspection of Fig. 4-8 and Fig. 4-9 indicate that acceptable values of $c_{flareT2}$ (i.e. touchdown velocity < 5ft/s) lie in the range $0.5 - 0.75$.

4.5.3 Display Options Reduction

The discussion outlined above indicates that a number of decisions needed to be made or unknowns to be defined for the final flare display design. It was clear at this stage that to achieve a design within the timescales of the

project, the number of unknowns had to be reduced. A process of de-selection on the available options was therefore performed as follows.

The first decision to be made for the flare MTE display concepts was whether to use a Type 1 or Type 2 flare τ profile. This would fundamentally influence the detailed design of the controlling algorithms for the target display symbol. The Type 2 flare was selected for three reasons:

1. Only one parameter had to be displayed to the pilot during the flare rather than a combination. For the Type 1 flare, the display would have to transition from showing $\dot{\tau}_{\Delta h}$ information, to $\tau_{\Delta h}$ and then back to $\dot{\tau}_{\Delta h}$ again.

2. To avoid the problem described above, $\dot{\tau}_{\Delta h}$ could be used as the sole display parameter. However, assuming a display showing $\dot{\tau}_{\Delta h}$ against a scale, this would mean that the display symbol would have to move from $\dot{\tau}_{\Delta h} = 1.0$, to 0.0 and then back to some other constant value (perhaps 1.0 to maintain the vertical velocity achieved) again. There is no way to arrange this motion such that one of the symbol movements is counter-intuitive to a flare command i.e. the symbol moves downwards instead of up or moves when the pilot should maintain a constant longitudinal stick position.

3. The algorithms that drive the BAE Systems VGS flare command display, whilst using a different method, command a target flare manoeuvre not dissimilar to the vertical velocity profile of the Type 1 flare. The question has been already asked as to whether displays would look as they do using motion perception as a basis. This result suggests that the displays may look different but the algorithms behind them may not be.

158

However, at the initial design stage, there was no reason to favour either a direct or an indirect method of τ-based flare command data. The initial testing therefore proceeded using both methods for the flare MTE. Section 3.5 provides a detailed description of the implementation of both types of flare command concept display. In summary:

- The direct display was implemented as a simple scale showing the commanded and actual value of $\dot{\tau}_{\Delta h}$.

- The indirect display showed actual flight path angle being flown. The command display symbol showed the desired flight path angle for a given value of $c_{flareT2}$.

4.5.4 Flare Command Display Design Parameter Shakedown

4.5.4.1 Direct Tau Information Concept

4.5.4.1.1 Performance Results

The full set of direct flare concept display results are summarised, to illustrate the major findings, in Fig. 4-13 ('$c_{flareT2}$' is denoted 'C6' in the
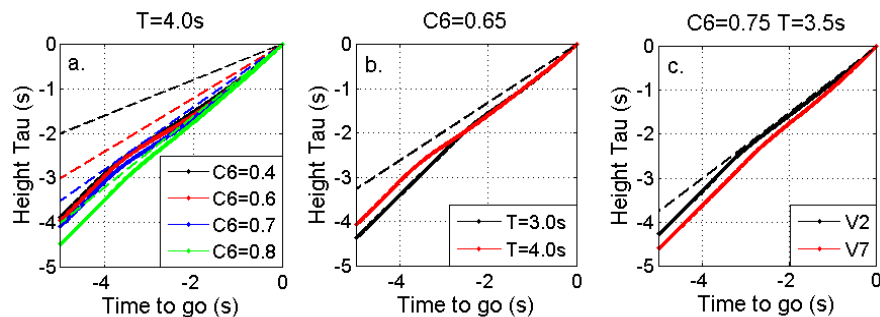

Fig. 4-13. Summary illustrations of flare height τ trajectories using the direct display concept: (a) manoeuvre duration, T=4.0s varying $\dot{\tau}_{\Delta h}$; (b) $\dot{\tau}_{\Delta h}$=0.65, varying T and (c) pilot's preferred variable combination in differing visibilities

figure and 'T' indicates the value of $\tau_{\Delta h}$ at which the flare command is initiated rather than total manoeuvre duration of Equations (2-8) to (2-11)). This shows a number of flare trajectories in the τ-domain for the flare test points flown. The dashed line is the target value of $c_{flareT2}$ and the colour of this line indicates which actual trajectory it should be compared with.

159

Fig. 4-13(a) shows that for a fixed flare initiation time (T), the trajectories defined by the lower values of $c_{flareT2}$ could not be achieved. As the value of $c_{flareT2}$ approach 0.7, the actual trajectory flown matches the command trajectory more closely. Fig. 4-13(b) simply indicates that the logic that defined the initiation of the flare command was working in the correct sense and at the appropriate time. Finally, Fig. 4-13(c) shows the trajectories flown with final design parameter values recommended by the pilot for this display concept in differing visibilities. Both show close adherence of the actual trajectory to the commanded value.

Fig. 4-14 further summarises the data by showing the vertical touchdown velocities achieved against the commanded value of parameter $c_{flareT2}$ using
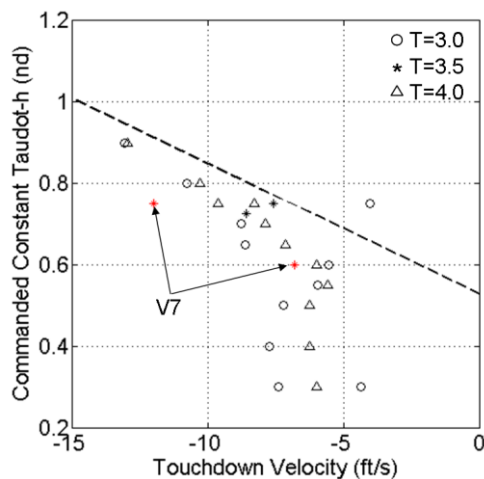

Fig. 4-14. Touchdown vertical velocity for flares performed using the direct τ-based flare command display

the direct flare display concept. Fig. 4-14 also shows the averaged best-fit line of the observed simulated and flight-test data of Eqs. (4-2) and (4-3). It can be seen that for values of $c_{flareT2} > 0.5$, the touchdown velocities achieved using the display concept approximately follow the slope of the trend line. However, the majority of the data lie on the side of the curve that is optimistic i.e. the curve 'predicts' a lower touchdown velocity than is achieved by using the display. In this sense, it might be said that the display concept under-performs the manual landings performed by pilots flying visually.

4.5.4.1.2 Pilot Comments

Pilot P1 commented that the display, as implemented, required an unnatural amount of piloting precision. This comment really applied to the

160

approach phase of the flare test points where the pilot was being asked to follow a $\dot{\tau}_{\Delta h} = 1.0$ command. Small longitudinal control inputs would cause a large movement of the 'actual' symbol making small, precise stick inputs necessary to arrive at the runway in the approximate touchdown zone. Ultimately, this comment may be attributable to the stick dynamics of the simulation facility. The control inceptor is a centre-stick (as opposed to a control yoke) arrangement. The stiffness and damping of the stick movement is controlled by electric motors and only one static value for each can be set. Approximately representative values used for the GLTA model were ascertained empirically by pilot P1. However, the control arrangement is a compromise solution for a simulator that can be re-configured to represent a wide range of air-vehicles. The fidelity of the control 'feel' cannot be claimed to be fully representative of a jet transport. As such, this aspect would make an interesting topic for further research. That is, what stick dynamics would be required to make the direct τ-based display concept more acceptable?

As for the flare itself, the pilot noted that low values of $c_{flareT2}$ (0.3, 0.4) caused bounces along the runway due to reasonably high touchdown velocities. This is not particularly evident in the results presented as the initial touchdown that caused the bounce has been used as the 'Time to go = 0' point. In reality, pilot P1 noted that the commanded flares in these instances would have resulted in a go-around.

In forming a judgement as to the preferred design parameters, P1 commented that he was trying to balance flight performance with the comfort of flying the flare manoeuvre. Initiating the flare at T=3.0s felt too close to the ground to the pilot and at T=4.0s as too far away. As the value of $c_{flareT2}$ was increased, an optimal deceleration command point was reached. Once beyond this point, the pilot commented that the pitch up

command came too late. The final pilot-preferred design values, therefore, were established as: $c_{flareT2}$=**0.75 and T=3.5s**.

A number of further comments were made by pilot P1 regarding what might be described as the 'look and feel' of the display as follows:

1. A clear indication of when touchdown occurs is required as the pilot needs to know when to de-rotate (this is also true of the indirect flare display).

2. The display is slightly misleading in one respect. The pitch-up motion is indicated by the command symbol moving from one rest position to another. This gives the impression to the pilot that s/he should commence a pull back on the stick and then stop. What is actually required to maintain the actual symbol over the command symbol is to pull back on the stick and continue that movement until touchdown.

4.5.4.2 Indirect Tau Information Concept

4.5.4.2.1 Performance Results

The full set of indirect flare concept display are summarised in Fig. 4-15 to illustrate the major findings. Fig. 4-15 shows a number of flare trajectories in the τ-domain for the flare test points flown ('$c_{flareT2}$' is denoted 'C6' in the figure).
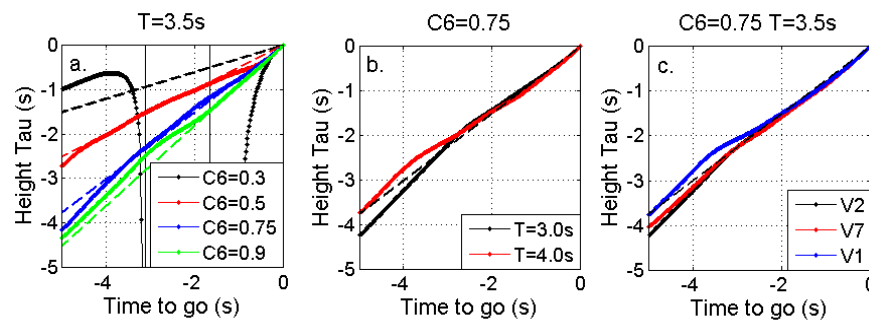

Fig. 4-15. Summary of flare $\tau_{\Delta h}$ trajectories using the indirect display concept: (a) T=3.5s varying $\dot{\tau}_{\Delta h}$; (b) $\dot{\tau}_{\Delta h}$ =0.75, varying T and (c) pilot's preferred combination of the two

As with the direct display concept, Fig. 4-15(a) is intended to show that the pilot was unable to achieve trajectories consist with that commanded for the lower values of $c_{flareT2}$. Indeed, for the example shown with $c_{flareT2}=0.3$, the commanded flare actually induces a ballooned landing. However, with $c_{flareT2}>=0.5$, the actual trajectory flown closely follows the theoretical command trajectory.

Fig. 4-15(b) shows that the flare initiation logic also worked as intended for the indirect display. Fig. 4-15(c) shows that the pilot-preferred design parameters resulted in consistent trajectories being flown in three different visual conditions that were almost exactly as that commanded.

Fig. 4-16 shows the vertical touchdown velocities achieved against the commanded value of parameter $c_{flareT2}$ using the indirect display concept.
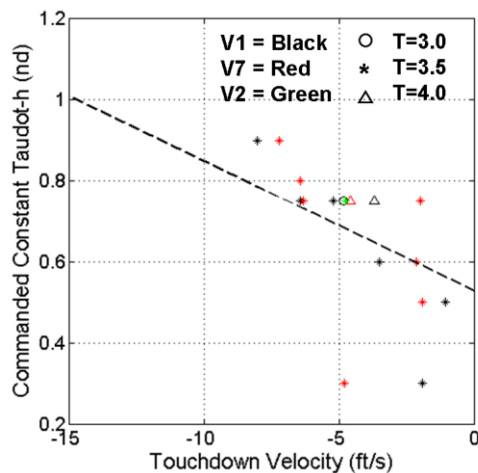

Fig. 4-16. Touchdown vertical velocity for flares performed using the indirect τ-based flare command display

Fig. 4-16 also shows the averaged best-fit line of the observed simulated and flight-test data of Eqs. (4-2) and (4-3). It can be seen that for values of $c_{flareT2}>=0.5$, the touchdown velocities achieved using the display concept approximately follow the slope of the trend line. A majority of the data ($c_{flareT2}>0.6$) lie on the side of the curve that is pessimistic i.e. the curve 'predicts' a higher touchdown velocity than is achieved by using the display. In this sense, it might be said that the display concept out- performs the manual landings performed by pilots flying visually.

4.5.4.2.2 Pilot Comments

The search for design variables for the indirect flare display concept was guided by the results of the direct display concept design parameters. The value of $c_{flareT2}$ was varied around the direct design parameter of 0.75. At lower and higher values of $c_{flareT2}$ (0.3, 0.8, 0.9), the pilot felt that the touchdown point was not predictable and that he could not comfortably track the command symbol. For intermediate points ($c_{flareT2}$=0.5, 0.6), bounces tended to be induced. As such, the same design parameters were set for the indirect display concept i.e. **$c_{flareT2}$=0.75 and T=3.5s**.

On the whole, the pilot felt that this display concept was less easy to fly than the direct concept. This was primarily due to:

1. a lack of indication as to when the flare would commence (there was no such indication on the direct display either) and

2. the display symbology was less well damped than the direct concept symbols.

However, in a contradictory statement, pilot P1 also commented that he perceived the workload involved in using this display to be lower.

4.5.5 Final Flare Command Display Selection

The second reason for performing this experiment was to enable a decision to be made as to which of the two flare display concepts should go forward into the final design for testing against a range of 'conventional' displays. Based upon pilot P1's comments alone, the direct display concept would have been selected. However, a number of factors led to the decision to **use the indirect display for the final design**:

1. The flare display would ultimately have to be integrated into commanding the flare following an approach using the lead-predictor concept. Assuming that the approach was stabilised, then the lead aircraft would already be indicating the required flight path

164

angle. It was therefore considered that the blend between the lead-predictor concept and indirect flight path command concepts would be more easily constructed than with the alternative.

2. If it were considered that the dashed line of Fig. 4-14 and Fig. 4-16 were some kind of 'law' or 'guide' that governed the vertical velocity at touchdown when using τ-based flare displays, then the majority of indirect results all fall on the 'safe' side of the 'law' (Fig. 4-16) i.e. touchdown velocities will be lower than anticipated whereas the opposite is true for the direct command display concept (Fig. 4-14).

3. Flight path vectors are a standard symbol on existing HUD and HDD and as such, integration of the indirect display concept control strategy would be less onerous than for the direct concept.

4.6 Display Trajectory Performance Comparison

This Section presents the summarised trajectory performance results obtained for the flare MTE test points. Averaged pilot ratings for each MTE are also presented. For all figures in this Section, **black** lines represent result data for pilot **P1** and **red** lines represent result data for pilot **P2**.
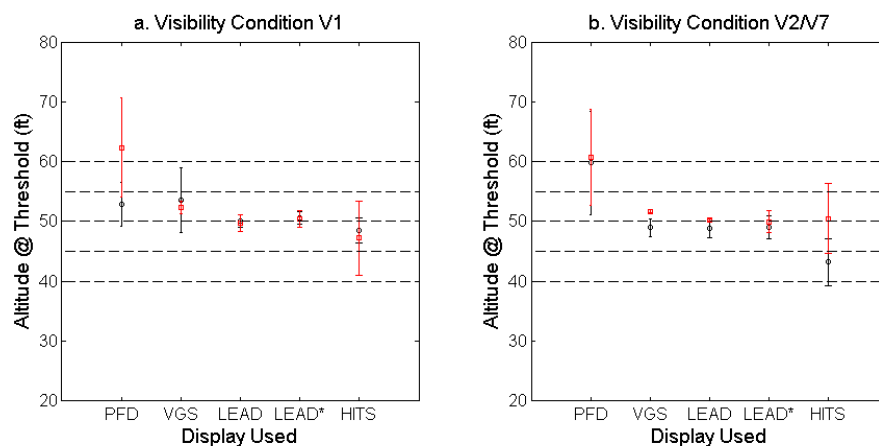

Fig. 4-17. Aircraft cg height AGL at runway threshold

165

The idealised trajectory placed the aircraft cg at an altitude above ground of 50ft as the aircraft crossed the runway threshold. Fig. 4-17 shows the mean aircraft cg altitude during the flare MTE at the runway threshold achieved by each pilot per display in both good and degraded visual conditions. On average, the PFD display format delivered the aircraft to the threshold high and the HITS display low. Both have a wide variation of threshold heights. With the VGS, LEAD and LEAD*, the pilot flies the aircraft more or less at the target altitude over the threshold (if anything, a small distance low). The variation in height above the threshold is much reduced compared to the PFD and HITS and is most tightly constrained when the LEAD and LEAD* formats are used.

The planned threshold speed for the approach is 140 knots. Fig. 4-18 shows the mean aircraft IAS during the flare MTE at the runway threshold
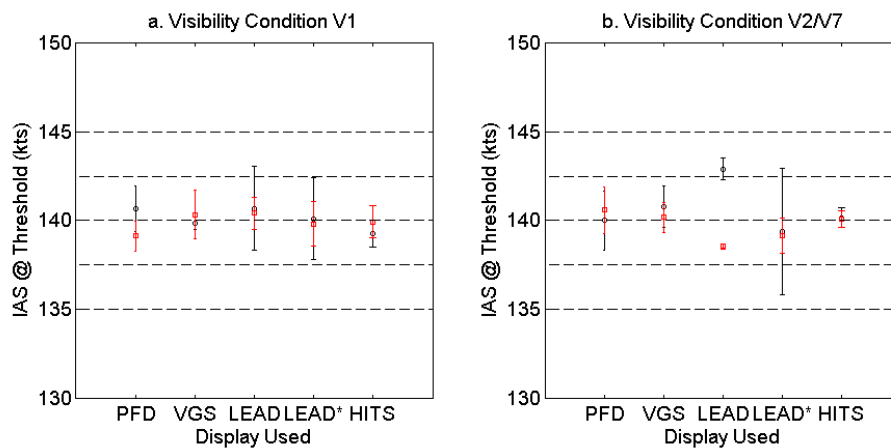

Fig. 4-18. Mean IAS at runway threshold

achieved by each pilot per display in both good and degraded visual conditions. In general, 140 knots is achieved at the threshold except when the LEAD concept is in use in visual conditions V2/V7. Both LEAD concepts exhibit the widest variations of threshold IAS with the HITS and VGS formats giving the least variation.
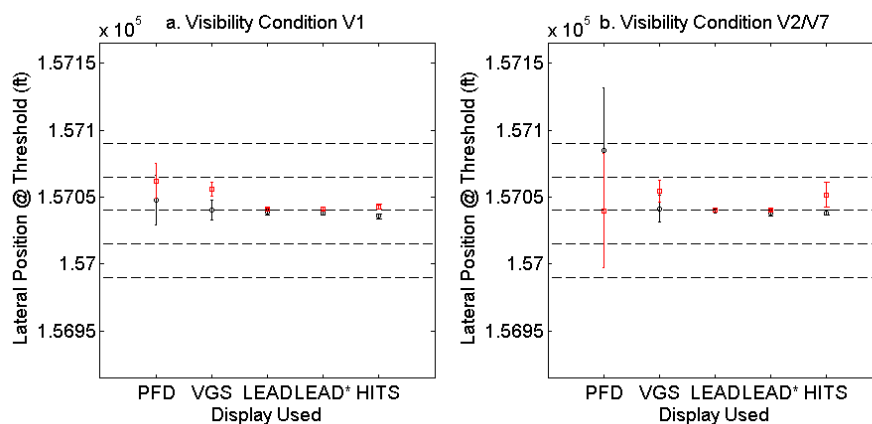
166

Fig. 4-19. Mean easterly coordinate at runway threshold

In an ideal situation, the aircraft ground track should be on the runway centre-line at the threshold (on the runway heading). Fig. 4-19 shows the mean aircraft easterly ('y') database coordinate at the threshold achieved by each pilot per display in both good and degraded visual conditions (runway centre-line database y-coordinate=157040ft). In general, all but the PFD display format result in desirable lateral positions in both good and degraded visual conditions. In degraded conditions, the PFD occasionally results in a lateral position at 50ft AGL outside of even the adequate performance objectives (pilot P1). There is little to choose between the LEAD, LEAD* and HITS concepts in a GVE, but the LEAD and LEAD* displays show a small advantage, in terms of consistency of threshold lateral position in a DVE.

167

The previous three flare analyses relate to the flare start conditions and as such, do not provide a measure of the performance of the flare command
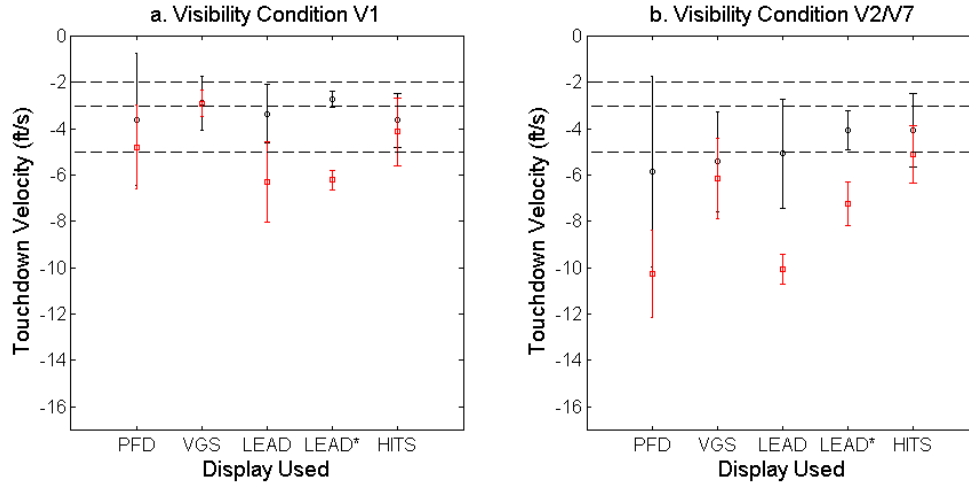

Fig. 4-20. Touchdown vertical velocity for flare MTE

algorithms in use. To achieve this, Fig. 4-20 illustrates the mean aircraft vertical velocity at touchdown i.e. at the end of the flare MTE achieved by each pilot per display in both good and degraded visual conditions. In general, the touchdown velocities achieved in degraded visual conditions are worse (greater in magnitude) than those achieved in good visual conditions. Additionally, on average, pilot P2 consistently makes heavier landings than pilot P1. Flares conducted using the PFD format provide the most inconsistent touchdown velocities whilst the LEAD (pilot P1) and VGS (pilot P2) produce the most consistent values of the same. Only the VGS and LEAD* displays result in desirable average touchdown velocities in visual condition V1 (pilot P1) and the best that can be achieved in degraded visual conditions is adequate performance by the LEAD* and HITS concepts (pilot P1).

Fig. 4-21 illustrates the mean aircraft easterly ('y') database coordinate at touchdown at the end of the flare MTE achieved by each pilot per display in both good and degraded visual conditions. Note that the performance criteria are more relaxed than in Fig. 4-19. The pilots expressed the opinion that in the worst case, touching down anywhere on the runway surface is acceptable. In general, there is little to choose between any of the display formats in good visual conditions. All result in touchdown lateral positions within desirable limits. For degraded visual conditions, the PFD format, once again, results in a variability outside of even adequate performance criteria. For the remaining display formats, there is little to choose between either overall positional accuracy or variability of touchdown lateral position. If anything, the HITS format shows the most
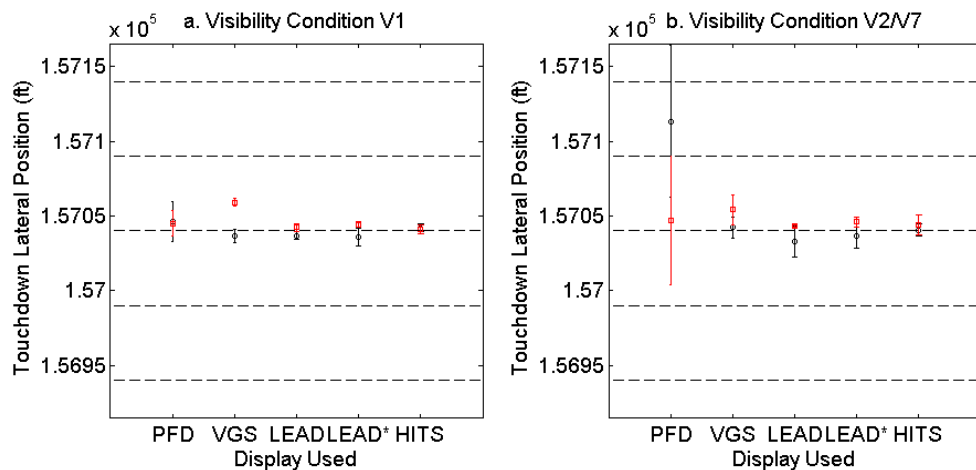

Fig. 4-21. Mean easterly coordinate at touchdown

accurate and consistent results in both visibility conditions. This results of this analysis is academic as the LEAD and LEAD* display formats actually used the same lateral guidance algorithm as the VGS so it is perhaps no surprise that the results are similar. It has been included primarily to show that using the τ-based algorithms for the vertical guidance did not upset the lateral positioning of the aircraft at touchdown.

Fig. 4-22 shows the mean northerly runway coordinate achieved at touchdown at the end of each flare MTE per pilot per display used. This

gives an indication as to the distance along the runway at which touchdown occurred. The mean actual touchdown position does not vary very much (~500ft) for all conditions and displays. Pilot P1 achieves the least variation in touchdown position along the runway using the LEAD* format in visibility condition V1, followed by the VGS format. Pilot P2 achieves an equally small variation in longitudinal runway touchdown position in visual condition V1 for the LEAD* and VGS displays. In visual condition V2/V7, pilot P1 appears to have performed the most consistently using the PFD display. This is interpreted as simply that he was unable to see the runway on this condition and flew into it at the same spot every time. Similarly, pilot P2 appears to touch down in a consistent manner using the LEAD concept. Again, the result of Fig. 4-20 suggest that not much of a flare was performed in these cases so the pilot simply flew into the runway at the approximate same location. Otherwise, both pilots perform equally well with the VGS and LEAD* display formats in visibility condition V2/V7.
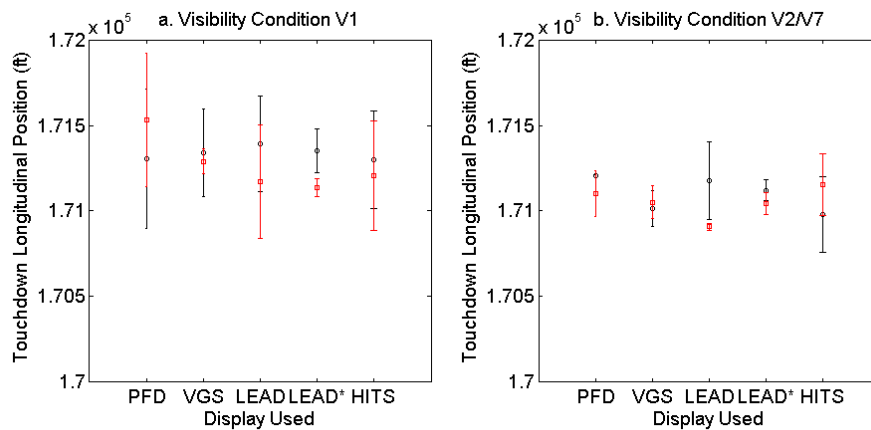

Fig. 4-22. Mean northerly coordinate at touchdown

4.7 Flare MTE Pilot Ratings

Fig. 4-23 shows the average ratings for all of the flare MTEs given by both pilots in the differing visibility conditions for each display format. No ratings are provided for the LEAD* format as these flare data were
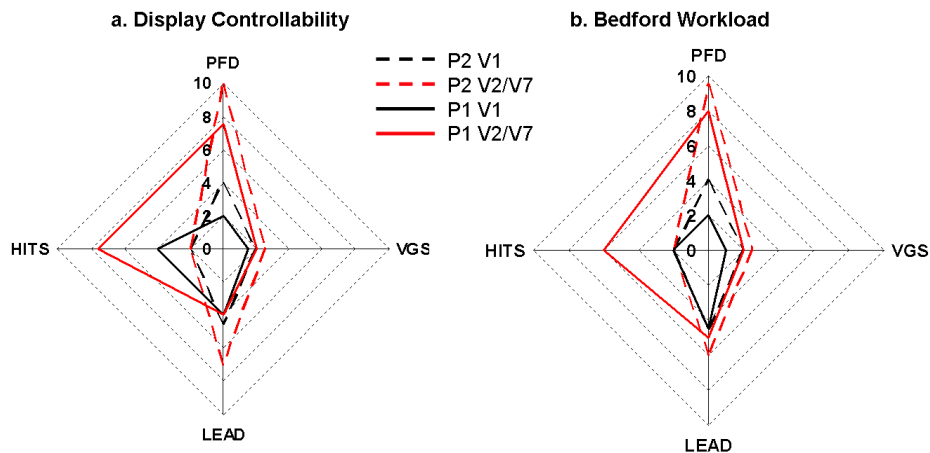

Fig. 4-23. Pilot ratings per display for the flare MTE: (a) Display controllability and (b) Bedford workload

collected from the Full and Curved Approach MTEs. The flares for these test points were not rated separately. In terms of analysis, this is acceptable since the flare is a short manoeuvre and speed can be considered constant throughout it so the absence of speed information is not critical. The only difference will lie in the initial conditions at the start of the flare whereby the IAS at the threshold might not be as consistent as with the LEAD* concept (see Fig. 4-18). Of course, any display would ultimately have to cope with whatever initial conditions were thrown at it by a line pilot so it is proposed that the ratings given for the LEAD display can be considered valid for the LEAD* as well.

Fig. 4-23 shows that the clear favourite for the flare in terms of both controllability and workload was the VGS. The high ratings for the PFD and HITS concepts in degraded visual conditions were awarded because both pilots felt that a safe flare was not achievable in the visual conditions presented (pilot P1 initiated go-arounds for 3 PFD test points). The LEAD

171

concept is generally rated somewhere in between these two extremes. The key comments that led to the LEAD concept being rated as it was are:

1. Low damping/command reversal makes the LEAD symbol a moderate workload format to follow successfully.

2. The display was not initially intuitive and the pilots had to think about which symbol to follow. This was exacerbated by difficulties telling the two display symbols apart when they are overlaid.

The key additional comments arising from the flare MTE for the VGS display concept were:

1. Initial attempts at flare not as easy as hoped it might be.

2. One or two occasions where the wrong symbol was 'followed' i.e. pilot being guided by the wrong symbol. The flare cue symbol automatically aligning itself with the guidance cue on one or two occasions.

3. Both pilots would have preferred the runway outline to have remained in place as a flare cue and found that its disappearance at 100ft slightly disconcerting/disruptive.

4. Only small pitch changes required to control flight path. The guidance provides a continuous movement of aft-stick but with a variable rate.

The key additional comments arising from the flare MTE for the HITS display concept were:

1. The guidance provided was insufficient. If the pilot flared too high, the tunnel frames disappeared from view before touchdown occurred. In visual condition V2, this was very uncomfortable for the pilots.

2. The HITS concept, or at least the tunnel frames, as tested are not suitable for use as a flare guide as they do not provide cues to allow the manoeuvre to be accomplished consistently and predictably.

3. With good visual conditions, the flight path vector by itself is a useful aid. The two other pieces of information required in the head-up field of view are airspeed and radar altitude above ground (although both pilots also stated that so long as speed was stable and at a sufficient value at the start of the flare, any change in IAS was not really an issue thereafter). Pilot P2 commented that he finds the talking radar altimeter in the Boeing 737 helpful during the flare manoeuvre. As an aside, it may be that the silence between height annunciations provides a suitable 'gap' that the pilot can use as a tau-based motion controller. This would be an interesting research topic for the future.

The key additional comments arising from the flare MTE for the PFD display concept were:

1. In the degraded visibility conditions used for the testing, in the real world, any form of landing would not be possible.

2. The ratings really relate to a visual landing since the PFD display itself provides no flare guidance.

3. Lateral characteristics of the aircraft model drove the workload ratings higher than might be given in a more stable aircraft as maintaining runway centre-line down to touchdown required significant attention to lateral stick inputs.

If the pilot controls the lateral axis of the aircraft model correctly, the only other task is to set the correct power to achieve the desired 140 knots at flare initiation.

4.8 Pilot Control Strategy

4.8.1 Pilot Control Strategy Background

The primary aim of the research was to produce guidelines for the development of future pilot vision aids. However, for the flare manoeuvre, it was noted that the trajectory (aircraft height) can be defined with respect to time with reference to only its total duration and the value of $\dot{\tau}_{\Delta h}$ selected by the pilot. At the same time, using the short-period linearised aircraft equations of motion, it is possible to derive an expression for aircraft elevator angle that includes derivatives of the flare trajectory. This is derived as follows.

The control of the height and vertical velocity of an aircraft is generally exercised using the phugoid mode of that aircraft's longitudinal motion [123]. The phugoid mode of an aircraft is generally a 'slow', low frequency mode, the implication being that it affords little or no short-term control over height. There are instances when the pilot of an aircraft will want to exercise tight, rapid control over the height of an aircraft, the flare manoeuvre being an obvious example. An alternative, therefore, is to consider that during the flare manoeuvre, it is the short period dynamics of the aircraft that are important. The short period mode is almost exclusively an oscillation in which the principle variables are pitch rate, 'q' and incidence angle, 'α', the speed remaining almost constant [120]. This description seems to fit that of the flare manoeuvre. The analysis can therefore now proceed on the basis of the short period dynamics equations. Fig. 4-24 shows the quantities of interest for the approach case.
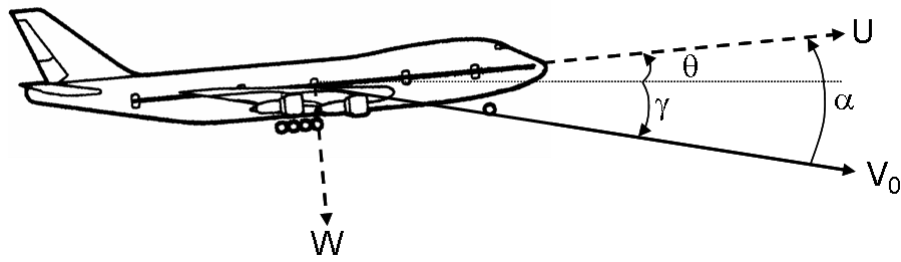
Fig. 4-24. Variable definition for derivation of pilot control input for constant rate of change of height tau

U and W are the aircraft body axis velocities, made up of trimmed and perturbation components (e.g. $U = U_{trim} + u$). V_0 is the total forward flight speed of the aircraft. The arrows show the positive directions for each value. From Ref. [120] we have the equations of motion that are relevant to the dynamics of the aircraft short period:

$$\begin{bmatrix} \dot{w} \\ \dot{q} \end{bmatrix} = \begin{bmatrix} z_w & z_q \\ m_w & m_q \end{bmatrix} \begin{bmatrix} w \\ q \end{bmatrix} + \begin{bmatrix} z_\eta \\ m_\eta \end{bmatrix} \eta \qquad (4\text{-}9)$$

For the analysis, the primary variable of interest is the inertial i.e. referenced to Earth axes vertical velocity W_e and specifically its perturbation from trim value, w_e (where $W_e = W_{etrim} + w_e$). For small pitch angles, θ, it can be said that:

$$w_e \approx w - V_0 \theta \qquad (4\text{-}10)$$

Assuming z_η to be negligibly small, the first two equations of Eq. (4-9) can then be further reduced to:

$$\dot{w} = z_w w + V_0 q \qquad (4\text{-}11)$$

$$\dot{q} = m_w w + m_q q + m_\eta \eta \qquad (4\text{-}12)$$

Differentiating Eq. (4-10) w.r.t time and substituting the result into Eq. (4-11) yields:

$$\dot{w}_e - z_w (w_e + V_0 \theta) = 0 \qquad (4\text{-}13)$$

175

Substituting Eq. (4-10) into Eq. (4-12) gives:

$$\dot{q} - m_w(w_e + V_0\theta) - m_q q = m_\eta \eta \qquad (4\text{-}14)$$

It is now necessary to eliminate q and $\dot{q}$ from Eq. (4-14) and this can be achieved by rearranging Eq. (4-13) for θ and differentiating the result to give:

$$\theta = \frac{\dot{w}_e - z_w w_e}{z_w V_0} \qquad (4\text{-}15)$$

$$q = \frac{\ddot{w}_e - z_w \dot{w}_e}{z_w V_0} \qquad (4\text{-}16)$$

$$\dot{q} = \frac{\dddot{w}_e - z_w \ddot{w}_e}{z_w V_0} \qquad (4\text{-}17)$$

Substituting Eqs. (4-15), (4-16) and (4-17) into Eq. (4-14) and re-arranging yields:

$$\dddot{w}_e - (z_w + m_q)\ddot{w}_e + (m_q z_w - m_w V_0)\dot{w}_e = m_\eta z_w V_0 \eta \qquad (4\text{-}18)$$

Eq. (4-18) provides an expression that relates elevator input angle to the derivatives of the (earth-referenced) vertical speed of the aircraft, w_e. An analytical solution is available for this equation because expressions are already available or can be derived for the derivatives of w_e if we assume a control strategy of $\dot{\tau}_{\Delta h} = c$. For the flare manoeuvre, in Eq. (2-1), $x = \Delta h$ so:

$$\ddot{h} = \dot{w}_e = -\left(\frac{h_0}{cT^{\frac{1}{c}}}\right)\left(\frac{1-c}{c}\right)t^{\frac{1-2c}{c}} \qquad (4\text{-}19)$$

Eq. (4-19) can be further differentiated to give:

$$\dddot{h} = \ddot{w}_e = -\left(\frac{h_0}{cT^{\frac{1}{c}}}\right)\left(\frac{1-c}{c}\right)\left(\frac{1-2c}{c}\right)t^{\frac{1-3c}{c}} \qquad (4\text{-}20)$$

$$h = \dddot{w}_e = -\left(\frac{h_0}{cT^{\frac{1}{c}}}\right)\left(\frac{1-c}{c}\right)\left(\frac{1-2c}{c}\right)\left(\frac{1-3c}{c}\right)t^{\frac{1-4c}{c}} \qquad (4\text{-}21)$$

One final step is to normalise Eq. (4-18) by the final elevator angle for the touchdown, η_f such that:

$$\overline{\eta} = \frac{\eta}{\eta_f} \qquad (4\text{-}22)$$

Inserting Eq. (4-22) into Eq. (4-18) gives:

$$\overline{\eta} = \frac{1}{\eta_f m_\eta z_w V_0}\left(\dddot{w}_e - (z_w + m_q)\ddot{w}_e + (m_q z_w - m_w V_0)\dot{w}_e\right) \qquad (4\text{-}23)$$

The w_e derivatives can be calculated from Eqs. (4-19), (4-20) and (4-21). V_0 and η_f are known from the flight data and m_η, z_w, m_q and m_w can all be

obtained from a linearised version of the GLTA FLIGHTLAB simulation model. Table 4-1 provides the values of the linearised coefficients for the GLTA in the final approach condition (140kts, FLAPS

Parameter	Value
m_η	0.00453
z_w	-0.787
m_q	-1.112
m_w	-0.0153

Table 4-1. Linearised derivatives for GLTA simulation model

50, gear down). The derivatives values used for the analysis of Section 4.8.3 are as per the output of FLIGHTLAB linearisation routines i.e. they are the 'semi-normalised derivatives' of Ref. [29] and are equivalent to the 'concise derivatives' of Ref. [120].

By combining the trajectory definition with the pilot elevator command, it was considered that the τ-based flare model might also provide the starting point for a pilot model of the flare. This idea has not been investigated during the course of this work.

4.8.2 Pilot Control Strategy Theory

Before presenting the results achieve with the test pilots, it is worth first re-considering the theoretical background presented in Section 2.4.1.5. This shows that if a pure constant $\dot{\tau}_{\Delta h}$ strategy is selected, then the resultant residual (touchdown) velocity should be zero. In practice, this is very rarely the case. The theory is then developed further to include a limiting acceleration (be that observer-selected or vehicle limited). When such a limit is imposed towards the end of the manoeuvre, it is shown that non-zero residual velocities are achieved.

Fig. 4-25 shows the theoretical values for normalised elevator input for varying values of $\dot{\tau}_{\Delta h}$ (denoted 'c' in the figure). As would be expected by the normalisation process, all but c=1.0 curves end at 1.0. Two special cases exist for c=0.5 and c=1.0. For the latter case, a constant velocity of approach to the target surface results. For the flare, this means that the aircraft is flown into the ground at the trimmed approach condition. No elevator input is made and this is shown as $\overline{\eta} = 0.0$. For the case of c=0.5, the surface is reached with zero residual velocity. In this case, the initial (step) input is just sufficient to bring the vertical descent rate to zero if it is maintained to touchdown. For the remaining cases, as 'c' moves from 0.5 to 1.0, a step elevator input of decreasing magnitude is made, followed by an increasing input commenced at an increasingly late stage of the manoeuvre. What is not shown, for reasons of figure clarity, is that for the larger the value of 'c' selected, the larger is the

Fig. 4-25. Theoretical normalised pilot elevator angle for flare MTE

maximum required elevator input compared to the elevator command at

178

touchdown (which is also reached at an increasingly late point during the motion).

4.8.3 Pilot Control Strategy Analysis Results

In order to be able to compare theoretical and actual normalised pilot elevator commands, a number of data items had to be established for each manoeuvre:

1. The value of $\dot{\tau}_{\Delta h}$, 'c', used. Only those flares that exhibited strong constant $\dot{\tau}_{\Delta h}$ behaviour were selected for analysis.

2. The nominal 'limiting acceleration' selected by the pilot.

3. The linearised aerodynamic and control derivatives for the aircraft model for the flare manoeuvre. These are provided in Table 4-1.

4. The moment of flare initiation. This is required since Eq.(4-23) provides the additional input required over and above the trimmed approach value.

Fig. 4-26 shows a small number of representative results from unguided flares i.e. flare conducted in V1 conditions with aircraft under manual control conducted by pilot P1 using the information detailed above. Normalised elevator input is plotted against (normalised) time for both theory and pilot. It can be seen that the theoretical input captures the general character of the pilot's input. The elevator input increases to a limited degree over the early portion of the manoeuvre which rises to a peak value prior to a reduced value at touchdown. However, the detail of the pilot input is not particularly well matched with the theory. In general, the pilot input overshoots the theoretical curve during the initial ramp up to the peak input value. The theoretical elevator response then consistently over-predicts the peak actual value. What is not captured is that the pilot elevator input is not one smooth pull back on the stick, but a small number of pulsed (stick moved fore and aft) inputs to the peak value. Again, it

may be that the simulation facility stick dynamics have their part to play in this result but no data has been collected to support this claim as yet.
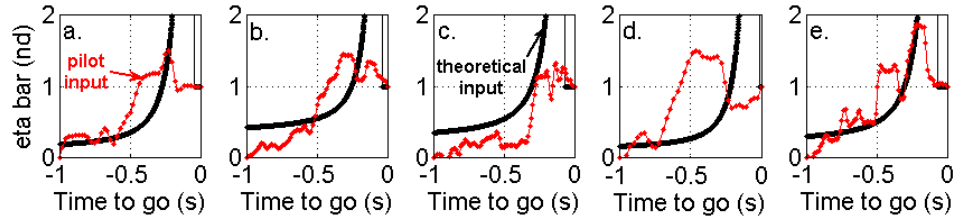

Fig. 4-26. Comparison of theoretical and actual normalised pilot elevator input for flare manoeuvre

4.9 Discussion of Results

The results of the analyses of the flare MTE have been presented in the preceding Sections. These present a number of interesting issues and opportunities which deserve further discussion.

4.9.1 Trajectory Definition

The results of the basic τ analysis of the flight test data from Ref. [122] show two different strategies for the flare in what might be called the $\dot{\tau}_{\Delta h}$ 'domain'. These provide a new means by which the trajectory of a flare can be defined. Furthermore, using the τ curves, it is possible to say, at a glance, the character of the trajectory followed in terms of the motion gap closure variable. The Type 2 flare trajectory definition has already been defined in Eqs. (2-25)-(2-31). There, it is shown that the motion gap changes as a function of a power law. For the Type 1 flare, it can be further shown that during the constant $\tau_{\Delta h}$ portion of the manoeuvre, the motion gap follows an exponential change (and hence so does the velocity and acceleration of that variable). The proof of this is straight-forward. For the closure of a motion gap, 'Δx', with τ, 'a':

$$\frac{\Delta x}{\dot{x}} = a \tag{4-24}$$

180

where 'Δx' is current gap to be closed and $\dot{x}$ is the instantaneous rate of closure of that gap. Rearranging Eq. (4-24) and writing in longhand form yields:

$$\frac{d\Delta x}{dt} - a\Delta x = 0 \qquad (4\text{-}25)$$

The general solution to the first order differential equation of (4-25) is:

$$\Delta x = Ae^{\frac{t}{a}} \qquad (4\text{-}26)$$

where 'A' is the integration constant that vary with the initial conditions as the pilot initiates the constant-τ phase of the flare manoeuvre. It is evident from Eq. (4-26) that the motion gap closure whilst τ is held constant is exponential in nature. This would result, theoretically at least, in a flare manoeuvre that never resulted in contact with the ground. Alternatively, in order to make contact with the ground using only this strategy, the pilot's 'aiming point' would have to be somewhere below the runway surface. Whilst it is not claimed that this observation has any major new applications, it does allow the character of the flare (or any other motion that follows similar trajectories) to be decomposed and described in a meaningful manner.

4.9.2   Type 1 vs Type 2 Flare Strategy

It is interesting to note that for both the flight test and simulated flight test flare summary touchdown velocity results, for all but one case of each type, the Type 1 flare always result in touchdowns with vertical descent rate below the nominal 'acceptable' value of 5ft/s. This is despite a wide range of $\dot{\tau}_{\Delta h}$ values used over the final portion of the manoeuvre. By the very definition of the groupings therefore, pilot groups 'FA' and 'SA' feature almost exclusively in Fig. 4-8(a). Section 4.5.3 outlines the primary reasons for selecting the Type 2 flare as a basis for a display control law. In addition to these, however, the Type 2 flare lends an air of

predictability to the display control algorithms in that the relationship between touchdown velocity and $\dot{\tau}_{\Delta h}$ selected can be approximated by a straight line in the first instance. The Type 1 flare touchdown velocity and $\dot{\tau}_{\Delta h}$ relationships is indicative of the inherent flexibility and adaptability of pilots to given situations. In order to start to develop guidelines for display design, it is necessary to take complex issues/problems and distil them down into a more manageable form. The Type 2 flare results lend themselves to such a process, whereas the Type 1 results do not. That is not say that the Type 1 results should be disregarded completely (Section 10.2.1 recommends that the Type 1 flare be investigated further). As a first pass, however, the Type 2 flare 'linear' results of Fig. 4-8 and Fig. 4-9 appeared to present a greater opportunity for success in this regard.

An alternative way to consider the results of Fig. 4-8 and Fig. 4-9. Is via the concept of τ-guides. The best fit lines cross the $\dot{\tau}_{\Delta h} = 0.5$ boundary at a touchdown velocity of 0ft/s and the $\dot{\tau}_{\Delta h} = 1.0$ at 15ft/s (approximately). The former case represents a 'perfect' touchdown i.e. the vertical descent rate reaches zero just as the main gear contact the runway surface. It is equivalent to the pilot following (i.e. coupling onto) a constant deceleration τ-guide with the coupling constant set to unity. The latter case is the ultimate 'imperfect' case where the aircraft strikes the runway surface at the approach descent rate (for the simulation flares, the approaches were conducted at 140 knots on a 3.5° glide slope. This equates to a vertical descent rate of 14.4ft/s. It is assumed that the actual flight tests conditions were similar). It equates to the pilot coupling onto a constant velocity τ-guide with the coupling constant set to unity. It is evident from the results that the 'coupling constant' selected by pilots falls somewhere in-between these extremes. The flight test results give an indication that a small majority of pilots use a guidance strategy that is closer to the 'perfect' solution. This is also evident, but to a lesser degree in the simulation data.

182

As such, τ-guidance can also be used as a model to describe pilot guidance strategies during the flare. This complements the previously reported research in Ref. [16].

4.9.3   Tau of Height as a Visual Perception Variable in GVE and DVE

The constant $\dot{\tau}_{\Delta h}$ hypothesis and the results presented to support it provide a deceptively simple potential solution to how pilots judge their descent to the runway surface during the flare. It is not the author's intention to present this as the 'final solution' to the perception of motion during this manoeuvre. Rather, it is only a part of the complete picture. The end result might well be simple, but the explanation of how this is achieved (beyond the scope of this thesis) is unlikely to be so. The evidence for this comes from two sources.

Firstly, $\tau_{\Delta h}$ relationships did not break down on every degraded visual landing. Even in some extremely degraded conditions, the pilot was able to carry out an acceptable touchdown, albeit extremely uncomfortably. One example of this was an approach carried out in V7 visual conditions. The pilots commented that their ability to carry out a flare was dependent upon whether a runway centre-line was visible just prior to touchdown. If it was not, then the colour of the runway merged with the fog colour. No flare was carried out and a hard landing resulted. If a white line did become visible, however momentarily, this sometimes proved sufficient to information to flare to some degree. This is perhaps again testament to the adaptability of the test pilots used but also to the information content available even in extremely poor visual conditions.

The second source of evidence comes from the eye-tracking analysis of Section 4.4. Here, pilots P1 and P3 are asked to carry out identical tasks. For them to be able to do this using $\tau_{\Delta h}$, Δh, or its corollary, must be visually available. The results from pilot P1 offer one solution to how this

is possible and ties in with instructions issued to student pilots during the flare. Pilots are encouraged to shift their gaze from the near-end of the runway during the approach to the far end of the runway (or horizon) during the flare. In doing so, motion due to the nose-up pitch of the aircraft is minimised and the runway end/horizon provides a point that does not move against which to judge aircraft motion. Pilot P1 appears to use a point a short distance ahead of the aircraft as a datum against which $\tau_{\Delta h}$ might be obtained by comparison with the horizon (see Section 2.4.1.2 on perception of τ). It is possible to offer an explanation of the degradation of performance during the flare manoeuvre with degraded visual conditions because the 'horizon' moves increasingly close to the pilot. The relative motion of this point due to aircraft pitch increases when compared to a more distant point and so the $\tau_{\Delta h}$ information available by comparing with the position ahead of the aircraft becomes less reliable. Unfortunately, pilot P3 uses a different technique and maintains gaze on the horizon during the flare. Despite this, pilot P3 makes successful landings with both Type 1 and Type 2 characteristics. Discussions revealed that pilot P3 maintained gaze on the horizon but used peripheral vision to detect descent to the runway. In this way, some point(s) in space not in the pilot's direct line of sight are being used to judge the descent to the runway surface. Of course, degrading the visibility means that the peripheral cues are also degraded and this, it is proposed, leads to the loss of τ information in this case. This difference of technique lends evidence to the suggestion that visual perception systems have evolved to be robust. It is not sufficient in terms of survival to rely on a single method of motion perception and so it should be no surprise that different techniques exist to judge observer motion. Of course, the foregoing argument does not rule out the possibility that pilots P1 and P3 are not both using $\tau_{\Delta h}$, just different means of detecting it (the explanation of Section 2.4.1.2 can be used equally well for points in the visual field not directly ahead of the observer).

184

There is an alternative explanation for the gaze position behaviour of pilot P1 and that is offered in Ref. [15]. Here, it is posited that the pilot of an aircraft (or an animal in flight) will land by coupling the τ of two distant points – one some distance from the observer and one nearer to the observer. It was not possible to test this hypothesis from the results taken for this work but suggests an intriguing possibility for future experimentation. This situation and the coupling required is shown in Fig. 4-27.
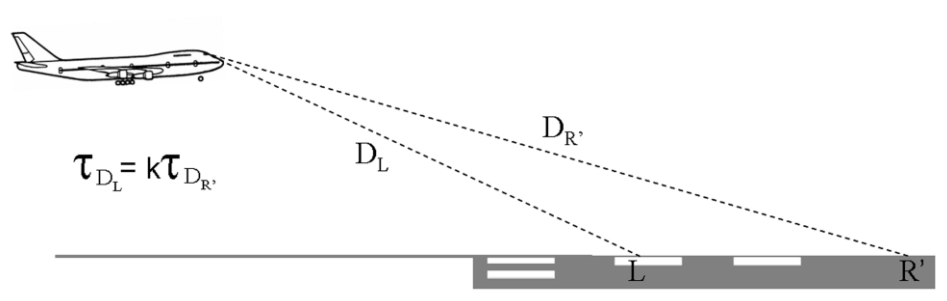

Fig. 4-27. Example of possible τ-coupling strategy used to land an aircraft

4.9.4 Tau of Pitch Angle as a Visual Perception Variable

The $\tau_{\Delta\theta}$ results have largely been ignored during the research beyond the basic τ analysis. This is because only small regions of coherence do exist, but not nearly to the same extent as for the Δh motion gap variable. For this reason, the variable was discarded as being useful for the initial pass at display design but it does raise a more interesting general question. The question that it raises relates to how τ might be used for dynamic pursuit manoeuvring and how this might then be used either in aircraft display or control systems. For the results presented in Fig. 4-7, it is clear that the pilot has a number of attempts at obtaining the correct pitch angle (described as 'hunting' in Section 4.2.2). This results in many 'zero crossings' for the pitch rate. From Eq. (2-1), $\tau_{\Delta\theta}$ must therefore become infinite. Yet it is clear from Fig. 4-7(c) that despite this, coherent constant $\dot{\tau}_{\Delta\theta}$ continuously re-emerge for short periods. It is as if the motion gap τ is

185

being 're-set' in some way once the target value is missed. This feature would be useful for pursuit-type command displays and should be further investigated as a continuation of this work.

One further point to note from the results presented in Fig. 4-7 is that there appears to be a 1-2Hz oscillation in the pitch attitude. Inspection of the pilot control activity also showed this oscillation to be present and in phase with the pitch oscillations. No pilot comments were recorded indicating that this was an issue that needed to be corrected. A brief analysis of $\tau_{\Delta\theta}$ using later trial data showed the oscillation to be less noticeable but the reduced coherence to still be an issue. As such, the decision to not continue the investigation using this parameter and the recommendation to use it as a basis for future studies still stand.

4.9.5   Display Selection Process and Initial Testing

Having made the decision to use a Type 2 flare as a basis for the flare command algorithms, it was necessary to decide between the 'direct' and 'indirect' methods of presenting command information to the pilot and the values of the parameters to use in the command algorithm. Section 4.5.4 reports on this process. There are a number of other issues worth reporting that were observed during this selection process.

The first of these relates to the temporary solution used to guide the pilot down to the runway for the direct display concept in order that the flare
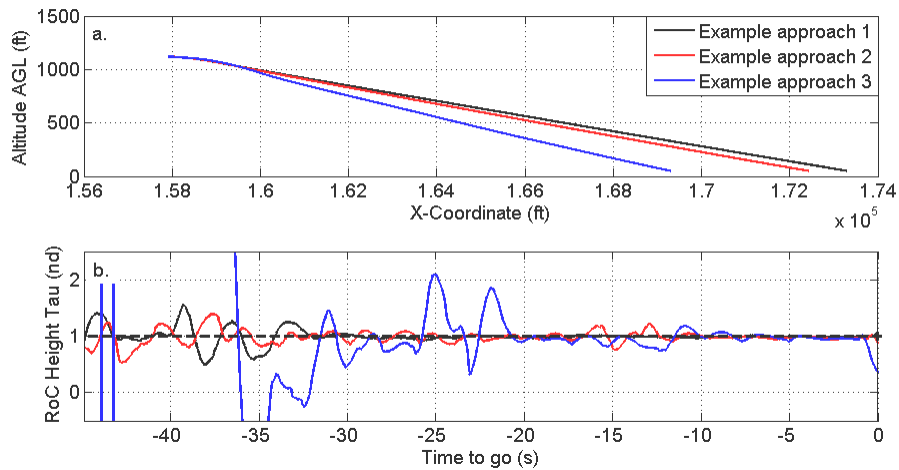

Fig. 4-28. Illustration of different approach trajectories flown using direct τ command display concept: (a) inertial trajectory and (b) commanded $\dot{\tau}_{\Delta h}$ against actual

algorithms could be tested. To allow the pilot to get down to within 3.5 seconds of contact with the runway surface, Ref. [30] suggests that the display concept should command an initial approach $\dot{\tau}_{\Delta h} = 1.0$. In theory, given identical start conditions, this should result in a constant approach path. This was found not to be the case. Fig. 4-28 shows a number of the approaches made by Pilot P1 using the direct command display. It can be seen that despite nominally identical start conditions, perhaps due to small differences in trim or initial pilot input when released from trim, or even not following the commanded $\dot{\tau}_{\Delta h}$ value (the black dashed line) accurately, large differences in flight-path trajectory result (by as much as 4000ft at threshold height between examples 1 and 3 above). This highlights two issues. The first is that using a simple $\dot{\tau}_{\Delta h} = 1.0$ algorithm to drive an approach display is unlikely to prove fruitful (when factors such as gusts and turbulence are included, for example). The second is that care must be exercised in the use of τ for trajectory control where the values are not supposed to be changing. By its very definition, there are many (parallel) paths that can be followed where $\dot{\tau} = 1.0$ for a given, fixed, gap closure rate. Moreover, if the gap closure rate varies, there is still a solution for the

187

instantaneous gap closure value that will meet the $\dot{\tau}_{\Delta h} = 1.0$ criteria. Fig. 4-29 shows this latter scenario. The final indirect flare command display was not susceptible to this error as $\dot{\tau}_{\Delta h} \neq 1.0$ and so Δh and its respective rate of change were supposed to be changing. This issue adds further weight to the decision not to use a Type 1 flare as the command algorithm as the very final portion of the flare would be prone to the unpredictability described.
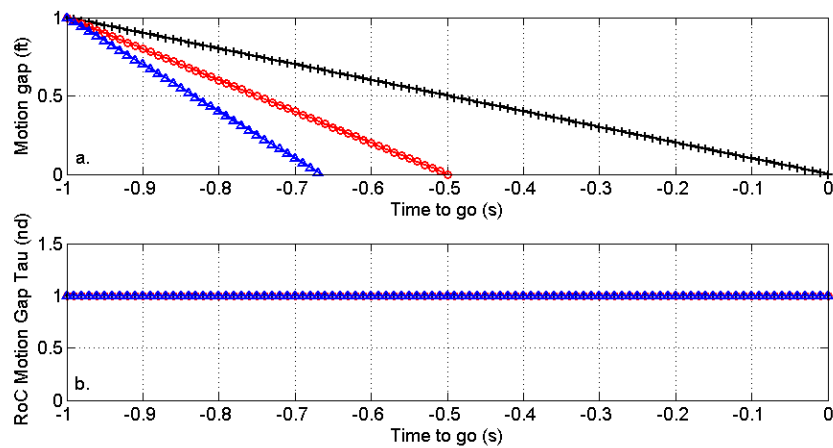

Fig. 4-29. Illustration of multiple trajectories that satisfy $\dot{\tau}_{x} = 1.0$

The second, related issue is one that was encountered during display development. In the same way that many trajectories satisfy the relationship $\dot{\tau}_{\Delta h} = 1.0$, there are two trajectories that fulfill the $\dot{\tau}_{\Delta h} = c_{flareT2}$ relationship, even if $c_{flareT2}$ does not equal 1.0. This arises from the definition of τ in Eq. (2-1). For the flare manoeuvre, x=Δh and Δh is measured as positive from the target surface. An approach to the surface means that the rate of change of Δh is negative and the opposite is true for motion away from the surface. $\tau_{\Delta h}$ is then positive or negative respectively. However, the rate of change of $\tau_{\Delta h}$ of can be the same in both cases. It is this parameter that is being used as the command variable for the flare display. In practice, in the early stages of display algorithm development, this led to a commanded pitch up if the flare was ballooned. Fig. 4-30 shows this situation schematically. Section 3.5.4.5.2 reports how

this issue was overcome for the display concept tested. A second method to overcome this issue would be to test for the sign of $\tau_{\Delta h}$.

The final issue, that of motion gap rate zero crossings, has already been discussed in terms of pitch angle and $\tau_{\Delta\theta}$.
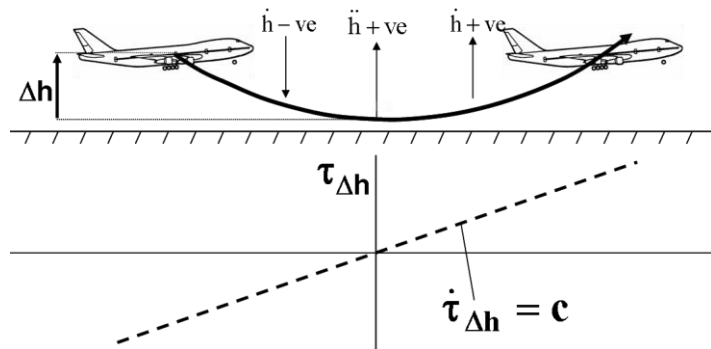

Fig. 4-30. Commanded $\dot{\tau}_{\Delta h}$ **can prescribe motion away from as well as towards a target surface**

This issue also arises for the flare command should the pilot be too aggressive and lead the flare command symbol. Occasionally, this led to the aircraft 'ballooning' (flying parallel to or ascending from the runway surface). The pilot would therefore correct for this and the sign of the vertical acceleration, $\ddot{h}$, would be changed. In turn, the display symbol would be driven to the limits of its travel on the screen (from Eq. (3-34), this gives the square root of a negative number). This was the primary cause of the 'jittery' behaviour reported by the pilots and hence the reason that, in some instances, the display was difficult to fly. The manual solution to this problem was to commence a small pull back on the stick just prior to the flare algorithm being phased in (i.e. when the 'FLARE' symbol starts to flash). This ensured that the vertical acceleration was always in the correct sense when the algorithm of Eq. (3-34) was blended in to control the flare command symbol. This is obviously not a satisfactory long term solution. Such a signal would need to be injected automatically or any solutions found to the pursuit issue already discussed could be implemented to resolve the issue.

4.9.6   Display Comparison

The results from the comparison of different display concepts for the flare MTE have been encouraging. In terms of both spatial position at the start of the flare and descent rate at touchdown, the LEAD and LEAD* concept performs on a par with or better than the implemented version of the VGS. It has to be said that pilot P1 out-performs pilot P2 in this regard and this is reflected in the ratings assigned to the display by each pilot, where the LEAD concept fares slightly less well with P2 than P1. The weak area identified for this concept is the speed control via optical looming and this shows as a wide spread of IAS values at threshold height. Paradoxically, pilot P2 out-performs P1 on this parameter. Again, this explains the higher workload ratings given by pilot P2 for the LEAD concept who reported working hard to maintain speed. This issue will be discussed further in Section 5.7.

What is noticeable across all display formats is that, generally speaking, adherence to target performance criteria worsens when visual conditions are degraded from V1 to V2 or V7. This implies that, however unconscious the process, the pilots are using additional information from the visual scene (over and above that provided by the display symbols) to fly the MTE. It is not at all clear, however, from the eye-tracking results (which only show point-of-regard), what form this information might take. This provides what may amount to a large source of research material that can be pursued in the future.

The HITS concept employed for the comparative trial essentially proved either little or no help to the pilots, despite performance results that might indicate the contrary. This was, in part, due to the fact that the tunnel frames ended at the nominal ideal touchdown point. If the pilot ballooned the aircraft or 'flared long', the aircraft would very often still be airborne by the time that the last tunnel frame had been reached. In V1 conditions

this was not too much of a problem but in V2, with no runway lights, the pilot was presented with a black screen. Any touchdown achieved was carried out blind. For any future work in this area, it is suggested that the tunnel frames be continued along the length of the runway. As such, the HITS concept has potentially been rated more harshly than it otherwise would, had this improvement been implemented for the reported trials.

4.9.7   Pilot Control Strategy

The results presented in Section 4.8 provide some encouragement in terms of being able to model pilot behaviour in terms of τ. The general character of the theoretical input matches practice but there are the noted significant differences. These differences are not entirely unexpected. Ref. [124] provides a similar pilot control strategy analysis for helicopter flight approaching rising ground (in itself, a manoeuvre not dissimilar from the fixed-wing flare). In this analysis, simulated flight test results are compared with theoretically derived inputs and it was found that the actual pilot inputs were larger and more aggressive than might otherwise have been predicted. It is suggested in the reference that this might be to stimulate the flow field to ascertain more quickly the motion that is being undertaken. The same might be said for the fixed-wing results. For the early to middle part of the manoeuvre, generally speaking, the elevator input is more aggressive (larger and applied more quickly) than theory would suggest. Although not visible from Fig. Fig. 4-25, large initial inputs result in lower peak values of elevator and this is clearly observed in the actual pilot results when compared to the 'required' normalised angle of the theory (the theoretical peak elevator angles being unattainable in some cases).

There is also the suggestion in Ref. [124] that the difference between theoretical and actual control inputs might be the generator of workload in

191

a manoeuvre. This would be an interesting avenue of research to pursue given the theoretical results presented in this thesis.

One further thought occurs on the issue of other avenues of research. The current work has made use of the spatial variable Δh as a means of cueing the pilot to perform the flare manoeuvre. An alternative might be to provide a cue to the pilot using the desired elevator input. For aircraft where the pilot stick is directly connected to the elevator (as in the GLTA simulation model), this translates directly into a commanded stick input. Of course, for more complex control systems, the relationship would need to be further manipulated to ensure that the actual pilot stick input resulted in the required elevator input.

4.9.8   Limitations of the Results

There are a number of limitations to the results presented and these will be discussed in this Section. The first is that for the simulation experiments, the number of pilots that has been used is limited to a maximum of 4 and for SKYG-FW-0001 and 0002, is limited to 1 and 2 respectively. This is, in part, due to the expense of professional (ex-test) pilots but was also deliberate in some cases. For example, the use of only a single pilot during the development of the display concepts allowed a rapid evaluation to be made of the unknown algorithm parameters. These 'final' parameter values were then evaluated by other pilots. If a number of pilots had been asked to indicate their preference for the parameters in question, there is no guarantee that any of the responses would have agreed. The decision as to which value to use per parameter would have been made increasingly difficult. This issue is also mitigated to some degree for the basic τ analysis for the flare by the inclusion of the results from Ref. [122]. It is recognised, however, that the results presented, particularly for the final performance evaluation, would be more compelling if results from a greater number of pilots had been obtained.

Much use has been made in the basic τ analysis of the use of correlation of $\tau_{\Delta h}$. A well correlated set of results does not imply causation Ref. [114]. As stated at the start of this thesis, the research did not set out to prove (or otherwise) the existence of τ in visual perceptual systems. However, the eye-tracking results and pilot comments from the same provide some indication of the pilot's point-of-regard during the flare and Section 2.4.1.2 provides a means by which such gaze positions might be capable of picking up τ information. Furthermore, flare manoeuvres were successfully commanded using algorithms based upon the τ results obtained. As such, it is suggested that the results presented herein lend weight to the use of τ as a visual perception variable for pilots landing an aircraft.

4.9.9 General Comments

The inference from the preceding discussion is not intended to be that the τ-based flare command display, as described, is in its final form. The key improvement required is a reduction in sensitivity (increase of damping) of the command display symbol to changes in the direction of the aircraft acceleration vector.

It might be considered that the display concept does not add much to the functionality provided by the VGS flare command. In one sense this is true. However, the algorithm that drives the LEAD and LEAD* concept flare command symbol are based upon an accepted theory of visual perception whereas the VGS algorithms have been developed in using traditional control systems theory. Both are, of course, valid (and the VGS, being a commercially available system, will always win any argument regarding practical application). It is argued, however, that a display algorithm based upon a theory of how pilots perceive their motion rests on a better foundation. It also opens up the possibility or the need for a new suite of τ-sensors. One might look forward to a time when a downward

looking τ-sensor detects the runway surface and τ-based algorithms such as those described in this thesis to bring the aircraft to which it is attached, safely onto the runway surface.

Having mentioned τ-sensors, it is an opportune moment to discuss the practical implementation of the ideas discussed so far. As already mentioned, in an ideal scenario, the aircraft would be equipped with an appropriate τ sensor that could measure the τ of the various gaps directly and hence its rate of change. The control algorithms would then operate on this information. At present, there are extensive efforts being made to produce and utilise optic flow sensors e.g. [68-70] but only a small number of sources have been found regarding the extraction the τ of motion gaps from that flow. Ref. [125] cites an approximate method of doing this (by measuring the divergence of the optic flow) and provides an example of a robot vehicle that employs this method (Ref. [126]). However, to the author's knowledge, there are no τ sensors currently available on the market. Use would have to be made, therefore, of other means of measuring the τ of the motion gaps. One of the primary attractions of τ theory as an explanation of how living organisms navigate around an environment is that it only requires an understanding of time and not measurements of distance, speed, force etc. It is therefore with some reluctance that it is suggested that the most practical means of obtaining τ for the displays described above is via the measurement of spatial variables. The first obvious candidate for the localiser and glide slope capture phases of the approach is to use signals from the satellite-based Global Positioning System (GPS). Typical horizontal accuracy figures for GPS receivers such as those used in Ref. [127] are 3.0m when used autonomously or 1.0m when used with reference to a base station. Vertical accuracy is likely to degrade by a factor of two [127]. Such accuracy would be satisfactory for the approach phases of the flight. By using GPS,

the aircraft inertial position is known. Onboard INS systems will provide aircraft attitude information and from this, the calculations detailed in Section 3.5.33.5.4 can proceed. For the flare MTE specifically, it is perhaps more likely that a radar altimeter would be used to ascertain Δh and hence provide the information required to be able to calculate its rate of change and τ.

The research has concentrated upon the degradation of the visual environment by simulating environmental effects such as fog and darkness. It is worth commenting that even in a visual conditions, the pilot's visual environment is degraded. The pilot's visual field is restricted to that which is available to the cockpit windscreen. Large portions of the available forward view are therefore obscured by aircraft structure. This was also true of the simulated field of view – simulator structure obscures some of the available outside world view. It would be a relevant topic for research to ascertain how a pilot's performance changes for manoeuvres such as the flare when such obscurations are removed. It is postulated that the flare performance would improve i.e. touchdown velocities would decrease in good visual conditions and that the visual environment could be degraded to lower levels (i.e. visibility further reduced) before deteriorations in τ-based relationships are observed. A corollary to this idea is that flare performance might also be improved if the main gear and runway surface are displayed directly to the handling pilot. In the case, the motion gap being controlled would be closely linked to $\dot{\tau}_{\Delta h}$ as used in this thesis.

4.10   Conclusions

A number of fixed-wing large jet transport aircraft flare manoeuvres have been analysed. The results from these analyses have been use to generate algorithms to drive a flare command display and this display has been

compared with existing operational and research display formats. From this work, the following conclusions have been drawn:

i.   Analysis of the flare manoeuvre can be greatly simplified using τ-theory as a basis with the motion gap variable being used as the τ parameter being defined as the distance between the aircraft cg during the flare and the aircraft cg at touchdown.

ii. $\tau_{\Delta\theta}$, whilst showing some coherence during the flare manoeuvre, does not conform to the hypothesis that $\dot{\tau}_{\Delta\theta}$ is constant to touchdown.

iii.   The hypothesis that $\dot{\tau}_{\Delta h}$ is constant during the flare has been shown to be correct. Such a hypothesis is consistent with the concept of the pilot coupling with a τ-guide to perform the manoeuvre.

iv.   Two distinct techniques exist to flare the aircraft that result in $\dot{\tau}_{\Delta h}$ being constant prior to touchdown. The first requires that $\tau_{\Delta h}$ be held constant for a period before touchdown. This results in an exponential trajectory which, if maintained, would never bring the aircraft into contact with the ground (or would require the pilot to 'aim' below the runway surface). The strategy is then changed to $\dot{\tau}_{\Delta h}$ being held constant, to provide a power law flight path to touchdown (Type 1 flare). The second strategy involves the steady descent rate being arrested by adopting a constant $\dot{\tau}_{\Delta h} < 1.0$ all the way to touchdown (Type 2 flare).

v.   Degrading the visual conditions, on occasion, disrupted the coherent τ relationships observed during the flare. This disruption appears to be due to the degradation of visibility interfering with the pilots mechanism that allows $\tau_{\Delta h}$

information (and hence its rate of change) to be picked up. The fact that the degraded visibility did not always result in this disruption is testament to the skill and adaptability of the pilots in question.

vi. Performance against the MTE criteria decreases when the same manoeuvre is flown in a DVE compared to the same manoeuvre in a GVE. None of the display formats tested therefore re-create entirely the information available to the pilot from the outside world visual scene.

vii. $\dot{\tau}_{\Delta h} = 1.0$ is not a suitable algorithm that will lead to a reliable approach to a runway threshold. Even in ideal simulator 'no wind or turbulence' conditions, extremely variable trajectory approaches resulted from this method of command.

viii. Pilots that use Type 1 flares when flying manually consistently produce touchdown velocities within acceptable values. Pilots that naturally use a Type 2 flare strategy are more prone to misjudge the flare, resulting in harder landings.

ix. The Type 2 flare is more amenable to engineering analysis for display algorithm generation. This conclusion is based not only upon the apparent linear relationship between touchdown velocity and value of $\dot{\tau}_{\Delta h}$ used but also the fact that only one parameter is used to command a Type 2 flare ($\dot{\tau}_{\Delta h}$).

x. For the Type 2 flare, there is a constant relationship of the approximate form: $\dot{\tau}_{\Delta h} = -0.032\dot{h}_{td} + 0.53$. This is a linear relationship that bisects zero touchdown velocity for $\dot{\tau}_{\Delta h} = 0.5$ and the approach vertical descent rate at $\dot{\tau}_{\Delta h} = 1.0$. If this relationship were to be normalised, it is postulated it would be independent of aircraft type.

xi. An acceptable display design using the basis of the Type 2 flare was found to be an indirect command-type display with the following flare parameters: Total flare manoeuvre duration, T = 3.5s; $\dot{\tau}_{\Delta h}$ =0.75. The actual parameter commanded was flight path angle, γ.

xii. The simple τ-based display concept performed at least as well as and in some cases better than the version of the VGS implemented on the UoL flight simulator in terms of MTE performance criteria.

xiii. Pilot preference, both in terms of controllability and workload rated the VGS as first with the τ-based concept second.

xiv. In order to successfully fly the flare command display, a particular technique was required. If this was not followed, then the motion characteristics of the display were such that significant pilot compensation was required to try to re-establish a sensible flare trajectory. Clearly this is an undesirable characteristic of a display symbol.

4.11 Recommendations

Based upon the work reported in this Chapter is it recommended that:

i. A solution to the concept display's sensitivity to reversal of the acceleration vector be sought and implemented.

ii. A means of injecting a small 'pre-flare' input should be sought to assist with recommendation (i).

iii. Investigate the possibility of using the elevator angle as a means of cueing the pilot in the flare. The first issue to resolve here will be how to ascertain the final value of the elevator angle required. One suggested means of calculating this is to

compute the elevator angle required for a flare with $\dot{\tau}_{\Delta h} = 0.5$. All other solutions converge on this value at the end of the flare manoeuvre.

iv.   Devise an experiment to test the τ-coupling hypothesis discussed in Section 4.9.3. Given pilot P1's technique in terms of flare gaze position, consideration should be given to using P1 as a subject for such an experiment.

v.   Limited τ guide (τ_G) results are reported by the author in Ref.[128] for the flare and it has been stated in this thesis that constant $\dot{\tau}$ strategies are equivalent to the pilot using a τ-guide. However, much more use has been made of τ guide analysis in rotary wing work (Refs. [16, 124]) and it may be that using this formulation to command trajectory control has its advantages . Of course, it may not but it would be useful to find out. As such, it is recommended that this exercise be repeated but using either τ_g or τ_G as a basis for the algorithms.

vi.   The algorithms used to command the pilot flare symbol could be used equally well as a basis for automatic control of an aircraft. Consideration should be given to using the τ-based approach to implement, for example, an automatic landing system.

vii.   It has been shown that the approximate relationship $\dot{\tau}_{\Delta h} = -0.032\dot{h}_{td} + 0.53$ exists for two aircraft types (DC-10 and GLTA simulation model). It has further been suggested that normalising this relationship would make it applicable to all aircraft flare manoeuvres. It would be an interesting research topic to establish whether this is so.

viii.   It has been hypothesised that providing the pilot with a view of the runway that is not obscured by aircraft structure or a direct view of the main gear would improve flare manoeuvre performance. This hypothesis should be tested using the flight simulation in the first instance.

C h a p t e r   5

LOCALISER AND GLIDE SLOPE CAPTURE MTES

5.1 Introduction

This Chapter reports on the results obtained for the localiser and glide slope capture MTEs. Section 5.2 reports on the preliminary testing performed to establish whether coherent τ relationships were observed and whether such relationships are affected by a degradation in the visual environment. A residual aircraft vertical velocity analysis was not considered appropriate for the MTEs contained in this Chapter since the motion gap closure 'target' is not a physical surface but a virtual one. Section 5.3 details an evaluation undertaken using the eye-tracking system purchased for the research project. Unlike the results of the previous Section, this was not to try to provide a direct explanation for the results obtained, but to establish a basis for the information to be presented to the pilot in the novel display concept. Section 5.4 reports on the development process undertaken for the τ-based localiser and glide slope capture display concept. Section 5.5 provides a comparison of the performance results obtained for each of the display formats tested and Section 5.6 reports upon the associated pilot display controllability and workload ratings. Finally, Sections 5.7, 5.8 and 5.9 summarise all of the learning points for the localiser and glide slope capture MTEs.

5.2 Basic Tau Analysis

As discussed in Section 3.4.4.1, the 'basic τ analysis' consisted of the selection of a number of potential motion gaps over which the pilot might have visual control. The τ of these gaps was then calculated during the

MTE (using the extended runway centre-line and glide slope as the 'target' values) and observations made about the coherence (or otherwise) of the τ of those values with time. The motion gaps of interest for the localiser and glide slope capture MTEs are shown in Fig. 3-6.

5.2.1 Lateral Distance to Runway Centre-Line Motion Gap

The localiser capture manoeuvre is performed during all of the approach MTEs and is also a dedicated MTE in its own right. The difference between the localiser capture MTEs (i.e. visual or precision) is the manner in which it is executed. For a visual approach, the appropriate ground track along which to approach the runway must be judged with reference to the outside world. For the non-precision and precision approaches, localiser information is provided by the aircraft instrumentation. Fig. 5-1 shows the first of the τ analyses performed for a sample of the localiser capture MTEs, $\tau_{\Delta y}$.
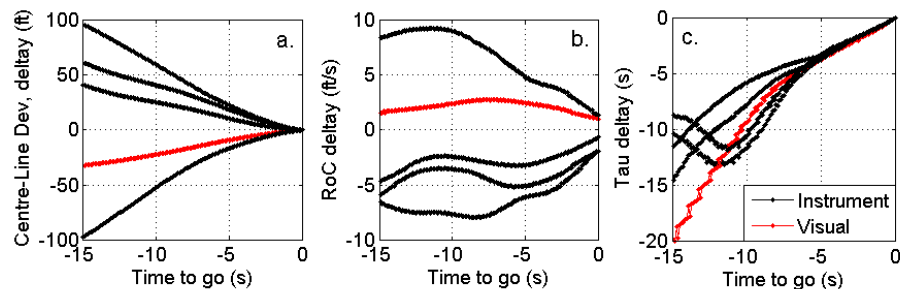

Fig. 5-1. Tau Analysis of the Localiser Capture Manoeuvre: a. Runway Centre-line Gap Closure; b. Rate of Change of Runway Centre-line Gap and c. Tau of Runway Centre-line Gap for Approach MTEs

It can be seen from Fig. 5-1(c) that, in general, for both visual and instrument-based localiser captures, there is a linear relationship between the $\tau_{\Delta y}$ and the time to close the runway centre-line gap i.e. constant $\dot{\tau}_{\Delta y}$. The data for all of the localiser capture MTEs performed during this phase of testing are summarised in Table 5-1. This relationship appears to hold for a wide-range of localiser capture events, ranging from rapid instrument closures to a much more tentative visual approach. As with previous analysis, the linear regions of the constant $\dot{\tau}_{\Delta y}$ portions of each manoeuvre (the last 5 seconds or so) are very well correlated. If anything, after a visual inspection of the visual approach τ relationship, one might be tempted to claim that it appears be one of the more coherent and 'τ-like' of the set of results. The majority of the slope values are greater than 0.5, indicating some overshoot on the final value of 'Δy' selected.

Type	Slope	Intercept	R^2
Instrument	0.49	-0.12	0.99
Instrument	0.77	0.13	0.99
Instrument	0.65	-0.25	0.99
Instrument	0.75	0.20	0.99
Instrument	0.63	-0.09	0.99
Instrument	0.68	-0.09	0.99
Instrument	0.67	-0.10	0.99
Instrument	0.65	-0.02	0.99
Instrument	0.68	0.01	0.99
Instrument	0.77	0.03	0.99
Visual	0.77	0.11	0.99

Table 5-1. Linear Regression Parameters for Runway Centre-line Gap Closure Tau Analysis for the Localiser Capture MTEs

5.2.2 Localiser Deviation Angle Motion Gap

Fig. 5-2 shows the results of the second τ analysis conducted for the same sample of localiser capture manoeuvres as in Section 5.2.1, $\tau_{\Delta locdev}$. As for
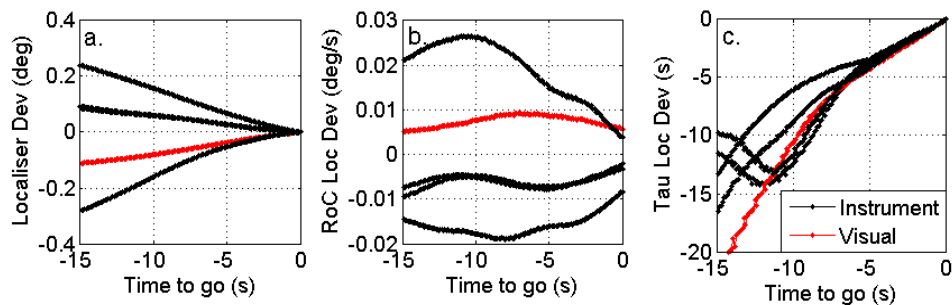

Fig. 5-2. Tau Analysis of the Localiser Capture Manoeuvre: a. Localiser Deviation Angle Gap Closure; b. Rate of Change of Localiser Deviation and c. Tau of Localiser Deviation Angle Gap for Various Approach MTEs

the $\tau_{\Delta y}$ analysis, a constant $\dot{\tau}_{\Delta locdev}$ relationship exists over the last 5 seconds or so of the manoeuvre and Table 5-2 shows that these too, are well correlated. Indeed, the curves of Fig. 5-1 (c) and Fig. 5-2(c) appear very similar. This is perhaps not too surprising since the calculation of the localiser deviation angle includes Δy.

MTE	Slope	Intercept	R^2
Instrument	0.52	-0.17	0.99
Instrument	0.82	0.15	0.99
Instrument	0.65	0.05	0.99
Instrument	0.87	0.29	0.99
Instrument	0.71	0.07	0.98
Instrument	0.73	0.12	0.99
Instrument	1.01	0.12	0.99
Instrument	0.72	-0.05	0.99
Instrument	0.79	0.08	0.99
Instrument	0.92	0.25	0.99
Visual	0.69	0.22	1.00

Table 5-2. Linear Regression Parameters for Runway Centre-line Gap Closure Tau Analysis for the Localiser Capture Manoeuvre MTEs

5.2.3 Orthogonal Distance to Glide Slope Motion Gap

Fig. 5-3 shows the results for the τ analysis of the motion gap $\tau_{\Delta xz}$. Over the last 3.5 – 4.0 seconds of the manoeuvre, a linear relationship i.e. constant $\dot{\tau}_{\Delta xz}$ is observed.
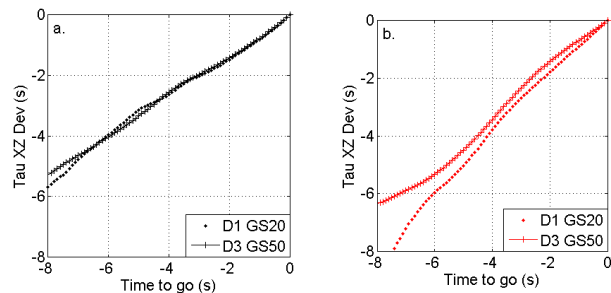

Fig. 5-3. Glide slope Δxz gap closure tau for visual conditions: (a) V1 and (b) V2

5.2.4 Glide Slope Deviation Angle Motion Gap

The glide slope capture manoeuvre is performed during all of the approach MTEs and was also a dedicated MTE in its own right. The difference between the capture manoeuvres is the manner in which it is executed. For a visual and non-precision approach,

MTE	Slope	Intercept	R^2
Glide slope Capture	0.86	0.01	0.99
Precision	0.62	0.03	0.98
Precision	0.74	0.02	0.98
Non-Precision	0.66	0.06	0.98
Visual	0.56	0.05	0.98

Table 5-3. Linear Regression Parameters for Glide Slope Deviation Angle Gap Closure Tau Analysis for the Glide Slope Capture Manoeuvre for Various Approach MTEs

the appropriate glide slope along which to descend must be judged with reference to the outside world. For the precision approach, glide slope information is provided by the aircraft instrumentation. Fig. 5-4 and show the τ analysis performed on the glide slope capture manoeuvres in both circumstances, τ_{gsdev}.
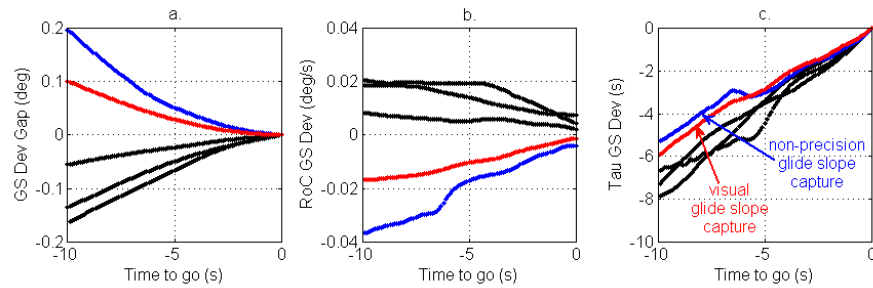

Fig. 5-4. Tau Analysis of Glide Slope Capture Manoeuvre: a. Glide Slope Deviation Angle Gap Closure; b. Rate of Change of Glide Slope Deviation and c. Tau of Glide Slope Deviation Angle for Various Approach MTEs

It is apparent from Fig. 5-4 that an approximately linear τ_{gsdev} coherent relationship exists over the last 5 seconds of the glide slope capture. Table 5-3 shows the linear regression data for the various approach MTEs. These data show that the implied constant $\dot{\tau}_{gsdev}$ relationship is well correlated.

5.3 Eye-Tracking Analysis

The eye-tracking equipment was used for the localiser and glide slope capture MTEs for a different purpose than with the flare MTE. For the flare, a set of results in both good and degraded visual conditions were obtained and the eye-tracker used to try to help explain them. In degraded visual conditions, there is no information available regarding the localiser or glide slope location save that from any instruments. The design philosophy for the novel concept included the reduction in the number of display symbols used with the aim of reducing display clutter and increase the pilot's ability to interpret the aircraft state 'at a glance'. Instead therefore, the eye tracker was used to ascertain what information the pilot sought and the frequency of this during the approach to the runway surface.

These analyses were carried out in both good and degraded visual conditions using all display formats. Fig. 5-5 presents sample results from pilots P3 and P4 conducting approaches in visual condition V1 (GVE) using the PFD.
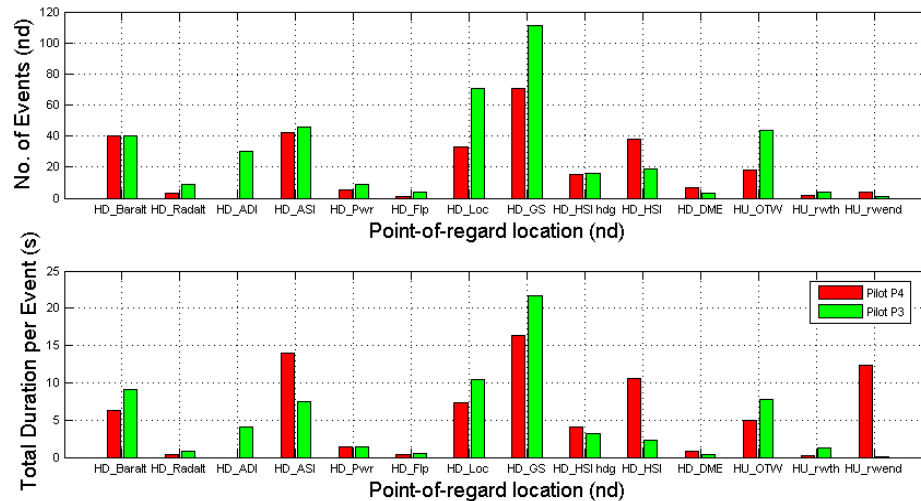

Fig. 5-5. Summary analysis for eye-tracked approach to runway in visual condition V1 (a) number of times point-of-regard moves to a particular location and (b) total duration of point-of-regard remaining at location during MTE

As might be expected, the number of events generally correlates with the total duration data and the trend for both pilots is approximately the same across the results. From the results of Fig. 5-5, the pilot's information requirements during the approach in descending order are:

1. Glide slope location (HD_GS. HD refers to head-down instrument panel).

2. Localiser location. (HD_Loc).

3. Airspeed (HD_ASI).

4. Altitude (HD_Baroalt, HD_Radalt).

5. Aircraft roll and pitch attitude (HD_ADI).

6. Horizontal situation/heading/distance to go (HD_HSI / HD_Hdg / HD_DME).

7. Outside world information such as the view from the centre-channel display and the location of the runway end/threshold (HU_OTWC, HU_rwth, HU_rwend. 'HU' refers to head-up).

8. Aircraft condition such as power and flap settings (HD_Pwr and HD_Flp).

From the perspective of display design, the question as to which information items to include had to be addressed. Having decided upon the 'lead-predictor' concept in principle, it was considered that the lead aircraft symbol provided localiser, glide slope, (desired) altitude and heading information. The looming function of the combined predictor and lead symbols was intended to provide airspeed information (against a target), the horizon line would provide roll information and, in conjunction with the predictor symbol, pitch information. The display was intended to look at aircraft guidance so aircraft condition symbols were not included and no runway symbology was used as the intention was that the pilot would simply follow the flare guide down to the runway surface.

Given the above argument, it was considered that the initial version of the lead-predictor display (LEAD) provided the pilot with all of the guidance cues necessary to perform a successful airfield approach.

5.4 Initial Display Design

Section 4.5.1 starts by asking a number of questions regarding what information should be presented to the pilot and whether τ information should be presented directly or indirectly. The decision to use the LEAD concept, based upon the results of the previous Section appeared to be capable of providing the pilot with the correct guidance information to perform the approach. The method chosen to do this was via an indirect means: the lead aircraft symbol would indicate the position of a pre-defined desired aircraft trajectory and when motion gaps needed to be

closed, the closure is defined by a constant rate of change of τ law. The reason for pre-defined trajectories being chosen was that it was considered that this is a practical solution to implementing such a display concept on board a real aircraft – the destination airfield approach procedures could be stored on or broadcast to the aircraft.

5.4.1   Trajectory Generation

In order to make the LEAD concept design work, a number of design decisions had to be made:

1. Which motion gaps should be used for the localiser and glide slope capture MTEs ?

2. What value of $\dot{\tau}$, T and t_{pred} should be used for each MTE ?

To answer the first question, given that the linear and angular relationships for both MTEs gave similar results, to be consistent with the flare command algorithm, the linear τ relationships were selected i.e. use $\dot{\tau}_{\Delta y}$ and $\dot{\tau}_{\Delta xz}$ as a basis for motion gap closure.

To answer the second question, a series of trajectories were generated and flown by Pilot P1 to establish the optimum values of the motion gap closure variables ($\dot{\tau}$, T and t_{pred}).

5.4.1.1 Localiser Capture

The duration of the localiser capture MTE was fixed at 10s (30° turn onto heading at 3°/s. In the airline community, this is known as a 'rate 1 turn'). A number of differing lead aircraft trajectories therefore had to be computed using varying values of $\dot{\tau}_{\Delta y}$ and
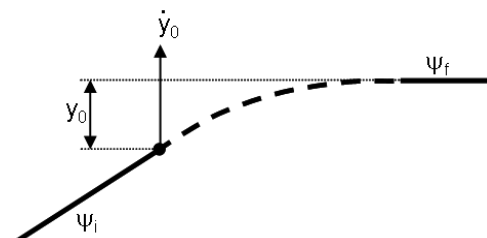

Fig. 5-6. Parameters used to define localiser capture command trajectories

208

t_{pred}. Varying $\dot\tau_{\Delta y}$ was achieved, with reference to Fig. 5-6 as follows:

1. Target indicated (V_{IAS}) and hence true-airspeed (V_{TAS} in ft/s) and aircraft heading are known for the approach phase (ISA conditions assumed). The initial target closure rate is given by:

$$\dot y_0 = V_{TAS} \sin(\psi_f - \psi_i) \qquad (5\text{-}1)$$

2. Calculate the distance from target that the turn onto the localiser should commence. If Eq. (2-30) is rearranged with $\Delta x = y0$ and $t = -T$ (start of manoeuvre), then:

$$y_0 = \dot y_0 (c1)T \qquad (5\text{-}2)$$

Now generate trajectory data using Eq. (2-29) with y_0 obtained from Eq. (5-2).

Fig. 5-7 shows the localiser capture trajectories generated using the procedure given above for a target V_{IAS}=160.0 knots.
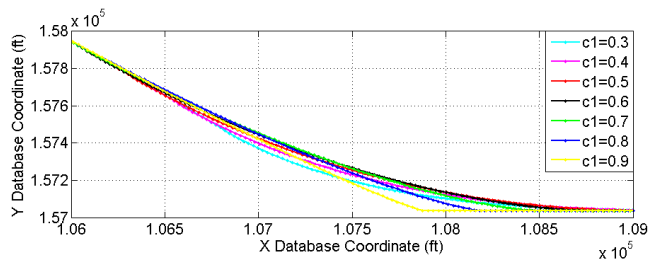

Fig. 5-7. Localiser capture trajectories defined by different values of C1 where $\dot\tau_{\Delta y} = $ C1

t_{pred} was varied at simulation run time by setting the model variable that represented t_{pred} in Eq. (3-19) to the appropriate value.

Note: in the following discussion $\dot\tau_{\Delta y}$ is referred to as 'C1'.

5.4.1.2 Glide Slope Capture

Establishing the optimum glide slope trajectory parameters was slightly more complicated than for the localiser capture because:

1. Both manoeuvre duration, T, and $\dot{\tau}_{\Delta xz}$ can vary. In the discussion that follows, $\dot{\tau}_{\Delta xz}$ is also referred to as C3.

2. All calculations had to be transformed from the earth-referenced 'xyz' axis system into an axis system that was orthogonal to the steady approach path in the vertical plane i.e. the new x-axis ('X') for the calculation was the glide slope trajectory itself. The glide slope capture trajectories were derived in the same manner as described for the localiser capture as defined in Fig. 5-8 (Δxz_0 and its derivatives replace Δy_0 and its derivatives in Eqs. (5-1) and (5-2).

Fig. 5-8 shows the resultant glide slope capture trajectories from this analysis for V_{IAS}=140.0 knots. To incorporate these trajectories into the final, full approach solution, they all had to be shifted to the right as represented in the figure to intercept the 3.5 degree glide slope at the correct point. The trajectories have been left in the format of Fig. 5-9 to try to illustrate more clearly the effect of varying the parameters T and $\dot{\tau}_{\Delta xz}$.
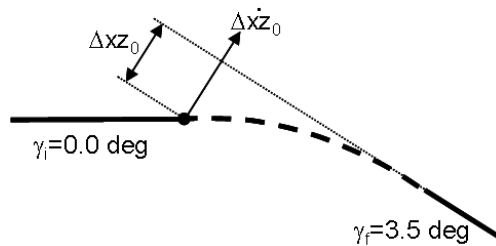

Fig. 5-8. Glide slope capture trajectories defined by different values of C3 where
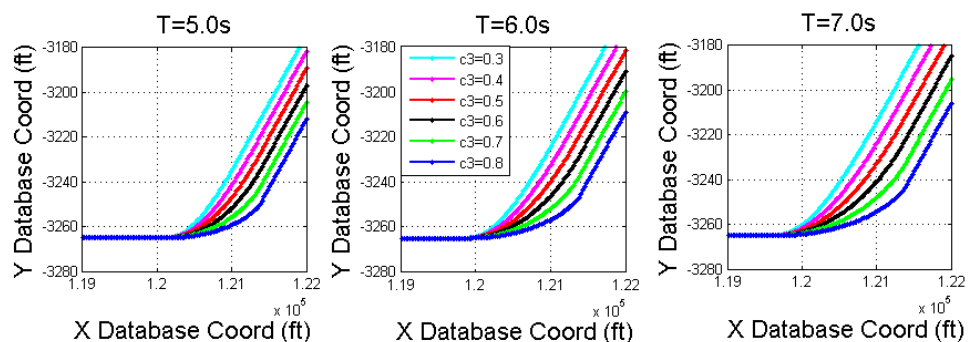
$$\dot{\tau}_{\Delta xz} = C3$$

Fig. 5-9. Glide slope capture trajectories defined by different values of C3 and T where

$$\dot{\tau}_{\Delta xz} = C3$$

210

5.4.2   Trajectory Selection

5.4.2.2 Trajectory Performance

5.4.2.2.1   Localiser Capture

Fig. 5-10 shows the aircraft trajectory for each test point flown in the x-y

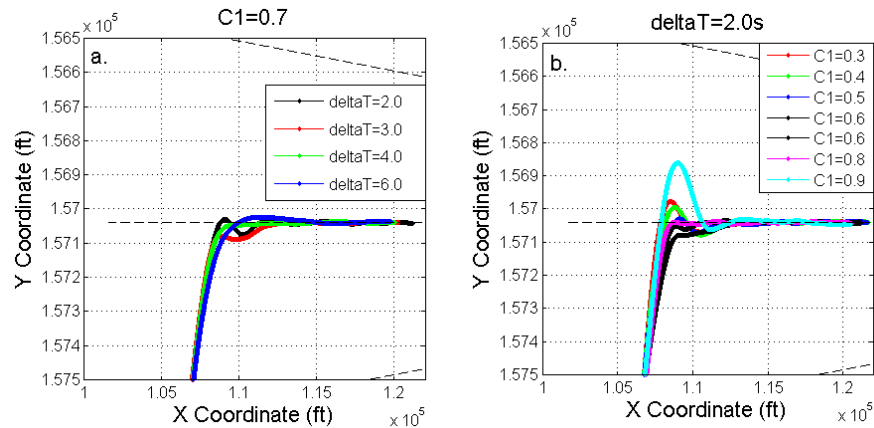(North-East) inertial plane, focusing primarily on the turn onto the

**Fig. 5-10. Horizontal trajectory flown using lead-predictor display: (a) C1=0.7 varying
prediction time ahead and (b) t_{pred}=2.0 varying C1**

localiser. Just visible on the plots (dashed lines) are the ideal localiser

track and the desired overshoot boundaries based upon the MTE definition

of Appendix B. It can be seen from Fig. 5-10 that in each case the localiser

track is eventually captured. In some cases however, the capture only

occurs after one or two overshoots. Fig. 5-10(a) indicates that the most

direct intercept with C1=0.7 was achieved when the 'look-ahead' or

prediction time (t_{pred}) was 4.0 seconds. However, the pilot's preference

was for t_{pred}=2.0 seconds (see next Section) and in this case the least

overshoot is observed in Fig. 5-10(b) when C1=0.6, although the localiser

capture is not as continuously progressive as for the C1=0.7, t_{pred}=4.0s

case. All turns onto localiser including the overshoots are well within the

desirable performance boundaries of ±0.5°.

Fig. 5-11 shows the variation of aircraft height AMSL during the same

localiser capture manoeuvres using the lead-predictor symbology as Fig. 5-

10. More clearly visible this time are the MTE performance boundaries

211

from Appendix B. The centre dashed line represents the target altitude for the manoeuvre. The innermost off-centre lines represent the desired performance limits and the outermost lines the adequate performance limits.
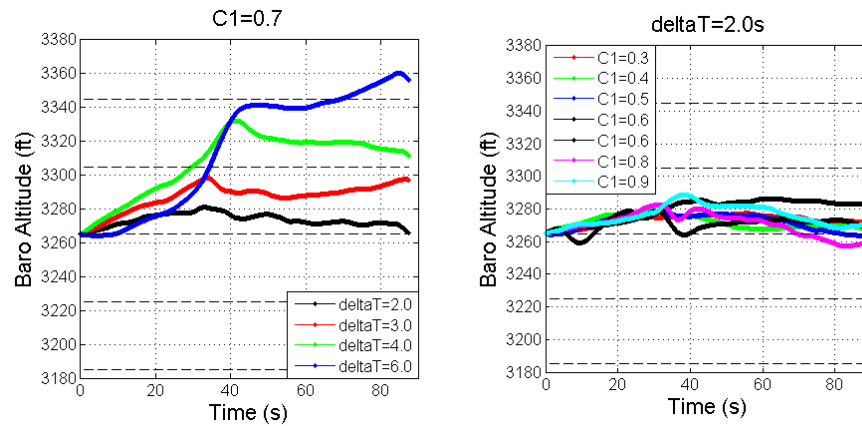

Fig. 5-11. Vertical trajectory flown using lead-predictor display: (a) C1=0.7 varying prediction time ahead and (b) t_{pred}=2.0 varying C1

With C1=0.7, for the t_{pred}=6.0s case, aircraft height is not maintained within the adequate boundary of +80ft whilst for the t_{pred}=4.0s case, the pilot manages to just hold the aircraft between the desirable and adequate performance boundaries. Finally, for the t_{pred}=2.0s and 3.0s cases, the aircraft altitude is kept within desirable performance criteria.

When t_{pred} is set at 2.0s, the pilot is able to fly the aircraft such that the altitude remains within desirable performance boundaries for all values of C1.

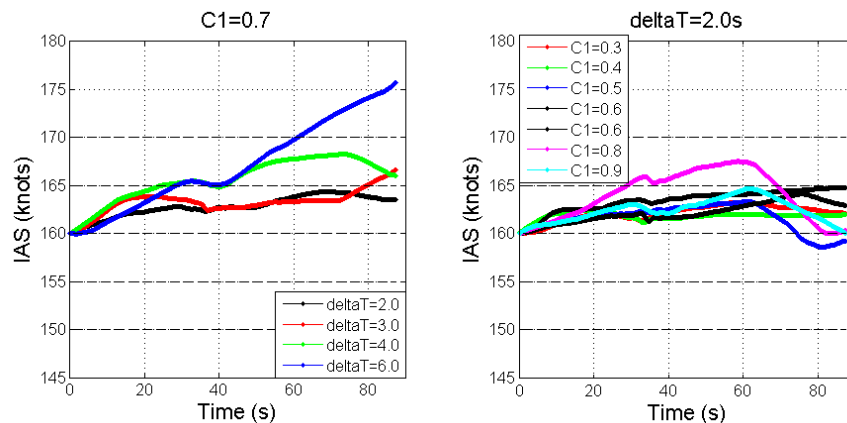Fig. 5-12 shows the variation of IAS for each of the test points flown for the localiser capture MTE.

Fig. 5-12. IAS profile flown using lead-predictor display: (a) C1=0.7 varying prediction time ahead and (b) t_{pred}=2.0 varying C1

The IAS plots essentially mirror the aircraft altitude plots. However, due to the different performance boundaries, when C1=0.7 (Fig. 5-12(a)), only the t_{pred}=2.0s case remains within desirable criteria, whilst the t_{pred}=3.0s and 4.0s cases remain within the adequate criteria. For the t_{pred}=6.0s case, the pilot fails to maintain aircraft speed within even the adequate performance criteria.

When t_{pred} is set at 2.0s (Fig. 5-12(b)), the pilot is (just) able to maintain the aircraft IAS within desirable performance criteria except in the case when C1=0.8 when the desirable criteria are exceeded but the adequate criteria are still maintained.

5.4.2.2.2   Glide Slope Capture

Fig. 5-13 shows the vertical trajectories flown by pilot P1 for each test point using the lead-predictor display concept for the glide slope capture MTEs. Also shown are the performance boundaries as defined in Appendix B (their relevance is reduced here because the glide slope capture trajectories are all still offset from their correct inertial position for this experiment).
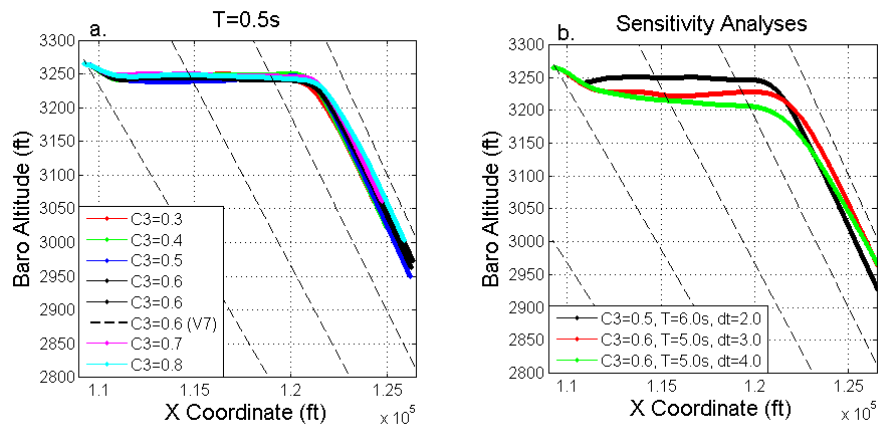
213

Fig. 5-13. Vertical trajectories flown for the glide slope capture MTE test points: (a) manoeuvre duration = 5.0s varying C3 and (b) assorted sensitivity analyses

All glide slope capture manoeuvres were completed successfully. The desirable and adequate overshoot criteria are also shown on Fig. 5-13. These are, to some degree, irrelevant at this stage as the lead aircraft trajectories were not in the correct inertial position for this trial. However, it is evident from Fig. 5-13 that any overshoot would be well contained within the desirable performance criteria.

There is a noticeable consistent drop in altitude of approximately 25ft for all glide slope capture MTE test points. This was found to be due to the small error in positioning of the predictor aircraft which ultimately caused an offset in its screen position. This error was corrected for the display performance testing reported in Section 5.5.

Fig. 5-14 shows the IAS profiles flown for each glide slope capture test point and the associated performance boundary criteria as defined in Appendix B.
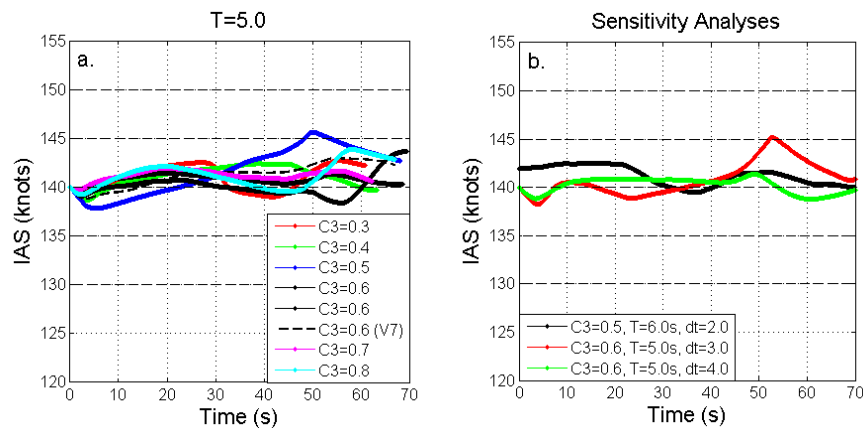
214

Fig. 5-14. IAS profile flown for the glide slope capture MTE test points: (a) manoeuvre duration = 5.0s varying C3 and (b) assorted sensitivity analyses

For all cases of the glide slope capture MTE test points, it can be seen that the aircraft IAS is maintained within the desirable performance criteria with just two very minor excursions into adequate.

5.4.2.3 Pilot Comments

5.4.2.3.1 Localiser Capture

The pilot's first comments concerned the form of the display as initially presented. It was P1's opinion that:

1. The style of the lines should be reversed i.e. the lead aircraft should be the dotted line and the predictor aircraft should be the full line. It was P1's preference to 'fly' the full line symbol.

2. The box format for the predictor aircraft was not necessary and that a single line symbol was sufficient i.e. a copy of the lead aircraft symbol but with a full line style was all that was required.

3. A means was required to stop the chase aircraft overtaking the lead aircraft and making it obvious to the pilot when this had happened. In the form tested in this experiment, if the chase aircraft did overtake the lead aircraft, then the looming worked in the opposite sense to that intended, so as the 'chase' aircraft moved further ahead of the 'lead' aircraft, the looming indicated that the lead aircraft was actually pulling away from the chase aircraft. This

215

effect 'commanded' the pilot to catch up with the chase aircraft (the opposite of what was required), making the situation worse, rather than better.

The initial investigation fixed the value of C1 at 0.7 (based upon an approximate average of the values observed in experiment SKYG-FW-0001) and varied the prediction time, t_{pred}. The pilot comments for this phase of the testing were as follows:

1. t_{pred}=6.0s: symbol too far away and hence too small to be seen and used effectively for speed control. In terms of following the localiser capture profile itself, pilot P1 commented that it was 'comfortable'.

2. t_{pred}=4.0s: symbol still perhaps a little too far away i.e. too small and hence the looming effect caused by speed changes difficult to pick up. This is evident in Fig. 5-12(a). Flying the localiser capture profile in this case was less comfortable and not intuitive during the initial stages of the turn (large lateral stick movements were required).

3. t_{pred}=3.0s: The symbol sizes were considered to be more useable and speed control was more accurate

4. t_{pred}=2.0s: Pilot P1 considered that fine speed control i.e. within 2.0knots of target was achievable with this 'look-ahead' time setting.

5. t_{pred}=1.0s: The symbology was now considered to be too large so no test point conducted.

Based upon the pilot comments above, it was decided to fix the prediction time, t_{pred}, to 2.0s and try to optimise the value of C1. The pilot's comments for this phase of testing were as follows:

1. C1=0.3, 0.4: The turn commanded by these values of C1 was too rapid in the translational sense. The swift movement of the lead aircraft symbol across the screen was 'disconcerting'.

2. C1=0.5: The bank angle required to follow the symbol was 'concerning' i.e. too high.

3. C1=0.6: The turn rate required for this manoeuvre was much more acceptable and flying the manoeuvre felt much more comfortable.

4. C1=0.8, 0.9: For both of these test points pilot P1 observed that the bank angle required to follow the lead aircraft appeared to be discontinuous and that this feature was unacceptable in a command display.

With the above comments in mind, the recommendation of pilot P1 was to opt for the following design parameters: **C1=0.6, t_{pred}=2.0s (and T=10s by default)**.

5.4.2.3.2 *Glide Slope Capture*

With t_{pred} effectively set by the localiser capture test results, the first batch of test for the glide slope capture MTE were used to establish and acceptable value of C3 with T (manoeuvre duration) set at 5.0s. The pilot's comments for these were as follows:

1. C3=0.3, 0.4: capture manoeuvre manageable but with a level of aggression that was noticeable but not inappropriate.

2. C3=0.5: capture manageable with no specific problems.

3. C3=0.6: capture manageable with very accurate tracking of lead aircraft possible.

4. C3=0.7: capture manageable but felt a little less progressive then the C3=0.6 case.

5. C3=0.8: again, the capture was considered to be manageable but there was a feeling that the manoeuvre progressed in a non-linear manner which is less desirable.

With pilot preference indicating C3=0.6, a small number of test points were conducted around this value to check for sensitivity to variation of other parameters (Fig. 5-13(b)). However, increasing T simply made the manoeuvre increasingly gentle. Increasing t_{pred} had no noticeable effect in this instance. With this in mind, pilot P1 recommended that the following design parameters be used for the glide slope capture phase of the lead-predictor display concept: **C3=0.6, T=5.0s and t_{pred}=2.0s**. One further important comment was made by the pilot during a test point conducted in degraded visibility condition V7. For this test point, it was indicated that the horizon line became very important ('came into its own') as the downward motion of the lead aircraft as the capture manoeuvre was commenced was made more obvious by the inclusion of the horizon line. This gave the pilot an obvious 'gap' on which to close.

5.5   Display Trajectory Performance Analysis

This Section presents the summarised trajectory performance results obtained for the localiser and glide slope capture MTE test points. For all figures in this Section, **black** lines represent result data for pilot **P1** and **red** lines represent result data for pilot **P2**.

5.5.1   Localiser Capture

This Section presents the results obtained for the localiser capture MTE test points.

5.5.1.1 Start On Condition

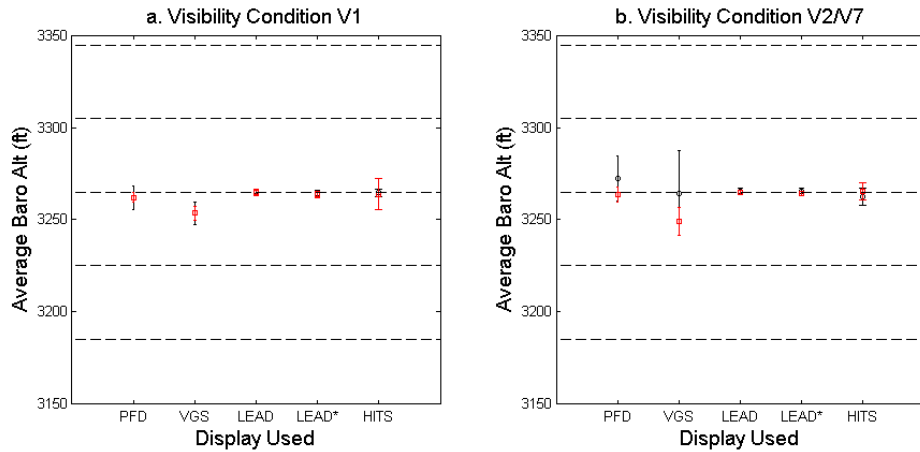Fig. 5-16 and Fig. 5-15 show summarised trajectory data for all test points

Fig. 5-16. Summary altitude data for the localiser capture MTE with 'on condition' start conditions

flown for the localiser capture MTE starting 'on condition' i.e. on height track and heading. Fig. 5-16 shows the mean aircraft altitude during the MTE by each pilot per display in both good and degraded visual conditions. The error bars indicate ± one standard deviation for the error between the actual altitude and the mean, giving an indication the variation of the data. The MTE desired and adequate performance boundaries are shown on the figures. For all test points, both pilots maintained the aircraft
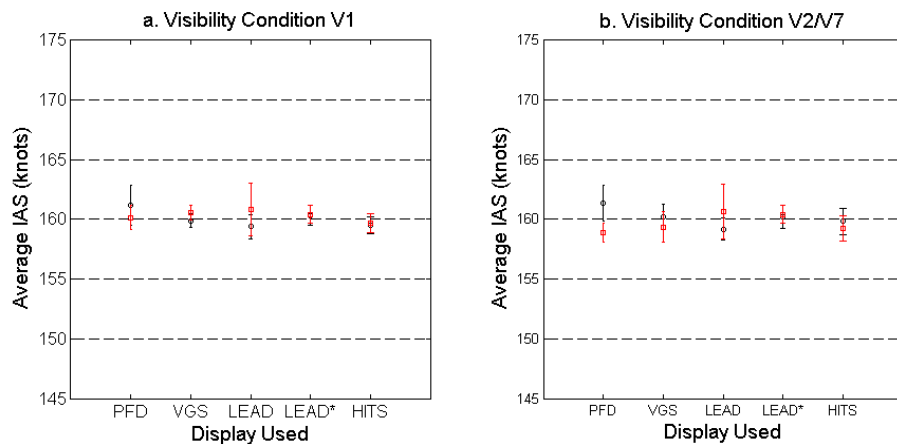

Fig. 5-15. Summary IAS data for the localiser capture MTE with 'on condition' start conditions

219

altitude within the desired performance boundaries. Both the LEAD and the HITS formats maintain the average altitude at the desired value and the least variation is observed in the two LEAD display formats. The PFD and VGS displays give average altitude values, generally slightly below the target and with higher standard deviations.

Fig. 5-15 shows the average IAS achieved over the localiser capture MTEs and the standard deviation of the errors obtained per display format. As for the altitude results, in all cases, the IAS is maintained within the desired performance boundaries. The largest standard deviations are observed in the PFD and LEAD display test points and the smallest variations observed for the VGS and LEAD* display formats.

To facilitate ease of visualisation, rather than summary data, the actual trajectory data for the localiser capture MTEs with 'on condition' start condition are shown in Fig. 5-17. The LEAD, LEAD* and HITS display

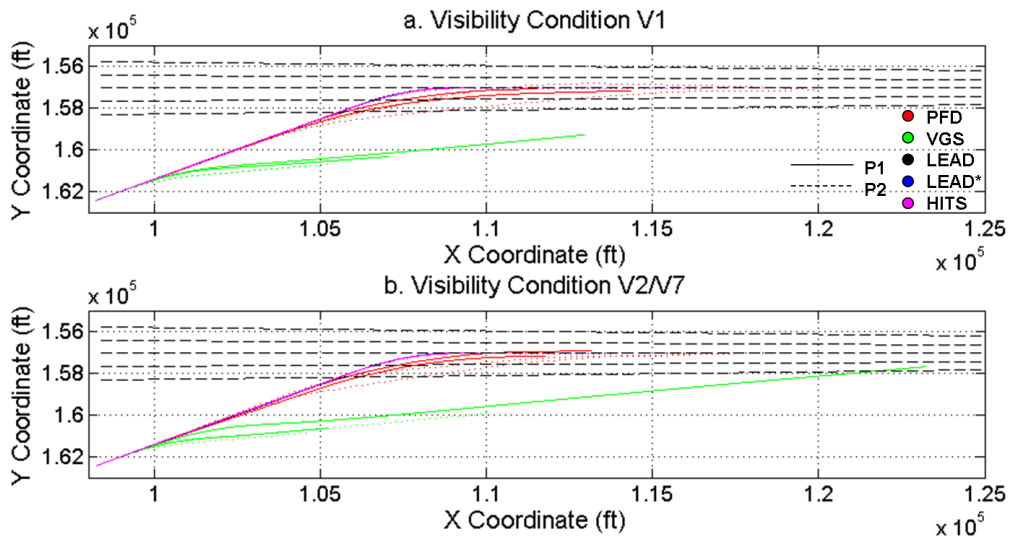**Fig. 5-17. Lateral trajectory data for localiser capture MTE with 'on condition' start conditions**
concepts give virtually identical flight paths with no discernible localiser overshoot. Slightly more variable tracks over the ground result when using the PFD display and some over- and under-shooting is evident. The VGS results are a consequence of the control laws that govern localiser capture.

220

These bring the aircraft onto the localiser at a target angle of around 10°
and as such, the lateral track is very different from that defined by the τ-
based control law. In each case however, the pilot terminated the MTE
when the localiser capture was considered to be stabilised.

5.5.1.2 Start with Lateral Offset

Fig. 5-18 and Fig. 5-19 show summarised trajectory data for all test points
flown for the localiser capture MTE starting with a lateral offset from the
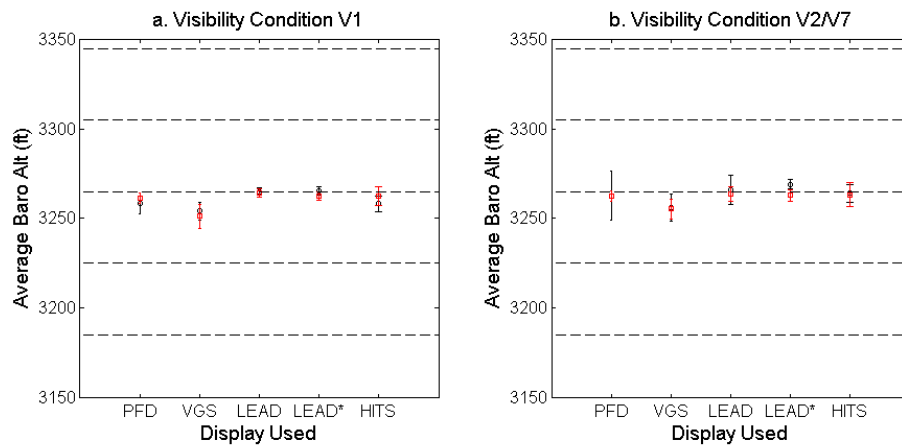desired track. Fig. 5-18 shows the mean aircraft altitude during the MTE

Fig. 5-18. Summary altitude data for the localiser capture MTE with a lateral offset from the desired track start condition

by each pilot per display in both good and degraded visual conditions. As
for the 'on condition' case, the pilots maintain aircraft altitude well within
desired performance boundaries. The two LEAD display concepts and the
HITS display provide average altitudes closest to the target and the two
LEAD formats give the smallest variations, particularly in visual condition
V1. The HITS and VGS give an average altitude generally slightly lower
than average with marginally larger variations in aircraft altitude.

221

Fig. 5-19 shows the average IAS achieved over the localiser capture MTEs per display format. In this case, there is a slightly more complex picture.
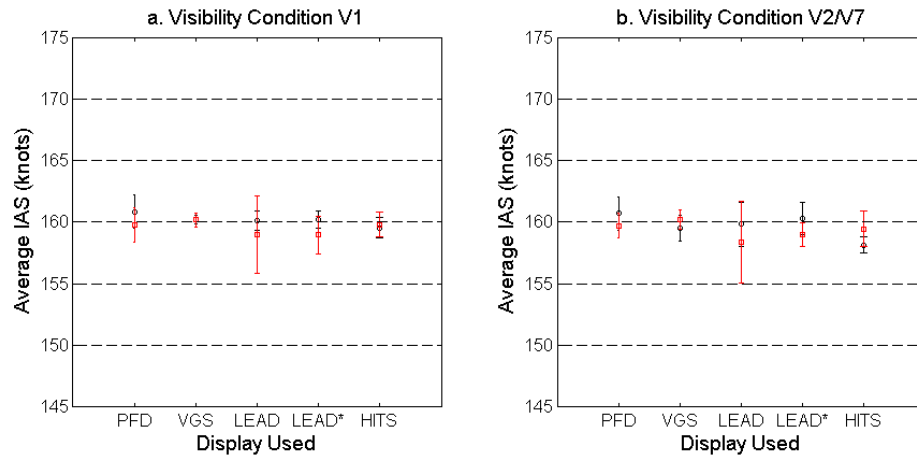
Fig. 5-19. Summary IAS data for the localiser capture MTE with a lateral offset from the desired track start condition

For both pilots, the VGS, LEAD* and HITS displays give comparable performance results in terms of the average IAS deviation from target and spread of results. The PFD and LEAD display formats generally give slightly larger deviations from target and larger standard deviations. However, pilot P1 performs better with the LEAD display and pilot P2 with the PFD format. In both cases, the pilot's 'strong' display results compare favourably with the results obtained with the other three formats.

Fig. 5-20 shows the actual trajectory data for the localiser capture MTEs with a 'lateral offset' start condition. The same trends are apparent as for the 'on condition' case with the exception now that where the trajectory is defined to the pilot with reference to the inertial frame i.e. LEAD, LEAD* and HITS, there is a small correction required back to desired track at the start of the MTE.

Fig. 5-20. Lateral trajectory data for localiser capture MTE with 'lateral offset' start conditions

5.5.1.3 Start with Lateral and Heading Offset

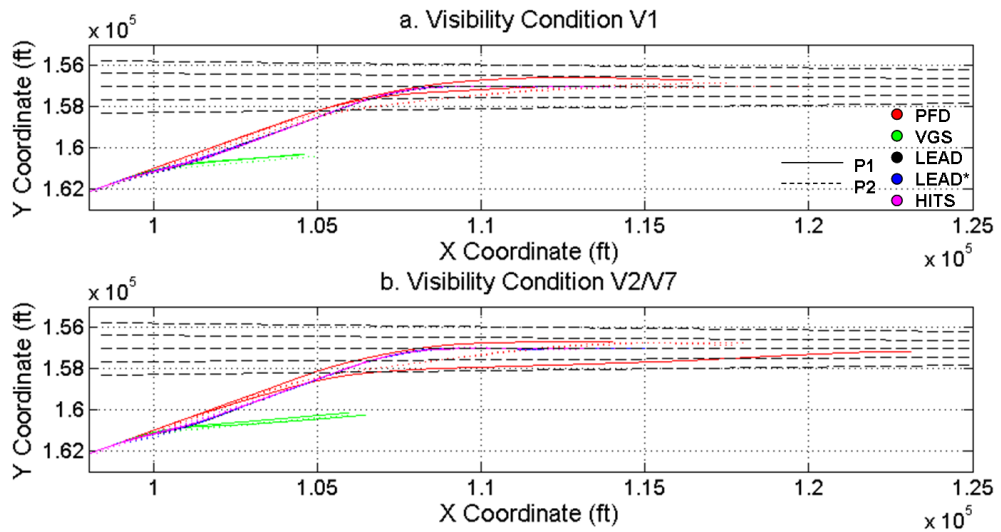Fig. 5-21 and Fig. 5-22 show summarised trajectory data for all test points
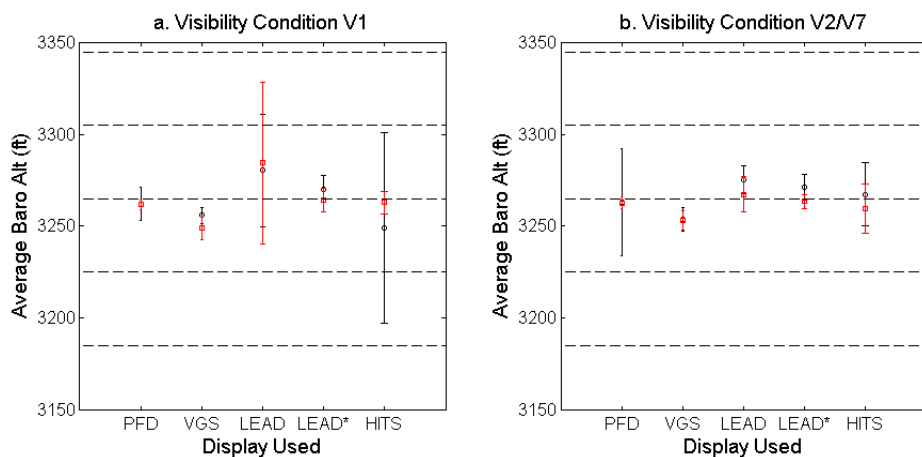

Fig. 5-21. Summary altitude data for the localiser capture MTE with both lateral and heading offsets from the desired track start condition

223

flown for the localiser capture MTE starting with both a lateral track and heading offset from the target values. Fig. 5-21 shows the mean aircraft altitude during the MTE by each pilot per display in both good and degraded visual conditions. In general, the performance of the pilots in maintaining altitude is now degraded. In visual condition V1, both pilots fail to maintain altitude within the desired performance boundaries with the LEAD display and pilot P1 also exceeds this boundary with the HITS display. Desired boundaries are maintained in all cases in visual conditions V2/V7 but with larger standard deviations than previously observed. The displays used to give the best or at least most consistent performance (in terms of data scatter across both visual conditions and pilots) are the VGS and LEAD* concepts.
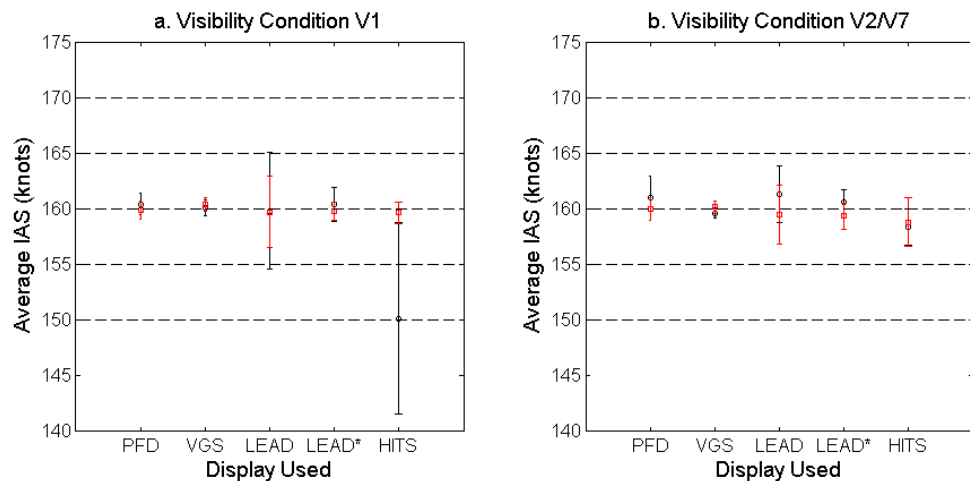
Fig. 5-22. Summary IAS data for the localiser capture MTE with both lateral and heading offsets from the desired track start condition

Fig. 5-22 shows the average IAS achieved over the localiser capture MTE starting with both a lateral track and heading offset from the target values. For these data, the desirable performance boundaries are exceeded by the pilot when flying using the LEAD and HITS concepts. The VGS gives the most consistent pilots and visual conditions, closely followed by the LEAD* and PFD displays.

Fig. 5-23 shows the actual trajectory data for the localiser capture MTEs with a 'lateral and heading offset' start condition. The same trends are apparent as for the 'on condition' case with the exception now that where the trajectory is defined to the pilot with reference to the inertial frame i.e. LEAD, LEAD* and HITS, there is a now a more pronounced correction required back to desired track at the start of the MTE. For the PFD case, the over-shoots of the localiser are now more severe although they still generally remain within the MTE desirable performance boundaries.
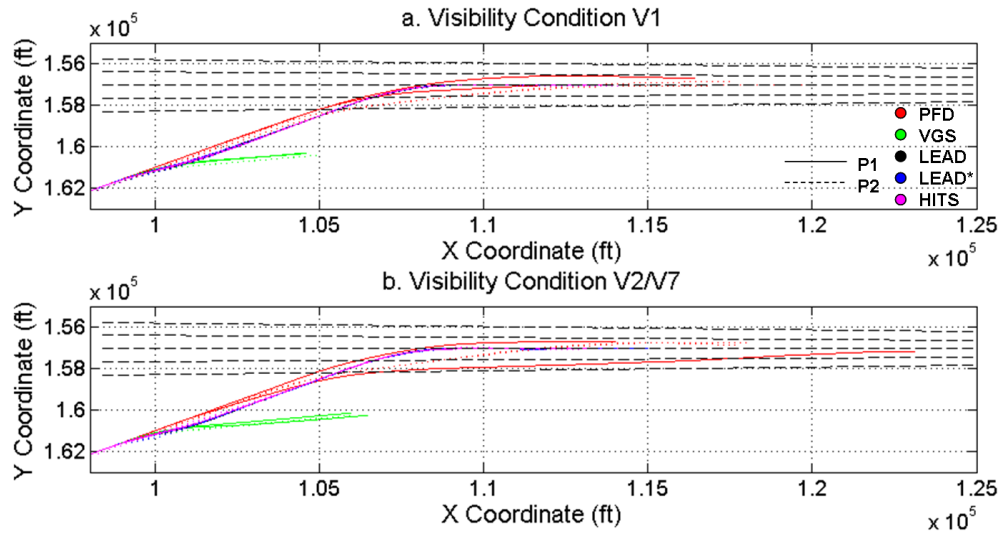
Fig. 5-23. Lateral trajectory data for localiser capture MTE with 'lateral offset' start conditions

5.5.2   Glide Slope Capture

5.5.2.1 Start On Condition

Fig. 5-24 to Fig. 5-27 show the summarised trajectory data for all test points flown for the localiser capture MTE starting 'on condition' i.e. on height, track and heading.

Fig. 5-24 shows the mean aircraft glide slope during the MTE by each pilot per display in both good and degraded visual conditions. The LEAD and
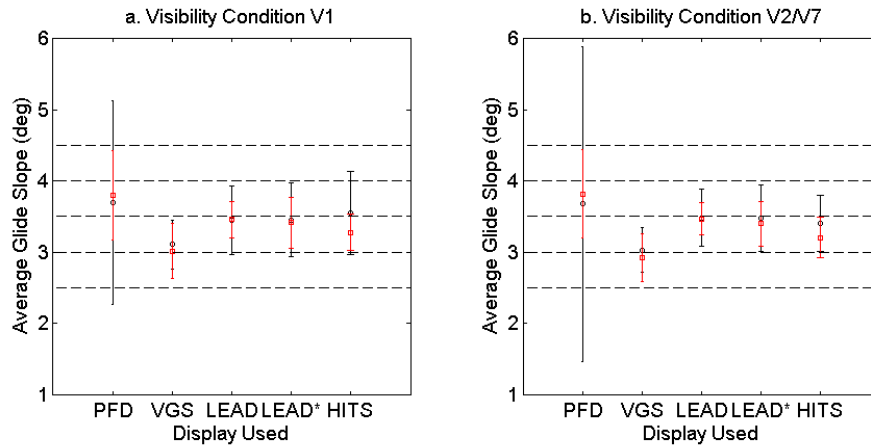
Fig. 5-24. Mean aircraft glide slope during capture MTE with 'on condition' start conditions

LEAD* displays give an average glide slope closest to target for both pilots followed by the HITS, PFD and VGS respectively. The PFD format results in the widest variation in glide slope angle in both visual conditions whereas the remaining displays tested all result in approximately the same data spread.
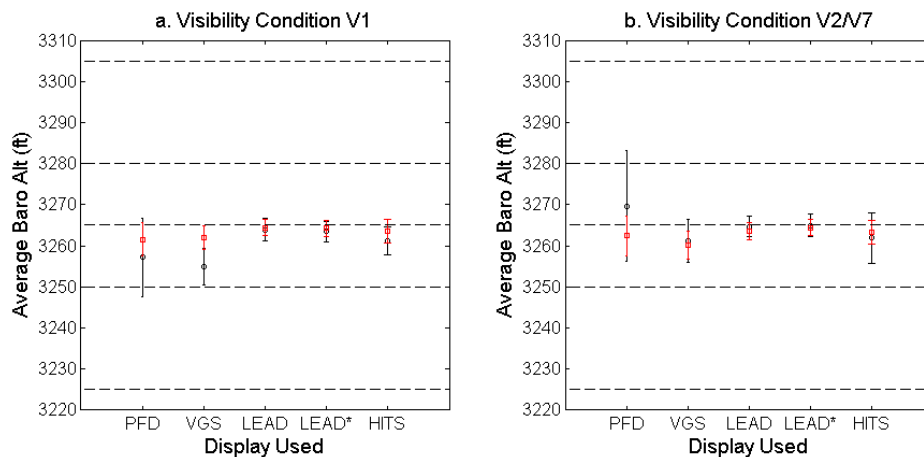
Fig. 5-25. Mean aircraft altitude during level phase of glide slope capture with 'on condition' start conditions

Fig. 5-25 shows the mean aircraft altitude during the level portion of the MTE by each pilot per display in both good and degraded visual

226

conditions. Again, the LEAD and LEAD* displays allow the pilot to fly at an altitude closest to target and per pilot, these displays result in the smallest variation in altitude. The VGS and HITS provide approximately equivalent results, the pilots flying slightly low on average with the largest deviation from target and variation in altitude resulting from the PFD display format.

Fig. 5-26 shows the mean aircraft y (east) coordinate during the MTE by each pilot per display in both good and degraded visual conditions. This is a measure of the aircraft's lateral deviation from the extended runway
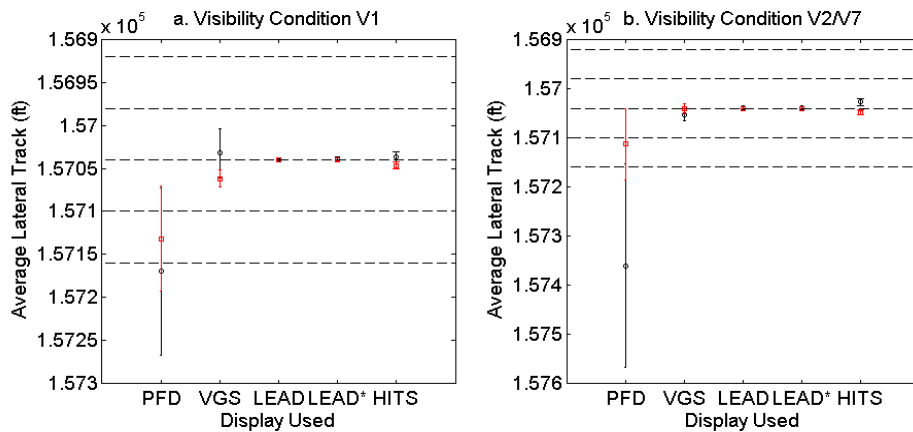
Fig. 5-26. Mean lateral deviation from extended runway centre-line during glide slope capture MTE with 'on condition' start conditions

centre-line during what is essentially a longitudinal manoeuvre. The LEAD and LEAD* displays provide the closest average adherence to the target value followed by the HITS, VGS and PFD displays respectively. This order also reflects the variations in y-coordinate observed during the MTE.

Fig. 5-27 shows the mean aircraft IAS during the MTE by each pilot per display in both good and degraded visual conditions. For all cases, the IAS is maintained within the desired performance boundaries. The VGS format
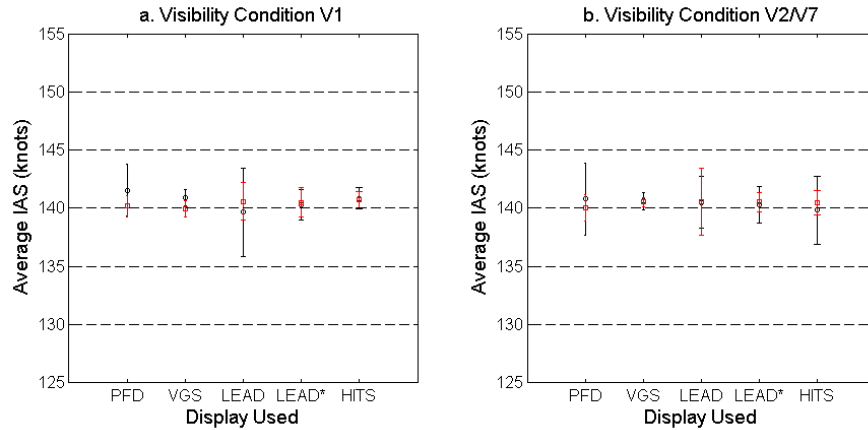
Fig. 5-27. Mean IAS during glide slope capture MTE with 'on condition' start conditions

delivers the least variance in the average IAS, followed by the LEAD* display. In visual condition V1, the HITS display format provides a low spread of IAS values but this significantly degrades in visual condition V2/V7. The highest spread of IAS values is observed for pilot P1 using the LEAD concept in visual condition V1.

5.5.2.2 Start With Vertical Offset

Fig. 5-28 to Fig. 5-31 show the summarised trajectory data for all test
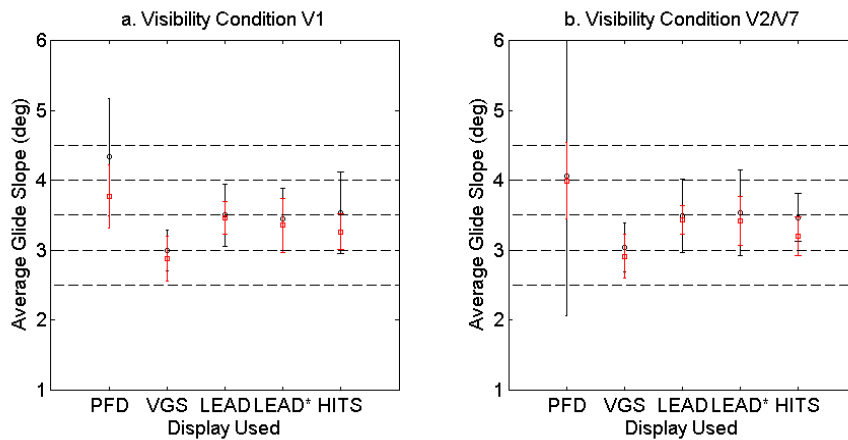
Fig. 5-28. Mean aircraft glide slope during capture MTE with a vertical offset from the desired start condition altitude

points flown for the localiser capture MTE starting with a vertical offset from the target altitude. Fig. 5-28 shows the mean aircraft glide slope during the MTE by each pilot per display in both good and degraded visual conditions. The LEAD and LEAD* displays result in the closest average glide slope to target for both pilots. The largest deviation from target is observed when the PFD display is used and flights using this format also exhibit the largest variation in glide slope angle.

Fig. 5-29 shows the mean aircraft altitude during the level portion of the MTE by each pilot per display in both good and degraded visual

Fig. 5-29. Mean aircraft altitude during level phase of glide slope capture MTE with a vertical offset from the desired start condition altitude

conditions. Test points conducted with the LEAD, LEAD* and HITS result in approximately consistent results in terms of both deviation from the target altitude and variation in the data over the course of the manoeuvre. A larger deviation from target and variation about the average altitude is evident for the PFD display and the VGS display exhibits a curious result. This will be discussed further in Section 5.7.

Fig. 5-30 shows the mean aircraft y (east) coordinate during the MTE by each pilot per display in both good and degraded visual conditions. As with the previous case, the LEAD and LEAD* concepts provide the closest
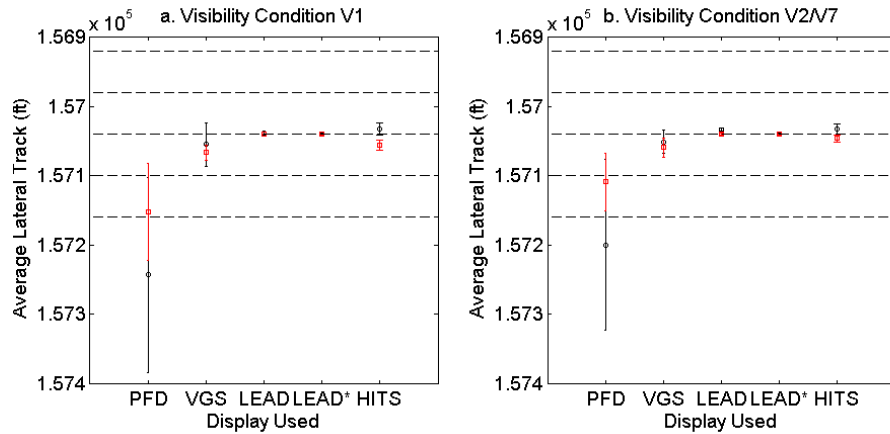
Fig. 5-30. Mean lateral track along extended runway centre-line during glide slope capture MTE with a vertical offset from the desired start condition altitude

adherence to target and least variation from runway centre-line track, followed by the HITS and VGS formats. The PFD display lead to the worst performance for both pilots in both visual conditions.
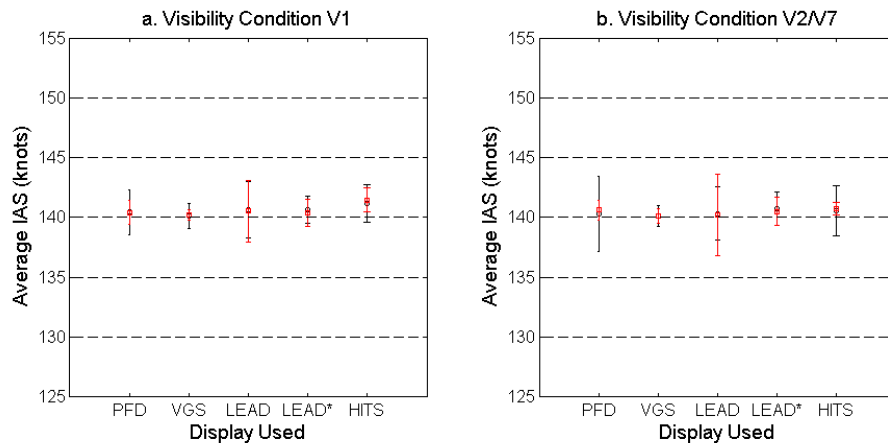
Fig. 5-31. Mean IAS during glide slope capture MTE with a vertical offset from the desired start condition altitude

Fig. 5-31 shows the mean aircraft IAS during the MTE by each pilot per display in both good and degraded visual conditions. Again, for all cases, the IAS is maintained within the desired performance boundaries.

230

Adherence to the target speed is good in all cases and formats VGS,
LEAD*, HITS, PFD and LEAD provide increasing variance of the speed
from the average, in the order given.

5.5.2.3 Start With Altitude and Vertical Flight Path Offset
Fig. 5-32 to Fig. 5-35 show the summarised trajectory data for all test
points flown for the localiser capture MTE starting with a vertical offset
from the target altitude and in a 3.5deg climb. Fig. 5-32 shows the mean
aircraft glide slope during the MTE by each pilot per display in both good

Fig. 5-32. Mean aircraft glide slope during capture MTE with both altitude and vertical flight path offsets from the desired start condition

and degraded visual conditions. The LEAD, LEAD* and HITS display
formats provide comparable performance in both visual conditions whilst
the VGS and PFD resulted in approximately equivalent deviations from
target with flights conducted using the PFD display format resulted in the
widest variation in glide slope.

231

Fig. 5-33 shows the mean aircraft altitude during the level portion of the MTE by each pilot per display in both good and degraded visual
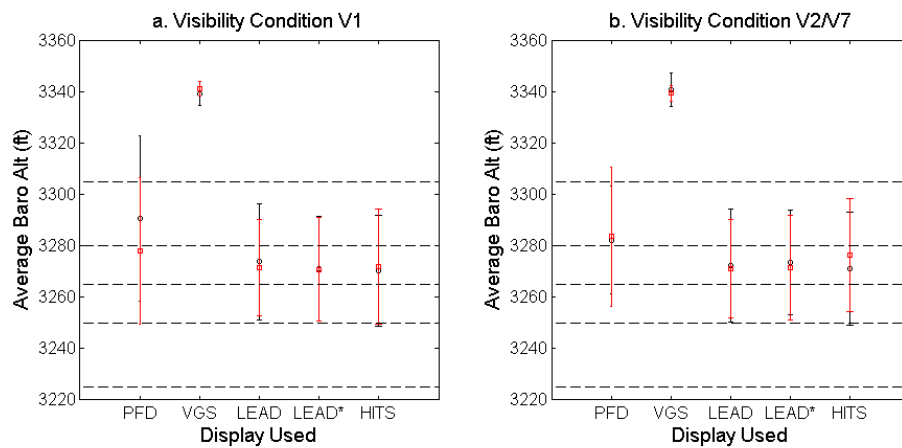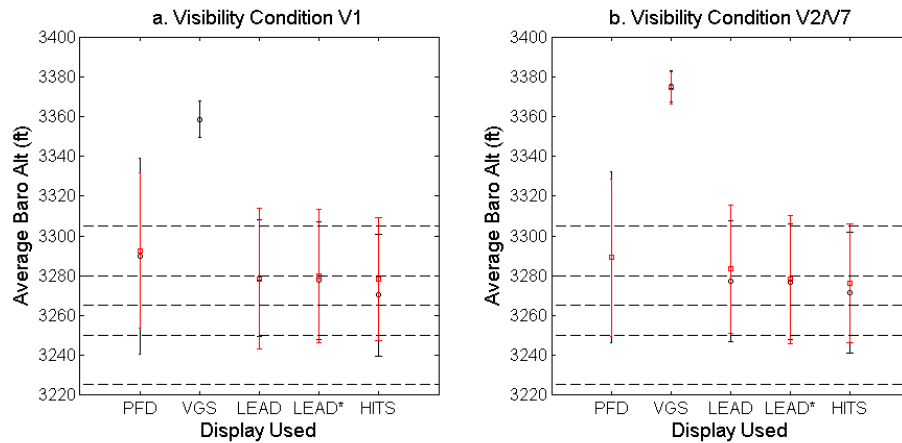

Fig. 5-33. Mean aircraft altitude during level phase of glide slope capture MTE
with both altitude and vertical flight path offsets from the desired start condition

conditions. The LEAD, LEAD* and HITS again resulted in comparable performance in terms of both deviation from the target altitude and the variation in the aircraft altitude. The PFD format resulted in the slightly larger deviation and variation in altitude and the VGS again exhibited the behaviour to be discussed in Section 5.7.

Fig. 5-34 shows the mean aircraft y (east) coordinate during the MTE by each pilot per display in both good and degraded visual conditions. The
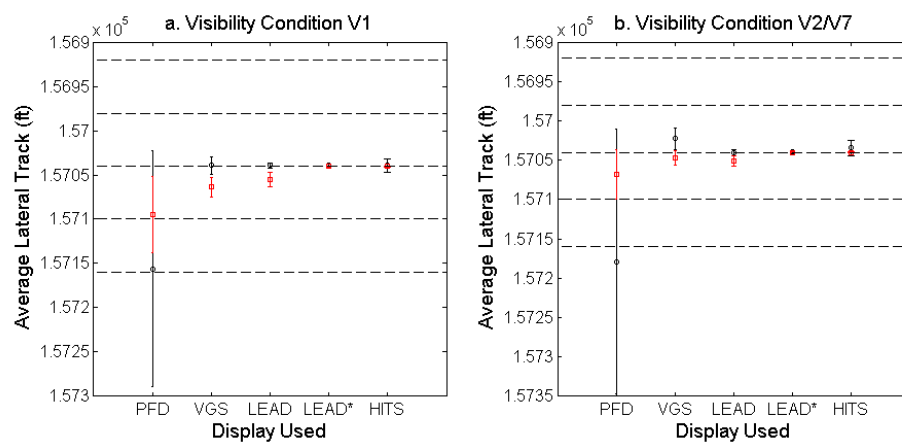
Fig. 5-34. Mean lateral track along extended runway centre-line during glide slope capture MTE with both altitude and vertical flight path offsets from the desired start condition

232

LEAD, LEAD* and HITS formats all result in comparably good performance in terms of deviation from the extended runway centre-line and the variation in y coordinate in general. The VGS performance is only marginally worse and the track achieved using the PFD significantly less tightly controlled.

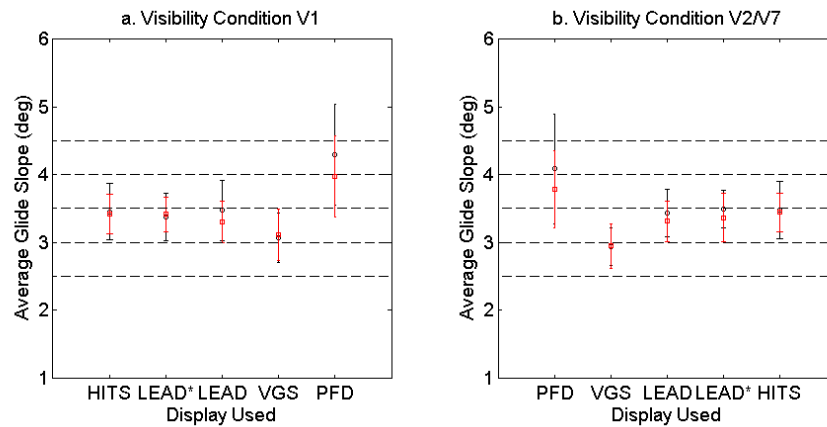Fig. 5-35 shows the mean aircraft IAS during the MTE by each pilot per
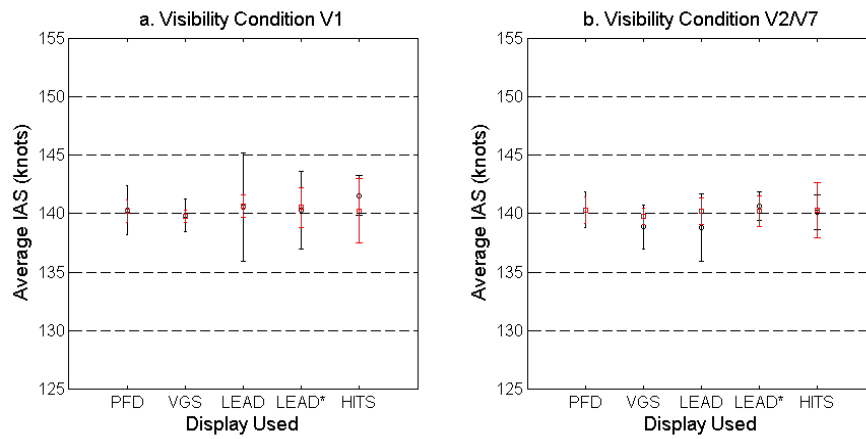
Fig. 5-35. Mean IAS during glide slope capture MTE with both altitude and vertical flight path offsets from the desired start condition

display in both good and degraded visual conditions. Again, for all cases, the IAS is maintained within the desired performance boundaries. The pattern of results is more mixed than the previous cases here. Average IAS values are all close to target but pilot P1 achieves generally a wider spread of data with the poorest adherence to target IAS being observed with the LEAD display format. Again, the VGS gives the lowest IAS variation but pilot P2 manages to achieve similarly low IAS variations with all but the HITS concept.

5.6   Localiser and Glide Slope Capture MTE Pilot Ratings

This Section reports on the averaged pilot ratings for all of the localiser and glide slope capture MTEs conducted during the display performance assessment.

5.6.1   Localiser Capture

Fig. 5-36 shows the average ratings for all of the localiser capture MTEs given by both pilots in the differing visibility conditions for each display format.
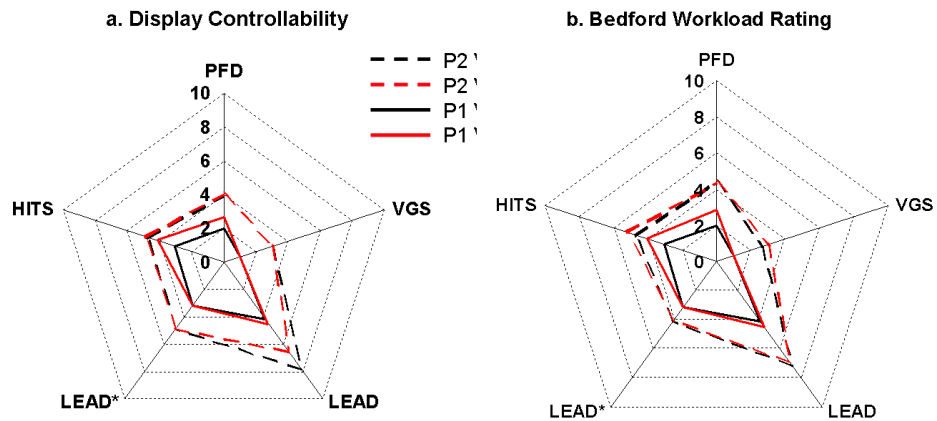
Fig. 5-36. Pilot ratings per display for the localiser capture MTEs: (a) Display controllability and (b) Bedford workload

The trend for both rating scales is consistent for both pilots, with pilot P2 giving slightly higher ratings than pilot P1 (a trend which continues throughout the remainder of the rating results). The most obvious result apparent from Fig. 5-36 is that the LEAD concept was the least favoured of all of the concepts tested in terms of both controllability and workload. The VGS is rated the best (lowest) with the PFD, LEAD* and HITS concepts all being rated at an approximately equal level. Some of the key factors provided by the pilots for the ratings given for the LEAD display are:

1. The looming effect by itself provides effective speed control if the speed is maintained around the target speed. To do this effectively though, was a high workload task. However, once the speed deviates significantly from the datum, then the looming cue is not sufficient to maintain target speed accurately.

2. The looming effect provided by the symbols was not intuitive. The pilots had to think i.e. compensate as to what one symbol being larger than the other meant and then act accordingly.

234

3. Linked in with the lack of speed cueing, the pilots found it difficult to know what throttle setting to apply to maintain speed at the target. If they 'guessed' the power setting and happened to get it right, then speed control was significantly easier to control than if they were having to constantly adjust the throttle position. In fact, throughout the testing, the pilots learned what power settings to apply and used this as a guide to control their speed, using the looming cue for fine adjustment.

4. The roll cueing for the capture manoeuvre, whilst useful for the roll in and out of the turn, was disconcerting in the turn itself. This was because matching the predictor symbol bank angle with that of the lead aircraft symbol did not result in the correct rate of turn. This, in turn, resulted in the pilot having to compensate with bank angle corrections to maintain the correct trajectory.

The remaining ratings are reasonable similar. The pilot key comments that pertain to the LEAD* display being rated as per Fig. 5-36 are:

1. Addition of IAS display makes the speed control issue disappear and therefore trajectory control can be concentrated on. The localiser capture manoeuvre then becomes accurate and straight-forward.

2. For the lateral and heading offset test case, the initial turn cueing was not at all intuitive (the symbology indicated a rapid pitch up and then pitch down motion). From the pilots viewing position, when this happened, there were also occasions when the lead aircraft symbol was lost from sight and this causes anxiety.

The pilot key comments that pertain to the VGS display being rated as per Fig. 5-36 are:

1. It was sometimes difficult to discern which symbol was being controlled and which symbol was being used as the guide.

2. However, the fact that the guide and symbol remained overlaid despite the lateral snaking characteristic of the aircraft model used gave a useful cue to the pilot that the motion was not being caused by them and that so long as the two symbols remained overlaid, no corrective action needed to be taken.

3. The guidance symbol did not take the aircraft to the correct height if off condition but to the height that the aircraft started at.

4. The display, whilst providing all of the information that a pilot would require, is cluttered, looks messy and in some cases, the symbology is indistinct.

5. The guidance provided is straight-forward and intuitive.

The pilot key comments that pertain to the HITS display being rated as per Fig. 5-36 are:

1. Difficult not to believe that the tunnels are not 'real' and 'solid' so slightly disconcerting when off condition and flying through them.

2. Pilot P2, at times, found himself concentrating on the tunnel 'symbols' almost to the exclusion of everything else.

3. 'Approximate' bank angle of tunnels for the localiser capture itself requires some pilot compensation to obtain the correct angle to ensure that the trajectory through the tunnels is correct.

4. When off-condition, it is an easy task to see where 'on-condition' is and this allows the pilot to choose the rate at which the aircraft is returned to the desired trajectory. Pilot P2 specifically commented that he 'instinctively liked' the tunnel concept.

5. However, the number of tunnel segments ahead should be varied depending upon the manoeuvre involved. The five tunnel segments used for the research was fine for straight and level segments, however, this was not considered sufficient in the turn as it did not

give sufficient 'look-ahead' time in terms of where the aircraft should be going. In this case, the pilots tended to concentrate on the furthest tunnel segment for guidance.

6. The natural horizon is a powerful cue and pilot P1 felt that for the degraded visual condition test points, he was not able to fly as accurately without it.

The pilot key comments that pertain to the PFD display being rated as per Fig. 5-36 are:

1. The display contained a number of minor but annoying deficiencies. These were: the scan required to achieve desirable performance, particularly in poor visual conditions was wide and 'busy'; a PFD in operational service would have target altitude and speed bugs to assist with observing any deviations from that set and the vertical speed scale required an element of interpretation.

2. Accurate speed and altitude control presented a small issue in that the tapes and digital displays had to be interpreted. This is particularly true given that the localiser capture target height was 3265ft and the altitude display only gave read-outs to the nearest 10ft.

For the lateral and heading offset test cases in degraded visibility, the pilot's situational awareness is very much reduced and to get back onto condition and capture the localiser proved quite challenging.

5.6.2 Glide Slope Capture

Fig. 5-37 shows the average ratings for all of the glide slope capture MTEs given by both pilots in the differing visibility conditions for each display format. Pilot P2 did not test the LEAD display format in visual condition V2/V7 so no rating is recorded.
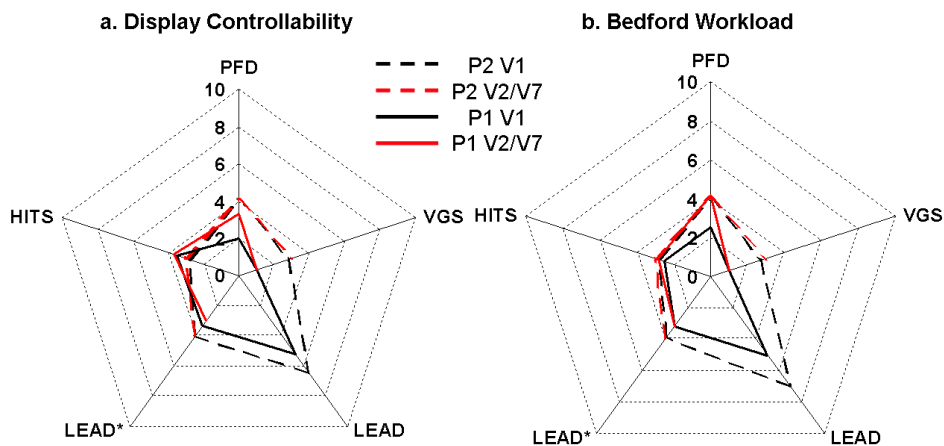
Fig. 5-37. Pilot ratings per display for the glide slope capture MTEs: (a) Display controllability and (b) Bedford workload

As for the localiser capture MTE, the LEAD display format was least favoured by both pilots in terms of being able to control the test parameters with the display and the workload involved in doing so. As before, the ratings for this display were primarily driven by the issues already reported regarding speed control and the related issue of power setting. The VGS scores consistently best and the LEAD*, PFD and HITS concepts are all rate approximately the same. The key additional comments arising from the glide slope capture MTE for this display concept were:

1. The display would be improved by providing some warning of the imminent change in attitude/power setting required for the capture of the glide slope itself.

2. Visual condition V1 allowed the pilots to have a better understanding of what was going on as the outside world provided situational awareness cues in terms of relative position of airfield, attitude cues etc.

3. Pilot P2 commented that this MTE was easier to fly than the localiser capture manoeuvre using the LEAD display.

The key additional comments arising from the glide slope capture MTE for the LEAD* display concept were:

238

1. The addition of the IAS symbol is not necessarily the end of the issues with this display. The aircraft symbols provide predictive information whereas the IAS gives current speed. What is missing is some form of prediction as to whether the aircraft needs to be accelerating or decelerating to be at the target speed at the predicted 'look ahead' time (author's note: of course, this was the intended purpose of the looming cue).

The key additional comments arising from the glide slope capture MTE for the VGS display concept were:

1. Moderate increase in workload to maintain/re-capture speed once the descent is initiated.

2. Pilot P2 did not 'trust' the acceleration caret display and was 'mildly irritated' by having to glance down for throttle setting information. Pilot P1 did find the acceleration cue to be useful for power setting.

3. Both pilots had enough spare capacity to carry out other tasks (such as talk to the simulator operator) whilst using the VGS. This is indicative of an easy-to-use display.

The key additional comments arising from the glide slope capture MTE for the HITS display concept were:

1. Pilot P2 had a tendency to fly close to the upper edge of the tunnel frames.

2. To get to a control rating of 1 or 2, pilot P2 requested that the flight path vector provide some form of flight path prediction capability.

3. Different coloured tunnel frames may be useful at key points e.g. at point to initiate descent.

4. The lateral instability of the aircraft model caused a slight increase in workload as it was not clear to the pilot if he were the cause of it or not so was making inputs to try to dampen it out.

The key additional comments arising from the glide slope capture MTE for the PFD display concept were:

1. Workload higher than localiser capture as attention is divided between controlling the flight path and reducing power to maintain the target IAS as the descent is initiated.

2. For the height offset with a 3.5deg climb start condition, the workload is increased as the manoeuvre is not stable from the outset.

3. A particular difficulty was encountered in visual condition V2/V7 where the outside world visual cues are very much reduced. Due to the lateral instability of the aircraft model, the task to maintain a steady approach was made artificially high with the only source of information being the cockpit head-down instruments.

5.7 Discussion of Results

5.7.1 Trajectory Definition

The same comments used for the flare apply here in that trajectories that conform to constant $\dot{\tau}_{\Delta y}$ or $\dot{\tau}_{\Delta xz}$ can be said to follow power-law inertial paths. However, what has been introduced here is that there is a further predictive element that can be utilised, if required by knowing the power law relationships of Eq.(2-30) and (2-31). Initial velocity and acceleration conditions can be calculated by knowing that at time, $t = 0$, $t = -T$.

5.7.2   Speed Control via Looming

Fig. 5-38 shows examples of pilots P1 and P2 trying to maintain a target speed of 160knots (IAS) using the LEAD concept during a localiser capture manoeuvre. The figure shows that both pilots are reacting to the speed warning annunciations which were triggered when the IAS reached 5knots above or below target, and not the looming effect.
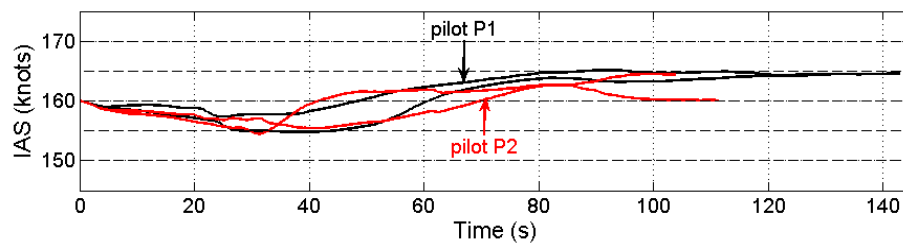
Fig. 5-38. Illustration of looming proving to be ineffective for speed control

It was somewhat surprising to discover, during the display performance trials, the extent to which the looming effect on the LEAD concept did not provide adequate speed control capability as problems of the same magnitude were not encountered during the development process. The only explanation that can be offered is that during development, the pilot was being asked to concentrate specifically on elements of the display functionality and with this focused concentration, speed control was possible. However, during the performance comparison trials, the pilot's attention was divided on other tasks (flying more complex manoeuvres with offsets, assessing the display as a whole, consideration being given to ratings etc.), revealing the limitations of the concept.

The failure of this particular concept does not necessarily spell the end of the idea (the author uses optical looming every day maintaining station behind the car in front whilst travelling to work). It is believed that the 2D aircraft representation was, in fact, too simple a representation of a lead aircraft. Consider the situation for real. A lead aircraft is not 2D but 3D. 'Looming' is not only perceived by the change on size of the wingspan and the fuselage cross-section. The entire aircraft shape contributes to the looming effect, which includes angular changes due to the length of

241

aircraft structure (the third dimension which is missing from the LEAD and LEAD* concepts). It is therefore suggested that, for future iterations of the concept, the information regarding the lead aircraft is presented in 3D form. This may be via a simple '3D' line drawing or via a 3D graphical model such as that shown in Fig. 3-31.

It is also interesting to speculate that a 'closed' shape e.g. a triangle would have performed more efficiently as a looming speed controller than the 'open' shape of the aircraft symbol. Fig. 5-39 illustrates such a concept. It is interesting in that it not only ties in with pilot anecdotal evidence (pilot P2 reported that some previous flight director display testing he had performed found that closed symbols were preferable to open ones), but links to the closure law of the Gestalt Theory of motion perception. It may be that closed two-dimensional shapes are more representative of the three dimensional world and therefore are more effective at representing 'looming'. The LEAD display does, of course, feature a closed shape – the circle of the 'fuselage'. It would be an interesting experiment to test which, if any, of the two concepts of Fig. 5-39 perform more effectively as a looming speed controller.

Fig. 5-39. Open and Closed Figures

5.7.3 $\tau_{\Delta y}$, $\tau_{\Delta xz}$, $\tau_{\Delta locdev}$ and $\tau_{\Delta gsdev}$ as a Visual Perception Variables

It is clear from the results of Fig. 5-1 and Fig. 5-2 that the analysis of $\tau_{\Delta y}$ and $\tau_{\Delta locdev}$ provide very similar results. It is less clear from Fig. 5-3 Fig. 5-4 of any similarity between $\tau_{\Delta xz}$ and $\tau_{\Delta gsdev}$ but they are conceptually identical, just in a different plane of reference. Overall, then, it would seem that there is evidence to support individual hypotheses that pilot control strategies, during the approach, strive to achieve the closure of aircraft motion gaps using constant $\dot{\tau}$ of those gaps. This is of interest

from a display design perspective because there has long been a debate about the form that design symbology should take. There is an argument that providing displacement-only information does not provide sufficient information to allow the pilot to control the parameter being displayed effectively and that rate information is also required to improve the situation [129]. This argument still persists in the design of both head-up and head-down displays in the form of the dial-vs-tape debate [130] (it is argued that moving–tapes that are now almost universal for airspeed and altitude display on HDDs and HUDs deprive the pilot of rate information that a rotating needle on a dial provides). It should be noted that the definition of τ incorporates both displacement and rate information. It is possible to hypothesise, therefore, that pilots have always sought out τ information.

The question arises as to how these variables might be perceived by the visual system. For the localiser and glide slope capture MTEs, both instrument and visual techniques were employed by the pilots. For the instrument cases, the pilot reported that the instrument scan employed concentrating primarily on the respective localiser or glide-slope deviation indicator. Once established, for the glide-slope capture specifically, this scan is supplemented by an occasional glance at the vertical speed to ensure that it is about right for the combination of desired glide-slope descent angle and airspeed. Any τ relationship observed can therefore be reasonably assumed to arise from the gap of the indicator needle and the desired location on the instrument (which, for the instruments used in this experiment, is directly proportional to the deviation angle itself).

For the case of visual flight, the localiser must be visualised in the pilot's mind by mentally extending the runway centre-line over the terrain between the runway and the aircraft such that as the turn onto it is complete, for nil-wind conditions, the runway is lined up in the centre of

the display directly ahead of the pilot. For glide-slope capture, pilots are trained to 'remember the picture' of what the runway should look like during the descent to it. For a visual glide-slope capture, the pilot must initiate a descent as that mental picture begins to emerge and then maintain it to the initiation of the flare. There are a number of cues available to the pilot that will allow him to do this that relate to the relative size and shape of the runway, the layout of its surroundings and its position in the windscreen in front of the pilot (see, for example Refs. [93], [92] and [91] for various attempts to quantify, by analysis, how a glide-slope angle is detected and maintained using variables visually available to the pilot). It would be an interesting next step in the research to ascertain whether any of the variables suggested in this reference also demonstrate coherent τ relationships during the motion gap closure manoeuvres. It could be argued that if this were the case, the variable in question might be the most fundamental invariant in the visual scene that is being used to close the gap. Overall, however, the evidence suggests that pilots use τ gap closure strategies not only when using the outside world as a reference, but also for null-selection of instruments.

For each of the motion gaps discussed, therefore, there is a plausible means for the pilot to detect any change in that gap from visually available information. However, some care must be taken with the selection and definition of the motion gaps as there are issues that require careful handling with analyzing τ. Traditional τ analyses (plummeting gannets, pigeons landing on perches, somersaulters landing etc.) have a very clearly defined end-point. The same can be said of the flare manoeuvre – the moment that the main gear comes into contact with the ground. However, for capture manoeuvres analysed, the end-point is 'virtual', there is no hard-stop at the end of the manoeuvre. To cope with this, the end-point was taken to be when key variable in question changed by less than 1% of the total gap. For a localiser capture, for example, the pilot may overshoot

the nominal runway centre-line and then re-capture it from the other direction. Where is the end point in this case ? For this specific example, the view was taken that there are two gaps closed. The first is the closure to the overshoot value and the second the re-capture to the runway extended centre-line. This is why, on Fig. 5-1 and Fig. 5-2, for instance, there are both positive and negative values of gap closure. For such dynamic manoeuvring, τ analysis can be difficult, if not impossible, because reversals of the rate of change of the motion gap can lead to large excursions of the value of τ as they return from close to $\pm\infty$ as the rate of change term approaches zero. This 'pursuit' guidance has already been discussed, but its relevance to 'soft-stop' τ analysis merits a further mention

5.7.4 Display Parameter Selection and Initial Testing

In general terms, the design parameters recommended by the pilot for the LEAD concept are those that would have been selected on the basis of the performance results alone. For the localiser capture MTE, t_{pred}=4.0s looks promising on the basis of the capture of the localiser track alone. However, this parameter did not provide as good speed control using the looming concept as for t_{pred}=2.0s or 3.0s. The decision to go with t_{pred}=2.0s therefore came down to pilot preference for a slightly larger symbol. C1=0.6 then represents the value for which the least overshoot (and indeed some undershoot) is observed and for which the pilot is most comfortable performing the turn onto track. One limitation of the simulation facility that may have contributed in part to this decision process was that of display blurring. The displays were developed on a standard computer monitor (resolution 1280x1024 pixels) and the displays appeared crisp and easily visible. This was also true of the HELIFLIGHT monitors in the flight simulator pod. Unfortunately, there is a collimation lens between the monitor image and the pilot's eye. This places the image at infinity but also results in a slight shadow image being cast. This second image caused

a distinct blurring of all of the HUDs used in this research. Short of using an alternative simulation facility, there was no way of getting around this issue. There is an argument here that using a fixed-base simulation facility has merit and a rudimentary one could quite easily be constructed for future work from desk-top personal computers. One of the cited advantages of using HELIFLIGHT is that it has a motion base. However, the motion cues that such a facility can provide are always going to be corrupted by the motion limits of the platform itself and of the washout filtering that has to occur. In any case, pilots are trained to ignore in-flight acceleration cues as these can be deceptive and rely instead on their instruments or visual cues [4]. It can be argued that a good visual environment (free of display blurring) would be more useful in display development than a facility with motion cues but a reduced ability to provide clear displays.

For the glide slope capture MTE, there is actually little to choose between the test points flown and so the selection of the final design parameters rests solely with pilot opinion. However, all of the MTE test points flown were benign and one of many values could have been chosen.

5.7.5   Display Comparison

For the MTEs that start 'on condition', the LEAD and LEAD* concepts perform well in terms of adherence to desired value and variation away from that target for spatial parameters (altitude, lateral track etc.). They out-perform, if only by a small margin, HITS, VGS and PFD display concepts in both good and degraded visual conditions. The LEAD concept is poor at speed control cueing and that has already been discussed. With the addition of the IAS to the LEAD* concept, it performs as well as HITS or VGS but this is to be expected.

For the start conditions with offsets introduced, the LEAD and LEAD* again perform well, but not significantly better than HITS, for example.

Using the HITS format, the pilots commented that they liked the 'freedom' to choose their own rate of return to the desired flight path. The similarity of the spread of spatial data for these concepts indicate that the same approach was taken to re-acquiring the lead aircraft (again, this simply indicated where the aircraft should be with no sense of urgency implied as to how quickly to return to the desired position). In this regard, the VGS shows some curious results outside of adequate performance boundaries. This was discovered (too late to do anything about it) during testing that the VGS algorithms, as implemented, would, on occasion, guide the aircraft onto a height other than the initial height of the start conditions. The pilot followed the guidance, as instructed, but this guidance was 'incorrect'. The absolute values should therefore be ignored but the deviation still provides a comparative indication with the other display concepts. In this regard, the VGS performs well.

In general terms, unlike for the flare MTE, there is no degradation in performance compared to the MTE criteria and in some cases, there is actually an improvement when the visual environment is degraded. This is least true for the LEAD concept and is interpreted as follows. The outside world view, according to Gibson, contains a wealth of information for the observer when under motion. Of course, for the results presented, the pilots also flew with reference to instruments and guidance. However, the HUDs, at least, were overlaid onto that visual scene. Even if it were a sub-conscious process, it appears that the information available from the visual scene is influencing aircraft guidance decisions in some cases. This results in less consistent trajectory performance. In the severe DVE tested, the only information available is from the displays and the pilot can devote all attention to these. It is this 'de-cluttering' of information that results in more consistent trajectories being flown.

In terms of pilot ratings, the LEAD and LEAD* perform better for the localiser capture MTE than for the glide slope capture. In general, pilot P1's ratings are lower i.e. more favourable than pilot P2. Following discussion with the pilots it became clear that the reason for this was that pilot P1 had been providing ratings based upon the guidance capability for the concepts alone, whilst pilot P2 had been taking a more holistic approach and rating the display in totality. The general trends indicated across pilot ratings are similar so it is not considered that this discrepancy is too detrimental. However, it may be that the HITS, LEAD and LEAD* concept may have been more severely rated by pilot P2 using the holistic approach as they are not, and were never intended to be, polished display formats, like the VGS for instance.

There is one further reason why the LEAD and LEAD* concepts were rated slightly more severely during the comparative display testing. For the localiser capture MTE start conditions with offsets, the initial position commanded by the lead aircraft directed a climb and then descent when none was required. This was later found to be a 'feature' of the logic used to constrain the lead aircraft symbol to the centre visual channel screen. This will need to be corrected for any future work conducted using this display format. As such, this has added an unintended extra element of compensation to control the symbol and has contributed to the ratings for this display being artificially high.

Overall, it should be remembered that the LEAD and LEAD* concepts did provide suitable guidance in both good and extremely degraded visual environments to allow the pilot to perform the MTEs at least as well as, and in many cases better than the alternative display formats. This showed that using the τ of a motion gap is suitable for driving a display that defines a flight path trajectory.

5.7.6 Roll Command

Both the LEAD and LEAD* concepts provided roll cueing in the turn for the localiser capture MTE. This proved to be adequate but not ideal. The roll angle commanded was 'averaged' from a number of trial runs flown by pilot P1 during initial testing of the display. As such, it did not always command a roll consistent with the chase aircraft's current actual speed or desired turn radius to re-acquire desired track. This attracted some pilot comment and is suggested as an improvement for the next iteration of the display concept.

5.7.7 Limitations of the Results

The same limitations apply to the results presented for the localiser and glide slope capture MTEs as for the flare MTE. In addition, it should be noted that the degraded visual conditions used for each display format are not quite 'symmetrical'. The HITS format was created using 3D models of the tunnel frames placed in the outside world database. Using fog to create visual condition V7 obscured these models as much as the surrounding scenery. To solve this problem, V2 was used as the degraded visual environment and V7 for the remainder of the display formats. It is not considered that this had a major impact as it resulted in the surrounding environment appearing black rather than grey. It was, however, a difference in test conditions and, as such, represents something to be improved next time.

The test of a display being 'more or less' acceptable than another has been measured using MTE performance criteria and pilot ratings. However, the use of τ-based displays implies that the use of such formats should provide the pilot with guidance information that is more recognisable, more intuitive. The measures used do not necessarily translate to a direct measurement of this 'cognition' of the information. For one thing, pilots are used to using certain types of displays e.g. PFD and VGS and it is

suggested that, however unintentionally, ratings awarded might lean favourably towards the familiar rather than the unfamiliar. A true measure of the effectiveness of a display is how quickly a pilot's brain can process the information that it provides. This is beyond the scope of the current thesis but perhaps provides an interesting research topic for the future.

5.7.8   General Discussion

One of the initial goals of the design process was to try to minimise the display symbology that is used on any concept developed. For the case of LEAD*, only four symbols are presented (lead and predictor aircraft, horizon, IAS). The pilot should be using the VGS in much the same manner (flight path symbol, guidance cue, horizon and IAS tape/digital readout). It can be argued that the number of symbols being used has not really been reduced but, with reference to the specific tests, the total number of symbols required to perform the task satisfactorily that are displayed to the pilot has been significantly reduced. Of course, the VGS additional symbology is assumed to be there for good reason but an interesting proposition for future displays is to project only that symbology set that is absolutely necessary for the phase of flight ahead of the pilot (such a function already exists in part in terms of 'de-clutter' modes on existing HUDs).

5.8   Conclusions

A number of fixed-wing large jet-transport localiser and glide slope capture manoeuvres have been flown and analysed. The results from these analyses have been used to generate τ-based trajectories. Algorithms have been developed to drive a lead aircraft symbol and predictor aircraft symbol to provide guidance such that a pilot can manually fly the aircraft around those trajectories. From this work, the following conclusions have been drawn:

i.   During the final segment of the localiser capture manoeuvre, the hypothesis that $\dot{\tau}_{\Delta y}$ and $\dot{\tau}_{\Delta locdev}$ remain constant has been shown to be correct.

ii.   During the final segment of the capture of a glide-slope, the hypothesis that $\dot{\tau}_{\Delta xz}$ and $\dot{\tau}_{\Delta gsdev}$ remain constant has been shown to be correct.

iii.   In a GVE, the constant $\dot{\tau}_{\Delta y}$ and $\dot{\tau}_{\Delta xz}$ pilot strategies can be achieved with reference to the visual information available in the outside world.

iv.   In a DVE, the constant $\dot{\tau}_{\Delta y}$ and $\dot{\tau}_{\Delta xz}$ pilot strategies is achieved with reference to the nulling of gaps indicated by cockpit instruments (in this case, localiser and glide slope angle deviation indicators).

v.   In general, for the approach MTEs, performance against the MTE criteria is either equivalent to, or improved, when the same manoeuvre is flown in a DVE compared to the same manoeuvre in a GVE. This is true for the PFD, VGS, LEAD* and HITS display formats. In this case, it is interpreted that the wealth of information available to the pilot from the outside world visual scene actually hinders the manoeuvre being flown accurately and consistently. The display formats provide sufficient information to fly the manoeuvre, with the degradation in visual conditions removing the 'unnecessary' clutter of additional information.

vi.   The use of a simple 2D representation of a lead aircraft provides insufficient speed cueing to provide satisfactory IAS guidance.

vii.   The use of average roll values to provide roll cueing was an unsatisfactory solution and exact roll angle cueing would

251

need to be introduced (or the roll cueing removed altogether) to provide a more satisfactory pursuit guidance solution.

viii. A lead and predictor aircraft symbol display concept provides the means to indicate and fly very precise and invariant flight paths.

ix. Acceptable τ-based values for the lead-predictor aircraft symbol concept are as follows: prediction time, t_{pred}=2.0s; for the localiser capture MTE: $\dot{\tau}_{\Delta y}$ =0.6 and total manoeuvre duration, T=10.0s; for the glide slope capture MTE: $\dot{\tau}_{\Delta xz}$ =0.6 and total manoeuvre duration, T=5.0s.

x. The HITS concept finds acceptance with pilots in that it provides the required guidance information but allows them to choose the rate at which any deviations can be corrected. The LEAD and LEAD * concepts also perform this function but the effect is more subtle.

5.9 Recommendations

Based upon the work reported in this Chapter, it is recommended that:

i. Consideration should be given to using a pseudo- or actual-3D lead aircraft symbol to establish whether this improves the speed cueing provided.

ii. Investigation into methods to measure human cognitive function should be made with pilots using various display formats. The absence or reduction of cognitive processing would be a measure of success of the ability of that display to provide the pilot with the guidance information that is required more effectively. It is hypothesised that a τ-based display would be more effective in this regard than a spatially-based display.

iii.   The τ-based relationships used to define the approach trajectories could equally well be used as a basis for automatic control of an aircraft along those trajectories. Consideration should be given to using the relationships reported to implement automated localiser (or general track) and glide-slope (or general descent and climb flight-paths) capture manoeuvres.

iv.   If recommendation (i) yields more successful speed control, the LEAD and HITS concepts be combined into a single display format.

C h a p t e r 6

FULL AIRFIELD APPROACH MTES

6.1 Introduction

This Chapter reports on the results obtained for the large jet transport
MTEs where the pilot conducted an approach to the airfield all of the way
to touchdown. Specifically, results from the following MTEs are reported:

1. Full Standard Visual Approach;

2. Full Standard Precision Approach and

3. Curved Approach

The Full Approach MTE is the localiser capture, glide slope capture and
flare MTEs linked together with steady state flight segments. As such,
Chapters 4 and 5 cover the basic analyses that relate to the extended MTEs.
The purpose of using the 'extended' MTEs was to establish whether the
display concepts performed acceptably over an entire approach, rather than
limited portions of the approach, and that no problems were encountered at
'the seams'. As such, a more limited analysis has been performed on these
MTEs. Section 6.2 reports the results of a trajectory performance analysis
and Section 6.3 reports on the corresponding pilot ratings.   Sections 6.4,
6.5 and 6.6 bring together the learning points from those results.

6.2 Display Trajectory Performance Analysis

6.2.1   Full Standard Approach

Fig. 6-1 to Fig. 6-5 show the summarised trajectory data for all test points
flown for the Full Approach MTE for pilots P1 and P2 in visual conditions
V1 and V2/V7. Fig. 6-1 shows the mean aircraft cg altitude during the
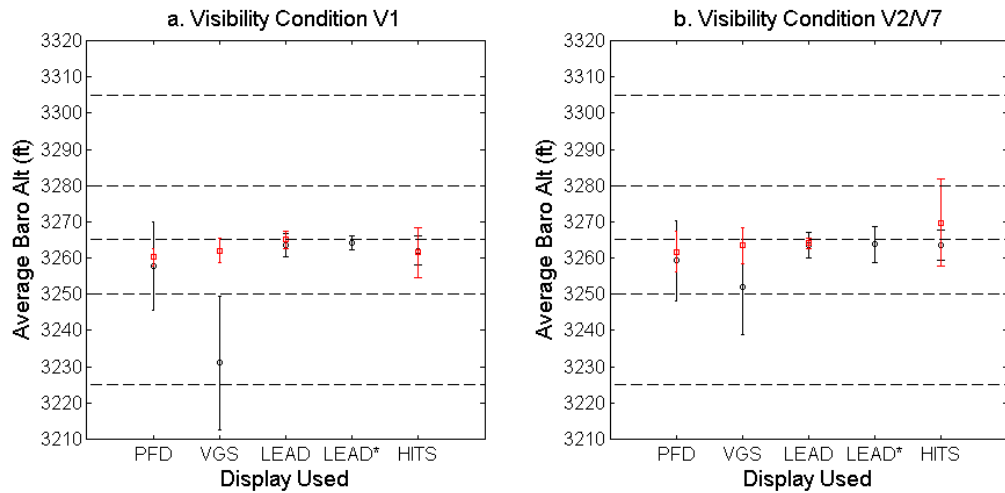
Fig. 6-1. Mean Altitude during approach to localiser during Full Standard Approach MTE

level portion of the MTE achieved by each pilot per display in both good and degraded visual conditions. In general, the LEAD and LEAD* displays resulted in the closest adherence to altitude in terms of deviation from target and variation in altitude over the course of the manoeuvre. The VGS and PFD formats also provided comparable if not more impressive results for pilot P2 but much less so for pilot P1. Conversely, for pilot P1, the HITS display results in altitude adherence comparable with the LEAD and LEAD* displays but less so for pilot P2.
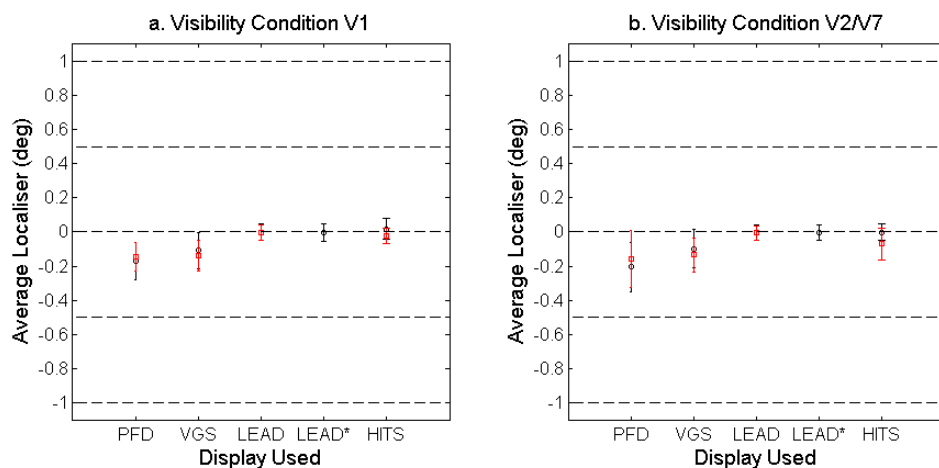
Fig. 6-2. Mean localiser overshoot during glide slope capture and descent phase of Full Standard Approach MTE

255

Fig. 6-2 shows the localiser overshoot achieved during the MTE achieved by each pilot per display in both good and degraded visual conditions. The LEAD, LEAD* and HITS (pilot P1) formats provide an average localiser deviation very close to the target value and with the smallest variation over the MTE. The VGS and PFD formats provide similar levels of degradation in the deviations and variations observed in both visual conditions.

Fig. 6-3 shows the average glide slope achieved during the MTE by each
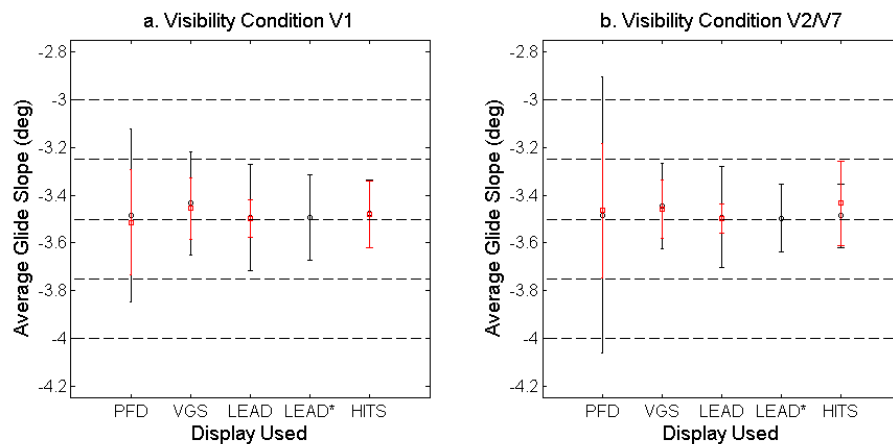
Fig. 6-3. Mean glide slope during descent phase of Full Standard Approach MTE

pilot per display in both good and degraded visual conditions. The VGS, LEAD, LEAD* and HITS all provided comparable results for pilot P1 with pilot P2 generating his best performance with the LEAD display. For both pilots, the PFD display format resulted in glide slope maintenance tasks that were on average as close to target as the four other displays but with the greatest variation over the MTE.

Fig. 6-4 shows the IAS achieved during the localiser capture portion of the MTE achieved by each pilot per display in both good and degraded visual
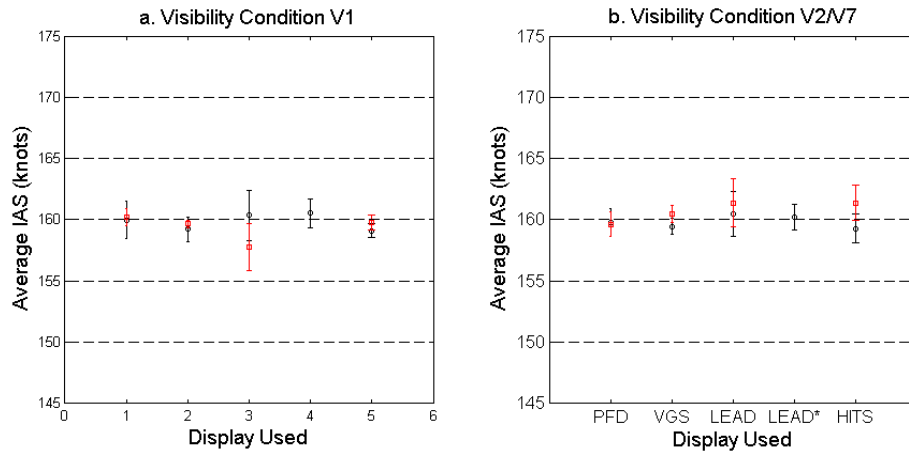
Fig. 6-4. Mean IAS during approach to and capture of localiser during Full Standard Approach MTE

conditions. The LEAD display format resulted in the widest variation in speed for both pilots in visual condition V1 whilst the LEAD* format provided a reduced variation for pilot P1 in visual condition V2/V7. The PFD, VGS and HITS displays provide comparable average IAS values and variations from that mean for both pilots in visual condition V1 with the performance observed in visual condition V2/V7 degrading somewhat for pilot P2.
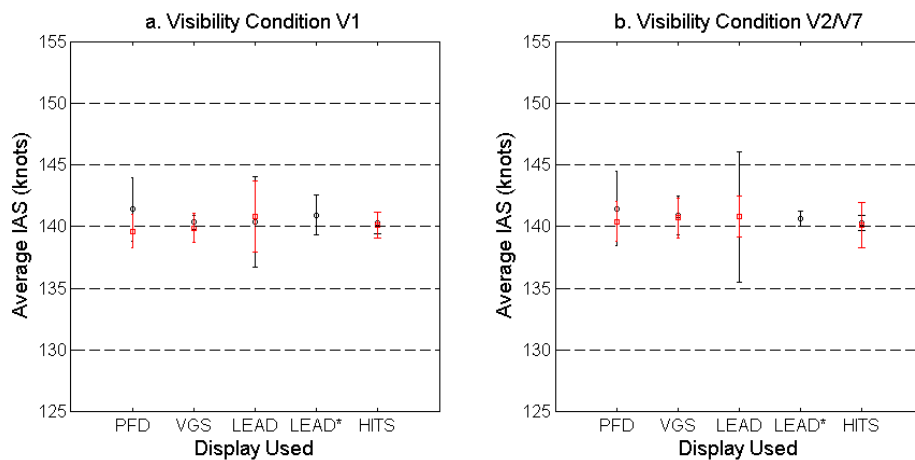
Fig. 6-5. Mean IAS during capture and descent phases of Full Standard Approach MTE

257

Fig. 6-5 shows the mean IAS achieved during the glide slope capture and descent phases of the MTE achieved by each pilot per display in both good and degraded visual conditions. For all displays formats, the average IAS achieved is close to the target of 140 knots. The LEAD display resulted in the widest variation in airspeed for both pilots in visual condition V1 and for pilot P1 in visual condition V2/V7. The pilots performed well using the VGS and HITS formats in V1 but less so in V2/V7, the LEAD* display producing the least variation in IAS in this visual condition.

6.2.2 Curved Approach

Fig. 6-6 shows the mean lateral track deviation achieved during the entire
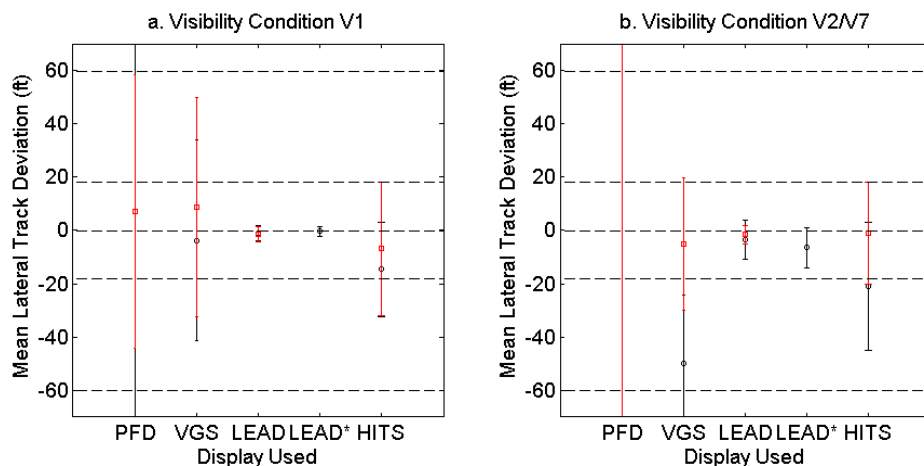
Fig. 6-6. Mean lateral deviation from desired track for the Curved Approach MTE

Curved Approach MTE by each pilot per display in both good and degraded visual conditions. It is clear that the LEAD and LEAD* concepts provide the best performance, both in terms of adherence to desired track and deviation from it. For these cases, the mean and standard deviation fall within the desirable performance criteria boundaries. The HITS concept performs well, maintaining average and variation deviations at least within adequate boundaries (though pilot P2 just maintains desirable). The VGS concept performs less well, however, Section 6.4.3 reports on why this is the case. When the pilot has only reference to the PFD symbology, unsurprisingly, adherence to track is not maintained very well at all.

258

Fig. 6-7 shows the mean vertical track deviation achieved during the entire
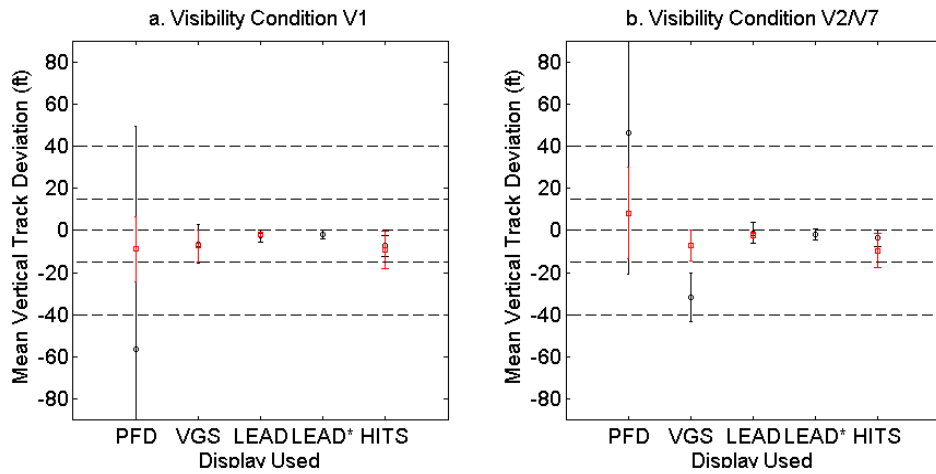
Fig. 6-7. Mean lateral deviation from desired track for the Curved Approach MTE

Curved Approach MTE by each pilot per display in both good and degraded visual conditions. As with the lateral deviation results, both LEAD concepts provide the most accurate and consistent adherence to desired flight path, with HITS, VGS and PFD following on respectively.

Although not strictly an MTE performance criterion, the curved approach was constructed such that the average glide slope during the descent was
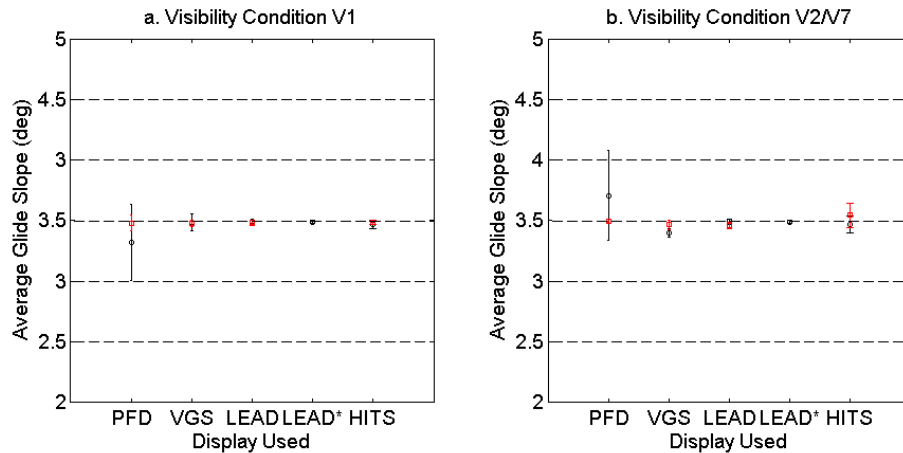
Fig. 6-8. Mean glide slope for Curved Approach MTE

3.5 °. Fig. 6-8 shows the mean aircraft glide slope during the MTE achieved by each pilot per display in both good and degraded visual conditions. These are, of course, a corollary to the results of Fig. 6-7. Both pilots achieved average glide slopes within the desired performance

259

boundaries. The VGS, LEAD and LEAD* displays resulted in the least variation form the respective averages.

Fig. 6-9 shows the mean aircraft IAS during the MTE achieved by each pilot per display in both good and degraded visual conditions. Both pilots
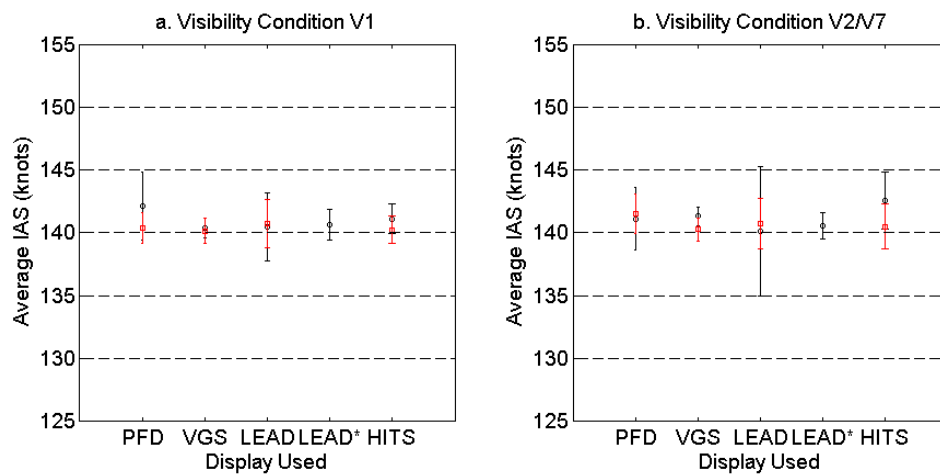
Fig. 6-9. Mean IAS for Curved Approach MTE

achieved average IAS values within desired performance boundaries, VGS and LEAD* producing comparable accuracy and least variation from this mean. The PFD, LEAD and HITS formats show worse performance, but still within desirable boundaries.

6.3 Full Approach MTE Pilot Ratings

6.3.1   Full Standard Approach

Fig. 6-10 shows the average ratings for all of the full approach MTEs given by both pilots in the differing visibility conditions for each display format.

Fig. 6-10. Pilot ratings per display for the Full Standard Approach MTE: (a) Display controllability and (b) Bedford workload

As with previous results, pilot P2 tends to rate the displays more severely than pilot P1. For visual condition V1, pilot P1 rates the VGS as the most controllable and resulting in the least workload followed by the PFD, HITS, LEAD and LEAD* formats. In visual condition V2, the VGS is still rated the best but the LEAD* becomes more comparable with HITS and the PFD is rated as being difficult to control and as having high workload. The same sorts of trend emerge for pilot P2.

Some of the additional pilot comments for the reasoning behind the ratings follow. For the PFD format:

1. In visual condition V1, the approach is primarily a visual task, making reference to the instruments occasionally. As such, it is well within the capabilities of the average line pilot.

2. Lateral 'instability' of the GLTA model makes the task much harder in visual condition V7 as it is not clear whether indicated heading changes are real or a function of the 'snaking' motion that the instability causes.

For the VGS display format:

1. Control of trajectory is very accurate and precise with 'instantaneous' guidance. Very little compensation required.

261

2. Loss of the runway outline in visual conditions V1 is less of an issue than in V7. In V7, the pilot's preference was to keep the outline of the runway on the display (it appears at 500ft AGL and disappears at 100ft AGL).

3. The flare guidance did cause a number of bounced landings and this has driven the ratings up on occasion.

4. Both pilots were occasionally confused by which symbol to follow during the flare. The flare alert cue moves up from the bottom of the display to provide pitch rate information for when the flare commences. The arrival of this cue added an element of uncertainty as to whether to follow it or the guidance cue (pilots were briefed to follow the guidance cue at all times).

For the LEAD and LEAD* display formats:

1. Most difficulty (and hence higher ratings) was with speed control during the approach (particularly with the LEAD format).

2. Due to the difficulties with the speed control, the flare annunciation and speed warnings could activate together and this could be distracting at a critical moment.

3. For the offset start conditions, the lead aircraft symbol occasionally disappeared from the pilot's sight and this was reported as disconcerting (the symbol was still on the screen but was obscured from view by the simulator structure around the display monitors).

4. Control activity generally perceived to be higher throughout the approach when compared to the VGS.

5. Some warning as to when the glide slope manoeuvre was about to commence would be useful.

6. It would be desirable to know how far to go. The pilots felt disconcerted, in visual condition V7, descending towards the

ground for some time without any indication of how close they were to it.

7. The ease or difficulty with which a particular approach could be flown was a function of how quickly the desired track could be re-established from any offset condition.

For the HITS format:

1. In straight sections of the tunnel, workload is very low.

2. The turn portions of the manoeuvre raised 3 issues. The first is that there is an apparent descent required when it is known that this is not the case (this is an optical illusion). The second is that the bank angle indicated is not necessarily the one that is flown. Finally, the number of tunnel frames that can be viewed ahead is fixed at 5. This is fine for straight sections of tunnel but needs to be increased during turning manoeuvres.

3. The tunnel elements lend themselves to stable flight as there is no chasing of localiser or lead aircraft required. The pilot can 'close the loop' on trajectory control less tightly (less gain). This is particularly true in visual condition V1 when the horizon assists with peripheral vision attitude control.

6.3.2   Curved Approach

Fig. 6-11 shows the average ratings for all of the Curved Approach MTEs given by both pilots in the differing visibility conditions for each display format.
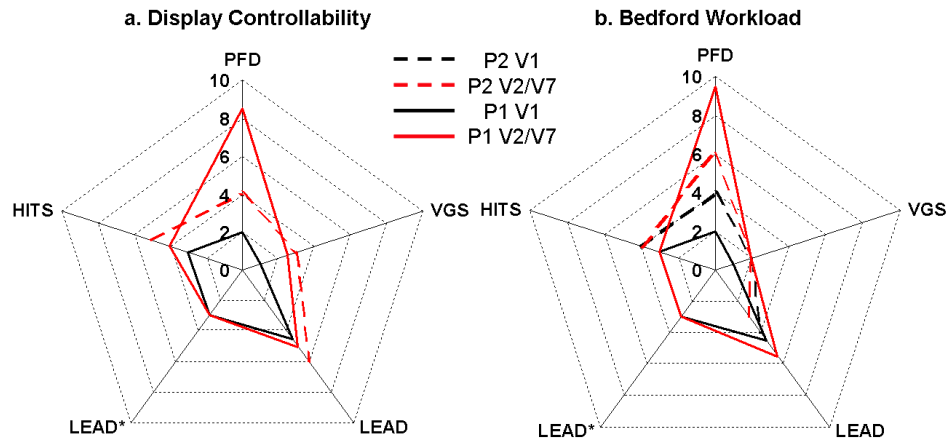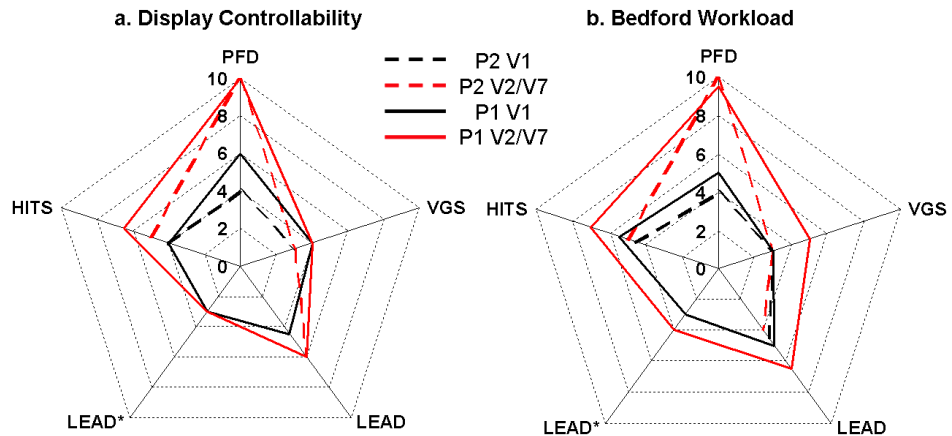

Fig. 6-11. Pilot ratings per display for the Curved Approach MTE: (a) Display

Some of the additional pilot comments for the reasoning behind the ratings follow. For the PFD format:

1. In visual condition V1, if the turn onto localiser is left until the localiser indicator needle starts to move, then a large overshoot occurs and regaining a stable approach is a high workload task. The task of anticipating when to turn on to localiser is therefore left to the pilot's own judgement.

2. In visual condition V7, the guidance is insufficient and almost impossible to complete. With no view of the runway, anticipating when to turn is guesswork. This test point resulted in the most number of 'go-around' decisions.

For the VGS display format:

1. The method used to provide guidance cue information i.e. the 'stepped' ILS input meant that at no point around the turn was the aircraft ever stabilised. It led to control reversals all of the way round the approach profile. Neither pilot enjoyed this form of

264

guidance. It was difficult to predict was the next required control input would be.

2. Once round the turn, the control and workload issues disappeared and the display performed as well as for the Full Standard Approach MTE.

For the LEAD and LEAD* display formats:

1. On the first attempt at this MTE, it was not obvious to the pilots where the power should be to maintain desired speed and so made the task 'hard work'.

2. The guidance, when flown with accurate speed control, did result in a stable approach on 'Final'.

3. In visual condition V7, the absence of peripheral cueing made the task feel harder to complete. After a number of practice runs in this condition, the display format was considered to be 'not that bad'.

4. For the LEAD format, speed control was the determining issue for the ratings. If datum speed was lost, it was very difficult to recover due to the only source of speed information being the looming cue.

5. Overall, despite the aforementioned issues, the display did provide guidance down to the threshold and resulted in 'reasonable' touchdown.

For the HITS display format:

1. It was difficult to establish a stable turn using the tunnel frames as a reference.

2. Knowing the height to initiate the flare proved difficult with reference to only the tunnel elements in visual condition V2. This task was a lot easier to perform in visual condition V1 due to horizon and peripheral cueing.

6.4 Discussion of Results

6.4.1 Trajectory Definition

The use of τ-based trajectories to drive the LEAD and LEAD* display formats allowed standard and a continuous descent curved approach to be flown to touchdown in a GVE and severely DVE. The PFD format, with only localiser and glide slope deviation indicators was found to be inadequate in a DVE. The VGS format implementation of the desired trajectory definition led to some adverse pilot comments during the turn onto the localiser. The HITS format used proved suitable for use in guiding the aircraft around the desired trajectory but with a number of shortcomings.

6.4.2 Display Comparison

With the exception of the PFD in visual condition V7, all the display formats tested guided the pilot down to the runway surface. It is clear, however, that if the trajectory to be flown is a specific earth-fixed path, then the LEAD* and HITS concepts provide the means to do this. The LEAD concept is not suitable in this regard as the speed control cueing is insufficient. If the VGS guidance cue can be made to respond to curved path trajectories rather than traditional straight-line ILS radio beams, then it too would be able to perform the task well.

For a Full Standard Approach, there is little to choose between the HITS and LEAD* formats. For the more dynamic continuous descent Curved Approach, however, the LEAD* concept demonstrates the ability to guide the pilot with much closer adherence to the desired flight path. Of course, HITS concepts are already flying on operational aircraft for en-route phases of flight. However, if and when proposed airspace changes occur, it is proposed that this method will need to be supplemented by something like the LEAD* concept to ensure that the proposed required navigation performance standards are met.

266

It is interesting to note that the pilots complained of power-setting issues when using the LEAD and LEAD* displays. The only display format that provided power setting cueing was the VGS. The same issue must therefore have been present for the PFD and HITS display formats. This is interpreted as meaning that other issues such as trajectory guidance were more apparent for the PFD and HITS testing and that this was not as big an issue for the LEAD formats. Because of this, alternative (and arguably, increasingly minor) issues came to the fore.

6.4.3   Limitations of the Results

The major limitation as far as the Full Standard approach MTE is concerned is that the PFD format results are perhaps more severe than they should be. As reported in Section 2.2.3.1, modern jet transports are equipped with a flight director capability. The PFD format did not possess this function (although the VGS did). As such, the format tested is not quite representative of the tools at the disposal of today's pilot.

The Curved Approach MTE analysis also has a small number of limitations. The first of these is that the VGS results, whilst an accurate reflection of its performance in the simulator, are not representative of how the display would work in the real world for such a trajectory. To reduce the development time required for the trial, the curved approach trajectory was divided up into 5 straight-line ILS trajectories. In this way, the existing VGS guidance algorithms could be used to guide the aircraft around the (approximate) desired path. As each pseudo-ILS beacon was passed, the simulation automatically updated the control signal to the next. As such, the trajectory travelled using the VGS was not commanded to be the accurate circular path and the command that was issued was 'stepped' and not continuous. The adherence to the desired spatial track obtained with the VGS would always, therefore, be reduced. Nevertheless, in reality, the VGS would not have been able to perform the MTE as tested in

the simulation environment. Had this manoeuvre been flown with the display as originally defined i.e. with an ILS straight-in approach function only, would have performed much less adequately and presumably been rated accordingly.

The second issue with the Curved Approach MTE, from the perspective of this thesis, is that, given the inadequacy of the looming speed cue, there is no τ content to it, except for the flare. The curved approach trajectory was constructed as a circular arc, as described in Ref. [3] to try to establish whether any τ-based concepts developed could cope with other trajectories. To that end, the LEAD* concept proved more than adequate. However, the continuous descent approach would also seem to be a prime candidate for an investigation into τ-coupling. To arrive at the threshold, the vertical and lateral motion gaps must be closed simultaneously and that is exactly what would result from an algorithm that couples the two τs of those motion gaps together.

6.4.4 General Comments

The work carried out is intended to provide guidelines for the development of guidance displays. A number of the pilot comments indicated that whilst the LEAD and LEAD* did provide this guidance function, their comfort levels when doing so in a DVE were not as high as for the PFD and VGS displays (even though the trajectory performance was worse). Examples of comments made concerned how far from the airfield the aircraft was i.e. how long was left to go, how high above the ground the aircraft was, particularly towards the end of the glide slope descent etc. Whilst these issues are not specifically pure guidance issues, they do reflect the pilot's need to be aware of their and the aircraft's general situation (their 'situational awareness (SA)'). The PFD and VGS provide this in terms of DME and radar altimeter readings. So, whilst the guidance issue

is of prime concern, thought must also be given to symbology to provide greater SA.

Overall, the results suggest that for 'standard' approaches to an airfield, the symbology of the VGS provide suitable guidance for jet transport aircraft (as might be expected for a production system). However, as airspace usage changes, paradoxically, stringent airways usage will be abandoned but the constraints upon navigational accuracy during terminal manoeuvring will increase. To achieve the greatest levels of spatial accuracy the results suggest that a HITS display is satisfactory but a lead aircraft can improve on this.

6.5 Conclusions

A number of fixed-wing large jet transport aircraft approaches to an airfield have been conducted and analysed. These included a full standard approach to an airfield using localiser and glide slope capture techniques and a more intensive continuous curved descent to the runway. From this testing, the following conclusions are drawn:

i. The τ-based display algorithms provided trajectory guidance that equalled or out-performed the other display formats tested in both a GVE and severely DVE.

ii. Good trajectory adherence does not guarantee that pilots will find the display easier to use. The VGS and HITS formats were generally rated as being more controllable and inducing less workload.

iii. Pilots appear to make use of peripheral vision cueing and when this is lost, e.g. in visual condition V7, they become sufficiently aware of this to comment upon the perceived degradation in their ability to fly a given manoeuvre.

iv.   Consideration of pure guidance cueing alone will not result in a display format with which pilots are automatically comfortable. Consideration needs to be given to symbology to provide additional situational awareness to aircrew.

6.6 Recommendations

Based upon the work recommended in this Chapter, it is recommended that:

i.   The use of τ-coupling should be investigated for use in continuous descent approaches similar to the Curved Approach MTE trajectory.

ii.   The use of symbology to provide peripheral cues should be investigated for use in a DVE. In the UoL Bibby flight simulation facility, this would mean using displays on the out-the-window-left and –right display channels.

iii.   The use of a combined HITS and LEAD* type display should be investigated, particularly for continuous descent (curved) approaches. En-route flight would utilise only the HITS format but as the airfield terminal manoeuvring area was approached, a lead aircraft symbol would be introduced to increase the precision with which a desired trajectory is flown. Issues surrounding how the symbol should be introduced and display de-cluttering would make interesting topics for research.

iv.   The next iteration of the LEAD* display should include limits of travel that restrict the symbology to the pilot's line of sight in the simulator.

C h a p t e r   7

CONCLUSIONS AND FUTURE WORK

7.1 Introduction

The research presented in this thesis casts the pilot's task of guiding the aircraft through its surrounding environment using manual control as one of perceived self- or ego-motion. Ecological psychology and specifically tau(τ)-theory provides an explanation for how an observer can be provided with temporal ego-motion perception information directly from the visual field. The temporal element is important because an observer in motion needs to be able to assess not only its current position but also its position at some time in the future i.e. its prospective position. Only in this way can the motion be guided such that collisions are avoided, prey is captured etc. A central tenet of τ-theory is that motion is guided via the closure of perceived motion gaps. A number of motion gaps available visually to the pilot were proposed for the following in-flight manoeuvres:

- Glide slope capture

- Localiser capture

- Landing flare

The gap closure strategy was hypothesised to be one where the rate of change of τ ($\dot{\tau}$) of the gap was kept constant by the pilot. The research that follows can then be divided into 3 main components:

1. Initial application of τ-theory to a range of flight manoeuvres to test the constant $\dot{\tau}$ hypothesis;

2. Development of a small number of novel display concepts based upon the results of the constant $\dot{\tau}$ analysis of the flight manoeuvres and

3. Testing of the novel displays and comparing the trajectory and pilot rating results with 3 alternative formats.

Each Chapter in this thesis contains its own set of results and detailed conclusions for these strands of the work. This Chapter summarises the major conclusions of the research in terms of the overall objectives of the project (the specific objective is mentioned in the text). It also presents recommendations for future work to be carried out.

7.2 Conclusions of the Research

7.2.1 Initial Tau-domain Analysis

The τ-domain analysis of the flight manoeuvre motion gaps in Chapters 4 and 5 provide supporting evidence for the constant $\dot{\tau}$ gap closure hypothesis. A constant $\dot{\tau}$ motion gap closure strategy is the same as the pilot τ-coupling with a constant velocity or a constant deceleration τ-guide. As such, the results presented within this thesis are consistent with the findings of Ref. [16] where evidence for the use of τ-guides in rotary-wing flight is also presented. As such, it is concluded that the use of τ-guides and of τ-based motion gap closure strategies is of fundamental importance in the understanding of how pilots guide their vehicles through the environment. Any research that includes a pilot should include τ-based strategies within the model of the pilot or in the subsequent analysis.

For the flare in particular, other research, such as that presented in Ref. [87] has concentrated specifically on the flare initiation τ (rather than $\dot{\tau}$ or τ_g) and the impact of visual scene texture has on flare initiation. The conclusions of such research are never particularly definitive. Within the current research, pilots were able to accomplish acceptable landing flares

in a wide variety of good and degraded visual environments with a wide range of flare initiation τ values. It appears that pilots can be extremely adaptable to the visual conditions with which they are presented. As such, the time to contact the runway surface by itself is concluded to be less important as a flare initiation parameter. Of greater importance is the combination of initiation τ and the associated $\dot{\tau}$ or τ_g coupling constant (and hence motion duration, T) selected.

Other research, such as [94] has concentrated on trying to isolate the motion gaps that a pilot uses to control the approach and flare. This was the initial approach adopted during the current research with some success. However, pilot models such as that developed by [91] predict that the weighting that a pilot applies to visually available motion gap may actually change during the course of the approach. During the flare, the pilots used in the current research also demonstrated different techniques in terms of their eye fixations but with the same net result in the τ-domain. It is likely that the visual information that a pilot picks up for guidance purposes comes from a variety of sources and that any attempt to isolate individual sources will either fail or encounter difficulties. If any particular source is removed, the pilot will use another. In this regard, τ-based motion gaps are useful constructs for motion control in that they provide a plausible explanation of how the aircraft motion is being guided without relying on specific sources of information having to be present.

The motion gaps identified in this thesis for which coherent τ-based closure strategies exist constitute a set of informative optical flow-field variables that a pilot requires for flight (Objective 1). In terms of the above argument, however, it is concluded that these only form a sub-set of the variables that are likely to exist for the manoeuvres considered.

7.2.2 Novel Display Development

There are three main conclusions to be drawn from the development of the novel display formats. The first is that whilst a single development pilot has its advantages in terms of a rapid implementation of ideas and corrections, it does not guarantee a successful implementation. Specifically, the optical looming feature of the LEAD and LEAD* formats was not flagged as problematic during the development testing. However, a speed control issue did manifest itself during the comparative testing phase (including for the display development pilot).

The second conclusion to be drawn from the development trial phase of the research is that the research presented in this thesis would truly come into its own with the development of a motion gap τ-sensor. The parameters used to provide τ information to the novel displays were conventional in the sense that they already exist for jet transports e.g. radar altitude, localiser and glide slope etc. The use of τ-based gap closure algorithms puts the use of these parameters onto a valid, pilot-centric, motion perception basis. However, the ultimate use to which the algorithms could be put is if the τ (or its derivative) of a particular motion gap could be fed to the flight control computers directly. One might imagine a downward 'looking' sensor on an aircraft that could supplement or replace the radar altitude function for the flare. The advantage of such a device would be in that it is passive rather than active. This is perhaps more of an advantage for a military vehicle than a civil one but any reduction in electromagnetic emissions into the environment should be seen as an improvement. Such a sensor would complement or be a development of the optic flow based sensors (e.g. Ref. [68]) that already exist.

The final conclusion to be drawn from the development phase of testing is that the mixing of prospective or predictive displays with direct command displays should be avoided or minimised wherever possible. Where such a

mix is essential, every effort should be expended to ensure the blending of the two is seamless to the pilot. This issue did take some time to resolve and even then, was not truly seamless in the LEAD and LEAD* concepts. This 'join' between the two algorithms was noticed by the pilots and led to less favourable ratings as a result.

7.2.3 Novel Display Comparative Results

In general, the novel displays that were developed as part of this research performed as well as or better than the alternative formats tested in terms of the objective parameters measured. This was generally accomplished at the expense of lower overall controllability and a greater workload than the PFD and VGS formats (objective 3). Pilots are trained to use the displays that are currently available and experienced pilots such as those used during the research will be used to interpreting the information that they provide. It is therefore a conclusion of this research that to be able to implement a truly novel display format within the jet transport industry would be a significant undertaking. This would not only be from a certification standpoint but from a crew training and acceptance perspective. Even the tunnel-in-the-sky formats have 'conventional' display symbology super-imposed upon them (see Fig. 2-16) and specific rule-changes had to be made to allow their use. The corollary to this conclusion is that if τ-based motion control is to be accepted or used, it would first have to be implemented using conventional display symbology.

A significant point to note is that truly equivalent performance in good and degraded visual environments was not achieved for any of the display formats tested (Objective 2). In general, the good visual environment objective measurements demonstrated less error from desired performance than their equivalent degraded environment results. It must be concluded from this that none of the display formats used entirely re-create the information available in a good visual environment when that environment

275

is degraded. From a motion perception perspective, the optic flow field of a good visual environment must be providing the pilot with increased guidance information with which to use τ than the display formats alone.

7.2.4 Overall Conclusion

The overall objective of the research project was to develop guidelines for the development of future pilot vision aids (Objective 4). It is intended that the detailed conclusions of Chapters 4, 5 and 6 should serve this purpose in the first instance. The conclusions of the previous Sections in this Chapter should also serve as higher level guidelines. An overall conclusion of the work however, is that the process undertaken resulted in novel display formats that utilised τ-based motion gap closure strategies to successfully guide pilots in flight. In terms of the design of future pilot vision aids, the process adopted appears a valid one and is commended to those that choose to use it:

1. Break the aircraft mission into a number of small, repeatable flight test manoeuvres.
2. For each manoeuvre, identify the motion gaps that the pilot will be closing in flight.
3. Analyse the motion gap closure strategy adopted by a number of pilots in terms of $\dot{\tau}$ and coupling with the τ-guides.
4. Consider commanding the aircraft motion using any τ-based relationships that emerge.

7.3 Future Work

Significant progress has been made during the research project described in this thesis. However, there is still much to understand in terms of how τ-based control strategies are used in the piloting task. Each individual experimental results Chapter has its own set of recommendations for future work. This Section summarises these recommendations under common headings.

7.2.1 Incremental Improvements to Display Formats Developed

This Section records the recommendations made that pertain to direct improvements that could be made to the display concepts developed and to the experimental procedures employed.

7.2.1.1 Display Concept Improvements

    i.   A solution to the flare command concept display's sensitivity to reversal of the acceleration vector be sought and implemented.

    ii.   A means of injecting a small 'pre-flare' input should be sought to assist with recommendation (i).

7.2.1.2 Experimental Procedure Improvements

    iii.   All of the testing reported in this thesis was conducted using simulated nil-wind and nil-turbulence conditions. A selection of the trial test points should be repeated with simulated wind and atmospheric turbulence. Of particular significance would be assessment of approach guidance displays in severe turbulence and the flare guidance displays in strong cross-wind conditions.

    iv.   For the research presented, no modelling of sensor errors were incorporated into the simulation test points. A future iteration should include such errors to ascertain the effect that this would have on all formats tested. Of specific interest would be errors on the localiser and glide slope receivers, the radar altimeter and the sensed accelerations.

    v.   To support recommendation (i) the GLTA aircraft model lateral flight characteristics should be enhanced. Specifically, the 'snaking' behaviour observed during the testing, indicative of poor low lateral stability, should be eliminated. It is believed that this instability is caused by the

277

GLTA wing horseshoe-vortex model not solving correctly in the simulation time step. The first avenue of investigation should therefore be an adjustment of the horseshoe vortex model solution parameters.

vi. The number of MTEs tested using the assorted display concepts should be expanded to the full set originally developed for jet transport operations during the course of the project. Only those relevant to the research are included in Appendix B.

vii. The use of a wider pilot population for final display testing purposes should be utilised.

7.2.2 Additional Research Possibilities

This Section records the recommendations made that pertain to new experiments that should be carried out to further add to the body of knowledge in the field of display design. These recommendations are further broken down into fundamental and applied research.

7.2.2.1 Fundamental Research

i. Limited τ-guide (τ_G) results are reported by the author in Ref.[128] for the flare and it has been stated in this thesis that constant $\dot{\tau}$ strategies give similar results to the τ guide. However, much more use has been made of τ guide analysis in rotary wing work (Refs. [16, 124]) and it may be that using this formulation to command trajectory control has its advantages . Of course, it may not but it would be useful to find out. As such, it is recommended that this exercise be repeated but using τ_G as a basis for the algorithms.

ii. Consideration should be given to using a pseudo- or actual-3D lead aircraft symbol for the LEAD concept to establish whether this improves the speed cueing provided.

278

iii.   Investigation into methods to establish human cognitive efficiency should be made and used as a measure of success of the ability of a display to provide the pilot with the guidance information that is required.

iv.   The use of symbology to provide peripheral cues should be investigated for use in a DVE. In the UoL Bibby flight simulation facility, this would mean using displays on the out-the-window-left and –right display channels.

v.   The ability of a pilot to flare an aircraft, using τ-based strategies, without the restrictions of aircraft structure or with a direct view of the main gear and runway surface should be investigated.

vi.   The next iteration of the LEAD* display should include limits of travel that restrict the symbology to the pilot's line of sight in the simulator.

vii.   A solution to the pursuit guidance problem, with specific reference to τ guidance should be investigated.

viii.   Type 2 flare linear touchdown velocity with $\dot{\tau}_{\Delta h}$ results spurred the design of the control algorithm for the flare-command display. However, it has been noted that the Type 1 flare results in touchdowns with consistently low descent rates. This is interpreted as some pilots being better able to deal with the wide variety of conditions that exist during the flare. The nature of the Type 1 flare should be further investigated to establish whether such adaptability can be incorporated into the flare command control algorithms.

7.2.2.2 Applied Research

ix.   Investigate the possibility of using the normalised elevator angle as a means of cueing the pilot in the flare. The first

issue to resolve here will be how to ascertain the final value of the elevator angle required. One suggested means of calculating this is to compute the elevator angle required for a flare with $\dot{\tau}_{\Delta h}$ =0.5. All other solutions converge on this value at the end of the flare manoeuvre.

x.   Test the τ-coupling hypothesis discussed in Section 4.9.3 for a flare manoeuvre. Given pilot P1's technique in terms of flare gaze position, consideration should be given to using P1 as a subject for such an experiment. The use of τ-coupling should also be investigated for use in continuous descent approaches similar to the Curved Approach MTE trajectory.

xi.   The algorithms used to command the pilot flare symbol and close the localiser and glide slope motion gaps could equally well be used as a basis for automatic control of an aircraft. Consideration should be given to using the τ-based approach to implement, for example, an automatic landing system.

xii.   It has been shown that the approximate relationship $\dot{\tau}_{\Delta h} = -0.032\dot{h}_{td} + 0.53$ exists for two aircraft types (DC-10 and GLTA simulation model). It has further been suggested that normalising this relationship with respect to vertical descent rate would make it applicable to all fixed-wing flares. It would, therefore, be an relevant research topic to establish whether this is true.

xiii.   The use of a combined HITS and LEAD* type display should be investigated, particularly foe continuous descent (curved) approaches. En-route flight would utilise only the HITS format but as the airfield terminal manoeuvring area was approached, a lead aircraft symbol would be introduced

to increase the precision with which a desired trajectory is flown. Issues surrounding how the symbol should be introduced and display de-cluttering would make interesting research questions.

xiv.   A τ-based take-off display be developed using the relationships uncovered during the basic τ analysis for this manoeuvre.

A p p e n d i x   A

GLTA WING MODEL

This Appendix provides details on the modelling and validation of the
FLIGHTLAB GLTA model's wing. However, before this description,
given that this is the first detailed discussion of FLIGHTLAB-related
activities, the Appendix provides a brief introduction to the software and
the philosophy that defines it.

A1 FLIGHTLAB Simulation Tool

"*The objective of FLIGHTLAB is to promote Concurrent Engineering by
providing a simulation tool capable of multidisciplinary support with
selective fidelity modelling options*"[131]. The FLIGHTLAB approach to
achieve this is a modular approach to simulation model building at a level
appropriate to the simulation data available (so, e.g., an engine could be a
simple power/thrust against throttle position look-up table or it could be a
more detailed thermodynamic representation where individual components
such as crankshafts and gearboxes are modelled). The philosophy is that
individual engineering disciplines within a project can attend to the
components of a model for which they are responsible. All of the
individual components can then be brought together under a common
simulation framework. FLIGHTLAB's capabilities are provided in Ref.
[131] and a more readable summary version is Ref. [132].

In addition to the flexibility afforded by FLIGHTLAB, the simulation
engineer can further choose to model a vehicle using a variety of
techniques, primarily:

282

1. Full vehicle model data. FLIGHTLAB can process multi-variable datasets that represent the dynamics of the total simulated vehicle. This method is akin to how an industrial aerospace company might store its model datasets.

2. Multi-body modelling. Using this method, individual airframe and system components are connected to form larger sub-systems of the vehicle. The complete model is then built up from the interconnected subsystems [132].

Due to the nature of the (albeit limited) data available for the B707, the multi-body approach to modelling was adopted for the GLTA.

A2 GLTA FLIGHTLAB Simulation Model

A2.1 Model Structure

The GLTA model is organized into a hierarchical structure as depicted in Fig. A1. Each layer, or '*group*', of the structure is populated by relevant configuration i.e. layout and aerodynamic data.
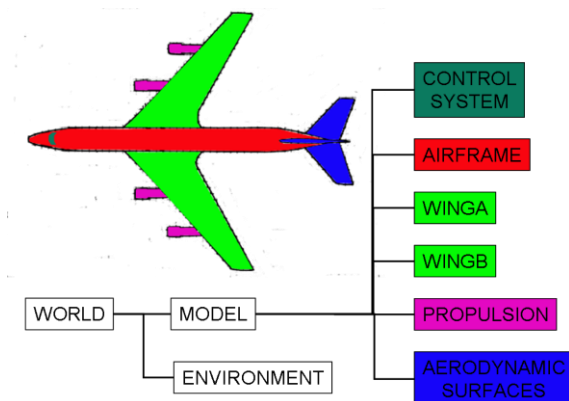
Fig. A1. Schematic Group Structure of GLTA FLIGHTLAB Model

The data used to validate each element of the model structure is discussed in the following Sections.

A2.2 Wing Model

The GLTA wing comprises an aerofoil, trailing edge flaps, inboard and outboard ailerons and spoilers. This configuration was selected for the B707 to provide satisfactory roll control throughout the flight envelope

283

[121]. With flaps up, the outboard ailerons are not required (and their effects are actually reversed at high speed due to aeroelastic twisting of the wing) and are locked out. At low speed, with flaps down, the roll control provided by the inboard ailerons and spoilers is not sufficient and so the outboard ailerons are brought into use. FLIGHTLAB provides a standard aerodynamic component that caters for an aerofoil with a flap (AEROWFLAP) that can be used to model both trailing-edge flaps and ailerons. However, there is no provision for spoiler effects and so a bespoke component had to be created to model the B707 wing for the GLTA. This component and the associated control mechanisms are discussed in Section A2.2.2.

The wing itself is modelled as a rigid lifting line surface (see for example, Ref. [133]). Fig. A2 shows the division of the wing into 'panels' for the aerodynamic force calculations. The wing's physical dimensions were taken from Ref. [110]. The wing model was populated with two-dimensional aerodynamic data which was converted into three-dimensional form through the application of a standard FLIGHTLAB horseshoe vortex model.
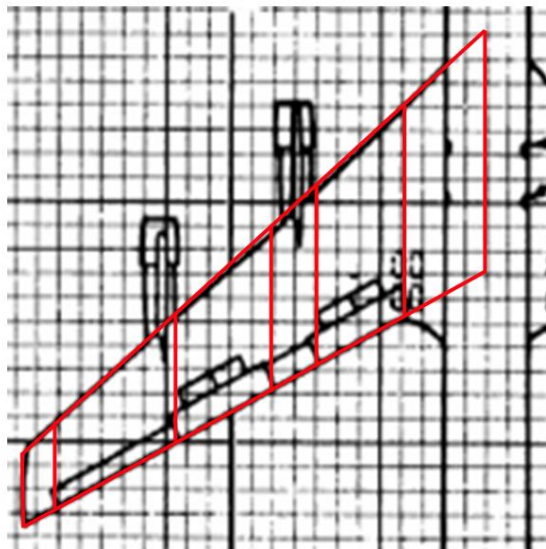
Fig. A2. Aerodynamic panel structure for GLTA wing

The following Sections provide the detailed methods used to generate the data required for the wing model and its control surfaces.

284

A2.2.1 Existing FLIGHTLAB Aerofoil Component

A2.2.1.1 Two-Dimensional Aerofoil Data

The start point for the GLTA wing model is two-dimensional aerofoil data. To generate these data, an example of the B707 wing aerofoil section was obtained from Ref. [134] and lift, drag and pitching moment coefficient data generated using the XFOIL program (Ref. [135]). The data were generated in viscous mode using as high a Reynolds Number as the code would allow, usually in the region of 1×10^6. According to Ref. [134], the B707 wing actually comprises of a number of different sections that are blended together along the span of the wing. In order to ease the burden of construction and the complexity of the model itself, it was decided to use only the inboard section as analysis showed that this provided the most comprehensive dataset of the five analysed by XFOIL. The section used is shown in Fig. A3. Fig. A4 shows the XFOIL-generated two-
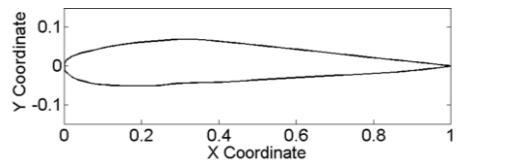
Fig. A3. Aerofoil Section Used for GLTA Wing Model.

dimensional lift, drag and pitching moment coefficient data, for a selection of Mach numbers for the section. Data beyond any identifiable stall were ignored as the validity of these is questionable.
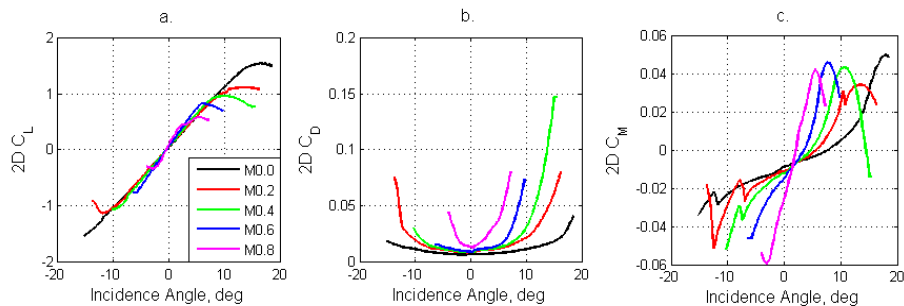
Fig. A4. GLTA 2D Wing Section Aerodynamic Coefficient Data: (a) Lift; (b) Drag and (c) Pitching Moment

It can be seen from Fig. A4 that the data is non-symmetric and increasingly limited over the incidence angle range as Mach No. increases. The lack of symmetry reflects the nature of the shape of the aerofoil. The limited incidence angle range of the data needed to be addressed due to the way that FLIGHTLAB handled data at the extremes of the ranges. Within the confines of the data provided to the model, linear interpolation is used between data points to provide intermediary values of coefficient data. For values of wing incidence outside of those provided, the early version of the GLTA model was configured such that the last value in the data range was retained. This resulted in some unrealistic stalling behaviour (the aircraft didn't stall but 'floated' in a nose-high attitude). Whilst the aircraft model was never intended to be used to explore the extremes of the flight envelope, it was felt that if the aircraft ended up there, its behaviour should indicate to the pilot that corrective action needed to be taken. To that end, additional wing data had to be provided to cover the incidence range ±180º. This was achieved by merging the FLIGHTLAB-supplied NACA0012 aerofoil dataset with the datasets of Fig. A4.

A2.2.1.2 Control Surface Aerofoil Data

Fig. A5 shows the B707 wing plan form from Ref. [110] with its control surfaces highlighted. The standard FLIGHTLAB aerodynamic (AEROWFLAP) component caters for an aerofoil with a flap. It can be used to model both trailing-edge flaps and ailerons. It computes the airloads for a 2-D aerodynamic segment with a trailing flap using lifting line theory [131]. Force and moment increments due to flap
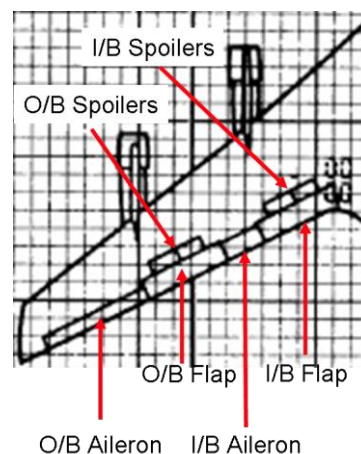
Fig. A5. Layout of the GLTA Wing Control Surfaces

286

deflection, δ_f, are calculated using [133]:

$$\Delta C_{lf} = C_{l\alpha} \tau \eta \delta_f \qquad (A1)$$

$$\Delta C_{df} = C_{df} \left(\frac{c_f}{c_w} \right)^{1.38} \left(\frac{S_f}{S_w} \right) \sin^2 \delta_f \qquad (A2)$$

$$\Delta C_{mf} = \delta C_{ml} \Delta C_{lf} \qquad (A3)$$

$C_{l\alpha}$, the aerofoil lift curve slope is computed from the user-provided tabulated data (Fig. A4(a)). The correction factors η and τ are shown in Fig. A6 (Ref. [133]). Both plain and slotted correction factors were included in the model to account for ailerons and trailing edge flaps respectively.
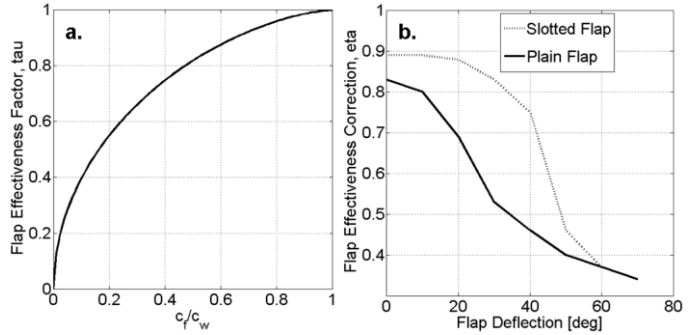
Fig. A6. Aerofoil aerodynamic data correction factors: (a) flap effectiveness and (b) flap effectiveness correction.

In Eq. (A2), C_{df} is a constant factor depending upon the type of flap being used (plain flaps=1.7; slotted flaps=0.9). The chord and area ratios are calculated based upon the wing geometry definition provided to the model.

Fig. A7 shows the values of the coefficient δC_{ml} used in Eq. (A3), taken from [133]. The total lift produced by the 2D aerofoil element is
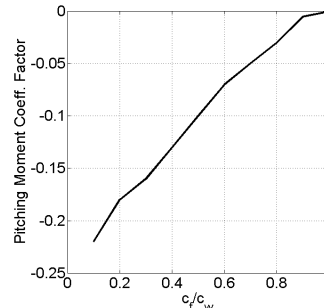
Fig. A7. Pitching Moment Coefficient Factor

then calculated using:

$$C_1 = C_{l\text{basic}} + \Delta C_{lf} \qquad\qquad (A4)$$

Where 'basic' denotes the data of Fig. A4(a). Similar expressions are used to calculate the total drag and pitching moment on the section.

A2.2.2 Modified FLIGHTLAB Aerofoil Component

The AEROWFLAP component lacked the capability to model spoilers. Therefore, a bespoke aerodynamic component had to be created to fully model the B707 wing for the GLTA. The existing AEROWFLAP component was modified to incorporate the incremental lift and drag effects due to the deployment of spoilers in an aerofoil section. No information could be found regarding the commensurate change in pitching moment so this effect is not directly calculated in the new component.

A2.2.2.1 Lift Increment Due to Spoiler Deflection

Refs. [136, 137] provide an empirical method for estimating the change in lift on a wing due to the deflection of a spoiler with flaps undeflected and deflected. The two-dimensional element of these methods has been incorporated into a new FLIGHTLAB aerofoil component (AEROWFLAPSP3).

AEROWFLAPSP3 assumes flap-type spoilers with no porosity as defined in Fig. A8. Two increments (although these will usually be decrements) have been added to the lift of a given aerofoil section, one for flaps undeflected, $\Delta C_{ls\infty}$ and one for flaps deflected, $\Delta C_{lsf\,2D}$.
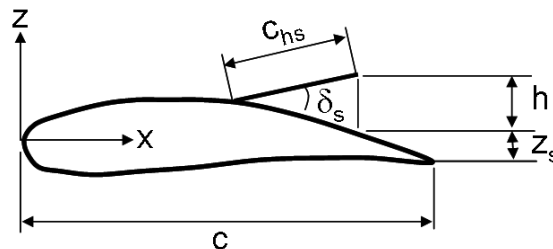
Fig. A8. Spoiler definition for AEROWFLAPSP3

288

The total two-dimensional increment in lift due to spoiler deflection is then given by:

$$\Delta C_{ls} = \Delta C_{ls\infty} + \Delta C_{lsf\,2D}$$ (A5)

These values were tabulated for two wing incidence values and included in the aircraft model. The component reads the appropriate increment, interpolating as necessary, and adds it to the aerofoil section lift coefficient for the onward wing loads calculation.

Table A1 shows the 2D increments for flaps undeflected, $\Delta C_{ls\infty}$. These are read from a figure in Ref. [136] and are functions of H/c and x_s/c where:

$$H = h_{eff} + z_s$$ (A6)

$$h_{eff} = hk$$ (A7)

$$h = c_{hs} \sin \delta_s$$ (A8)

z_s is the ordinate of the wing section at x_s which is given by:

$$x_s = x_h + c_{hs} \cos \delta_s$$ (A9)

Spoiler Deflection Angle, δ_s (deg)	Alpha=0 ^{0}		Alpha=10^0	
	I/B Spoiler	O/B Spoiler	I/B Spoiler	O/B Spoiler
0	0	0	0	0
10	0.15	0.25	0.1	0.25
20	0.35	0.49	0.25	0.45
30	0.49	0.7	0.45	0.7
40	0.63	0.85	0.6	0.8
50	0.73	1	0.7	0.95
60	0.8	1.05	0.8	1.1
70	0.84	1.1	0.85	1.2

Table A1. 2D Spoiler lift decrements,

The 2D component of $\Delta C_{lsf\,2D}$, the additional lift increment due to spoiler deflection with flaps deflected is calculated as follows:

$$\Delta C_{lsf\,2D} = -\left(k_f \frac{h_{te}}{c} \right) \qquad (A10)$$

where k_f is a flap-type dependent factor provided by the method and:

$$h_{te} = c_f \sin \delta_f \qquad (A11)$$

Table A2 shows the calculated values for the GLTA model.

	Alpha = 0			Alpha = 10		
δ_f/deg	k_f	h_{te}/c	$\Delta C_{lsf\,2D}$	k_f	h_{te}/c	$\Delta C_{lsf\,2D}$
0.00	5.00	0.00	0.00	6.00	0.00	0.00
10.00	5.00	0.05	-0.23	6.00	0.05	-0.28
20.00	5.00	0.09	-0.46	6.00	0.09	-0.55
30.00	5.00	0.13	-0.67	6.00	0.13	-0.81
40.00	5.00	0.17	-0.86	6.00	0.17	-1.04
50.00	3.30	0.21	-0.68	2.00	0.21	-0.41
60.00	0.00	0.23	0.00	0.00	0.23	0.00

Table A2. 2D spoiler lift decrements, flaps deflected

The total lift produced by the 2D aerofoil element, including the effect of spoilers can now be calculated using:

$$C_l = C_{lbasic} + \Delta C_{lf} + \Delta C_{ls} \qquad (A12)$$

Due to the two-dimensional nature of the AEROWFLAP3 component, it was necessary to ensure that wing-model panel boundaries coincide with the edges of the spoiler panels.

A2.2.2.2 Drag Increment Due to Spoiler Deflection

Ref. [138] provides an empirical method for calculating a drag increment due to spoiler deflection on a 3D wing. Again, only the 2D components i.e. profile drag have been included in AEROWFLAP3 as follows:

$$\Delta C_{ds} = \Delta C_{d0s} = 1.2 \sin^2 \delta_s \frac{sc_s}{S_w} \qquad (A13)$$

All of the parameters are known to the simulation solution so this calculation was included directly into the new component. The total drag produced by the 2D aerofoil element, including the effect of spoilers can now be calculated using an expression similar to that of Eq. (A12).

A3 Validation of GLTA FLIGHTLAB Simulation Model

A3.1 Wing Lift Curve Slope

For wing validation purposes, global wing lift curve slope data for a rigid B707 aircraft, available from Ref. [121], are plotted against equivalent data for the GLTA model in Fig. A9 (no aeroelastic effects are included in the

FLIGHTLAB simulation model but these data do include the effect of the horseshoe vortex model). It can be seen that there is reasonably good agreement between simulation model and the real (rigid) aircraft. The GLTA lift curve slope remains within 5% of the 'target value' and is a higher value up until around Mach 0.8 when the two

Fig. A9. Comparison of GLTA and B707 (rigid aircraft) wing lift curve slope variation with Mach No.

values converge. Both sets of data, however, show the same trend. A larger value of wing lift curve slope means that for a given change of incidence, the GLTA will develop slightly more lift than the real rigid aircraft. However, a <5% error was considered acceptable for an empirically developed flight model such as the GLTA so no further corrective action was taken.

A3.2 Fuselage Aerodynamic Data

Unfortunately, no fuselage-only aerodynamic data were available to validate the fuselage aerodynamic modelling. However, total clean aircraft drag polars were available for Boeing aircraft from Ref. [139]. Fig. A10 shows the GLTA FLIGHTLAB model drag polar data against the publicly available data. It can be seen that the model data compares well with the real aircraft except at the lowest values of lift coefficient, C_L. Given that the aircraft model would not be operated at these low C_L values, it was concluded

Fig. A10. Drag polar comparison: GLTA and other Boeing aircraft, Mach 0.7

that the GLTA model was representative of a large jet transport aircraft.

A3.3 Empennage Data

Ref. [121] provides two longitudinal stability derivatives that were used to validate the GLTA empennage data. These are:

1. Stabiliser effectiveness ($C_{m_{i_t}}$), defined as the rate of change of pitching moment coefficient with the tail angle-of-attack.

2. Elevator effectiveness (C_{m_δ}), defined as the rate of change of the pitching moment coefficient with elevator deflection.

Fig. A11 shows the B720 values for these derivatives from Ref. [121] Compared with the values calculated for the GLTA. It can be seen in Fig.
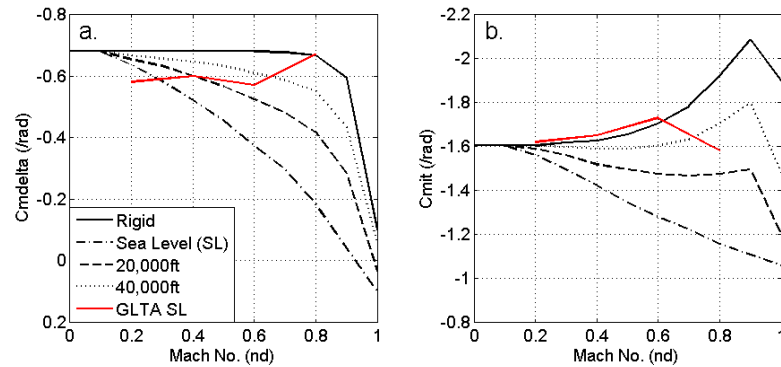
Fig. A11. Empennage longitudinal data comparison for GLTA and B720: (a) C_{mit} and (b) $C_{m\delta}$

A11(a) that the GLTA model elevator effectiveness trend is a reasonable approximation of that of the real aircraft. The GLTA stabiliser appears less effective in Fig. A11(b) than on the actual B720 above M0.6. The general trend below this Mach number is well captured however. Pilot comments indicated that the elevator power was consistent with their experience. No further modifications were made to the empennage on that basis.

The major pilot criticism of the empennage was that the stabiliser trim function was actuated too slowly. This made the aircraft difficult to trim longitudinally. The actuation rate was therefore doubled, giving a more satisfactory trim response.

A3.4 Validation of Engine Response Characteristics

The engines for the GLTA FLIGHTLAB were modelled as simple turbojets. There were no Boeing 707 engine response data available so Boeing 747 engine response data, from Ref. [140], were used to gain confidence in the GLTA engine responses. Fig. A12 shows a comparison of throttle input (normalised against maximum throttle value) and resulting engine thrust (normalised against maximum thrust produced) for a full throttle slam open and then closed.
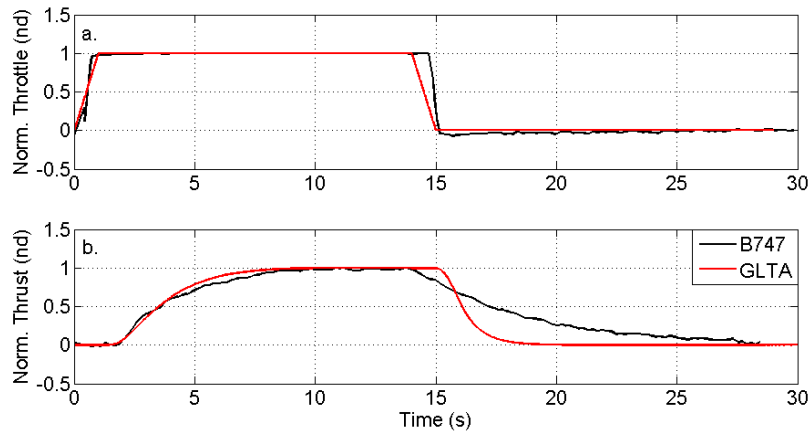
Fig. A12. Engine model response validation: comparison with Boeing 747 throttle slams

It can be seen from this figure that good agreement is achieved for the thrust increase but that the thrust reduction is less well modelled. It was considered for the purposes of the research that this was acceptable. The only adverse pilot comment regarding throttle operation was that the aircraft slowed down too quickly compared to real Boeing aircraft. This is, at least in part, related to the increased rate of reduction of thrust in the aircraft model noted in Fig. A12(b).

Appendix B

MISSION TASK ELEMENT DESCRIPTIONS

To be able to break jet transport operations into manageable 'chunks' that can be analysed in a laboratory, a method common in the rotary-wing community, but less so in the fixed-wing community (although not unheard of) was adopted. Aircraft operations were broken down into individual missions. Each mission was broken down into its respective phases. Finally, each phase was further broken down into individual task elements that can be conducted under controlled conditions in a laboratory. This Appendix provides the detailed results of such an analysis for jet transport operations.

B1 Fixed-Wing Aircraft Missions

A number of fixed-wing aircraft missions were identified as follows:

- Transport;

- Search and Rescue (SAR);

- Training;

- Emergency Medical Services;

- Fire-Fighting;

- Eye-in-the-sky;

- Patrol and

- Aerial Work.

The most pertinent mission to the research described within this thesis is the 'Transport' mission. In this context, the 'Transport' mission comprises the movement of passengers and/or freight from one location to another or to and from the same location. This would include passenger flights, freight activities, air taxi operations, VIP and corporate communication flights, pleasure flights, private flights and humanitarian aid/famine relief operations.

B2 Jet Transport Mission Phases

Having identified the mission(s) in question, it was then necessary to break them down into specific phases of flight. For a transport mission, these are:

- Taxi;
- Take-off;
- Initial Climb;
- Climb;
- Cruise;
- Loiter;
- Descent;
- Approach and finally
- Land.

It is clear from the safety statistics review of Section 2.1 however, that the key phases to concentrate on Approach and Land.

B2.1 Approach

Before landing the aircraft, the pilot must set up an approach to the runway to be used for landing. This means lining the aircraft up with the desired runway and configuring the aircraft for a landing (undercarriage and flaps down as required). The pilot must take account a number of elements to

ensure that the aircraft intercepts the runway. These are worthy of further discussion, as follows.

a. Wind direction. The ideal scenario is to fly an approach into wind i.e. where the prevailing wind is blowing down the runway towards the aircraft. Where this is not the case, any aircraft flying the runway heading will be blown away from the runway centreline (unless, of course, the wind is blowing from directly behind the aircraft). The pilot must take account of this drift by altering the aircraft heading. The goal of this exercise is to ensure that the ground track of the aircraft ends up at the runway threshold.

b. Wind speed. The aerofoil sections of a fixed wing aircraft are subject to two components of air velocity. The first is due to the movement of the aircraft through the air. In still air, this velocity would then be equal to the aircraft speed across the ground. The second component is due to any movement of the air itself i.e. wind speed. The indicated airspeed that is displayed to the pilot in the cockpit, is the sum of these two velocity components. On an approach, the aircraft is being flown slowly, at a particular approach speed, close to the ground. If the wind speed is high, then this will form a relatively large proportion of the indicated approach speed. Problems can occur when the wind speed and/or direction change suddenly (a phenomenon known as wind-shear). If this change is a sudden reduction, the indicated airspeed will also reduce suddenly. The concern here is that the speed reduction is sufficient to take the aircraft below its stall speed. Close to the ground, a stalled aircraft can be impossible to recover. The pilot must therefore be aware of any change in indicated speed

that cannot be accounted for i.e. the aircraft is at a constant power or thrust setting and is being flown at a constant pitch angle.

c. Descent Rate. The pilot of a fixed wing aircraft must ensure that the aircraft does not touch down too early (the aircraft has missed the runway) or too late (insufficient runway available to brake the aircraft to a halt). The pilot must therefore modulate the descent rate to ensure that the aircraft does not over- or under-shoot the runway. Further care must be taken as a too-high descent rate on touchdown could cause a failure of the landing gear.

d. Aircraft speed. As the aircraft approaches a runway, flaps/slats are deployed. These provide a means of slowing the aircraft down (due to extra drag) whilst providing additional lift for a given airspeed (change in aerofoil camber). However, these devices cannot be deployed at any speed that the pilot might choose. Flap schedules are produced for each aircraft type that provides pilots with the speeds below which it is safe to deploy a specific stage (i.e. 5, 10, 15 etc degrees) of flap. These ensure that the flaps are not deployed at speeds above which the forces acting on them will cause them to fail. The schedule also tries to provide a minimum pitch change in the aircraft (a common consequence of flap deflection is a pitch attitude change) due to flap deflection. The pilot must therefore monitor aircraft speed and ensure that flaps are deployed at appropriate speeds. The pilot must also, of course, modulate the aircraft power/thrust to ensure that the aircraft speed does not decay below the stall speed.

Whilst approaching the airfield, the pilot must be alert for conflicting air traffic (there will often be traffic ahead and behind of the aircraft on the same approach) and any ground-based obstacles and terrain.

B2.2 Land

Following a successful approach, the pilot will attempt to land the aircraft. This involves pitching the aircraft up to reduce its descent rate (the flare) followed by one of two desirable possibilities:

a. Hold the aircraft flying parallel to the ground to allow its speed to decay causing it to sink onto the ground (can be used if there is an excess of runway available to land in).

b. Positively place the aircraft on the ground at the reduced sink rate (used if there is the possibility that there is insufficient runway available if the aircraft where to 'float' too far down it).

There is, of course, always the possibility that the pilot cannot land the aircraft following an approach. This might be because a visual approach has been misjudged and the aircraft is too high with little possibility of descending in time to land, because the runway is not visible in poor weather or because wind shear has been detected. In these instances, the pilot would initiate a go-around. In this case, the aircraft is pitched up into a climb attitude and the aircraft power set to an appropriate climb setting. For instrument approaches, an airfield-specific missed approach procedure is flown. In visual conditions, the manoeuvre is flown visually.

B3 Jet Transport MTEs

Having defined the mission phases, the final stage of the process is to divide these up into specific mission task elements. Ref. [141] provides a

full list of these for a fixed-wing aircraft. For the priority mission phases
given in Chapter 3 for a jet transport aircraft, the key MTEs were defined
as per Table B1.

Mission	Phase	Sub-Phase	MTE
Transport	Approach	Visual Precision	Localiser capture Glide slope capture Full Standard Curved
Transport	Land	-	Flare

Table B1. Jet Transport MTEs for Key Mission Phases

A detailed description of the MTEs used during the research is given in the
following Sections.

B3.1 Localiser and Glide Slope Capture

Mission	Transport	Phase	Approach
MTE	ILS Localiser and Glide Slope Capture		
MTE Start Condition	Aircraft positioned in trimmed flight at a suitable location to initiate an approach to the airfield.		
MTE End Condition	ILS localiser and glide slope indicators stable.		
Context			
To allow aircraft operations in weather conditions that would otherwise prevent them, major airports have runways equipped with an ILS. The ILS provides guidance information to allow the pilot to fly a prescribed glide slope and ground track even if the runway/airfield is obscured. The ILS system consists of two radio beams: a. a beam angled outward - the localiser. This helps the pilot align the aircraft with the runway and b. a beam angled upward - the glide slope. This provides an obstruction-free path towards the runway). Before such an approach can be attempted, the pilot must align the aircraft flight path with the localiser and commence the descent when the glide slope beam commands it.			
Piloting Requirements			
Align the aircraft flight path with the runway heading. Deploy flaps at appropriate speeds during the aircraft deceleration. Initiate a descent must then be initiated at the appropriate moment to maintain a 3-degree glide slope to the runway threshold. This requires that a specific approach speed and descent rate be maintained.			
Manoeuvre Description			

The simulated airfield will have an approach plate generated for it. This plate will provide appropriate navigation information to allow the pilot to capture the airfield ILS (the 'ILS' in this case, may be a sky-guided simulated one of course). The pilot must navigate to the airfield as per the approach plate (observing headings relative to navigation aids and altitudes at distances from the airfield etc) and align the aircraft with the ILS localiser. When the ILS commands a descent be initiated, the pilot must set up a suitable descent rate to track the ILS glide slope.

Objectives

Intercept a nominal runway localiser (i.e. a ground track lined up with runway heading and centreline).

Maintain nominal localiser ground track to runway.

Intercept a nominal runway glide slope.

Commence and maintain a descent at a nominal 3 degrees to the runway.

Performance Standards

Desirable	Adequate
IAS (Localiser) : 160 +/- 5 knots	160 +/- 10 knots
IAS (Glide slope) : 140 +/- 5 knots	140 +/- 10 knots
Altitude (Level Flight): Target +/- 15ft	Target +/- 40ft
Glide slope = ILS glide slope +/- 0.5 deg.	Glide slope = ILS glide slope +/- 1.0 deg.
Localiser = ILS localiser +/- 0.5 deg.	Localiser = ILS localiser +/- 1.0 deg.
Track deviation = Target +/- 60ft	Target +/- 120ft

a. Localiser Capture
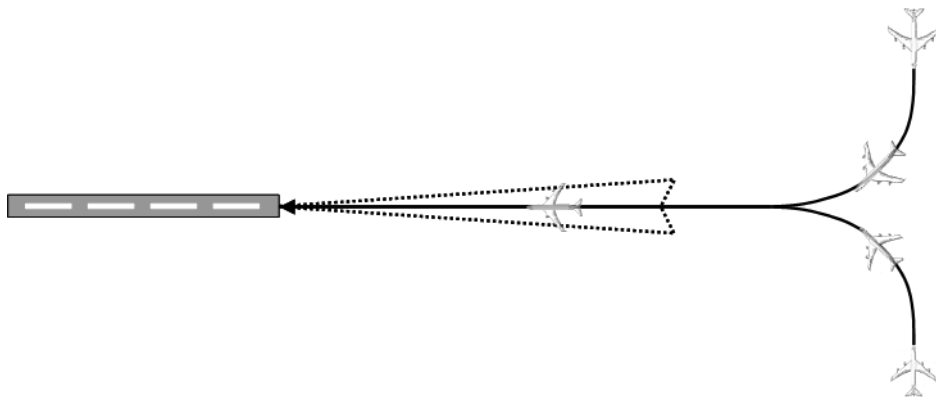
b. Glide slope Capture

B3.2 Full Standard Visual Approach

Mission	All	Phase	Approach
MTE	Full Standard Visual Approach		
MTE Start Condition	Aircraft positioned at a suitable location in trimmed flight to initiate a visual approach to the airfield.		
MTE End Condition	Aircraft above threshold of runway in use.		
Context			
When an airfield does not have any ground-based navigational equipment (or when the equipment that it has available is unserviceable), then a visual approach must be made to the runway. The pilot can be assisted in this type of approach by the use of suitable runway lighting e.g. PAPI, VASI etc.			
Piloting Requirements			
Intended runway and any obstacles in sight. Correct any deviation from the intended glide slope/intended touchdown point. Arrive at runway threshold at indicated altitude of 50ft with approach power and flaps set, gear down.			
Manoeuvre Description			
The aircraft will be placed within sight of the airfield. It must then be lined up with the runway, and a descent initiated and maintained to the runway threshold.			
Objectives			
Demonstrate that a 'visual approach' and landing can be made to a runway in visual conditions that would otherwise exclude this possibility or would require an instrument approach to be flown.			
Performance Standards			

Desirable	Adequate
IAS = target IAS +/- 5 knots.	IAS = target IAS +/-10 knots.
Glide slope = target glide slope +/- 1 deg.	Glide slope = target glide slope +/- 2 deg.
Localiser = r/w c/l +/- 1 deg.	Track = target track +/- 2 deg.

B3.3 Full Standard Precision Approach

Mission	Transport	Phase	Approach
MTE	Full Standard Precision Approach		
MTE Start Condition	ILS localiser and glide slope captured, wings level, descent rate steady		
MTE End Condition	Aircraft above threshold of runway in use.		

Context

To allow aircraft operations in weather conditions that would otherwise prevent them, major airports have runways equipped with an ILS. The ILS provides guidance information to allow the pilot to fly a prescribed glide slope and ground track even if the runway/airfield is obscured. The ILS system consists of two radio beams:
 	
    a. a beam angled outward - the localiser. This helps the pilot align the aircraft with the runway and
 	
    b. a beam angled upward - the glide slope. This provides an obstruction-free path towards the runway).
 	
A precision approach is one where both lateral and vertical descent information are presented to the pilot from a system such as an ILS (though more recently, GPS has been used to provide vertical height information).

Piloting Requirements
Maintain a rate of descent to track the glide slope down to the runway. Ensure that the aircraft is aligned with the nominal runway localiser. Arrive at runway threshold at indicated altitude of 50ft with approach power and flaps set, gear down.

Manoeuvre Description
The aircraft will be aligned with the runway localiser and glide slope at a specified altitude. These will be followed down to the airfield threshold.

Objectives
Maintain nominal localiser ground track to runway. Maintain a descent at a nominal 3 degrees to the runway threshold.

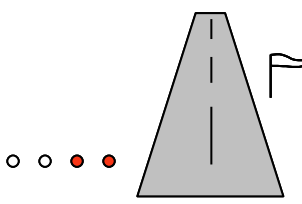| Performance Standards	
Desirable	**Adequate**
IAS (Localiser) : 160 +/- 5 knots	160 +/- 10 knots
IAS (Glide slope) : 140 +/- 5 knots	140 +/- 10 knots
Altitude (Level Flight): Target +/- 15ft	Target +/- 40ft
Glide slope = ILS glide slope +/- 0.5 deg.	ILS glide slope +/- 1.0 deg.
Localiser = ILS localiser +/- 0.5 deg.	ILS localiser +/- 1.0 deg.
Track deviation = Target +/- 60ft	Target +/- 120ft

ILS Glideslope

ILS Localiser

B3.4 Curved Approach

Mission	Transport	Phase	Approach
MTE	Curved Approach		
MTE Start Condition	Stable level approach condition (appropriate flaps and power setting, gear down, ground track perpendicular to the runway centre-line).		
MTE End Condition	Aircraft above threshold of runway in use.		

Context
Airspace capacity is continuously increasing and many international airports are close to or at traffic saturation during peak periods. At the same time, pressure is growing on the aviation industry to reduce its environmental impact. To start to resolve these issues, new methods are being sought to maximise the number of aircraft arriving at an airport whilst reducing environmental nuisances such as noise. Continuous descent approaches (CDA) are one proposed solution. A CDA reduces or eliminates level flight segments with flaps and gear deployed (and hence high thrust engine settings) and allows the aircraft to approach the airfield at higher IAS. A Curved Approach is an example of a CDA and contains constant radius turning segments.

Piloting Requirements
The pilot is required to initiate a descent whilst simultaneously performing a turn onto the runway localiser. Descent rate should be modulated to arrive at the runway threshold at 50ft indicated.

Manoeuvre Description
The aircraft will be in trimmed straight and level flight at 140kts on a heading of 270 with DME indicating 4.6nm. When DME indicates 4.1nm, the pilot will initiate a descent and turn onto 360. The descent rate should be such that the nominal vertical glide slope of 3.5 deg is maintained. The turn rate should be such that the localiser is captured at 2.1nm DME. The glide slope and localiser are then to be tracked as usual to the runway threshold. The entire manoeuvre is to be carried out at 140 knots.

Objectives
Demonstrate that a continuous descent approach can be performed to the runway threshold
Maintain trajectory within the navigation performance boundaries set.
To arrive at the runway threshold centre-line at 50ft

Performance Standards	
Desirable	**Adequate**
IAS: 140 +/- 5 knots	140 +/- 10 knots
Lateral position: Target +/- 18ft	Target +/- 60ft
Vertical position: Target +/- 15ft	Target +/- 40ft

B3.5 Flare

Mission	Transport	Phase	Approach
MTE	Flare		
MTE Start Condition	Stable approach condition (appropriate flaps and power setting, gear down, ground track along runway centre-line) at 3nm from threshold.		
MTE End Condition	Main gear touch down on runway surface		
Context			
A modern jet transport aircraft approach to a runway will be carried out with a typical glide slope value of 3 degrees. At current approach speeds, the aircraft flew into the runway surface at this angle, the vertical velocity at runway contact would be 10-15ft/s. This would be an uncomfortable experience for those on board and unacceptably high (on a regular basis) for the undercarriage. The rate of descent must therefore be reduced to a more acceptable value and this is achieved by 'flaring' the aircraft.			
Piloting Requirements			
Ascertain suitable flare commencement height			
Reduce vertical rate of descent by pitching aircraft nose up			
Main gear contacts runway surface with wings level and aircraft heading aligned with that of the runway			
Manoeuvre Description			

The landing process can most generally be divided into three distinct phases: final approach; flare and touchdown control [142]. .An ideal approach will result in the aircraft arriving above the runway threshold centre-line at 50ft. At a suitable height above the runway surface (typically around 30ft indicated) the pilot must pitch the aircraft nose up to reduce the rate of descent to the runway surface. This is the flare manoeuvre. For modern jet transports, the aircraft should then be flown positively onto the runway i.e. the target surface contact vertical velocity > 0. This requirement is specified to avoid excessive 'float' down the runway. If a cross-wind exists then one wing may be 'low' and/or the aircraft heading will not be aligned with that of the runway. The pilot must bring the wings level and/or align the aircraft and runway heading ('kick off the drift') to avoid striking an engine pod on the runway and causing excessive lateral loads in the main gear struts. There will be occasions when, for whatever reason, the pilot will not make the appropriate control input for the flare. In this case, in particular when the flare initiation is carried out at too great an altitude, there will be a period of control inputs and adjustment to try to ensure a suitable touchdown velocity. This period might then be termed touchdown control.

Objectives

To arrive at the runway threshold centre-line at 50ft

To maintain runway centre-line below 50ft

To contact runway surface with aircraft main gear at an acceptable vertical rate of descent

Performance Standards

Desirable	Adequate
Aircraft Lateral Position: +/- 1/8 r/w width	+/- ¼ r/w width (flare initiation)
Aircraft Lateral Position: +/- ¼ r/w width	+/- ½ r/w width (touchdown)
IAS at threshold: 140 +/- 2.5 knots	140 +/- 5 knots
Altitude AGL at threshold: 50 +/-5ft	50 +/-10ft
Touchdown vertical velocity: < 3.0 ft/s	3.0 – 5.0 ft/s
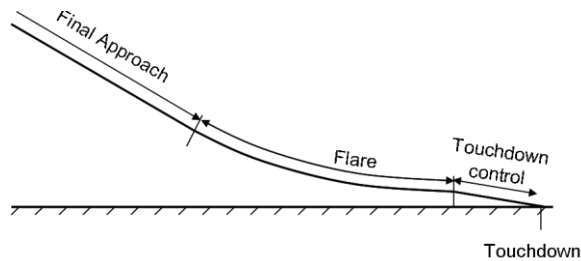
A p p e n d i x   C

FLY DATABASE MILITARY AIRPORT APPROACH PLATES

C1 Military Airfield Layout

Fig. C1 shows the plan-view layout of the outside world 3D database model airfield (termed the 'military airfield') used for all research work described in this thesis. All approaches were carried out to runway 36L.

Elev	Var	A/D	LAT				
232	**0°W**	REF PT	*LONG*		*MILITARY A/F* **AERODROME**		

NAME **Tower**	**Approach**	**ATIS**	**D1**	**ID**
Frequency	*Frequency*	*Frequency*	**6 May 04**	

R/W	VASIS	APPROACH	THR	RUNWAY	L.DIST	SLOPE
12 (120°T)		*CD5B-1*	*Gr*	*HRL EL*	*3500m*	*0.07D*
30 (300°T)						
18L (180°T)						
18R (180°T)						
36L (360°T)	P3.5°					
36R (360°T)						

OTHER LIGHTING:

NOTES
Non-standard aerodrome markings
CIRCUITS
All circuits must be to the East due to terrain. Avoid circuits to r/ways 18L/R.

1. Terrain North through West to South within 5nm and from North through East to South within 15nm.
2. High ground on approach to and climb out from r/ways 36L/R.

REV:

Fig. C1. Aerodrome Chart for the 'FLY' 3D outside world database military airfield

C2 Military Airfield Precision Approach Plate

Fig. C2 shows the side-view layout of the precision approach to the outside world 3D database model airfield (termed the 'military airfield') used for all research work described in this thesis.
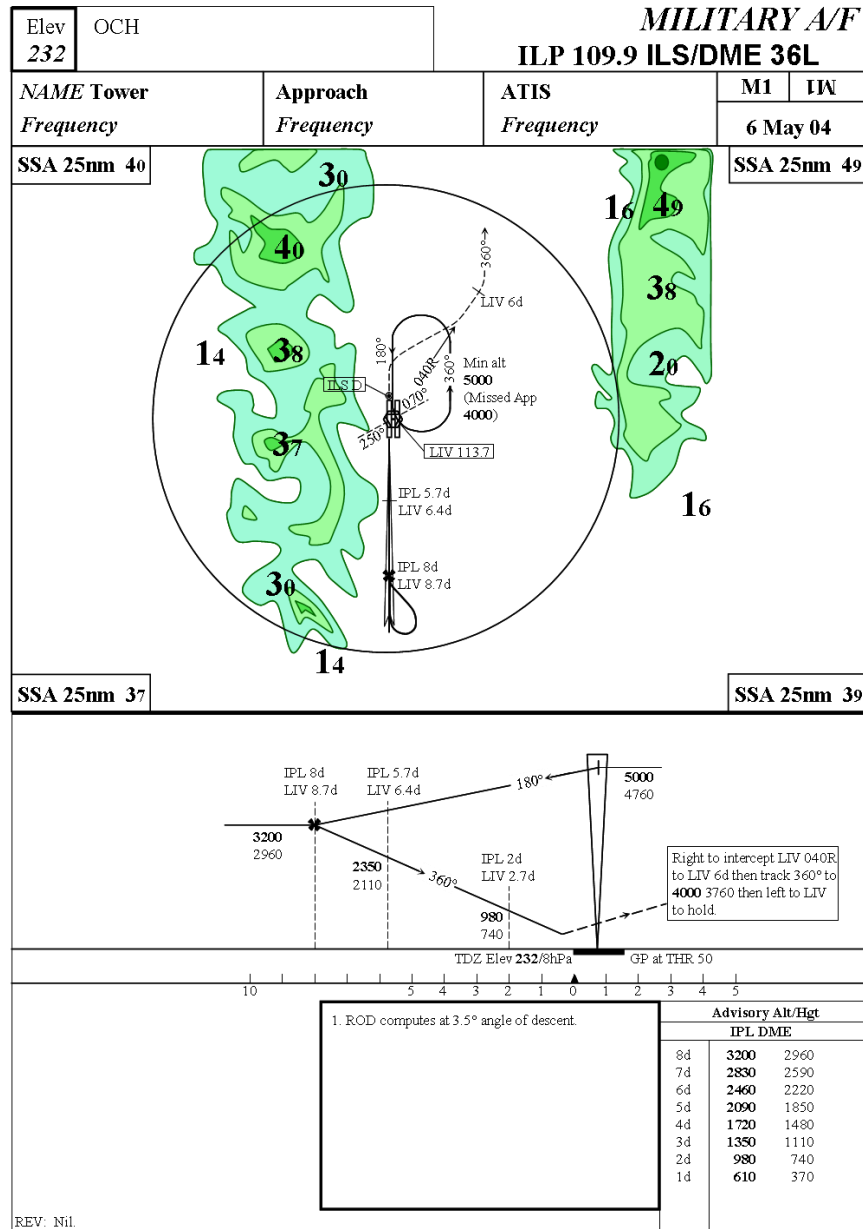
Fig. C2. Precision approach definition for 'FLY' 3D outside world database military

A p p e n d i x   D

PILOT RATING SCALES AND QUESTIONNAIRE

This Appendix defines the pilot opinion rating scales used to try to objectively assess each of the display concepts used by the research project.

D1. Display Controllability Rating Scale

Fig. D1 shows the Display Controllability Rating Scale of Ref. [116] (this is actually termed Display Flyability Rating in the reference) as used in the research. project.
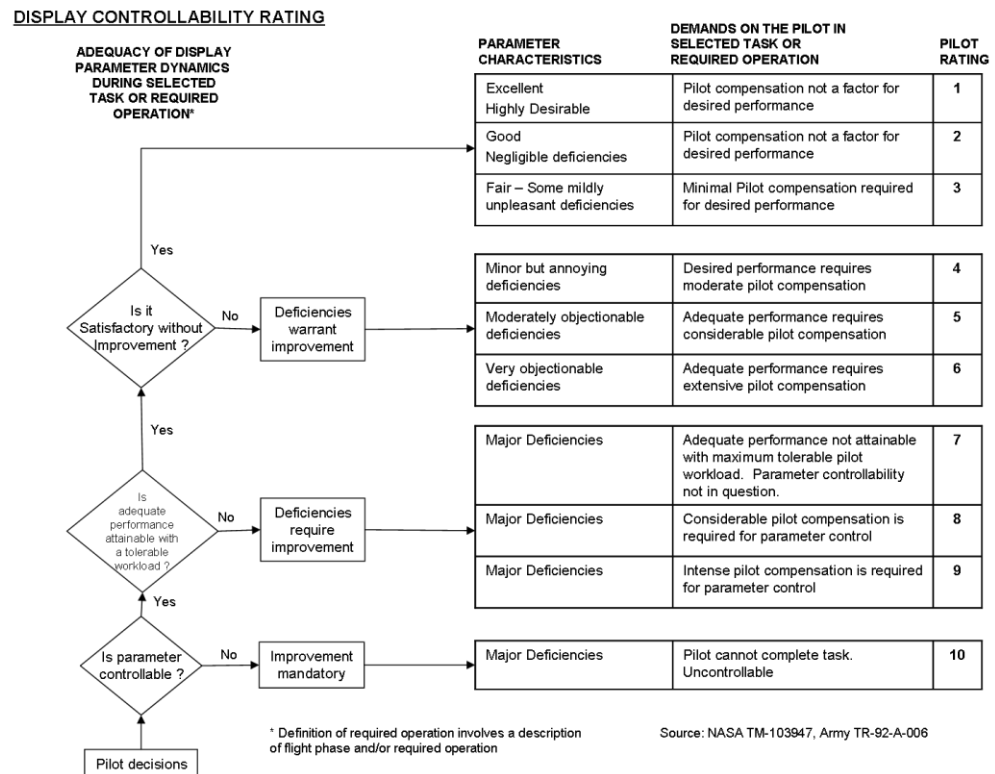
Fig. D1. Display Flyability Rating Scale

D2. Bedford Workload Scale

Fig. D2 shows the Bedford Workload Rating Scale of Ref. [117] as used in the research project.

BEDFORD WORKLOAD SCALE

WORKLOAD DESCRIPTION	PILOT RATING
Workload insignificant.	1
Workload low.	2
Enough spare capacity for all desirable additional tasks.	3
Insufficient spare capacity for easy attention to additional tasks.	4
Reduced spare capacity. Additional tasks cannot be given the desired amount of attention.	5
Little spare capacity. Level of effort allows little attention to additional tasks.	6
Very little spare capacity, but maintenance of effort in the primary task is not in question.	7
Very high workload with almost no spare capacity. Difficulty in maintaining level of effort.	8
Extremely high workload. No spare capacity. Serious doubts as to ability to maintain level of effort.	9
Task abandoned. Pilot unable to apply sufficient effort.	10

Fig. D2. Bedford Workload Scale

A p p e n d i x E

PILOT CURRICULUM VITAE

The research described in this thesis utilised the services of three professional fixed-wing jet transport aircraft pilots. As is the custom, the pilots are not identified by name but are designated P1, P2 and P3. The flying experience of pilot P1, pilot P2 and pilot P3 are given below.

E1. Pilot P1

Pilot P1 joined the Royal Navy in 1979 and served on 845 and 846 Squadrons as a Commando Helicopter pilot. He attended Central Flying School in 1985 and served on 705 Squadron as a Qualified Helicopter Instructor gaining an A1(H) QHI qualification. 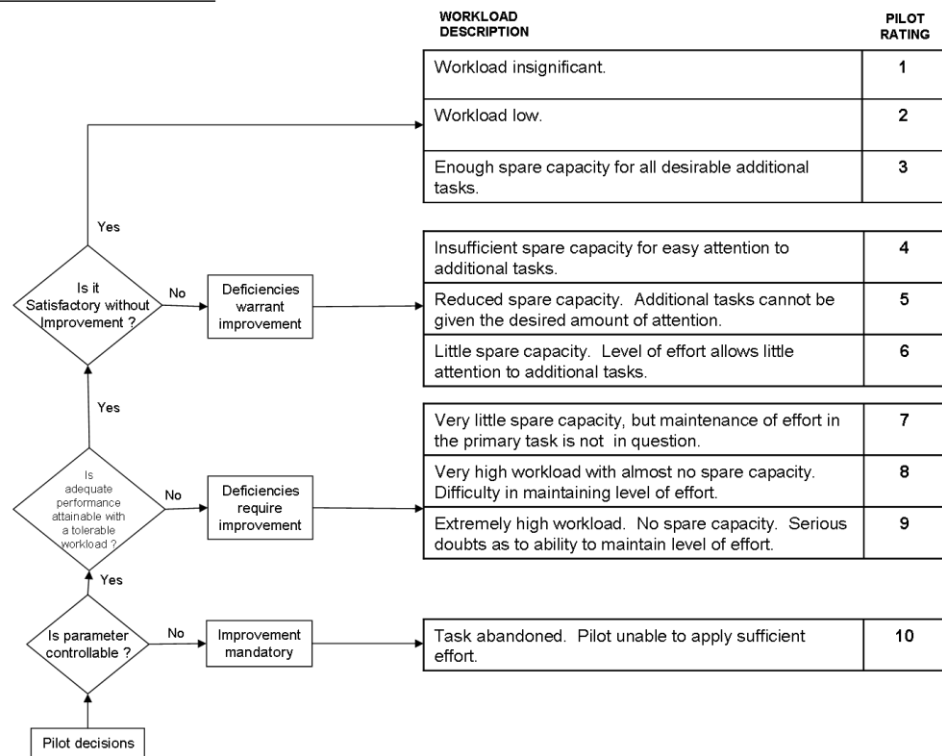He trained at the Empire Test Pilots' School in1989 before serving with Rotary Wing Test Squadron, Boscombe Down as test pilot. Responsibilities as test pilot included the introduction of the Lynx HAS Mk8 into Royal Naval Service; Sea King, Wessex and Gazelle project duties: icing project pilot, Night Vision Goggle (NVG) project pilot and SHOL project pilot.

Pilot P1 returned to operational service in 1992 with 846 Squadron including duties as Senior Pilot before returning to the Empire Test Pilots' School as a tutor. In 1995 he became Staff Aviation Officer to the Commodore Amphibious Warfare responsible for all aspects of amphibious aviation for the Royal Navy and Marines. He saw operational service in Northern Ireland, the South Atlantic, Lebanon and Bosnia. He completed three seasons as display pilot on Gazelle, both solo and as team leader in the formation team, and competed in both the World and British Helicopter Championships winning eleven national and international

trophies, including twice British Helicopter Champion on two occasions. Pilot P1 was awarded the Air Force Cross in 1989.

Pilot P1 left the Royal Navy in 1996 to become an airline pilot. He is currently flying Boeing 747-400 on long-haul routes with British Airways. In addition, he carries out instructional flying on light turbine helicopters and corporate helicopter operations on Agusta 109 and Gazelle aircraft. In total , pilot P1 has amassed 4750 rotary wing flying hours (4000 military, 750 civil) and 8500 fixed wing flying hours (500 military, 8000 civil).

Pilot P1 commissioned the James Bibby simulator at Liverpool University in 2000.

E2. Pilot P2

Pilot P2 undertook an engineering degree at Cambridge. While he was there, he flew with the Cambridge University Air Squadron. After graduating he joined the RAF and flew Lightnings with 92 Sqn in Germany before attending the Empire Test Pilots School. He then spent over four years at RAE Bedford. Amongst the projects he took part in were the Economic Cat III landing trials, Sea Harrier HUD development, and pilot workload assessment. Together with Dr Alan Roscoe, he designed the Bedford pilot workload rating scale.

In 1980 pilot P2 left the RAF and joined BAe at Hatfield, later at Woodford, where he was project development test pilot for the 125 -800, -1000 and 800XP series business jets, as well as doing some work on the 146. He then joined the Raytheon Aircraft Company and moved to Kansas. He came back to the UK in 1997 and became a commercial airline pilot. From 2000, he has been a captain with easyJet, flying the 737 out of Liverpool.

Since 1978 pilot P2 has been one of the pilots at the Shuttleworth collection of historic aircraft and has flown almost all of them.

He flew 2,300 hours with the RAF and has done almost 10,000 since becoming a civilian, nearly half of which were on the various versions of the HS/BAe 125 (now known as the Hawker).

E3. Pilot P3

Pilot P3 joined the Royal Navy on a Medium Career Commission, after first completing an honours degree in Mechanical Engineering. Following flying training Pilot P3 joined 845 Commando Squadron for the first of three consecutive tours, initially on the Wessex then on the Sea King. During this time he served as the principle NVG Instructor, Helicopter Warfare Instructor and finally as a Flight Commander with responsibility for Special Forces Operations. In 1991 Pilot P3 was appointed to Boscombe Down where he completed No 29 Rotary Wing course at The Empire Test Pilots' School. On graduation he was appointed to the Royal Aircraft Establishment at Bedford as the rotary wing experimental test pilot. Whilst serving on the Aerospace Research Squadron Pilot P3 completed a fast jet and also a multi-engine fixed wing conversion and carried out experimental research on both fixed and rotary wing aircraft.

When RAE Bedford closed down in 1994, Pilot P3 moved back to Boscombe Down for a year, serving on the Experimental Flying Squadron. In 1995 he was appointed to the US Naval Aviation Test and Evaluation Centre at Patuxent River Maryland, to instruct on the US Naval Test Pilots' School. Pilot P3 spent three years at USNTPS, instructing on both helicopters and fixed wing aircraft, eventually becoming the Senior Instructor. Whilst there, he also carried out classified work for the US Department of Defence. On his return from the States in 1998, Pilot P3 was appointed as the commander, of a tri-service specialist flying unit.

Joining the RNR Air Branch on leaving the RN, Pilot P3 holds the rank of Commander and serves as the CO (Reserves) Commando Helicopter Force. He currently flies the Boeing 747-400 for British Airways.

Pilot P3 has a total of 8000 flying hours of which 3500 are civil fixed-wing, 3500 military rotary-wing and 1000 were accrued on military fixed-wing types.

E4. Pilot EP1

Pilot EP1 qualified for the PPL(A) in 1996 and has flown 140 hours in civilian single-engine piston propeller driven aircraft since then. Pilot EP1 also served as a Grade 1 pilot for 635 Volunteer Gliding Squadron between 1996 and 1998.

References

1. Anon., *The Future of Air Transport - White Paper*, D.f. Transport, Editor. 16th December 2003.
2. Mulder, M., *Cybernetics of tunnel-in-the-sky displays*. 1999, Delft: Delft University Press.
3. Anon. *OPTIMAL. Optimised Procedures and Techniques for Improvement of Approach and Landing*. [cited; Available from: **http://www.optimal.isdefe.es/**.
4. *Aviation Safety and Pilot Control: Understanding and Preventing Unfavorable Pilot-Vehicle Interactions*. National Research Council. 1997, Washington D.C.: National Academy Press.
5. Sheridan, T.B. *Automation, Authority and Angst - Revisited*. in *Proceedings of the Human Factors Society - 35th Annual Meeting*. 1991.
6. Tanaka, K. and K. Matsumoto, *A Hierarchical Model of Pilot's Procedural Behavior for Cockpit Workload Analysis*. Transactions of the Japan Society of Aeronautical and Space Sciences, 1986. **28**(82): p. 230-239.
7. Weiner, E.L. and R.E. Curry, *Flight-Deck Automation: Promises and Problems*. Ergonomics, 1980. **23**(10): p. 955-1011.
8. Endsley, M., *Towards a Theory of Situation Awareness*. Human Factors, 1995. **37**(1): p. 32-64.
9. Sarter, N.B. *The Flight Management System - Pilot's Interaction with Cockpit Automation*. in *IEEE Conference on Systems, Man. and Cybernetics*. 1991.
10. Newman, R.L. and K.W. Greeley, *Cockpit Displays: Test and Evaluation*. 2001, Aldershot: Ashgate Publishing Ltd.
11. Anon. *Capstone Program: Frequently Asked Questions*. 2005 [cited; Available from: **http://www.faa.gov/about/office_org/headquarters_offices/arc/programs/capstone/index.cfm?Template=dsp_FAQ.cfm#phase1**.
12. Gibson, J.J., *The perception of the visual world*, ed. L. Carmichael. 1950, Boston: Houghton Mifflin Company.
13. Johnson, W.W. and C.A. Awe, *The Selective Use of Functional Optical Variables in the Control of Forward Speed. TM 108849*. NASA, September 1994.
14. Perrone, J.A., *The Perception of Surface Layout During Low-Level Flight. CP 3118*. NASA, 1991.
15. Lee, D.N., *Guiding movement by coupling taus*. Ecological Psychology, 1998. **10**(3-4): p. 221-250.

16. Padfield, G.D., D.N. Lee, and R. Bradley, *How Do Helicopter Pilots Know When to Stop, Turn or Pull Up?* Journal of the American Helicopter Society, 2003. **48**(2).

17. Anon. *Degree of Doctor in Philosophy. Notes for Guidance of Examiners*. [cited; Available from: **http://www.liv.ac.uk/sas/administration/phdguidance.pdf**.

18. Anon. *CAA Corporate Information*. [cited; Available from: **http://www.caa.co.uk/default.aspx?categoryid=286**.

19. Anon, *NTSB/ARC-02/03. Annual Review of Aircraft Accident Data. US Air Carrier Operations Calendar Year 1999*. 2004, NTSB.

20. Anon. *Aviation Safety Network*. [cited; Available from: **http://www.aviation-safety.net/about/**.

21. Anon, *CAP 681: Global Fatal Accident Review 1980 - 1996*. March 1998, Civil Aviation Authority.

22. Anon, *CAP 701: Aviation Safety Review*. October 2000, Civil Aviation Authority.

23. Anon, *NTSB/ARC-02/03. Annual Review of Aircraft Accident Data. US Air Carrier Operations Calendar Year 1999*. 1999, NTSB.

24. Anon. *Aviation Accident Database and Synopses*. [cited; Available from: **http://www.ntsb.gov/ntsb/query.asp**.

25. Rantner, H. *Airliner Accident Statistics 2005. Statistical summary of fatal multi-engine airliner accidents in 2005*. January 1st, 2006 [cited; Available from: **http://aviation-safety.net/pubs/**.

26. Ranter, H. *Airliner Accident Statistics 2002. Statistical summary of fatal multi-engined airliner accidents in 2002*. January 3rd, 2003 [cited; Available from: **http://aviation-safety.net/pubs/**.

27. Jukes, M., *Aircraft Display Systems*. Aerospace Series, ed. I. Moir and A. Seabridge. 2004, London and Bury St. Edmunds: Professional Engineering Publications Ltd.

28. Previc, F.H. and W.R. Ercoline, *Spatial Disorientation in Aviation*. AIAA Progress in Astronautics and Aeronautics. Vol. 203. 2004.

29. Padfield, G.D., *Helicopter Flight Dynamics: The Theory and Application of Flying Qualities and Simulation Modelling*. 1995, Oxford: Blackwell Science.

30. Jump, M. and G. Padfield, *Progress in the development of guidance strategies for the landing flare manoeuvre using tau-based parameters*. Aircraft Engineering and Aerospace Technology, 2006. **78**(1): p. 4-12.

31. Suijkerbuijk, M., et al. *Development and Experimental Evaluation of a Performance Based Vertical Situation Display*. in *AIAA Guidance, Navigation and Control Conference and Exhibit*. 15-18th August 2005. San Francisco, California.

32. Previc, F.H., *Visual Illusions in Flight*. Progress in Astronautics and Aeronautics, ed. F.H. Previc and W.R. Ercoline. Vol. 203. 2004, Reston, Virginia: AIAA.

33. Ford, T., *Increased Awareness.* Aircraft Engineering and Aerospace Technology, 1999. **71**(4): p. 362-364.

34. Wisely, P.L. and C.T. Bartlett, *Gate to Gate Operation of a Civil Transport Head Up Display.* SPIE, Cockpit Displays VII: Displays for Defense Applications, 2000. **4022**: p. 392-398.

35. Wilckens, V. and W. Schattenmann. *Test Results with New Analog Displays for All Weather Landing*. in *AGARD Conference Proceedings "Problems of the Cockpit Environment"*. 1968.

36. Anon., *Radio Navigation and Instrument Flying*. The Air Pilot's Manual, ed. P.D. Godwin. Vol. 5. 2004, Cranfield: Air Pilot Publishing Ltd.

37. Boeing. *Technology Flies High on Boeing 737*. 2003 [cited; Available from: **http://www.boeing.com/commercial/news/feature/737tech.html**.

38. Hughes, D., *Cockpits Shed Paper*, in *Aviation Week & Space Technology*. February 2nd 2004.

39. Wilckens, V. *Improvements in Pilot/Aircraft-Integration by Advanced Contact Analog Displays.* in *Proceedings of the Ninth Annual Conference on Manual Control*. 1973.

40. Olmos, O., C.C. Liang, and C.D. Wickens, *Electronic map evaluation in simulated visual meteorological conditions.* The International Journal of Aviation Psychology, 1997. **7**(1): p. 37-66.

41. Croft, J., *Alaska: Pioneering new vision for pilots*, in *Aerospace America*. June 2004. p. 13 - 15.

42. Ruley, J.D., *The FAA's Capstone Project*, in *Pilot Journal*. March/April 2005.

43. Anon. *Proposed Capstone Phase III Statewide Plan (Accelerated NAS Transition Proposal)*. 2005 [cited; Available from: **http://www.alaska.faa.gov/capstone/docs/Statewide%20v1.1H.pdf**.

44. Anon. *Implementation Progress of Capstone Phase II. Summary for 2004*. July 2005 [cited; Available from: **http://www.alaska.faa.gov/capstone/Capstone%20Phase%202%20Folder/Final%202004%20Phase%202%20Report.pdf**.

45. Scott, W.B., *The Collins View*, in *Aviation Week & Space Technology*. August 9th 2004.

46. Sachs, G., *Longitudinal flightpath predictor design for minimum pilot compensation.* Proceedings of the Institution of Mechanical Engineers, Part G: Journal of Aerospace Engineering, 2000. **214**(1): p. 41.

47. Sachs, G., *Tunnel/predictor Display with Two-axis Control Coordination and Simplification.* Aerospace Science and Technology, 2003. **7**: p. 621 - 631.

48. Sachs, G. and I. Sturhan. *Preview and Manual Control Modes with Tunnel-Predictor Display.* in *AIAA Guidance, Navigation and Control Conference and Exhibit.* Aug 15-18th 2005. San Francisco, California: AIAA.

49. Kaiser, J., et al., *Stereoscopic Head Up Display for aviation.* SPIE Stereoscopic Displays and Virtual Reality Systems VIII, 2001. **4297**: p. 117-126.

50. Verschragen, E., M. Mulder, and M.v. Paassen. *Track-Recovery Support for Tunnel-in-the-Sky Displays.* in *AIAA Guidance, Navigation and Control Conference and Exhibit.* August 15-18th 2005. San Francisco, California: AIAA.

51. Guy, A. and T. Schnell. *Terrain Awareness & Pathway Guidance for Head-Up Displays (TAPGUIDE); A Simulator Study of Pilot Performance.* in *22nd Digital Avionics Systems Conference.* 2003.

52. Schiefele, J., et al. *Human Factors Flight Trial Analysis for 2D Situation Awareness and 3D Synthetic Vision Displays.* in *22nd Digital Avionics Systems Conference.* 10-12th October2003. Indianapolis.

53. Reising, J.M., et al. *Evaluation of Pathway Symbology Used to Land From Curved Approaches with Varying Visibility Conditions.* in *Human Factors and Ergonomics Society 42nd Annual Meeting.* 1998.

54. Snow, M.P. and J.M. Reising, *Effect of Pathway-in-the-Sky and Synthetic Terrain Imagery on Situation Awareness in a Simulated Low-Level Ingress Scenario*, A.F.R. Laboratory, Editor. 1999.

55. Reising, J.M., et al. *A Comparison of Two Head-Up Display Formats Used to Fly Curved Instrument Approaches.* in *Humand Factors and Ergonomics Society 39th Annual Meeting.* 1995.

56. Hoh, R.H., A.J. Arencibia, and G.M. Hislop. *Development and Flight-Test of a Commercial Head-Up Display.* in *Society of Experimental Test Pilots 46th Annual Symposium.* 2002. Fort Walton Beach, Florida, US.

57. Still, D.L. and L.A. Temme. *OZ: A Human-Centered Computing Cockpit Display.* 2001. I/ITSEC.

58. Still, D.L. and L.A. Temme, *Oz: A Human-Centered Computing Cockpit Display User Guide.* 2003.

59. Foyle, D.C., et al. *Human Performance Models of Pilot Behaviour.* in *Human Factors and Ergonomics Society 49th Annual Meeting.* 2005. Santa Monica: HFES.

60. Johnson, W.W. and M.K. Kaiser. *Perspective imagery in synthetic scenes used to control and guide aircraft during landing and taxi:*

some issues and concerns. in *SPIE/International Society of Optical Engineers*. 1995.

61.   Cash, A., *Psychology for Dummies*. 2002, Indianapolis: Wiley Publishing Inc.

62.   Bruce, V., P.R. Green, and M.A. Georgeson, *Visual Perception: Physiology, Psychology and Ecology*. 3rd ed. 1996, Hove: Psychology Press.

63.   Gordon, I.E., *Theories of Visual Perception*. 1989, Chichester: John Wiley & Sons.

64.   Gibson, J.J., *Picture Testing and Research. AAF Aviation Psychology Research Report No. 7*, U.S.G.P. Office, Editor. 1947.

65.   Gibson, J.J., *The Ecological Approach to Visual Perception*. 1986, Hillsdale, New Jersey: Lawrence Erlbaum Associates.

66.   William H. Warren, J. and D.R. Mestre, *Perception of Circular Heading From Optical Flow*. Journal of Experimental Psychology: Human Perception and Performance., 1991. **17**(1): p. 28-43.

67.   William H. Warren, J., M.W. Morris, and M. Kalish, *Perception of Translational Heading From Optical Flow*. Journal of Experimental Psychology: Human Perception and Performance., 1988. **14**(4): p. 646-660.

68.   Humbert, J.S. *AIAA-2005-6280: Pitch-Altitude Control and Terrain Following Based on Bio-Inspired Visuomotor Convergence*. in *AIAA Atmospheric Flight Mechanics Conference*. 15 -18 August 2005. San Francisco, USA.

69.   Mueller, T.J., ed. *Fixed and Flapping WIng Aerodynamics for Micro Air Vehicle Applications*. Progress in Astronautics and Aeronautics, ed. P. Zarchan. Vol. 195. 2001, AIAA: Reston, Virginia, USA.

70.   Roderick, J., J. Kehoe, and R. Lind. *AIAA-2005-6280: Vision-Based Navigation Using Multi-Rate Feedback from Optic Flow and Feature Estimation*. in *AIAA Atmospheric Flight Mechanics Conference*. 15-18 August 2005. San Francisco, USA.

71.   Havron, M.D., *HSR-RR-62/3-MK-X: Information Available from Natural Cues During Final Approach and Landing*. 1962, Human Sciences Research Inc.: Arlington.

72.   Hecht, H. and G.J.P. Savelsbergh, *Theories of Time-to-Contact Judgement*. Advances in Psychology, ed. G.E. Stelmacht. Vol. 135. 2004, Amsterdam: Elsevier B.V.

73.   Gibson, J.J., *The ecological approach to visual perception*, in *The history of psychology: Fundamental questions*, M.P. Munger, Editor. 2003, Oxford University Press: New York, NY. p. 468-477.

74.   Morgan, M.J., *Computational Theories of Vision. (Review of Marr)*. Quarterly Journal of Experimental Psychology, 1984. **A36**: p. 157-165.

75. Lee, D.N., *Tau in Action and Development*. Action, Perception and Cognition in Learning and Development. 2005, Hillsdale, New Jersey: Erlbaum.

76. Lee, D.N., *How Movement is Guided*, submitted for publication, Psychology.

77. Lee, D.N., *A theory of visual control of braking based on information about time-to-collision.* Perception, 1976. **5**(4): p. 437-459.

78. Lee, D.N. and P.E. Reddish, *Plummeting gannets: A paradigm of ecological optics.* Nature, 1981. **293**(5830): p. 293-294.

79. Schoner, G., *Dynamic theory of action-perception patterns - the time-before-contact paradigm.* Human Movement Sciences, 1994. **13**(3-4): p. 415-439.

80. Savelsbergh, G.J.P., H.T.A. Whiting, and R.J. Bootsma, *Grasping Tau.* Journal of Experimental Psychology: Human Perception and Performance., 1991. **17**(2): p. 315-322.

81. Caljouw, S., J.v.d. Kamp, and G.J.P. Savelsbergh, *The Fallacious Assumption of TIme-To-Contact Perception in the Regulation of Catching and Hitting.* Advances in Psychology, ed. H. Hecht and G.J.P. Savelsbergh. Vol. 135. 2004, Amsterdam: Elsevier.

82. Lee, D.N., et al., *Visual Control of Velocity of Approach by Pigeons When Landing.* Journal of Experimental Biology, 1993. **180**: p. 85-104.

83. Wann, J.P., *Anticipating Arrival: Is the Tau Margin a Specious Theory ?* Journal of Experimental Psychology: Human Perception and Performance., 1996. **22**(4): p. 1031-1048.

84. Lee, D.N., C.M. Craig, and M.A. Grealy, *Sensory and intrinsic coordination of movement.* Proceedings of the Royal Society of London, 1999. **B266**: p. 2029-2035.

85. Kaiser, M.K. and W.W. Johnson, *How Now, Broad Tau ?* Advances in Psychology, ed. H. Hecht and G.J.P. Savelsbergh. Vol. 135. 2004, Amsterdam: Elsevier.

86. Pleijsant, J.M., et al. *Effects of Runway Outline and Ground Texture on the Perception of Time-to-Contact in Simulated Landings*. in *Fourth European Workshop on Ecological Psychology*. July 3-5 1996. Zeist, The Netherlands.

87. Mulder, M., et al., *The Effects of Pictorial Detail on the Timing of the Landing Flare: Results of a Visual Simulation Experiment.* The International Journal of Aviation Psychology, 2000. **10**(3): p. 291-315.

88. Kaiser, M.K. and L. Mowafy. *Visual Information for Judging Temporal Range*. in *Piloting Verticfal Flight Aircraft: A Conference on Flying Qualities and Human Factors*. 1993. San Francisco, California.

89. Gibson, J.J., P. Olum, and F. Rosenblatt, *Parallax and perspective during aircraft landings.* American Journal of Psychology, 1955. **68**: p. 372-385.

90. Calvert, E.S., *Visual Judgements in Motion.* Journal of the Institute of Navigation, 1954. **7**(3): p. 233-251.

91. Galanis, G., A. Jennings, and P. Beckett, *A Mathematical Model of Glide-Slope Perception in the Visual Approach to Landing.* The International Journal of Aviation Psychology, 1998. **8**(2): p. 83-101.

92. Lintern, G. and M.B. Walker, *Scene Content and Runway Breadth Effects on Simulated Landing Approaches.* The International Journal of Aviation Psychology, 1991. **1**(2): p. 117-132.

93. Perrone, J.A., *Visual Slant Misperception and the 'Black Hole' Landing Situation.* Aviation, Space, and Environmental Medicine, 1984. **55**: p. 1020-25.

94. Tiller, S.J., et al. *Learning to land: the role of perceptual cues, feedback and individual differences.* in *5th Aviation Psychology Symposium.* 2000. Manly, Australia.

95. Lee, D.N., *Aerial docking by hummingbirds.* Naturwissenschaften, 1991. **78**: p. 526-527.

96. Lee, D.N., et al., *Steering by echolocation: a paradigm of ecological acoustics.* Journal of Comparative Physiology A, 1995. **186**: p. 347-354.

97. Lee, D.N., J.R. Lishman, and J.A. Thomson, *Regulation of gait in long jumping.* Journal of Experimental Psychology: Human Perception and Performance, 1982. **8**(3): p. 448-459.

98. Lee, D.N., D.S. Young, and D. Rewt, *How do somersaulters land on their feet?* Journal of Experimental Psychology: Human Perception and Performance., 1992. **18**(4): p. 1195-1202.

99. Fajen, B.R., *Steering Toward a Goal by Equalizing Taus.* Journal of Experimental Psychology: Human Perception and Performance., 2001. **27**(4): p. 953-968.

100. Tresilian, J.R., *Empirical and Theoretical Issues in the Perception of Time to Contact.* Journal of Experimental Psychology: Human Perception and Performance., 1991. **17**(3): p. 865-876.

101. Tresilian, J.R., *Visually timed action:time-out for 'tau' ?* Trends in Cognitive Science, 1999. **3**(8): p. 301-310.

102. Jump, M. and G. Padfield, *Investigation of the flare maneuver using optical tau.* Journal Of Guidance Control And Dynamics, 2006. **29**(5): p. 1189-1200.

103. Padfield, G.D. and M.D. White. *Flight Simulation in Academia: HELIFLIGHT in its First Year of Operation.* in *The Challenge of Realistic Rotorcraft Simulation.* November 2001. RAeS, London.

104. Bickerstaffe, I.H. *Portrait of Landscape.* in *Proceedings of IMAGE Conference.* 1998. Scottsdale, Arizona.

105.   Anon., *VAPS User's Guide*. 2004, Engenuity Technologies: Montreal.

106.   Anon., *Eye Tracking System Instruction Manual. Model 501 Head Mounted Optics*. 2003, Applied Science Laboratories: Bedford, MA, USA.

107.   Anon., *Eyeanal (Eye-Analysis) Software Manual. Windows version for use with ASL Series 5000 and ETS-PC Eye Tracking Systems v1.3a*.

108.   Anon., *Pooley's Flight Guide. United Kingdom 2001.*, ed. R. Pooley, R. Patel, and W. Ryall. 2001, Elstree, England: Pooley's Flight Equipment Limited.

109.   Rendall, D., *Jane's Aircraft Recognition Guide*. 1999, London: Harper-Collins.

110.   *B707 Airplane Characteristics: Airport Planning*. December 1968, The Boeing Company Commercial Airplane Division.

111.   Anon., *Aeronautical Design Standard-33E-PRF. Perfromance Specification, Handling Qualities Requirements for Military Rotorcraft*. March 21, 2000, U.S. Army, AMCOM, Redstone, Alabama.

112.   Anon., *Pan-American World Airways Airline Manual System. Aircraft Operating Manual: B700*. 6th June 1969.

113.   Anon., *UK IFR Touring Guide*. 2006, Walton-on-Thames, Surrey, UK European Aeronautical Group UK Ltd.

114.   Ehrenberg, A.S.C., *A Primer in Data Reduction: An Introductory Statistics Textbook*. 2000: John Wiley & Sons.

115.   Cooper, G.E. and R.P. Harper, *The Use of Pilot Rating in the Evaluation of Aircraft Handling Qualities*, in *AGARD Report 567*. 1969.

116.   Haworth, L.A. and R.L. Newman, *Test Techniques for Evaluating Flight Displays*. February 1993, NASA TM 103947.

117.   Roscoe, A.H. and G.A. Ellis, *A Subjective Rating Scale for Assessing Pilot Workload in Flight: A Decade of Practical Use*. 1990, Royal Aircraft Establishment TR 90019.

118.   Hart, S.G. *Description and Application of the NASA Task Load Index (TLX). . in The Department of Defense Human Engineering Technical Advisory Group Workshop on Workload*. 1987. (NUSC 6688) Newport, RI: Naval Underwater Systems Center.

119.   Stewart, D., *Exotic Australia*, in *Pilot*. August 2005.

120.   Cook, M.V., *Flight Dynamics Principles*. 1997, Oxford: Butterworth-Heineman.

121.   Seckel, E., *Stability and Control of Airplanes and Helicopters*. 1964.

122.   Heffley, R.K., T.M. Schulman, and W.F. Clement, *NASA-CR-166404: An Analysis of Airline Landing Flare Data Based on Flight and Training Simulator Measurements*. 1982, NASA.

123. Pinsker, W.J.G., *R. & M. No. 3662: A Theoretical Study of Height Control in Flight Close to the Ground as Affected by Elevator Lift and Cockpit Position*, in *Aeronautical Research Council: Reports and Memoranda*. 1971, Aero F Dept., R.A.E. Bedford: London.

124. Padfield, G.D., G. Clark, and A. Taghizad. *How long do pilots look forward ?* in *31st European Rotorcraft Forum*. September 2005. Florence, Italy.

125. Barrows, G.L., *Mixed-Mode VLSI Optic Flow Sensors for Micro Air Vehicles*, in *Department of Electrical and Computer Engineering*. 1999, University of Maryland, College Park.

126. Coombs, D., et al. *Real-time obstacle avoidance using central flow divergence and peripheral flow*. in *Proceedings of the IEEE International Conference on Computer Vision*. 1995. MA.

127. Moralez, E., et al. *In-Flight Assessment of a Pursuit Guidance Display Format for Manually Flown Precision Instrument Approaches*. in *American Helicopter Society 60th Annual Forum*. June 7-10, 2004. Baltimore, Maryland, USA.

128. Jump, M. and G.D. Padfield. *Tau Flare or not Tau Flare? that is the question: Developing Guidelines for an Approach and Landing Sky Guide*. in *AIAA Guidance, Navigation and Control Conference*. 15 – 18th August 2005. San Francisco.

129. Lintern, G., C.E. Kaul, and S.C. Collyer, *Glideslipe Descent-Rate Cuing to Aid Carrier Landings*. Human Factors, 1984. **26**(6): p. 667-675.

130. Long, J., *Heads Up on Heads-Up: SDO Hazards from Moving-Tape HUD Symbology*. Flight Safety, June 2002.

131. Anon, *FLIGHTLAB Theory Manual (Vol. One)*. March 2004, Advanced Rotorcraft Technology: Mountain View, California.

132. Lawrence, D.B., *The Flying Qualities of the Wright Flyers*, in *Department of Engineering*. September 2004, The University of Liverpool.

133. McCormick, B.W., *Aerodynamics, Aeronautics and Flight Mechanics*. 1995, New York: John Wiley & Sons Inc.

134. Selig, M. *UIUC Airfoil Data Site*. 2002 [cited; Available from: **www.ae.uiuc.edu/m-selig/ads.html**.

135. Drela, M., *XFOIL 6.9 User Guide*. 11th January 2001, MIT.

136. Anon., *ESDU 90030: Lift and Rolling Moment Due to Spoilers on Wings with Flaps Undeflected at Subsonic Speeds*. 1999.

137. Anon., *ESDU 92002: Lift and Rolling Moment due to Spoilers on Wings with Trailing-Edge Flaps Deflected at Subsonic Speeds - Extension of Item No. 90030*. 1999.

138. Anon., *ESDU 96026: Drag and Yawing Moment Due to Spoilers*.

139. Roskam, D.J., *Airplane Design Part II: Preliminary Configuration Design and Integration of the Propulsion System* 2002, Lawrence, KA, USA: DAR Corporation.

140. Hanke, C.R., *The Simulation of a Jumbo Jet Transport Aircraft Vol. 1 & 2*. 1970, NASA-CR-114494.

141. Pinsker, W.J.G., *R. & M. No. 3602: The Landing Flare of Large Transport Aircraft*, in *Aeronautical Research Council: Reports and Memoranda*. 1969, Aerodynamics Dept., R.A.E. Bedford: London.